CHALMERS TEKNISKA HÖGSKOLA

CHALMERS UNIVERSITY OF TECHNOLOGY
GÖTEBORG
SWEDEN

FOOTINGS WITH SETTLEMENT-REDUCING PILES IN NON-COHESIVE SOIL

Phung Duc Long

Department of Geotechnical Engineering
1993

FOOTINGS WITH SETTLEMENT-REDUCING PILES IN NON-COHESIVE SOIL

Phung Duc Long

Submitted to the School of Civil Engineering, Chalmers University of Technology, in partial fulfillment of the requirement for the degree of Doctor of Philosophy

Department of Geotechnical Engineering
Chalmers University of Technology
S-412-96 Göteborg, Sweden

Göteborg 1993

FOOTING WITH SETTLEMENT-REDUCING PILES IN NON-COHESIVE SOIL

Phung Duc Long

Department of Geotechnical Engineering
Chalmers University of Technology
S-412 96 Göteborg, Sweden

ABSTRACT

Although the design concept based on the idea of limiting the settlement of footings by settlement-reducing piles is gaining more and more support, there have been very few experimental studies of the behaviour of piled footings in non-cohesive soil. The influences of the contact between the pile cap and the soil on the capacity and the load-settlement behaviour of a piled footing are considerable but this has not been well understood.

The purpose of this study is to clarify the overall interaction between the piles, the cap, and the soil in piled footings with friction piles in non-cohesive soil. The major part of the study consists of three extensive series of large-scale field model tests on single piles, free-standing pile groups, shallow footings and piled footings. The field tests were carried out in loose to dense sand, and with pile spacings of four, six and eight times the pile width. By performing the field model tests, the Author has tried to create a better understanding of the load-transfer mechanism and of the load-settlement behaviour of a piled footing in non-cohesive soil. The most important factors influencing the behaviour of piled footings have been investigated.

The study shows that in cap-pile interaction, the increase in the pile shaft resistance is most important and more pronounced than the increase in the pile base resistance and the change in the cap capacity. It is also found that the load-settlement behaviour of the cap in a piled footing is very similar to that of a shallow footing with the same geometry under equal soil conditions. This remark is used as the basis for the proposed simplified methods of predicting settlement of a friction piled footing in non-cohesive soil. The results calculated using the proposed methods are in good agreement with the measured values.

The reduction in settlement of a piled footing, in relation to a corresponding shallow footing, depends clearly on the relative cap capacity. With a high value of the relative cap capacity, i.e. when the capacity of the cap is predominant over that of the piles, the contribution of the piles has a clear effect in reducing the settlement of the footing.

Keywords: settlement-reducing piles, pile-cap-soil interaction, driven piles, non-cohesive soil, field tests, earth pressure cell, numerical analysis, simplified method.

CONTENTS

SUMMARY

Our knowledge of friction pile behaviour in non-cohesive soil has been greatly widened during the last decade. Many experimental studies have been performed on the behaviour of single piles and of free-standing pile groups. However, there have been very few experimental studies of the behaviour of piled footings with the cap being in contact with the soil. The influences of the contact between pile cap and soil on the capacity and the load-settlement behaviour of a piled footing are considerable but this has not been well understood. The mechanism of load transfer in a piled footing involves a highly complex overall interaction between piles, pile cap and surrounding soil. The interaction is influenced by the stress-strain-time and failure characteristics of all elements in the system. The soil may be changed considerably due to pile installation and to the contact pressure at the cap-soil interface. The load-deformation behaviour of the piled footing is affected by a lot of factors such as soil properties, group geometry, pile installation and interaction between different elements (piles and cap) in the footing. Due to the uncertainties or difficulties in defining such factors, there is no available analysis method capable of including them all.

The design concept based on the idea of limiting the settlement of footings by settlement-reducing piles is gaining more and more support. Only a small number of piles are required to reduce considerably the settlement of a footing. For a wide application of such footings, which would result both in economical advantages and in reduction of settlements and tilting, reliable methods of analysing the behaviour of piled footings are badly needed.

The purpose of this study is to clarify the overall interaction between the piles, the cap, and the soil in piled footings in non-cohesive soil. By performing large-scale field model tests, the Author has tried to create a better understanding of the load-transfer mechanism and of the load-settlement behaviour of a piled footing in non-cohesive soil. The most important factors influencing the behaviour of piled footings have been investigated.

Experimental investigation

The experimental part of the study consists of large-scale field model tests on piled footings, free-standing pile groups, single piles, as well as shallow footings under equal soil conditions. The problem of pile-cap-soil interaction

of a piled footing in sand includes interaction between the piles in the group, named as pile-soil-pile interaction, as well as between the pile group and the pile cap, which is in contact with the soil surface, named as pile-cap interaction. Comparisons of the test results on single piles with those on free-standing pile groups show the pile-soil-pile interaction, while comparisons of the test results on piled footings with those on free-standing pile groups and on caps alone clarify the pile-cap interaction. To make possible a study of the settlement-reducing effect of piles, the load-settlement behaviour of shallow footings and of piled footings have to be directly compared. Three different test series were carried out, each of which consists of four separate tests comprising a shallow footing, a single pile, a free-standing pile group and a piled footing under equal soil conditions and with equal geometry.

The model piles used in the field tests were hollow steel piles with a square cross-section, 60 mm by 60 mm. The length of the model piles was about 2.3m and the depth of embedment of the piles in each separate test varied slightly, depending on the testing procedure. The surface of the piles was covered with sand (grain size < 0.125 mm) glued to the surface. All the pile groups were square and consisted of five piles: one central pile, and four corner piles. As the main purpose of the research was to study the settlement-reducing effect of the piles, the pile spacing was chosen to be relatively large. The centre-to-centre pile spacing was $4b_p$ (four pile widths) in the first test series, and $6b_p$, $8b_p$ in the second and the third series. The pile caps (footings) were made of pre-fabricated reinforced concrete and were absolutely rigid. The size of the footings was chosen with regard to the pile spacing. In the first test series, the sand was quite loose; in the second and the third series, the sand was medium dense to dense. The geometry of the test models and the density of soil, used in the field model tests, are summarised in Table 1.

Axial pile loads were measured by means of load cells at the base and head of every pile. The load was also measured in the middle of one corner pile in order to investigate the distribution of the axial pile load with depth. The lateral earth pressure against the pile shaft was measured along the central pile by means of Glötzl total stress cells. In all the tests, the total applied load was monitored by an independent electric load cell. The load, carried by the cap in a piled footing, was then obtained by subtracting the load taken by the piles from the total load.

Table 1 Summary of the field model tests

Test Series	Pile Group and Cap	Sand	Pile Length (m)	Separate Tests
T1	five piles spacing $S=4b_p$ 46cmx46cmx25cm	I_D = 38%	- 2.0 2.1 2.3	T1C, shallow footing T1S, single pile T1G, pile group T1F, piled footing
T2	five piles spacing $S=6b_p$ 63cmx63cmx35cm	I_D = 67%	- 2.0 2.1 2.3	T2C, shallow footing T2S, single pile T2G, pile group T2F, piled footing
T3	five piles spacing $S=8b_p$ 80cmx80cmx40cm	I_D = 62%	- 2.0 2.1 2.3	T3C, shallow footing T3S, single pile T3G, pile group T3F, piled footing

The tests on the piled footings were performed using two different procedures. The first procedure, in which the test was started when the pile cap was already in good contact with the soil, had the advantage of making possible a direct comparison between the behaviour of a piled footing on the one hand and that of a shallow footing and a free-standing pile group on the other. However, using the second procedure, in which the test was started when the pile cap was 20 mm above the soil surface, the effect on the pile behaviour of the cap being in contact with soil is more obvious. Comparisons with other tests can be made by using the load-settlement curve, *modified* from the original one according to the method shown in Appendix A. The second test procedure is strongly recommended for testing piled footings both in sand and clay.

Bearing capacity

The bearing capacity of the piled footings was studied by using different *load efficiency coefficients*, based on comparison of capacities of the elements of a piled footing (piles and cap) with those of a single pile, a free-standing pile group, and a shallow footing. All the efficiency coefficients vary depending upon the settlement level. The bearing capacity of a piled footing can then be expressed according to Eq. (1):

$$P_n = n\,(\eta_{1s}\,\eta_{4s}\,P_{ss} + \eta_{1b}\,\eta_{4b}\,P_{sb}) + \eta_6\,P_c \qquad (1)$$

where, n = number of piles in the group,

η_{1s}, η_{1b} = influence factors of pile-soil-pile interaction on the pile shaft and pile base capacities,

η_{4s}, η_{4b}, η_6 = influence factors of pile-cap interaction on the pile shaft and pile base capacities, and on the capacity of the cap,

P_{ss}, P_{sb} = shaft and base capacities of the reference single pile under equal soil conditions as the pile group,

P_c = capacity of the shallow footing (cap alone)

The pile base efficiency η_{1b} was found to be equal to unity for medium dense to dense sand, and higher than unity for loose sand. The pile shaft efficiency η_{1s}, which represents the pile driving effect on the pile shaft resistance, was always higher than unity even for pile groups with large pile spacing. In the third test series, for example, the pile spacing was as large as eight times the pile width ($S= 8b_p$), but η_{1s} is still quite high, $\eta_{1s} \simeq 2$. The pile base efficiency η_{4b} is probably higher than unity for very short piles, but can be taken as unity when the piles are long enough, e.g. $l_p >$ (1.5 to 2) B_c. The pile shaft efficiency η_{4s} is the most important factor in the cap-pile interaction problem, especially under a high contact pressure at the cap-soil interface or at a large settlement. The cap efficiency η_6 is very close to unity. For practical design, it can be taken as 1.0 for loose sand, and 0.9 for medium to dense sand.

Load-displacement behaviour

The failure of a piled footing in non-cohesive soil is progressive, i.e. the applied load increases with increasing settlement. The load-settlement behaviour of the piles and the cap in the piled footings was compared to that of the corresponding free-standing pile groups and shallow footings. It was found that *the behaviour of the cap in a piled footing is very similar to that of a corresponding shallow (unpiled) footing* on both loose and dense sand (Fig.1). This is one of the most important conclusions drawn from the study and was used as a basis of the proposed simplified methods of estimating settlement of a piled footing in sand.

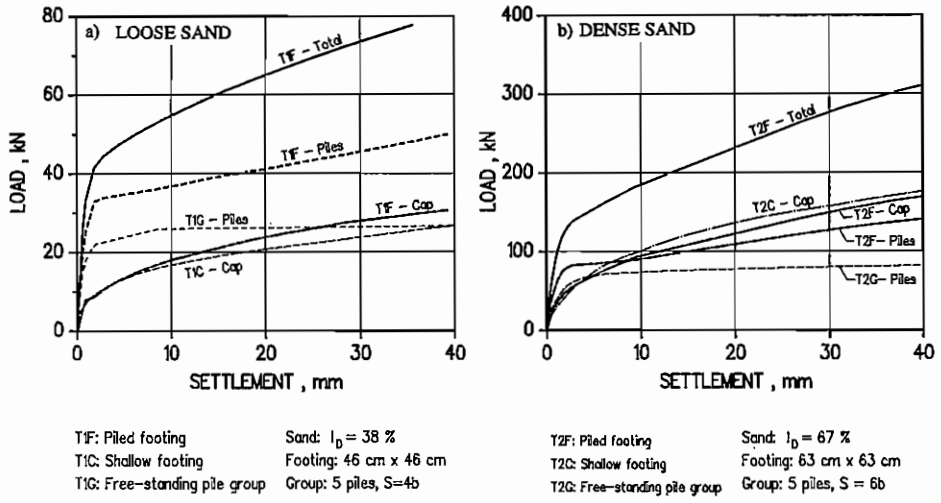

Fig. 1 Load-settlement behaviour, comparison between the tests on piled footing, free-standing pile group and shallow footing. (a) for loose sand; (b) for medium dense to dense sand.

Lateral earth pressure and skin friction along a pile

The increase in lateral earth pressure against the pile shaft in a piled footing consists of two components: the increase due to the cap in contact with soil on the one hand, and to the effect of the pile failure zone on the other. The cap effect is predominant for the upper part of the pile, while the effect of the pile failure zone is predominant for the lower part. However, in comparison with the increase in lateral pressure due to the cap effect, the increase due to the pile failure effect is small and can be ignored in practice. At a small cap load, the increase in lateral pressure due to the cap effect is small. When the cap load is large enough, so that the soil under the cap becomes plastic, it increases in proportion to the increase in the cap load. The lateral pressure against the pile shaft clearly decreases with increasing depth. It has its largest magnitude at the cap-soil interface, and is reduced to zero at a certain depth depending upon the size of the cap (Fig. 2).

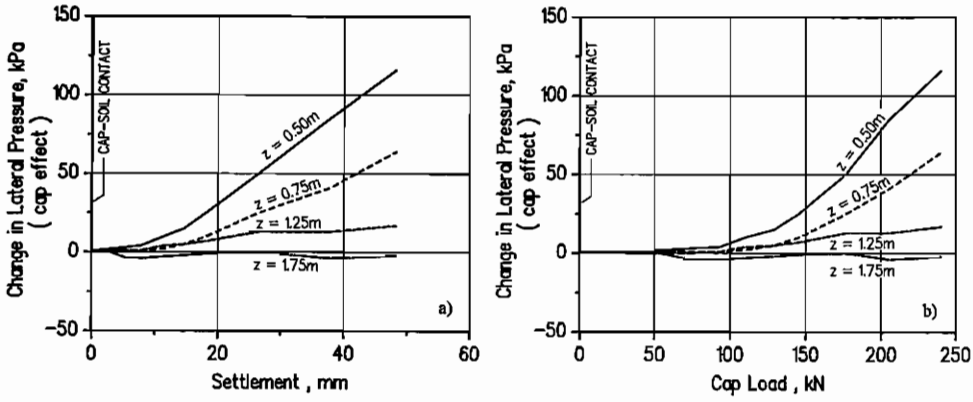

Fig. 2 Increase in lateral earth pressure along pile due to the cap effect (a) versus settlement; (b) versus cap load.

In a piled footing, the skin friction along a pile consists of friction due to pile-soil-pile interaction (as for single piles and free-standing pile groups), and friction due to an increase in lateral earth pressure $\Delta\sigma_h'$, caused by the cap-soil contact pressure and by the influence of the failure zone at the pile base. The increase in skin friction along a pile due to the cap effect and to the effect of pile failure is shown in Fig. 3.

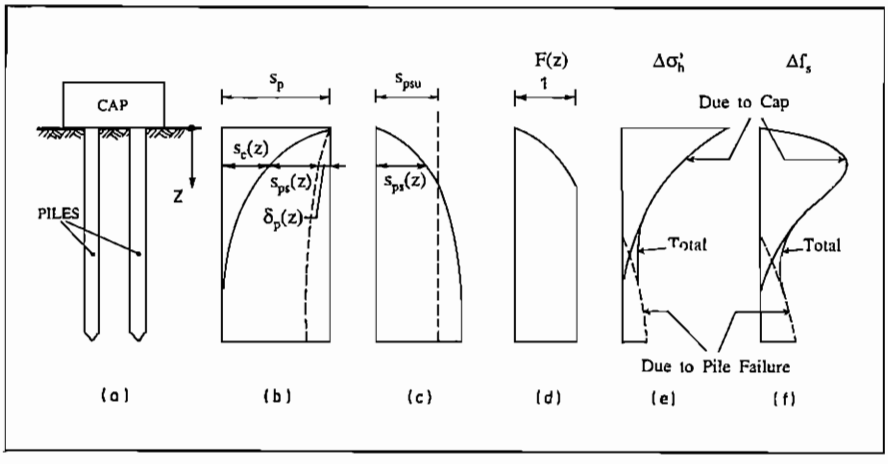

Fig. 3 Increase in skin friction along a pile due to effect of cap being in contact with soil and to effect of pile failure.

Settlement-Reducing Effect

The conventional settlement ratio, defined as the ratio of the settlement of a single pile to that of a pile group, has little practical meaning in estimating the settlement of piled footings. Different *settlement ratio coefficients* have been defined in order to compare the settlement of a piled footings with the settlements of a single pile, a free-standing pile group, and a shallow footing. The settlement ratio ξ_7, defined as ratio of the settlement of a piled footing to that of a corresponding shallow footing at the same applied load, seems to be the most practical, Fig. 4.

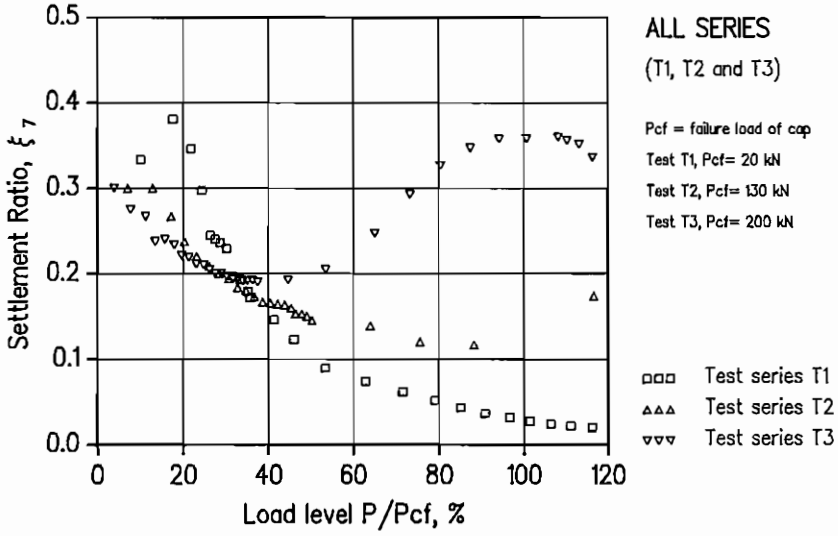

Fig. 4 Settlement ratio ξ_7 - Comparison of piled footings with shallow footings. Test series T1:relative density of sand I_D=38%, pile spacing $S=4b_p$; Test series T2: I_D=67%, $S=6b_p$; Test series T3: I_D=62 %, $S=8b_p$.

The ratio ξ_7 clearly depends on the *relative cap capacity* α, which refers to the relative contribution of the pile cap to the capacity of a piled footing. Fig. 5 shows an empirical relationship between ξ_7 and α, which can be used for a quick estimate of the reduction in the settlement of piled footings.

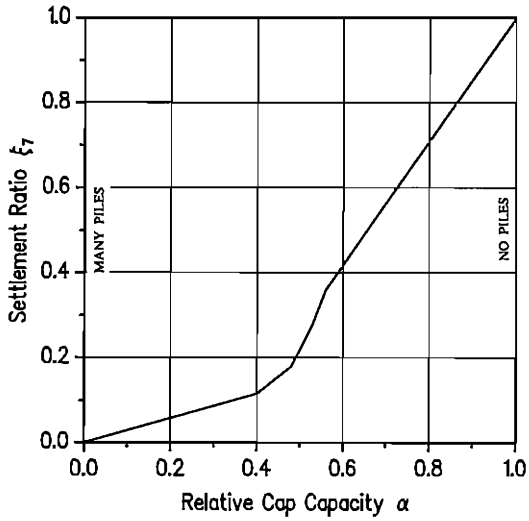

Fig. 5 Settlement reduction factor ξ_7 of piled footings, in relation to shallow footings, versus relative cap capacity α

Numerical Analysis

Most of the available computer programs for analysing pile groups and piled footings are based on the theory of elasticity. The DEFPIG code, presented by Poulos (1980a) is one of the most typical. The load-settlement behaviour of the piled footings, included in this research was compared with that calculated by means of the DEFPIG code. The comparison shows that, with well-selected soil properties, DEFPIG predicts quite well the load-settlement behaviour of the piled footing under the working load (or the elastic stage). However, the program fails to simulate the "settlement-hardening" response of the piled footing. This can also explain the incorrect conclusion drawn on the basis of the elastic methods, namely that the increase in stiffness of a piled footing due to the cap in contact with soil is small in comparison with that of a corresponding free-standing pile group.

The analysis of the load-settlement behaviour of the shallow footings by means of FLAC, an explicit finite difference code, gives an excellent agreement with the test results, provided that an elastic-plastic material according to the Mohr-Coulomb failure criterion is used for modelling the soil. In comparison with the elastic analysis, the horizontal pressure in the soil, obtained by

using the Mohr-Coulomb soil model, is much higher, and the depth of influence is much greater, Fig. 6. This explains why the elastic methods fail in simulating the load-settlement behaviour of a piled footing. The Mohr-Coulomb soil model is, therefore, suggested to be used where the horizontal soil pressure is part of the geotechnical problem.

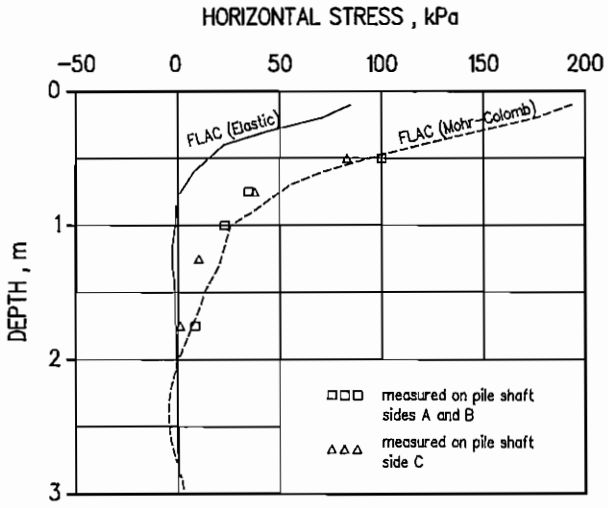

Fig. 6 Comparison of the horizontal soil stress under the shallow footing T2C analysed by FLAC with the measured earth pressure against the pile shaft due to the cap effect in the piled footing T2F at the load level $P_c = P_{fc}$ *= 175 kN.*

It is interesting to see that the measured lateral earth pressure against the pile shaft due to the cap effect in the piled footings has a surprising correspondence with the horizontal soil stress under the corresponding shallow footings analysed by the elastic-plastic theory. This fact once again supports the conclusion that the behaviour of the cap in a piled footing is similar to that of a corresponding unpiled footing. This can also be used as a basis for a theoretical estimation of the cap effect on the pile shaft resistance in a piled footing.

Proposed simplified calculation methods

Based on the above conclusion regarding the load-settlement behaviour of a piled footing, simplified methods of predicting the settlement of piled footings in

non-cohesive soil have been proposed in Chapter 8. Thus, the settlement of a piled footing can be approximately estimated as the settlement of a corresponding shallow footing at the same cap load level. The load-settlement behaviour of a shallow footing, in turn, can be analysed according to any method preferred by the reader. Thus, once the load-settlement behaviour of a shallow footing is determined, the behaviour of a corresponding piled footing can be approximately estimated, provided that the load carried by the cap in the piled footing is known. The key factor is to estimate the load carried by the cap P_{fc}, which can be obtained by subtracting the load taken by the piles P_{fp} in the piled footing from the total applied load P_{ft} :

$$P_{fc} = P_{ft} - P_{fp} \tag{2}$$

Based on the result of load tests on single piles, provided that the load efficiency for a free-standing pile group in relation to a single pile η_1 (at the same settlement) is known, the load taken by the piles can be estimated according to the first method as:

$$P_{fp} = n \cdot \eta_1 \cdot P_s \tag{3}$$

where, n = number of piles in the group
P_s = load applied on the single pile at the same settlement

If the load efficiency for piles in a piled footing versus piles in a free-standing pile group η_4 (due to the cap effect) is also known, the P_{fp} value can be estimated according to the second method as:

$$P_{fp} = n \cdot \eta_1 \cdot \eta_4 \cdot P_s \tag{4}$$

Generally, the efficiency η_4 is higher than unity whatever the relative density of the sand, and it increases when the settlement increases. The η_4 value is rarely known in practice due to the lack of experimental evidence. However, it can be estimated by means of the theory of plasticity as shown above.

The proposed simplified methods of settlement analysis, Methods 1 and 2, are exemplified for the piled footings in all three test series using the results of the corresponding tests on single piles and on shallow footings (Chapter 5), as well as the load efficiencies η_1 and η_4 (Chapter 6). The load-settlement behaviour of a piled footing predicted by the proposed simplified methods, is in good agreement with the measurement results, Fig. 7.

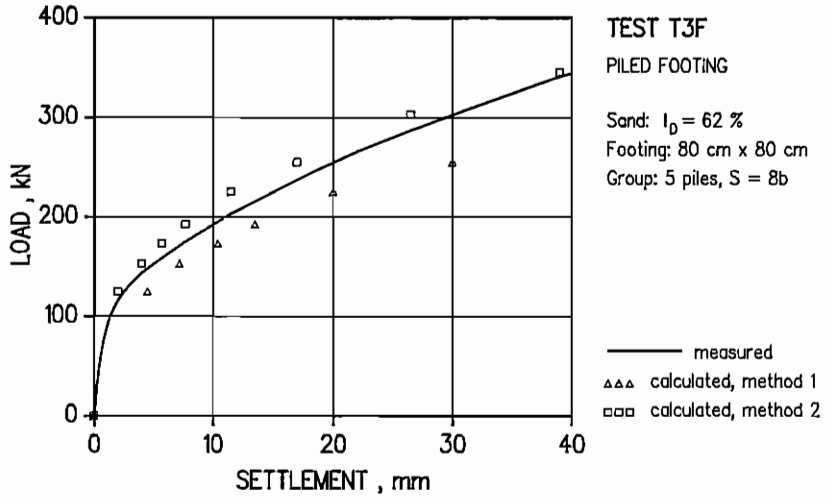

Fig. 7 Comparison between the settlements calculated according to the proposed simplified methods and the measured results - Test series T3.

For the determination of the reduction in settlement of a piled footing, in relation to a corresponding shallow footing, the settlement ratio ξ_7 can also be quickly estimated according to the third simplified method, with the help of the relationship between ξ_7 and the relative cap capacity α, as shown in Fig. 5. In comparison with the test results, the method gives a promising prediction.

NOTATIONS AND SYMBOLS

Roman Letters

a	length of cap/raft
A_j	area of surface load at node j
A_p	cross-sectional area of pile
b	width of cap/raft
b_p	pile width
B	width of shallow footing or piled footing
B_c	nominated width of cap
B_g	width of pile group
c	ratio of pile spacing to pile diameter (S/d)
C	compaction index
C_u	soil uniformity coefficient
d_p *or* d	pile diameter
d_{50}	mean grain diameter of soil
e	void ratio
e_{max}	maximum void ratio
e_{min}	minimum void ratio
E	Young's modulus
E'	Young's modulus for plain strain condition
E_D	dilatometer modulus (DMT)
E_i	initial Young's modulus
E_p	Young's modulus of pile material
E_s	Young's modulus of soil
E_{pr}	pressuremeter modulus (PMT)
E_t	tangent modulus
f_k	dimensionless coefficient
f_s	pile shaft resistance or CPT skin friction
f_{su}	ultimate pile shaft resistance
$f_s(z)$	pile shaft resistance at depth z
F(z)	level of mobilisation of skin friction
F	factor of safety
G_s	shear modulus of soil
G_{sb}	shear modulus of soil at pile base
i, i_k	dimensionless coefficients
I	influence factor
I_d	dilatometer material index (DMT)
I_D	relative density of sand
I_{bb}, I_{bs}	settlement influence factors
k	load transfer level
k_c, k_g, k_f	stiffness of pile cap, pile group and piled footing
k_B	modulus number for bulk modulus
k_E	modulus number for Young's modulus

K	relative pile stiffness
K_B	bulk modulus
K_d	dilatometer horizontal stress index (DMT)
K_o	coefficient of lateral earth pressure at rest
K_s	coefficient of lateral pressure at pile shaft
l_p *or* l	pile length
m	modulus number for constrained modulus
M	constrained tangent modulus
M_{DMT}	dilatometer constrained tangent modulus (DMT)
n	porosity
n	number of piles in a pile group
n_r	number of rows in a pile group
n_B	stress exponent for bulk modulus
n_E	stress exponent for Young's modulus
p	average distributed load from structure
p_0	self-weight of excavated soil
p_1	effective distributed load
$p_{1,k}$	distributed load at load transfer level k
p_o	horizontal pressure at rest (PMT)
p_l	limit pressure (PMT)
p_l^*	net limit pressure (PMT)
p'	mean effective stress
P	concentrated applied load
P_c	load applied on a shallow footing/cap
P_{cf}	failure load of a shallow footing/cap
P_g *or* P_{gr}	total load applied on a free-standing pile group
P_{gf}	failure load of a free-standing pile group
P_{gb}, P_{gs}	base and shaft loads of a pile group
P_{gfb}, P_{gfs}	ultimate base and shaft loads of a pile group
P_{ft}	total load applied on a piled footing
P_{fc}	load carried by cap in a piled footing
P_{fp}	load carried by piles in a piled footing
P_i, P_j	loads applied on piles i and j
P_s	total load applied on a single pile
P_{sf}	failure load of a single pile
P_{sb}, P_{ss}	base and shaft loads of a single pile
P_{sfb}, P_{sfs}	ultimate base and shaft loads of a single pile
$\bar{P}$	average load per pile in group
P(z)	pile axial load at depth z
q *or* q_j	uniform surface load
q_b *or* q_{bj}	pile base pressure
q_c	cone resistance (CPT)
r	radial distance from pile centre
r_0	pile radius

r_c	effective radius of cap element
r_m	influence radius of pile
s	settlement/displacement
s_c	settlement of shallow footing/cap
$s_c(z)$	settlement of soil due to cap-soil contact pressure
s_g *or* s_{gr}	settlement of pile group
s_{ft}	settlement of piled footing, corresponding to total load
s_{fp}	settlement of piled footing, corresponding to load taken by piles
s_s	settlement of single pile
s_p	settlement of pile head
$s_{ps}(z)$	relative displacement between pile and soil
s_{psu}	pile-soil displacement required to mobilise full skin friction
S	pile spacing, centre-to-centre distance
u	pore pressure
w	water content
w	displacement
w_1	displacement of single pile under unit load
w_0 *or* w_{0i}	displacement of pile head
V	volume of cavity (PMT)
V_c	initial volume of measuring cell (PMT)
V_m	mean volume in pressuremeter tests (PMT)
V_t	effective volume of the plotted tube (PMT)
w_s	displacement of pile head due to pile shaft compression
w_{bb}	displacement of pile base due to pile base load
w_{bs}	displacement of pile base due to pile shaft load
w_f	settlement of piled footing
w_{su}	settlement required to mobilise full pile shaft capacity
w_I, w_{II}	settlement components
z	depth
z_k	depth from $z_{LTL,k}$
$z_{LTL,k}$	depth of load transfer level k

Greek Letters

α	relative cap capacity
α	correction factor (CPT)
α_c	increase factor for capacity of cap in piled footing
α_g, α_g'	increase factors for capacity of piles in piled footing
α_{ij}	interaction factor between piles i and j
α_{rij}	interaction factor between pile-cap units i and j
α_b, α_s	base and shaft interaction factors
α_{cp}	cap-pile interaction factor
α_{bbij}	interaction factor of pile base i due to base load j
α_{bsij}	interaction factor of pile base i due to shaft load j

β	stress exponent for constrained modulus
β_c	cap-pile-soil interaction factor for cap capacity
β_b, β_s	cap-pile-soil interaction factors for pile base and shaft capacity
β_{pij}	pile-soil surface interaction factor
β_{sij}	soil surface-pile interaction factor
γ	bulk unit weigh
δ	angle of friction at pile-soil interface
δ_b, δ_s	pile-soil-pile interaction factors for pile base and shaft capacity
$\delta_p(z)$	compression of pile shaft
Δf_s	increase in pile skin friction
Δs	compression of soil layer
Δz	thickness of soil layer
$\Delta\sigma_h'$	increase in horizontal effective pressure
ε_1	vertical strain
ε_v	volumetric strain
η	group efficiency
ζ	parameter in solution for axial pile response
η_b, η_s	base and shaft efficiencies
η_i (i=1-7)	load efficiencies, defined in Table 6.1
θ	pile perimeter
μ'	factor allowing for grain shape and roughness
ν	Poisson's ratio
ν_p	Poisson's ratio of pile material
ξ	settlement ratio
ξ_i (i=1-7)	settlement ratios, defined in Table 6.8
ρ	parameter giving degree of homogeneity of soil
ρ	bulk densisty of soil
ρ_d	dry density of soil
ρ_{DMT}	bulk density of soil, estimated from DMT
ρ_s	specific gravity of soil
σ_v'	vertical effective stress
σ_h'	horizontal effective stress
σ_1	major principal stress
σ_2	intermediate principal stress
σ_3	minor principal stress
σ_r	reference stress = 100 kPa
τ_0	shear stress on pile shaft
ϕ'	effective angle of internal friction
ϕ_{cv}'	effective angle of internal friction at critical relative density (no volume change during shear)
ψ	angle of dilatancy
χ_s	parameter depending on shaft friction distribution along pile
ω	exponent for settlement ratio

Abbreviations

ASCE	American Society of Civil Engineers
ASTM	American Society for Testing and Materials
CIRIA	Construction Industry Research and Information Association
CPT	Cone Penetration Tests
CTH	Chalmers University of Technology
DMT	Dilatometer tests
ECSMFE	European Conference on Soil Mechanics and Foundation Engineering
FHWA	(U.S.) Federal Highway Administration
ICSMFE	International Conference on Soil Mechanics and Foundation Engineering
JGED	Journal of the Geotechnical Engineering Division
JSMFD	Journal of the Soil Mechanics and Foundation Division
NGI	Norwegian Geotechnical Institute
NTH	Norwegian University of Technology
PMT	Pressuremeter tests
Proc.	Proceedings
SGI	Swedish Geotechnical Institute

1. INTRODUCTION

1.1 Footings with Settlement-Reducing Piles

The current design practice for piled footings is based on the assumption that the piles are free-standing, and that all the external load is carried by the piles, with any contribution of the footing being ignored. This approach is illogical, since the footing itself is actually in direct contact with the soil, and thus carries a significant fraction of the load. The philosophy of design is recently undergoing a gradual change. The idea discussed by Burland et al. (1977) of using a few piles to reduce the settlement to the required level (and to improve the state of stress in the raft) is gaining more and more support. The piles are therefore termed "settlement-reducing piles". The design question becomes not "how many piles are needed to carry the weight of the building", but "how many piles are needed to reduce the settlement to an acceptable level"?, (Fleming et al, 1992).

There are a number of reasons why the idea of spread foundation design with settlement-reducing piles has not become widely used. One of the reasons is the lack of reliable calculation methods for predicting the settlement and for estimating the behaviour of such foundations. Moreover, there have been very few experimental studies of the behaviour of piled footings. Most of the tests previously made deal with free-standing pile groups. The effect of the footing (cap) being in contact with the soil on the settlement behaviour of the piled footing, as well as the bearing capacity of the piles, is therefore not well understood.

1.2 Scope of the Study

In the case of piled footings in non-cohesive soil, the settlement is often sufficient to mobilise the full bearing capacity of the piles. In order to study the settlement behaviour of a piled footing, it is thus necessary to understand the behaviour of the piles in the footing close to or at failure. Therefore, although this study mainly deals with the settlement of piled footings, both the settlement and the bearing capacity problems have been investigated. The aim of the investigations has been to establish different practicable *load efficiency* and *settlement ratio* coefficients.

Obviously there is a great need for a better understanding of the load-transfer

mechanism (both between the piles and between the cap and the piles), the interaction between the piles (pile-soil-pile interaction), and especially the interaction between the cap and the piles (cap-soil-pile interaction) in a piled footing in non-cohesive soil.

The experimental part of the study consists of three field test series comprising large-scale model tests in non-cohesive soil. In each test series, four separate tests on a shallow footing, a single pile, a free-standing pile group, and a piled footing were carried out under equal soil condition. Comparisons of the test results in one and the same test series clearly show the behaviour of the elements of a piled footing (the cap and the piles) and the overall behaviour of the piled footing itself. As regards the long-term settlement, the creep behaviour of the shallow footings has been compared with that of the corresponding piled footings. The results of this study can be used as a guideline in the analysis of a piled footing, the existing knowledge of which is quite limited.

Changes in the lateral earth pressure against the pile shaft were measured by means of pressure cells mounted along the pile shaft. The axial pile load distribution along the pile was also studied. The results have been interpreted with special attention to the effect of cap-soil contact pressure.

The change in soil properties due to pile driving and due to cap-soil contact pressure was investigated by sampling, and by different field investigation methods (pressuremeter, dilatometer and static penetrometer tests).

The applicability of existing methods for the prediction of settlement of piled footings has been investigated by comparing measured settlements with calculated values. Simplified methods of predicting settlement of piled footings in non-cohesive soil are suggested, based on the results of the experimental study.

2. LITERATURE SURVEY

2.1 Introduction

In piled foundations, the piles are conventionally designed to carry the total weight of the structure, with an appropriate safety factor against failure. Any contribution exerted by the pile cap in contact with soil is ignored. In many cases, however, the cap or raft has adequate bearing capacity itself. The piles are needed only because the predicted settlement of the foundation is in excess of permissible values. In such cases, piles will have to be included in the foundation to reduce settlement rather than to carry the total load of the structure. The working load will then be shared between the cap and the piles. Only a limited number of piles are used to reduce the settlement to the permissible level. Generally, the permissible settlement is sufficient to mobilise nearly the full bearing capacity of the piles. However, it does not involve any risk since the bearing capacity of the cap will ensure stability of the whole foundation. Studies on footings with settlement-reducing piles should be performed at loads close to failure of the piles, or at a sufficiently large settlement of the footings.

In piled footings in non-cohesive soil, the overall soil-cap-pile group interaction problem is complicated. The overall interaction consists of the pile-soil-pile interaction and the cap-soil-pile interaction. The pile-soil-pile interaction is studied experimentally by comparing a test on a free-standing pile group with that on a single pile under equal soil conditions. The cap-soil-pile interaction should be studied in a similar way by comparing tests on a shallow footing, a free-standing pile group and a piled footing. Unfortunately, most of the tests reported in the literature were performed on free-standing pile groups, and very few tests have been performed on pile groups with the cap resting on the soil surface. The most influential factors on the behaviour of a pile group, or a piled footing in sand are soil properties, pile spacing, and geometry of the group (layout of piles, ratio of pile length and footing width).

The principle problems studied in the literature on free-standing pile groups and piled footings in non-cohesive soil are:

(a) bearing capacity of the groups/footings (group efficiency);
(b) settlement of the groups/footings (settlement ratio); and
(c) load distribution among piles in the group (and/or load share between piles and cap).

The first two problems remain principally the same as those for shallow footings. The third one is necessary for a better understanding of the behaviour of pile groups, as well as for structural design of the cap/raft. In this chapter, the group efficiency and settlement ratio obtained from the previous tests will be surveyed. The existing methods for evaluating the settlement of free-standing pile groups, as well as of piled footings with the cap in contact with soil, will also be reviewed.

2.2 Previous Experimental Studies

The experimental studies previously performed on friction pile groups and piled footings in non-cohesive soil are summarised in Table 2.1 . In the table the tests are listed in chronological order. The main features of the respective investigations were presented in a previous, more complete literature survey (Phung, 1992).

As can be seen in Table 2.1, both free-standing pile groups and piled footings have mainly been studied experimentally by small-scale model tests. Among these small-scale model tests, there are only two studies concerning piled footings, namely those carried out by Kishida and Meyerhof (1965) and Akinmusuru (1980), while the others deal only with free-standing pile groups. In Akinmusuru's tests, the piles were provided with strain gauges at the pile top, which made it possible to study the load sharing between the cap and the piles. In the tests, the behaviour of free-standing pile groups and piled footings were also compared.

Few full-scale test or large-scale model tests have been reported in the literature, see Table 2.1. Most of the large-scale and full-scale tests carried out before 1960-1970 were performed with less advanced instrumentation, e.g. without separate measurement of loads carried by the cap and by the piles. Among the large- and full-scale tests on piled footings, only the tests performed by Vesic (1969), Garg (1979) and Liu et al. (1985) include a comparison between free-standing pile groups and piled footings. Vesic's study has been considered by many researchers as a major reference on pile groups with and without cap resting on the soil. However, in this study, the so-called tests on free-standing pile groups seem to be based on the penetration diagrams obtained during pile installation (pushing down the pile group into soil by hydraulic jack). Comparison of such results with static load test results on piled footings may lead to incorrect conclusions, especially regarding the

contribution exerted by the cap resting on soil. Such a comparison should be based on tests using the same standard testing procedure under equal soil conditions.

Table 2.1 Axially-loaded tests and prototypes on free-standing pile groups and piled footings in non-cohesive soil (after Phung, 1992)

Authors	Year	Full scale	Large scale	Small model	Free-stand pile group	Piled footing	Note
Press	1933	+			+		
Feagin	1948	+				+	(4)
Cambefort	1953		+		+		
Kezdi	1957		+		+		
Fleming	1958			+	+		
Kezdi	1960			+	+		
Stuart et al.	1960			+	+		
Berezantsev et al.	1961	+				+	
Pepper	1961			+	+		
Hanna	1963			+	+		
Kishida & Meyerhof	1965			+	+	+	
Beredugo	1966			+	+		
Kishida	1967	+			+		
Vesic	1969		+		+	+	(1)
Woodward-Clyde	1969	+			+		
Leonards	1972	+				+	(5)
Hartikainen (a,b)	1972			+	+		
Tejchman	1973			+	+		
Trofimenkov	1977	+				+	(4)
Garg	1979	+			+	+	(5)
Akinmusuru	1980			+	+	+	
Ko et al.	1984			+	+		(3)
Liu et al.	1985	+			+	+	(5)
Millan et al.	1987			+	+		(3)
Di Millio et al.	1987	+			+		
Ekström	1989		+		+		(2)

where, (1) laboratory test; (2) field test; (3) centrifugal test; (4) case histories; (5) bored piles

2.2.1 Group efficiency

It is well known that the ultimate load of a group is generally different from the sum of the ultimate loads of individual piles in the group. The *group efficiency*, η, is defined by the ratio:

$$\eta = \frac{P_{gf}}{nP_{sf}} \tag{2.1}$$

where, P_{gf} = ultimate load of a pile group
P_{sf} = ultimate load of a single pile under equal soil conditions
n = number of piles in the group

Similar definitions are used for the ultimate base load and shaft load of a group. *Base efficiency* η_b, and *shaft efficiency* η_s are defined as

$$\eta_b = \frac{P_{gfb}}{nP_{sfb}} \qquad \text{and} \qquad \eta_s = \frac{P_{gfs}}{nP_{sfs}} \tag{2.2}$$

where, P_{gfb}, P_{gfs} = ultimate base and shaft load of a pile group
P_{sfb}, P_{sfs} = ultimate base and shaft load of a single pile

It is noted that the definition given by Eq. (2.1) refers only to free-standing pile groups. The same definition has also been used for piled footings by several authors, such as Kishida & Meyerhof (1965), Vesic (1969), Garg (1979). This, however, is not logical because the contribution of the cap is quite independent of the geometry of the pile group and mainly depends on its size.

2.2.1.1 Free-standing pile groups

The most important factors influencing the group efficiency are soil property, pile spacing and method of pile installation. Different results are obtained for pile groups in loose (to medium dense) sand and for those in dense sand.

Pile groups in loose sand

For free-standing pile groups in loose to medium dense sand it has been fairly well agreed that the total group efficiency η is often greater than unity. The previous test results are reviewed in separate figures for laboratory small-scale model tests on the one hand, Figures 2.1 to 2.3, and for large-scale and

full-scale tests on the other, Fig. 2.4. For the small-scale model tests, the efficiency η reaches a peak value of 2.0 to 2.7 at a pile spacing S, between 2d and 3d (d is the pile diameter). The group efficiency approaches unity at a large enough spacing (6d to 10d). In these figures, S means a centre-to-centre spacing between piles. A spacing of 1d has no physical meaning and cannot be achieved in practice. Test values for a S/d ratio of unity were obtained by carrying out tests on block foundations of the appropriate size, Hanna (1992). For the large- and full-scale tests, a similar tendency can be seen in Fig. 2.4. For driven piles, an efficiency higher than unity can be explained by compaction of soil within the group due to pile driving. Ekström (1989) showed that the larger the pile group (larger number of piles), the larger the compaction effect. For bored piles, however, the group efficiency is very close to unity independent of the pile spacing, Liu et al. (1985).

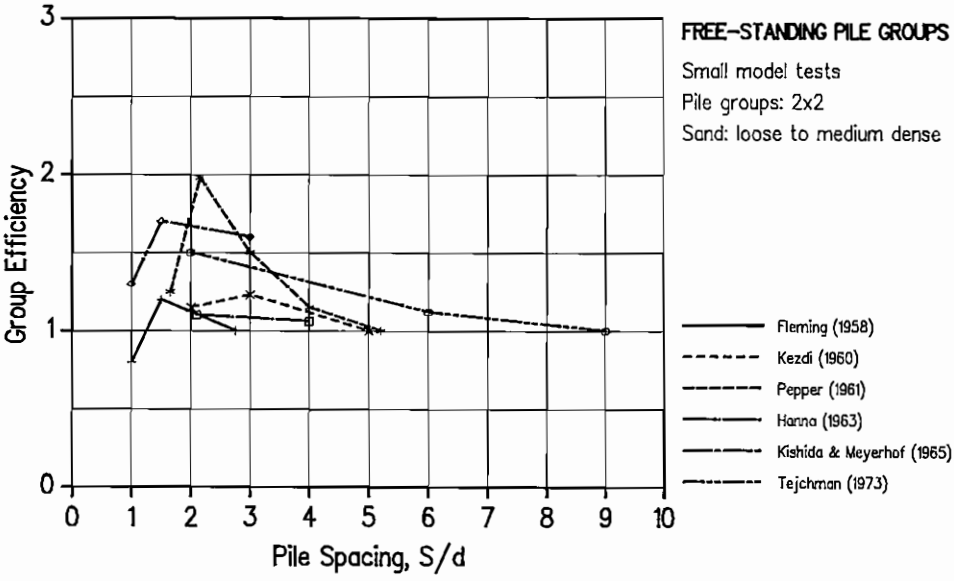

Fig. 2.1 Group efficiency η - Laboratory small model tests on free-standing pile groups in loose to medium dense sand. Groups of 4 piles (2 by 2).

For the base group efficiency η_b, different results have been reported. Most tests show a base group efficiency close to unity. The highest values of the base efficiency $\eta_b \simeq 1.5$ were found for groups of piles driven in very loose sand with a spacing of 2d to 3d (Kezdi, 1957, and Tejchman, 1973). At a large enough spacing (6d to 9d), the base efficiency reduces to unity. For bored piles, the base efficiency η_b seems to be less than unity, Liu et al. (1985), see Fig. 2.5.

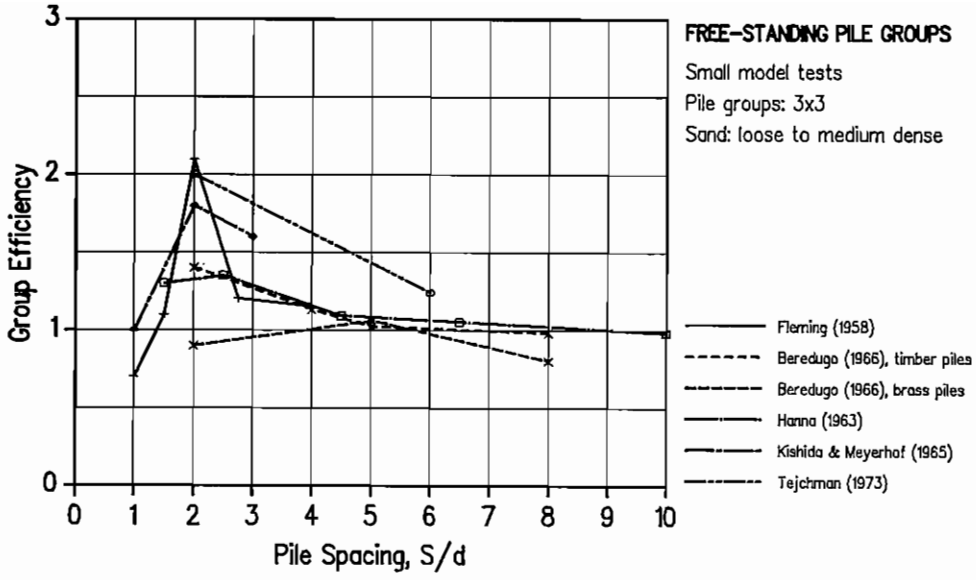

Fig. 2.2 Group efficiency η - Laboratory small model tests on free-standing pile groups in loose to medium dense sand. Groups of 9 piles (3 by 3).

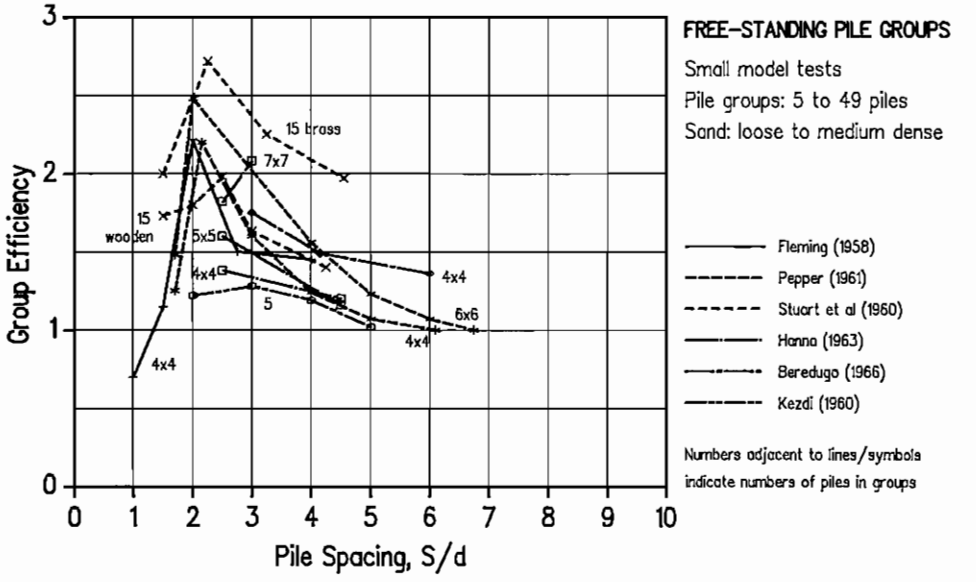

Fig. 2.3 Group efficiency η - Laboratory small model tests on free-standing pile groups in loose to medium dense sand. Other groups (5 to 49 piles).

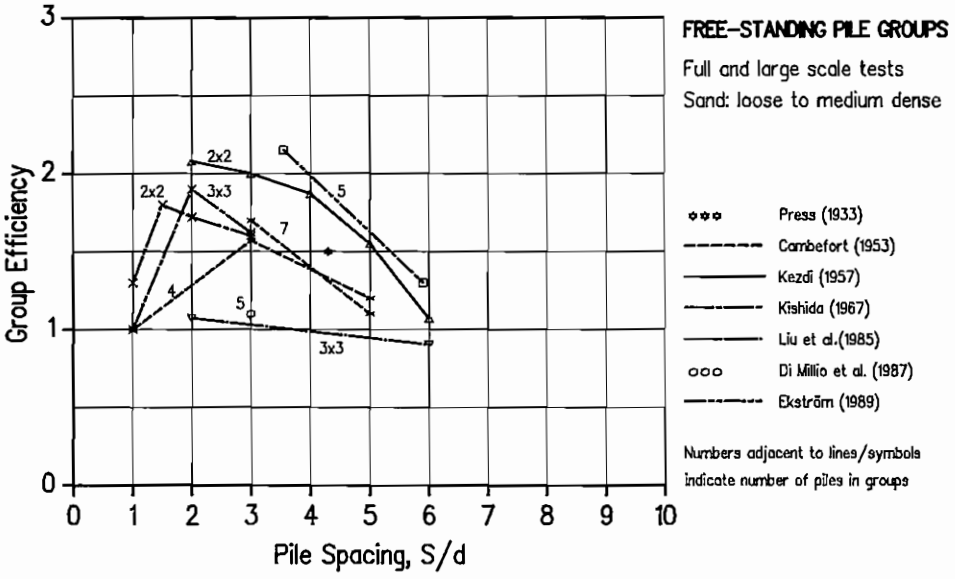

Fig. 2.4 Group efficiency η - Large and full scale tests on free-standing pile groups in loose to medium dense sand.

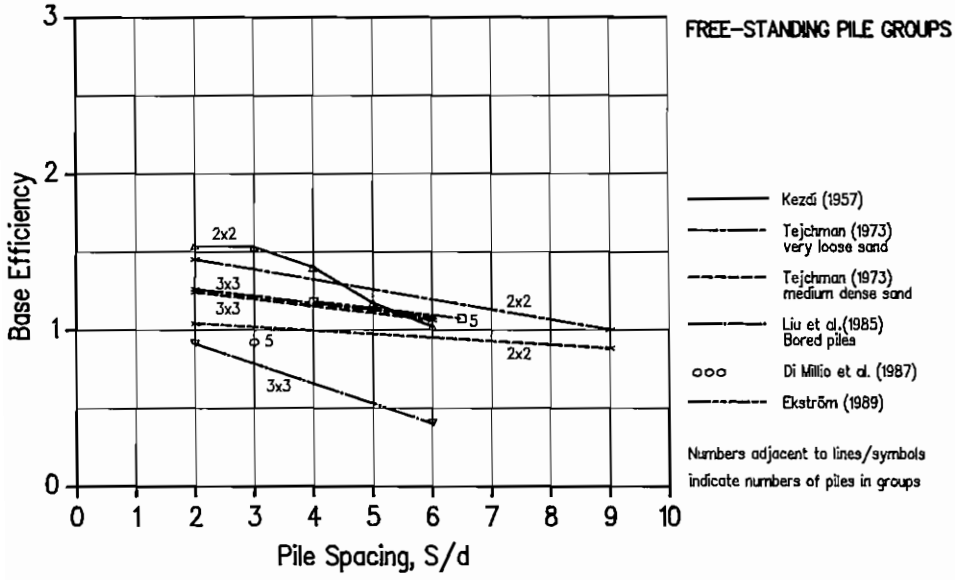

Fig. 2.5 Base Group efficiency η_b - Tests on free-standing pile groups in loose to medium dense sand.

Figure 2.5 shows that the suggestion of a unity base efficiency, Vesic (1969), may be right only for medium dense to dense sand. For pile groups in very loose to loose sand, the soil under the pile base is also compacted by pile driving, which results in a base efficiency higher than unity.

However, it can be established from all the tests that the base efficiency is always lower than the total group efficiency. This also means that the shaft group efficiency is always higher than both the total efficiency and the base efficiency.

Pile groups in dense sand

It has been agreed that the group efficiency of pile groups in very dense sand is lower than unity. An efficiency lower than unity can be explained by the fact that pile driving in dense sand decreases the relative density of soil because of the dilatancy of the sand. The loosened zone along the pile shaft has a width of about 5 times the pile diameter (Kerisel, 1961). Fig. 2.6 summarises the test results on pile groups in dense sand. In the figure, there are some tests that yield group efficiencies higher than unity with a peak value at a spacing of 2d, similar to what was found for pile groups in loose sands (Stuart et al., 1960, Tejchman, 1973).

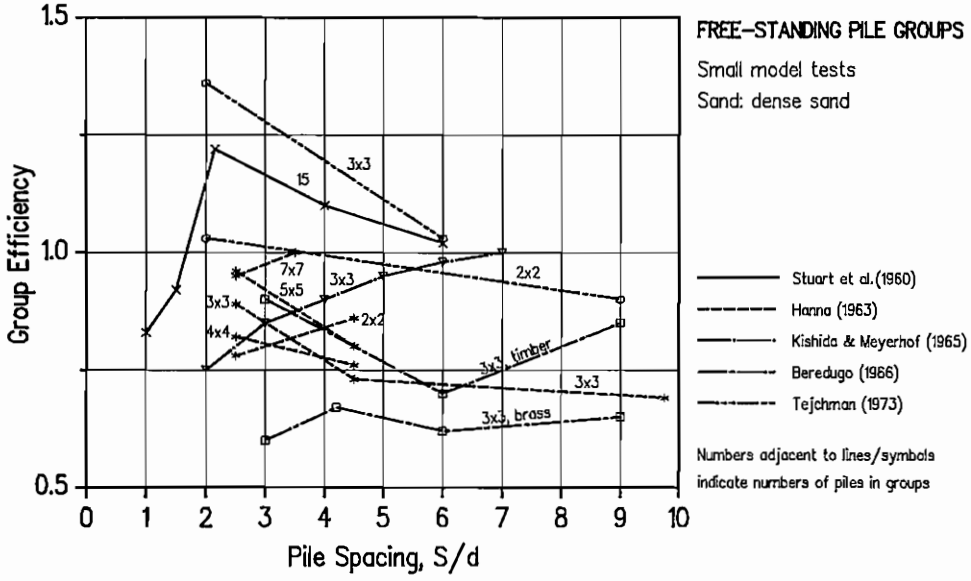

Fig. 2.6 Group efficiency η - Laboratory small model tests on free-standing pile groups in dense sand.

2.2.1.2 Piled footings

A pile cap in contact with the soil surface can contribute significantly to the load capacity of the group. Kishida and Meyerhof (1965) showed that the total bearing capacity of piled footings can be estimated from the bearing capacity of free-standing pile groups by allowing for the influence of the pile cap. This influence consists of the bearing capacity of the pile cap and its surcharge effect on the point resistance of the piles in the group, using the whole pile cap for individual pile failure for groups with a large pile spacing, Fig. 2.7b, or using the outer rim of the pile cap outside the equivalent pier area for pier failure for groups with a small pile spacing, Fig. 2.7a.

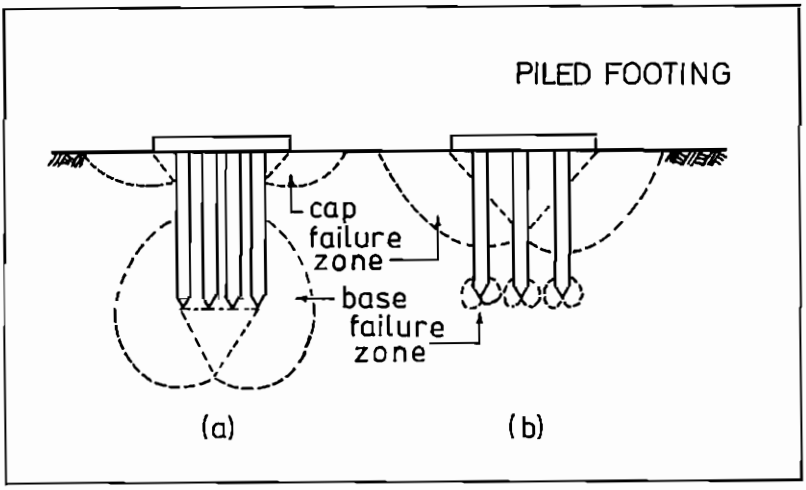

Fig. 2.7 Assumed failure zone at piled footings: (a) pier failure, (b) individual pile failure. (Kishida & Meyerhof, 1965)

Vesic (1969) did not support the concept of blocks or "equivalent piers", no matter how small the pile spacing, because the base load of the group is approximately equal to the sum of point loads of individual piles, and its magnitude is significantly different from the ultimate base load of the equivalent pier. However, he supported the suggestion that the contribution of the pile cap to the bearing capacity of a pile group results from a general shear failure under the outer rim of the cap contact surface, named as effective cap bearing area if the group fails as an equivalent pier. According to this

same suggestion, the cap would contribute by its entire contact surface, just as a shallow foundation of the same size, if the pile spacing is large enough for the piles to fail individually. But he had a remark that even for groups with piles at large spacings, the concept of outer rim support seems to give quite good estimations of cap loads. This remark, however, may be doubtful because his so-called tests on free-standing groups seem to be based on the penetration diagrams. A comparison between piled footings and free-standing pile groups should be based on test results using the same standard test procedure with the same soil conditions.

Garg (1979) performed systematic field tests on bored piled footings in sand. The test results show increasing contributions from the pile cap as the pile spacing is increased. Besides, the extent of the contribution is not a fixed quantity but is dependent on the number of piles and their spacing in the group, as well as on the load and displacement level of the group. The author suggested that the contribution of the pile cap to the load capacity of a pile group should not be defined as a certain percentage of the ultimate load. He also supported the account for the cap contribution in terms of the outer rim of the pile cap.

Akinmusuru (1980) showed that the capacity of a piled footing is not just the algebraic sum of the bearing capacities of the pile group and the cap. In non-cohesive soil, the capacity of a piled footing was found to exceed the sum of those of the pile group and the cap. This is due to the increase in bearing capacities of both the cap and the pile group by mutual interaction:

$$P_{ft} = \alpha_g P_g + \alpha_c P_c \tag{2.3}$$

where, P_{ft}, P_g, P_c = ultimate bearing capacities of piled footing, free-standing pile group, and cap alone, respectively

α_g, α_c = increase factors of bearing capacities of free-standing pile group and cap alone by mutual cap-soil-pile interaction

The test results showed that the contribution of the cap depends on both pile length and cap size. Moreover, it was shown that the change in pile capacity is more sensitive to the effect of the cap-soil-pile interaction than that of the footing, i.e. the α_g value is much higher and more variable than the α_c value, which is then suggested to be unity, Fig. 2.8. In this figure, α_g' means pile load increase factor obtained by assuming α_c=1.

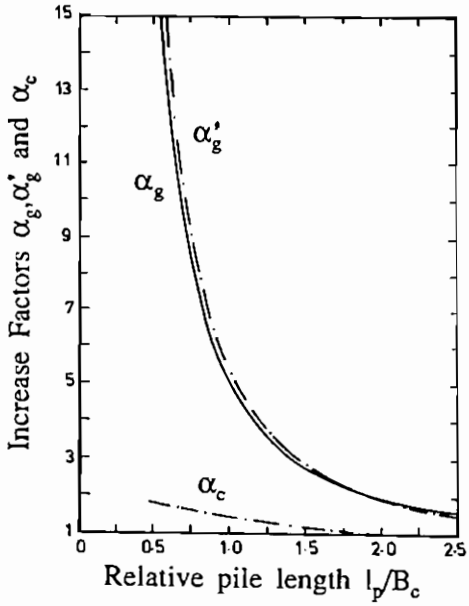

Fig. 2.8 Increase factors of pile and cap capacities due to cap-pile interaction. (Akinmusuru, 1980)

Liu et al. (1985) carried out systematic field tests on bored pile groups. The results showed different effects of cap-pile-soil interaction on both the shaft and the base resistance of the pile groups. The shaft efficiency η_s and the base efficiencies η_b, that are defined similarly to Equations (2.1) and (2.2), can be calculated as follows:

$$\eta_s = \beta_s \, \delta_s$$
$$\eta_b = \beta_b \, \delta_b \qquad (2.4)$$

where, δ_s, δ_b = coefficients considering effects of pile-soil-pile interaction on shaft and base resistances of the pile group, respectively

β_s, β_b = coefficients considering effect of cap-pile-soil interaction on shaft and base resistances of the pile group. (For free standing groups, $\beta_s = \beta_b = 1$ and $\eta_s = \delta_s$, $\eta_b = \delta_b$)

It was suggested that the β_s, β_b, δ_s, δ_b values should to be calculated by empirical formulae, depending on the number of piles in the groups, pile spacing, B_c/l_p ratio, etc., where l_p is the pile length, and B_c the nominated width of cap, $B_c = \sqrt{\text{cap area in plan}}$.

The ultimate bearing capacity of the piled footing is then calculated as the sum

of the capacity of the piles, considering both pile-soil-pile interaction and cap-soil-pile interaction by the factors β_s, β_b, δ_s, δ_b , and the cap capacity:

$$P_{ft} = n\,(\beta_s\,\delta_s\,P_{ss} + \beta_b\,\delta_b\,P_{sb}) + P_c \qquad (2.5)$$

where, n = number of piles in the group
P_{ss}, P_{sb} = shaft and base capacities of reference single pile under equal soil conditions as the pile group
P_c = ultimate capacity of cap alone
β_s, β_b, δ_s, δ_b = see Eq. (2.4)

One of the most important conclusions from their study is that "block failure" does not occur for groups of bored piles in sand.

Discussions and suggestions

Various test results, summarised in Figs. 2.9 and 2.10, show that the group efficiencies of piled footings, in both loose and dense sand, are much higher than unity. This means that the pile cap contributes significantly to the load capacity of the piled footing. This is true not only for driven piles but also for bored piles, although the group efficiency for free-standing bored pile groups is probably less than unity.

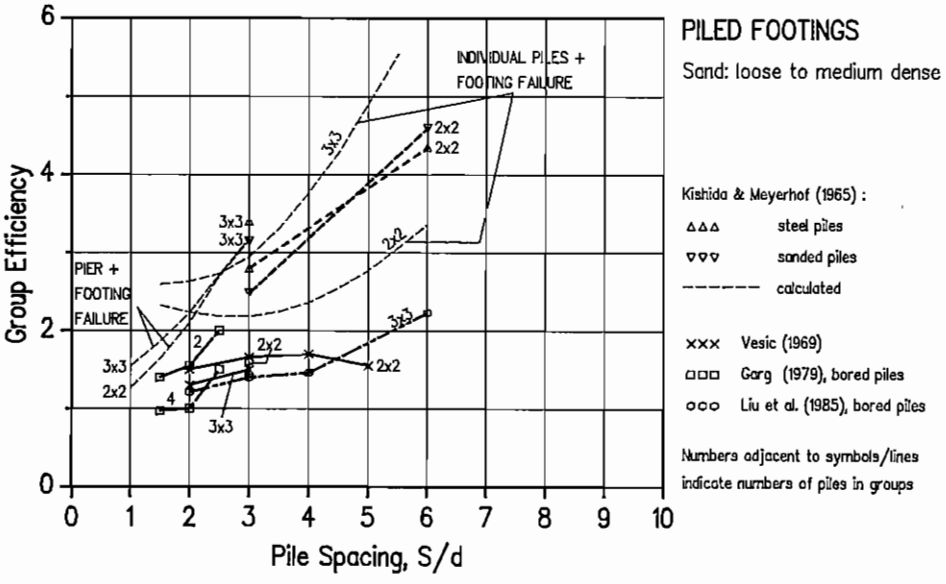

Fig. 2.9 Group efficiency η - Piled footings in loose to medium dense sand.

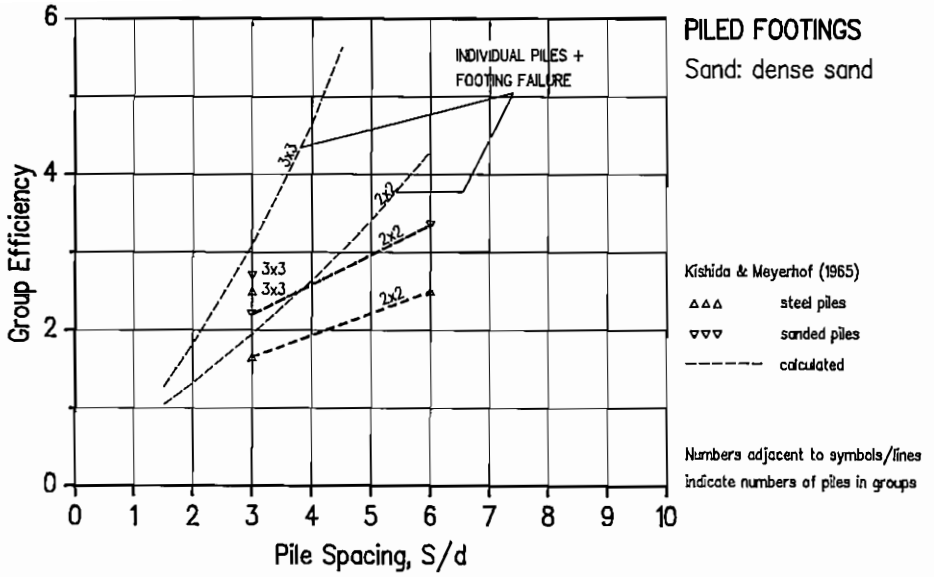

Fig. 2.10 Group efficiency η *- Piled footings in dense sand.*

The group efficiency for piled footings in both loose and dense sand increases with increasing pile spacing. This is partly due to the contribution of a larger cap (footing) to the capacity of a piled footing. The group efficiency also depends on the ratio of pile length to cap width l_p/B_c, the ratio of pile length to pile diameter l_p/d_p, and the number of piles in groups. Berezantsev et al. (1961) showed that the capacity of piled footings is strongly dependent on the ratio of group width to pile diameter.

In a general case, the total capacity of a piled footing may be calculated as

$$P_{ft} = n\,(\beta_s\,\delta_s\,P_{ss} + \beta_b\,\delta_b\,P_{sb}) + \beta_c\,P_c \qquad (2.6)$$

where, n = number of piles in the group,

δ_s, δ_b = influence factor of pile-soil-pile interaction on the pile shaft and pile base capacities,

β_s, β_b, β_c = influence factor of cap-pile interaction on the pile shaft and pile base capacities, and on the capacity of the cap,

P_{ss}, P_{sb} = shaft and base capacities of the reference single pile under equal soil conditions as the pile group,

P_c = capacity of the shallow footing (cap alone).

The cap capacity, P_c, in the case of pile groups with large pile spacing may be estimated as for a shallow footing, or in the case of pile groups with small pile spacing by using the concept of the outer rim capacity of the cap.

The influence of cap-pile-soil interaction on the capacity of the pile group is more significant than on the cap capacity, i.e. β_s and β_b are more important than β_c. For long enough piles, e.g. $l_p > (1.5 \text{ to } 2)B_c$, the surcharge effect on base resistance is negligible, i.e. β_b is equal to unity. The factor β_s is therefore most important in the cap-pile-soil interaction problem.

To get a better understanding of the behaviour of piled footings, load tests should be carried out on single piles, free-standing pile groups, piled footings, and on unpiled footings (cap alone), using the same standard testing procedure under equal soil conditions. To the knowledge of the writer, there has been only one study performed in this way so far , namely that by Akinmusuru (1980). However, in this study the tests were carried out on a laboratory scale and were not so well instrumented. Moreover, in laboratory small-scale model tests, it is almost impossible to simulate the pile installation effect, e.g. driving effect, which has an important influence on pile-soil-pile interaction. For the above reasons, large- or full-scale tests provided with advanced instrumentations are strongly needed.

To compare the load capacity of single piles, free-standing pile groups, piled footings, and unpiled shallow footings, it will be useful to define new *load efficiencies*, which are based on equal settlement. The displacement criterion is consistent with the concept of allowable settlement for structures.

2.2.2 Settlement Ratio

The settlement of a pile group as compared with that of a single pile under equal soil condition can be analysed in a way similar to the analysis of group efficiency. Different definitions of the settlement ratio, ξ, have been proposed, such as:

1) Ratio of the average settlement of a pile group $\bar{s}_{gr}$ to that of a reference single pile s_s under equal soil conditions, at a certain fraction of the failure load:

$$\xi = \frac{\bar{s}_{gr} \text{ (at } P_g = P_{gf}/F)}{s_s \text{ (at } P_s = P_{sf}/F)} \qquad (2.7)$$

where P_g, P_s = certain working load of the pile group and of the single pile
P_{gf},P_{sf} = failure loads of the pile group and of the single pile
F = certain factor of safety

2) Ratio of the average settlement of the pile group to that of the single pile at the same load per pile

$$\xi = \frac{\bar{s}_g}{s_s} \qquad (2.8)$$

where, $\bar{s}_g$ = average settlement of the pile group
s_s = settlement of the single pile at the same average load per pile as the group which can be a certain fraction of the failure load of the single pile

3) Ratio of the slopes of the load-settlement curves P-s of the pile group to that of the single pile

$$\xi = \frac{\text{slope of } \bar{P}\text{-s curve of the pile group}}{\text{slope of P-s curve of the single pile}} \qquad (2.9)$$

where, $\bar{P}$ = average load per pile in the group

The first definition was used by Whitaker (1957), Stuart et al. (1960) etc., but the second definition is more useful and more common. It seems, however, to be easier to determine the settlement ratio using Eq. (2.9) in many cases. Leonards (1972) suggested the calculation of such a ratio both for the initial slopes of the settlement-load curves, when shaft friction dominates, and for the final slopes, when substantial load is carried by pile point resistance. These are named "friction" and "bearing" settlement ratios, respectively. It is noted that the "friction" settlement ratio is very similar to the second definition for every load level in the initial linear part of the P-s diagram of a single pile, while the "bearing" settlement ratio is similar to the first definition for loads near ultimate loads with a safety factor near unity.

The settlement ratio depends on the pile failure criterion chosen. There are a number of methods that may yield different values of the failure load for one and the same test. Another factor which has a considerable influence on the

settlement ratio is the safety factor chosen. In the literature, safety factors of 1.5, 2.0 and 3.0 are often used. In addition to soil characteristics, pile spacing, number of piles in the group, group geometry, method of construction, the variation in choice of definition of settlement ratio, failure criterion and safety factor in the literature makes the review of the settlement ratios obtained from the previous studies very complicated.

2.2.2.1 Free-standing pile groups

There is a great disagreement among different researchers regarding the values of the settlement ratio for pile groups in sand. Many studies yield settlement ratios higher than unity while others show values lower than unity. This disagreement can be clearly seen in Fig. 2.11. Hanna (1963), Tejchman (1973) and Di Millio et al. (1987) indicate ξ values higher than unity, while Kezdi (1957) and Ekström (1989) show ξ values lower than unity for free standing pile groups in loose and medium dense sand. It should be noticed that the two tests made by Di Millio et al., and by Ekström, which both represent very well-instrumented full-scale or large-scale field tests, show opposite results on the settlement ratio. In dense sand, however, all the tests in the literature indicate ξ values higher than unity, see Fig. 2.12.

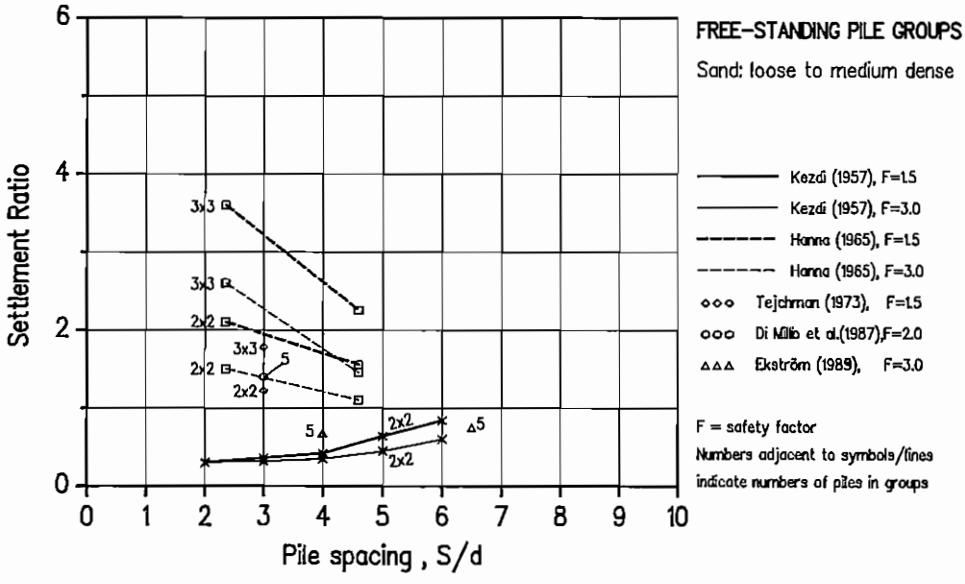

Fig. 2.11 Settlement ratio versus pile spacing - Free-standing pile group in loose to medium dense sand

No clear dependence of the settlement ratio on pile spacing can be seen for pile groups in loose to medium dense sand, Fig. 2.11. For groups in dense sand, however, the settlement ratio seems to decrease as the pile spacing increases, see Fig. 2.12.

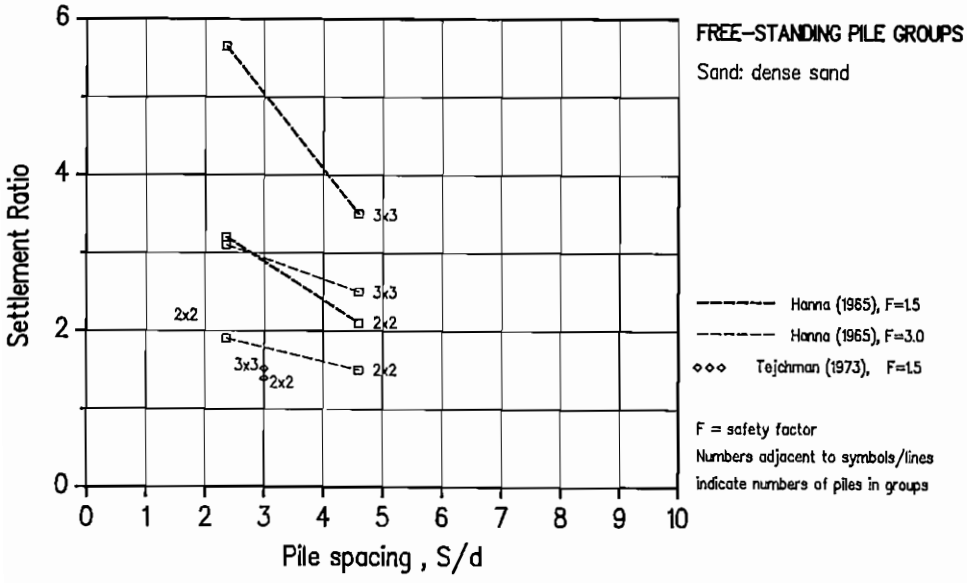

Fig. 2.12 Settlement ratio versus pile spacing - Free-standing pile group in dense sand

The settlement ratio is probably more dependent on the relative width of the group, defined as the B_g/d ratio, in which B_g is the centre-to-centre distance between the outer piles in the group, and d is the pile diameter. In Figures 2.13 and 2.14, the settlement ratios obtained in the literature are compared with those calculated according to Eq. (2.10), suggested by Vesic (1969) for piled footings. The figures show the ξ values much higher and lower than those calculated by Eq. (2.10). However, all the tests show that settlement ratios increase with increasing relative width of the group B_g/d, both in loose and dense sands. This also means that settlement increases with increasing width of a pile group. In Figures 2.11 to 2.14, the settlement ratio is calculated according to the second definition, Eq. (2.8)

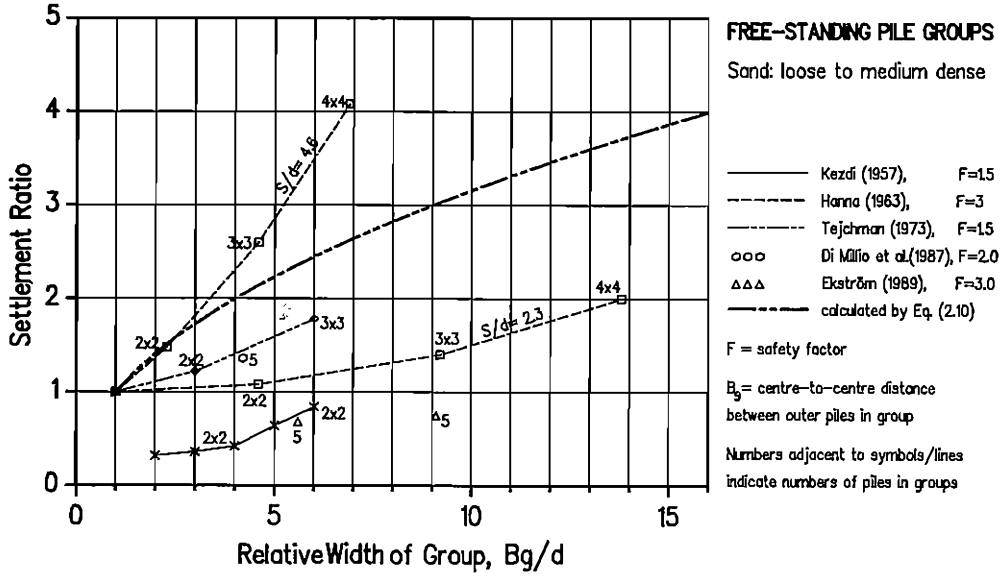

Fig. 2.13 Settlement ratio versus relative width of group B_g/d - Free-standing pile group in loose to medium dense sand

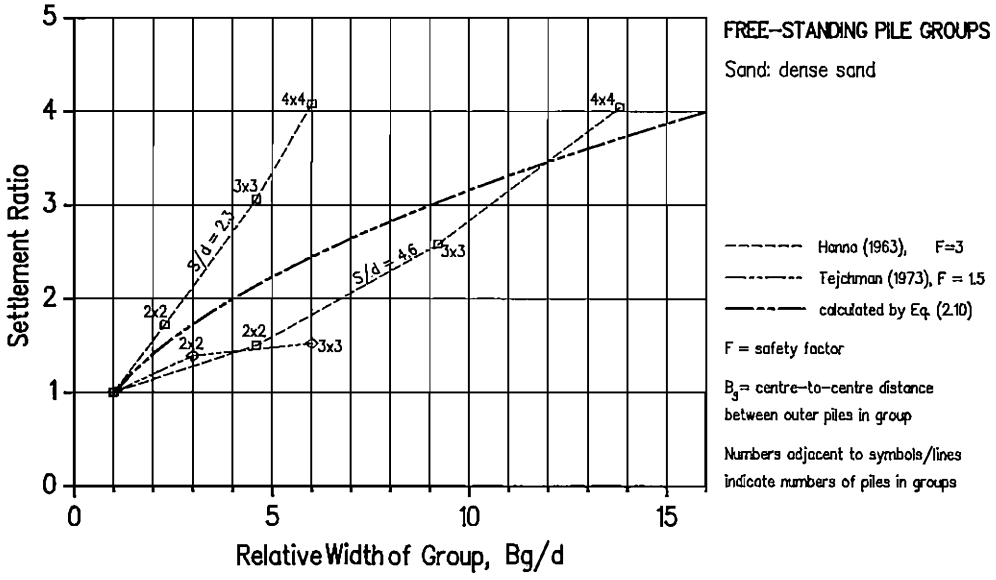

Fig. 2.14 Settlement ratio versus relative width of group B_g/d - Free-standing pile group in dense sand

A reasonable evaluation of the settlement ratio should also include the relative depth of the group, defined as the ratio of the pile length, l_p, to the group width (or pile spacing S). Unfortunately, such a study has not been available so far. O'Neill and Heydinger (1982) tried to establish the dependence of the settlement ratio on the l_p/S ratio from the previous field tests, but the data were insufficient, Fig. 2.15.

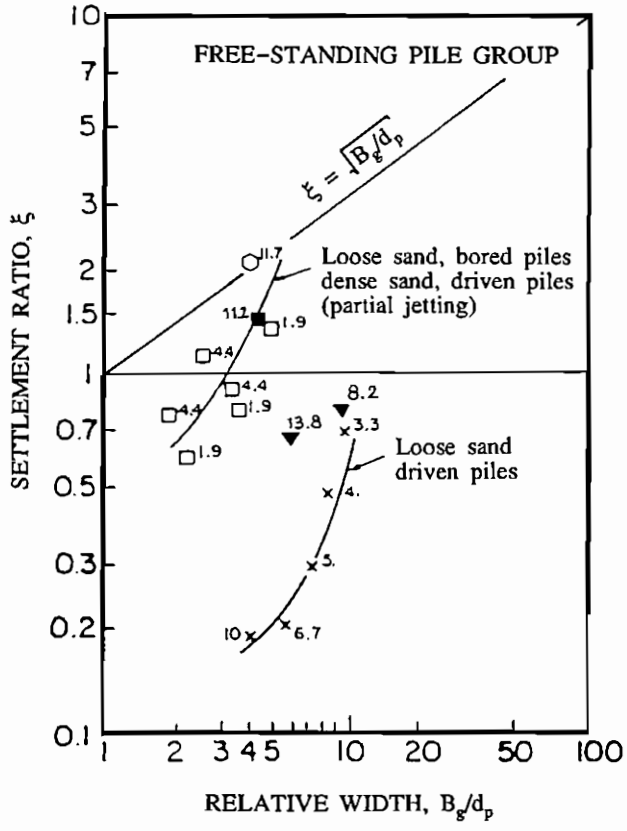

LEGEND

- □ Garg (1979), bored piles
- O Woodward-Clyde (1969), (partial jetting)
- × Kezdi (1957)
- ▼ Ekström (1989)
- ■ Di Millio et al. (1987)

B_g = group width,
Numbers adjacent to symbols indicate ratio l_p/S,
Settlement ratios are determined according to Eq. (2.8), at 50% of failure load of single pile

Fig. 2.15 Settlement ratio versus relative width of group B_g/d - Large and full scale tests on free-standing pile group in sand. (Modified from O'Neill and Heydinger, 1982).

2.2.2.2 Piled footings

Like free-standing pile groups, the test results show settlement ratios both higher and lower than unity for piled footings, see Figures. 2.16 to 2.18.

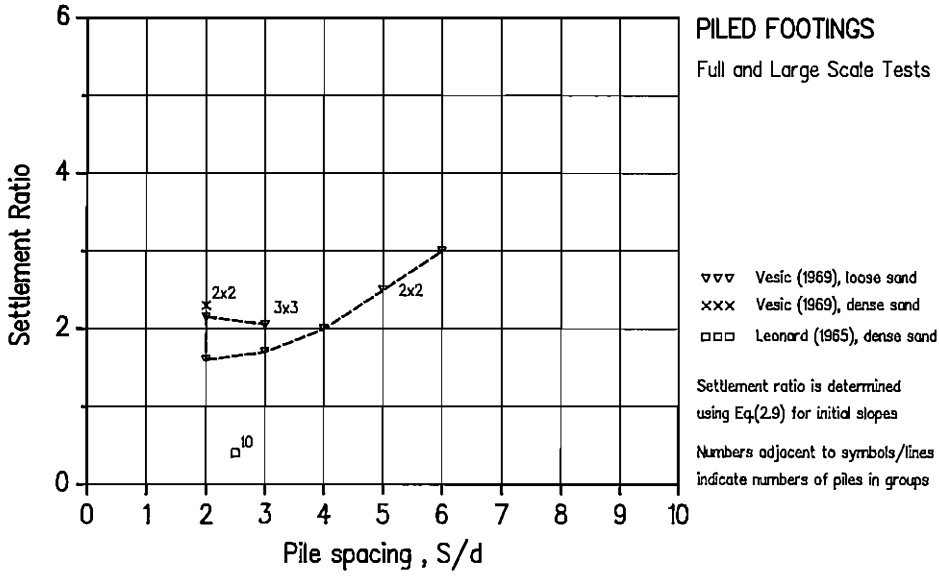

Fig. 2.16 Settlement ratio versus pile spacing - Large and full scale tests on piled footings in sand

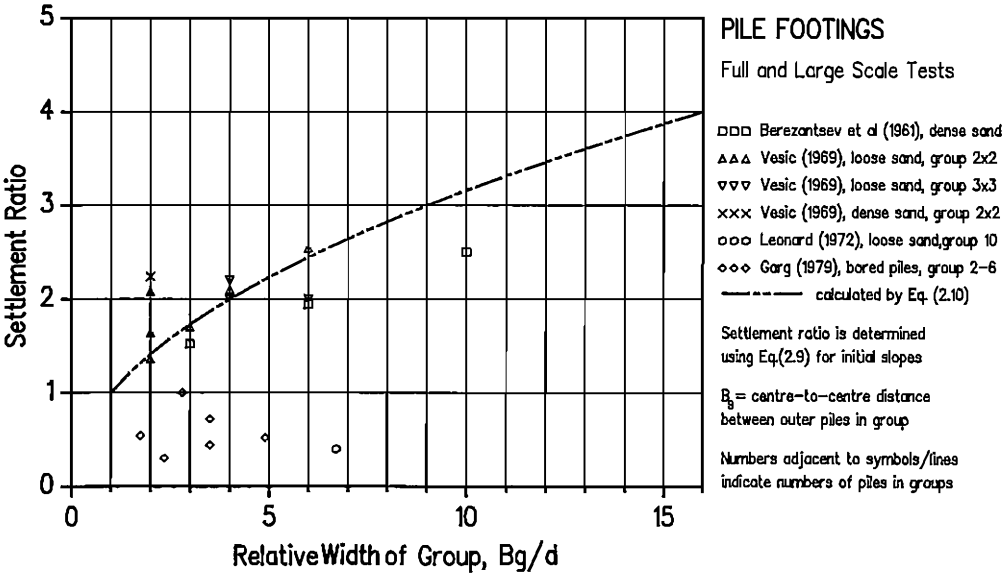

Fig. 2.17 Settlement ratio versus relative width of group B_g/d - Large and full scale tests on piled footings in sand

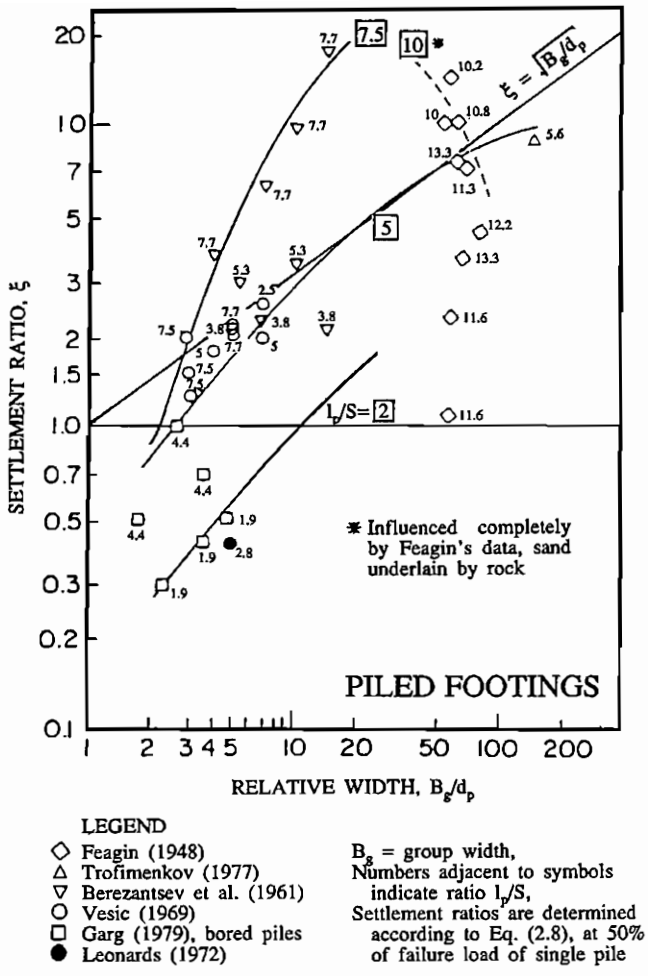

Fig. 2.18 Settlement ratio versus relative width of group B_g/d - Large and full scale tests on piled footings in sand. (Modified from O'Neill and Heydinger, 1982).

The test results obtained by Vesic (1969) show that the settlement ratio increases as the pile spacing increases, which is in agreement with the results reported by Meyerhof (1959). Leonards (1972), however, by restudying the results obtained by Berezantsev et al. (1961), drew an opposite conclusion.

Berezantsev et al. (1961) showed that the settlement of piled foundations is proportional to the square root of the load transference area in the plane of

the pile base. The load transference area is determined by drawing a surface inclined towards the outer face of the pile group at an angle of 0° to 7° depending on the type and density of the soil. This also means that the settlement of piled foundations depends mainly on the width of the foundations, and that both pile spacing and number of piles are less important.

Vesic (1969) collected the available data and suggested that the general trend of the relationship between the relative width of piled foundations B_g/d, and the settlement ratio can be expressed as

$$\xi = \sqrt{B_g/d} \qquad (2.10)$$

where, B_g = centre-to-centre distance between the outer piles in the group
d = pile diameter

Fig. 2.17 shows the settlement ratio obtained from full- and large-scale tests in comparison with Eq. (2.10). Restudying the results obtained by Berezantsev et al. (1961), Leonards (1972) also indicated that the slope ratio varies linearly with the relative foundation width. Moreover, the "bearing" ratio is lower and increases less rapidly with the relative width than the "friction" ratio.

No clear dependence of the settlement ratio on the relative depth can be seen, but the settlement ratio of piled footings tends to increase when the ratio l_p/S increases, see Fig. 2.18.

2.2.2.3 Discussions

There is no agreement so far on the value of the settlement ratio for pile groups in sand, neither in the case of free-standing pile groups, nor the case of piled footings. From the literature it can be noticed that the settlement ratio may be higher or lower than unity. A ratio lower than unity seems reasonable for small pile groups. It can be explained by compaction of soil within the group due to pile driving. For a large pile group, however, when the relative width of the group is large enough, a settlement ratio higher than unity seems probable. It is due to the fact that the stress increase in the soil induced by large pile groups is higher than in the case of single piles at the same load per pile due to superposition of stresses. Another reason is that compaction due to pile driving has less effect on the soil underneath the base

of the group. The ratio must be much higher than unity when the underlying soil is compressible.

There are contrary opinions on the relationship between settlement ratio and pile spacing. It seems, however, as if pile spacing is not as important for the settlement ratio as for the group efficiency. The settlement ratio is more dependent on the relative width of the group than on pile spacing. A definite relationship between the group width and the settlement ratio has not yet been agreed upon. Eq. (2.10) suggested by Vesic (1969) seems not to be so reasonable, though it is supported by some other researchers. However, it can obviously be seen that the settlement ratio increases with increasing width of pile group. The settlement ratio tends also to increase when the relative depth of the group increases. However, the existing data are not sufficient as yet. A reasonable evaluation of the settlement ratio of pile groups or piled footings in non-cohesive soil should include the relative width and relative depth of the groups, as well as the relative density of soil.

A survey of the literature on the settlement ratio should be based on the same definition of the settlement ratio, using the same fraction of failure load, i.e. the same safety factor. The definitions of the settlement ratio according to Equations (2.8) and (2.9) seem preferable. Besides, the same failure criterion should also be used. Briaud et al. (1985) showed that different criteria may yield a difference (in failure loads obtained) of over 100%, which emphasizes the importance of using the same failure criterion. Further studies should be performed to make possible a comparison of the settlement ratios of free-standing groups with those of piled footings.

The use of piled footings with a minimum number of piles to reduce settlement of the footings has recently become more and more common. A new concept of settlement ratio between the settlement of a piled footing and that of a shallow footing may also be practical. To avoid a confusing choice of failure criterion, which becomes more complicated when the shallow footings are also involved, settlements of the two footings should be compared at a chosen load level.

2.3 Methods of Calculating Settlement of Pile Groups and Piled Footings

The mechanism of load transfer in a piled footing involves a highly complex overall interaction between piles, pile cap and surrounding soil. The interaction is influenced by the stress-strain-time and failure characteristics of all elements in the system. The soil may be changed considerably due to pile installation. The load-deformation of the piled footing is affected by a lot of factors such as soil properties, group geometry, pile installation and interaction between different elements (piles and cap) in the footing. Due to the uncertainties or difficulties in defining such factors, there is no available analysis method capable of including them all. In this section available methods, currently used for predicting settlement of pile groups and piled footings, will be reviewed.

2.3.1 Simplified methods

Settlement ratio methods

Different empirical methods have been suggested for calculating the settlement ratio, defined as the ratio of the settlement of a pile group to that of a single pile carrying the same average load as a pile in the group. Most of the empirical methods were developed on the basis of full-scale or model test results and consider only the geometry of pile groups, but do not take the soil properties into account. These methods should be used with caution and only in those cases where the condition is similar to the tests on which the correlations are based.

Skempton (1953) proposed the following formula to calculate the settlement ratio

$$\xi = \frac{(13.1\ B_g + 9)^2}{(3.28\ B_g + 12)^2} \qquad (2.11)$$

where, B_g = width of pile group, in metres

Meyerhof (1959) suggested that the pile spacing should be accounted for and proposed the following formula for square pile groups

$$\xi = \frac{c\ (5 - c/3)}{(1 + 1/n_r)^2} \qquad (2.12)$$

where, c = ratio of pile spacing to pile diameter = S/d
n_r = number of rows in the pile group

Vesic (1969) suggested Eq. (2.10), as already presented in Section 2.2.2, for calculating the settlement ratio of piled footings:

$$\xi = \sqrt{B_g/d_p}$$

Randolph developed theoretically a useful approximation for the settlement ratio, see Fleming et al. (1992):

$$\xi = n^{\omega} \tag{2.13}$$

where, n = number of piles in the group
ω = exponent, generally lying between 0.2 and 0.6 for most groups

For floating pile groups, Poulos (1989) has derived solutions which suggest the practical values of ω: 0.33 for piles in sand, and 0.5 for piles in clay.

Equivalent raft method

The settlement of a friction pile foundation is still usually calculated according to the earliest proposed method given by Terzaghi (1943), which suggested that the building loads are imposed at a level corresponding to the lower third point of the piles, Fig. 2.19. The additional stresses in soil due to the building load can then be determined by the theory of Bousinesq, or by the "2:1-method". The method, however, does not take into consideration the number of piles, the stiffness of the piles, or the ratio between applied load and ultimate load, all being factors of great importance. The method is suitable for hand calculations, and a lot of case records show that with a well-chosen η-factor, satisfactory results are obtained, e.g. Bjerrum et al. (1957).

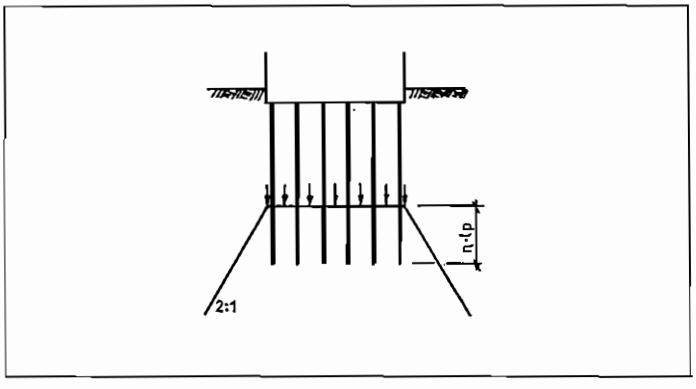

Fig. 2.19 Equivalent raft method for calculating settlement of friction pile group.

Modified equivalent raft method

A modification of the equivalent raft method was suggested by Thaher and Jessberger (1990a, b) in which the load applied is assumed to be transferred to the soil at several levels instead of only one level, as in the equivalent raft method. The determination of soil stress spread and distribution is a fundamental step for a proper estimation of settlements. The authors suggested that depending on the configuration of the foundation system, the effective load $p_l=p-p_0$ (where p is the average pressure from the structure, and p_0 presents the self-weight of the excavated soil) is transferred to the soil by the raft/cap in the form of contact pressure, and by the piles in the form of shaft and tip resistances. The effective load is transferred to the subsoil at several levels which are indicated as load transfer levels LTL, see Fig. 2.20. The load portion $p_{l,k}$ (area load) assigned to the load transfer level k (k =1 to n) at the depth $z_{LTL,k}$ can be estimated with reference to the expected distribution of the contact pressure and the pile load along piles, according to recommendations based on centrifuge modelling. The effective soil stress σ_v' is given by:

$$\sigma_v' = i \cdot p_l \tag{2.14}$$

where, i = dimensionless coefficient, $i = \sum_{k=1}^{n} i_k$

i_k = single coefficient corresponding to the load portion $p_{l,k}$, given by

$$i_k = \frac{f_k}{2\pi}\left[\arctan\frac{ab}{z_k\sqrt{(a^2+b^2+z_k^2)}} + \frac{abz_k}{\sqrt{(a^2+b^2+z_k^2)}}\left(\frac{1}{a^2+z_k^2}+\frac{1}{b^2+z_k^2}\right)\right]$$

$f_k = p_{l,k}/p_l$

a,b = length and width of the cap/raft

z_k = depth from the load transfer level k, see Fig. 2.20

This formula is a modification of the formula by Steinbrenner (1934), see Thaher and Jessberger (1990). After having estimated the distribution of the induced effective stress over depth, the compression Δs of the soil layer in question can be evaluated by common methods, e.g. with the help of the stress-settlement curve or compression modulus M: $\Delta s = \sigma_v' \Delta z/M$, where Δz is the thickness of the soil layer in question, and σ_v' is the mean vertical effective stress induced by the external load in the soil layer. As usual, the total settlement s at any point is obtained as the sum of compression of the regarded soil layers underneath this point: $s = \Sigma \Delta s$

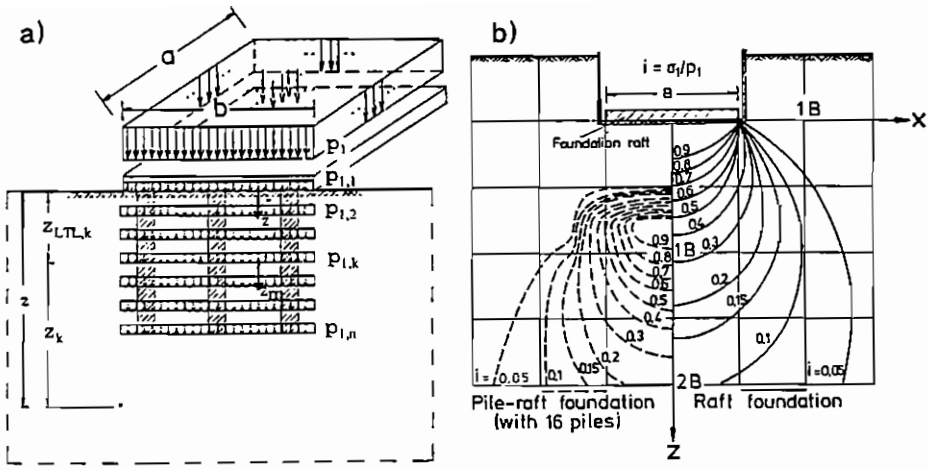

Fig. 2.20 Modified equivalent raft method for calculating settlement of a friction pile group. (a) Calculation scheme and notations, (b) Distribution of the induced effective soil stress. (Thaher and Jessberger, 1990)

2.3.2 Advanced methods

Theoretical methods for the analysis of settlement of pile groups and piled footings can be divided into different groups: (1) the continuum method, (2) the hybrid approach, (3) the approximate analytical method, and (4) the finite element method.

Boundary Element Method

The problem of pile groups with the cap being in contact with the soil surface was solved by Butterfield and Banerjee (1971) by means of the Boundary Element Method (BEM), also known as the integral equation method, using Mindlin's solution for a point load in the interior of a semi-infinite elastic homogeneous mass. Since this particular point force solution automatically satisfies the stress-free boundary conditions on the surface of the half space, only the cap-soil and the pile-soil interfaces have to be discretised. This method is a complete continuum method and is one of the most rigorous solutions so far for analysing pile groups and piled footings, but it needs considerable computing time. Fig. 2.21 shows the settlement ratio calculated using this method for different pile groups with and without the cap in direct contact with the soil surface. This figure indicates that the increase in stiffness of the piled

footings due to the cap is small (typically below 15%) for most common configurations of pile groups, although significant load may be carried by the cap (up to 36 + 50% of the total load). As discussed later, this conclusion is not correct for piled footings in sand, due to the inadequacy of the theory of elasticity in this case.

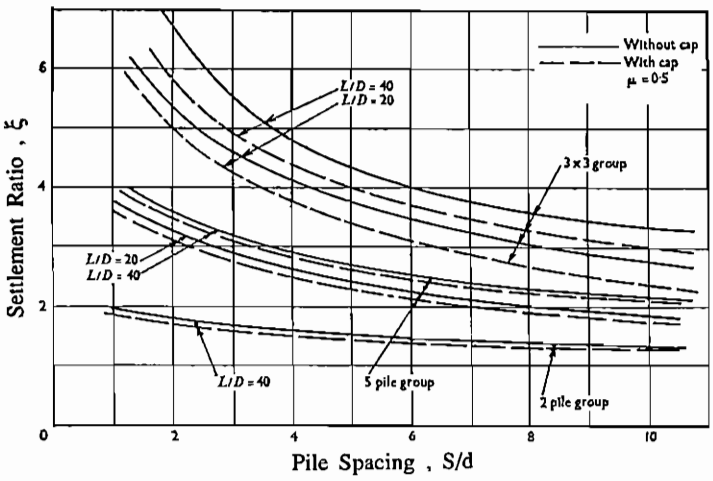

Fig. 2.21 Settlement ratio obtained by using the boundary element method - Comparison between free-standing pile groups and pile footings. (Butterfield and Banerjee, 1971)

Interaction factor method

This method, suggested by Poulos (1968), is based on the linear theory of elasticity. For free-standing pile groups, the basic unit to be considered is a single pile. The interaction factor between two individual piles is used and the displacement of one pile due to loading of other piles can be estimated by superposition. For pile groups with constant pile spacing and equal pile geometry, the displacement w_i of pile i can thus be calculated as:

$$w_i = w_1 \sum_{j=1}^{n} (\alpha_{ij} P_j) \qquad (2.15)$$

where, w_1 = displacement of the single pile under unit load
P_i, P_j = loads in pile i and j
α_{ij} = interaction factor between pile i and pile j, $\alpha_{ii}=1$
n = number of piles in the group

The interaction factor α_{ij}, which governs the additional settlement of the pile in question due to the loading of other piles, is defined as

$$\alpha_{ij} = \frac{\text{additional settlement of pile i due to unit load at pile j}}{\text{settlement of pile i under unit load}} \qquad (2.16)$$

The interaction factor α_{ij} is determined by integration of Mindlin's solution for a point load in the interior of a homogeneous elastic half-space. The interaction factor α_{ij} depends on pile spacing (S/d_p), relative pile stiffness ($K=4E_pA_p/E_s\pi d_p^2$), pile slenderness (l_p/d_p), and non-homogeneity of soil (Poulos and Davis, 1980). The factor decreases with increasing pile spacing. The interaction factor α_{ij} for two floating piles in a homogeneous semi-infinite mass ($\nu = 0.5$) is shown as a function of dimensionless pile spacing S/d in Fig. 2.22a for a value of $l_p/d_p = 25$ and various values of K.

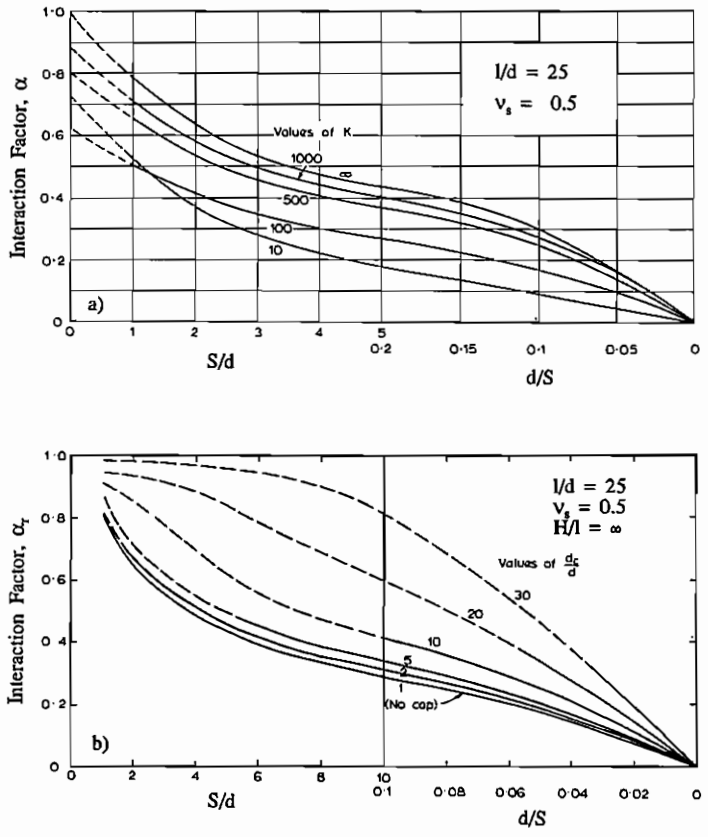

Fig. 2.22 Interaction factors: (a) for free-standing piles α_{ij}, (b) for pile-cap units α_{rij}. (Poulos and Davis, 1980)

For piled footings, the analysis is similar to that employed for free-standing pile groups, except that the basic unit to be considered is a single pile with an attached circular cap resting on the soil surface. The interaction of two pile-cap units can be expressed in term of an interaction factor α_r, defined as:

$$\alpha_{rij} = \frac{\text{additional settlement of unit i caused by unit load at j}}{\text{settlement of single unit i under unit load}} \qquad (2.17)$$

The settlement of a typical unit *i* can then be calculated similarly to Eq. (2.15), using the factor α_{rij} instead of the factor α_{ij}. The interaction factor α_{rij} for two identical pile-cap units in a homogeneous semi-infinite mass (ν = 0.5) is shown as a function of dimensionless pile spacing S/d in Fig. 2.22b, for a value of l_p/d_p= 25 and various values of d_c/d_p, in which d_c is the diameter of the cap unit. In all cases, the piles are incompressible (K = ∞) and the pile cap is rigid.

Hain and Lee's method

Another rigorous method is presented by Hain and Lee (1978). In the analysis, four independent modes of interaction are used: pile to pile, pile to surface, surface to pile, and surface to surface interactions, Fig. 2.23. For the pile to pile interaction, the interaction factors given by Poulos are used. The other interaction factors are derived from the theory of elasticity and are defined as follows:

$$\beta_{pij} = \frac{\text{additional settlement of pile i due to unit surface load j}}{\text{settlement of pile i due to unit load}} \qquad (2.18a)$$

$$\beta_{sij} = \frac{\text{additional settlement of surface i due to unit pile load j}}{\text{settlement of surface i due to unit load}} \qquad (2.18b)$$

where, β_{pij} = pile-soil surface interaction factor
β_{sij} = soil surface-pile interaction factor

The finite element subdivision of the raft contains m nodal points, in which the piles are located at n of these points. At the remaining m-n nodes, where the raft is directly in contact with the soil, a uniform pressure is assumed to act over a rectangular area surrounding a particular node. The vertical displacement w_i of pile node i, for example, is then given by:

$$w_i = w_1 \sum_{j=1}^{n} (\alpha_{ij} P_j) + w_1 \sum_{j=n+1}^{m} (\beta_{pij} q_j A_j) \qquad (2.19)$$

where, w_1 = displacement of the single pile under unit load
P_j = pile load at node j
α_{ij} = interaction factor between pile i and pile j
β_{pij} = interaction factor for pile i due to surface load at j
q_j, A_j = uniform pressure, and area of surface at node j

The overall stiffness matrix is established first, and the displacement of the soil surface is resolved. The raft is then analysed by means of the finite element method by setting the displacement of the raft equal to the above-solved soil surface displacement. The iteration necessary to satisfy all the given equations requires considerable computation time. By means of a "load cut-off" procedure, a maximum capacity of individual piles can be simulated.

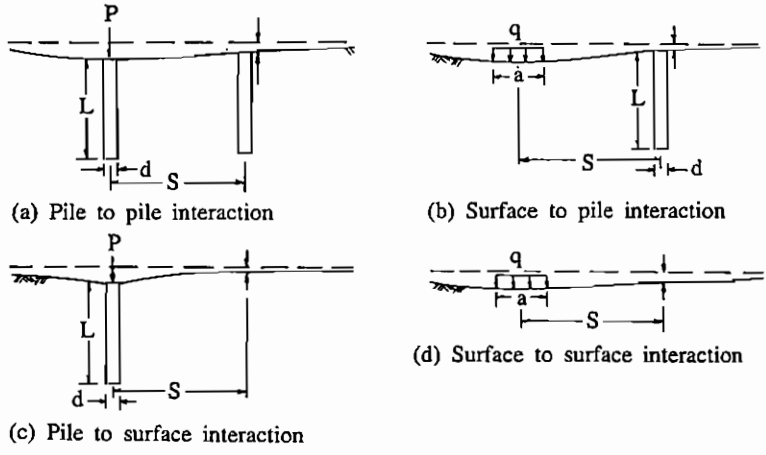

Fig. 2.23 Pile and surface interactions. (After Hain and Lee,1978)

Randolph and Wroth's method

Randolph and Wroth (1979) have introduced an approximate analytical model for computation of the vertical deformation of pile groups using the interaction factors. The method is based on the superposition of the displacement fields of individual piles within the group. The soil may be homogeneous, or its stiffness may increase linearly with depth. However, the method is confined to the assumption of linear elastic soil behaviour. Theoretical interaction factors are deduced from the form of deformation field around a single pile , treating the pile shaft separately from the pile base. Under axial load, the deformation field around the pile shaft varies approximately logarithmically with radius r,

according to:

$$w = \frac{\tau_0 r_0}{G} \ln(r_m/r) \tag{2.20}$$

where, τ_0 = shear stress on the pile shaft
r_0 = pile radius
r_m = radius of influence of the pile
G = shear modulus of soil

Empirically, the radius of pile influence r_m has been found to be of the order of the pile length, and can be estimated as: $r_m = 2.5\rho l_p(1-\nu)$; where l_p is the pile length, ν is Poisson's ratio of soil, and ρ is the degree of homogeneity of soil, varying between 0.5 for soil with stiffness proportional to depth and 1.0 for homogeneous soil (Randolph and Wroth, 1978). Thus, denoting $\zeta = \ln(r_m/r_0)$, the shaft interaction factor α_s for a pile at a distance r from the pile in question will be:

$$\alpha_s = \frac{\ln(r_m/r)}{\zeta} = 1 - \frac{\ln(r/r_0)}{\zeta} \tag{2.21}$$

At the level of the pile base, the deformation field due to the pile base load may be approximated by:

$$w = w_b \frac{2 r_b}{\pi r} \tag{2.22}$$

giving rise to a base interaction factor α_b, for a pile at a distance r, as:

$$\alpha_b = \frac{2}{\pi} \frac{r_b}{r} \tag{2.23}$$

where the subscript "b" refers to the pile base, and the deflection of the pile base is obtained from the standard solution (Timoshenko and Goodier, 1970) as $w_b = P_{sb}(1-\nu)/(4r_b G_{sb})$, where P_{sb} is pile base load, and G_{sb} is the shear modulus of soil at the pile base . The settlement ratio is then calculated according to Eq. (2.13), $\xi = n^{\omega}$, in which n is the number of piles in the group, and ω is the exponent, depending on pile slenderness, pile stiffness, pile spacing, soil homogeneity, and Poisson's ratio of soil, see Fleming et al. (1992).

A simplified approach for analysing piled footings by combining the separate stiffness of the cap and of the pile group has been suggested by Randolph (1983). The approach is based on the use of the average interaction factor α_{cp} between the piles and the cap. Writing the pile cap stiffness as k_c, and the

pile group stiffness as k_g, (the term stiffness refers to the total load divided by the settlement), the overall stiffness k_f of the footing is obtained from:

$$k_f = \frac{k_g + k_c(1 - 2\alpha_{cp})}{1 - \alpha_{cp}^2 k_c/k_g} \tag{2.24}$$

while the proportion of load carried by the cap P_c and by the pile group P_g is given by:

$$\frac{P_c}{P_c + P_g} = \frac{k_c(1 - \alpha_{cp})}{k_g + k_c(1 - 2\alpha_{cp})} \tag{2.25}$$

The stiffness of the pile cap and the pile group may be evaluated conventionally, while the interaction factor α_{cp} may be obtained from the following approximate expression, Randolph (1983):

$$\alpha_{cp} = \frac{\ln(r_m/r_c)}{\ln(r_m/r_0)} = 1 - \frac{\ln(r_c/r_0)}{\zeta} \tag{2.26}$$

where, r_c = effective radius of the cap element associated with each pile

The r_c value may be calculated so that, for a group of n piles, $n\pi r_c^2$ equals the total actual area of the pile cap A_c, or $r_c = \sqrt{(A_c/n\pi)}$. Fig. 2.24a shows how the stiffness of a single pile under axial load is increased by the presence of a pile cap in contact with the ground. In this figure, the ratio k_g/k_f gives the ratio of stiffnesses of the single pile without to that with the cap in contact with the soil surface. The results from this approximate method are compared with those from Poulos and Davis (1980) and show a good agreement. Similarly to the conclusions obtained by Butterfield and Banerjee (1971), the results show that due to the cap the increase in stiffness of the piled footings is small, although a significant portion of the overall load may be carried by the cap, Fig. 2.24b.

The settlement of the piled footing w_f is then calculated as:

$$w_f = w_I + w_{II} \tag{2.27}$$

where, w_I = settlement of the cap, taking the load as the total applied load minus that carried by the piles

w_{II} = additional settlement due to load carried by the piles

The settlement w_{II} may be estimated as: $w_{II} = \alpha_{cp} \cdot \xi \cdot w_{su}$ where w_{su} is the settlement at which a single pile mobilises its full shaft capacity, ξ is the settlement ratio, and α_{cp} is the interaction factor as given by Eq. (2.26).

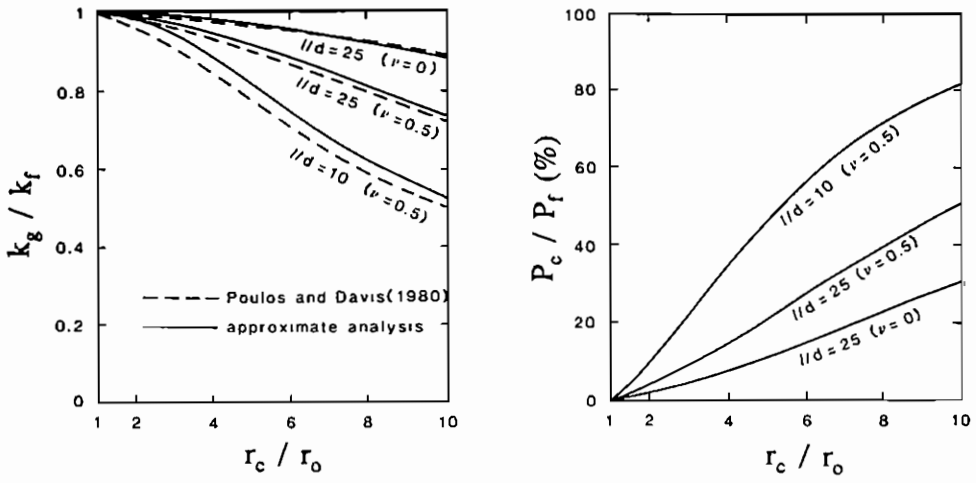

Fig. 2.24 Calculation according to Raldolph and Wroth method: (a) Effect of pile cap on single pile stiffness, (b) Portion of load carried by pile cap (Fleming et al, 1992)

Hybrid method

The problem of load transfer from the pile shaft and the pile point into the soil is very complex.The *load transfer method*, originally suggested by Coyle and Reese (1966), has served as a basis for different approaches to determining the load transfer curve for a single pile. In these approaches, a non-linear second-order differential equation, relating displacement along the pile shaft to a transfer function, can be set up and solved using an iterative finite-difference scheme. The results will then be heavily dependent on the transfer function selected, which can be obtained either experimentally or according to formulae suggested. The solution technique employed contained a hidden assumption that the pile settlement at any point is not affected by shaft loads at other points along the pile. This arises from the fact that the soil along the shaft is replaced by a set of non-linear springs, acting locally and totally independent of its neighbours. The load-transfer curves thus describe the relationship between mobilized shaft friction and pile displacement, and in the offshore industry they are commonly called "t-z" curves. Also, since the transfer function does not account for pile-soil-pile interaction, it can be directly applied for prediction of the settlement of pile groups. However, a *hybrid method* has been proposed in which transfer functions are partly used in the analysis of pile group settlement (O'Neill et al. 1977). Accordingly, each individual pile in the group is modelled by the use of

non-linear unit load transfer curves and the interaction among piles is presented by means of the elastic half-space deformation theory. Briefly, the method is as follows: (1) Determine the response of individual piles within the group, ignoring interaction effects; (2) Using soil reactions obtained from Step 1, compute additional soil displacements at the nodes of other piles in the group using Mindlin's solution. Interaction effects between nodes in the same pile are ignored; (3) The load-transfer curves for the individual pile nodes are adjusted using the additional soil displacements to account for the group effects. With the modified load-transfer curves, Steps 1-3 are repeated, and the solution proceeds in an iterative manner. The main limitation of the method is that true pile-soil-pile interaction is not directly considered, and that the convergence of the iteration has not generally been demonstrated. O'Neill and Ha (1982) compared the "hybrid" algorithm with Poulos's method (e.g. Poulos and Davis, 1980) and found that the two methods are in close correspondence. However, appropriate elastic constants had to be developed separately for each method, with the hybrid method requiring much larger Young's modulus for the soil because that modulus is not used in the near-field computations.

Chow (1986a) proposed an even simpler approach than the above-mentioned concept employing what he termed the "average Mindlin approach", which involved the computation of a mean correction term for pile stiffness due to group action in axially loaded groups. The governing differential equation is solved using the finite element approach to yield the stiffness matrices for the pile and the soil, in which the pile is modelled by two-node line elements, and the soil is presented by discrete vertical springs which are attached to the pile nodes. Extension to non-homogeneous soil is made by using the mean of soil shear modulus at node i (where the displacement is evaluated), and node j (where the unit load is applied) in the Mindlin's solution. Extension to non-linear soil behaviour is performed by assuming that at high soil strains at the pile-soil interfaces, slippage occurs only in a narrow zone of soil adjacent to the pile shaft, whereas the soil between the piles is subjected to relative low strain levels, and hence remains essentially elastic. Thus, the use of Mindlin's solution to determine the interaction effects is only approximate.

Polo and Clemente's method

The method was proposed by Polo (1982), Polo and Clemente (1988) using the concept suggested by Vesic (1977), in which the settlement w_0 of a single pile is split into three components: (1) settlement due to axial deformation of the pile shaft

w_s caused by the axial load along the pile; (2) settlement of the pile base w_{bs} induced by the load transmitted along the pile shaft; and (3) settlement of the pile base w_{bb} due to the load transmitted at the pile base:

$$w_0 = w_s + w_{bs} + w_{bb} \tag{2.28}$$

$$w_s = (P_{sb} + \chi_s P_{ss}) \frac{l_p}{E_p A_p}, \quad w_{bb} = \frac{q_b d_p}{E_s} I_{bb}, \quad w_{bs} = \frac{f_s d_p}{E_s} I_{bs} \tag{2.29}$$

where, P_{sb}, P_{ss} = pile base and pile shaft loads
q_b, f_s = pile base pressure and average pile shaft friction
l_p, d_p = pile length and pile diameter
E_p, E_s = Young's moduli of pile material and of soil
A_p = cross-sectional area of pile
I_{bb}, I_{bs} = settlement influence factors
χ_s = parameter depending on distribution of shaft friction along pile

Typical values of χ_s are: 0.5 for uniform or parabolic distribution; 0.67 and 0.33 for triangular distribution increasing and decreasing with depth. The settlements of pile groups are then obtained by using the interaction factors α_{bbij} and α_{bsij}, which correspond to increases in the settlement at the base of pile i due to the shaft load and base load of pile j, respectively. The settlement influence factors I_{bb}, I_{bs}, and the interaction factors α_{bbij}, α_{bsij} were obtained from FEM computations for a homogeneous linear elastic half-space with distributed loads along the surface of a hollow cylinder inserted in the soil. Assuming a uniform (average) shaft friction f_s for every pile, the settlement w_{0i} of pile i can be given as

$$w_{0i} = \frac{l_p}{E_p} q_{bi} + \frac{I_{bb} d_p}{E_s} \sum_{j=1}^{n} (\alpha_{bbij}\, q_{bj}) + \frac{2 l_p^2}{E_p} f_s + \frac{I_{bs} d_p}{E_s} f_s \sum_{j=1}^{n} \alpha_{bsij} \tag{2.30}$$

In the case of a group of n identical piles held together by a rigid cap, the procedure yields a set of equations with the following unknowns: the settlement of the group w_0, the average pile shaft friction f_s, and the base pressure for each pile q_{bi} (i=1 to n).

In the elastic methods, a constant ratio of the pile shaft load to the pile base load is assumed throughout loading of individual piles in the group. In the above-mentioned method (Polo and Clemente, 1988), the assumption is made that the pile base load does not develop before the ultimate shaft load is reached. However, field measurements indicate that the shaft load P_{ss} usually increases very rapidly and non-linearly with the total applied load P_s, reaching the ultimate value P_{sfs},

while the base load P_{sb} develops simultaneously at a much lower rate, which increases significantly as P_{ss} approaches P_{sfs}. Clemente (1990) suggested a new method, in which variable shaft-load to base-load ratios are used during loading.

Finite Element Method

The finite element method (FEM) has been used to study axially loaded single piles, for instance by Ellison et al. (1971), Desai (1974), Ottaviani (1975), Trochanis et al. (1991a), etc. Compared with the other methods, the FEM has superiority in modelling the soil as a non-linear and/or inhomogeneous body. The method is also capable of simulating the effects of pile installation, e.g. soil compaction and residual stresses in piles due to pile driving. The method is often used to check or establish the other analytical models. Poulos and Davis (1980) have compared results from elastic solutions with the FEM. Randolph and Wroth (1978) used the FEM to check the applicability of their simplified analytical approach. With the help of the FEM, Trochanis et al. (1991b) suggested a simplified model for the analysis of one or two piles. Despite its advantages, the FEM is rarely used for practical purposes because it is time consuming and expensive in three-dimensional analyses. The FEM is often used as an effective tool for parameter studies.

The FEM have also been used for analysing pile groups and piled footings. The use, however, is more complex than for single piles because of a lack of axial symmetry. Three approaches have been used:

a) Full three-dimensional analysis, Ottaviani (1975);
b) Idealisation of the group as an equivalent two-dimensional plane strain model, Desai et al. (1974);
c) Idealisation of the group as an equivalent axisymmetrical model, Hooper (1973), Pressley and Poulos (1986).

The first approach a) involves the least amount of simplification required. It is, however, also the most expensive one to run and the most complex one to set up. Ottaviani (1975) has used this approach to study the linear elastic behaviour of pile groups with 9 piles (3 by 3) and 15 piles (3 by 5) with and without the cap being in contact with the soil surface. He concluded that the cap being in contact with soil does not only transmit a portion of load directly to the soil, it also modifies considerably the load transfer mechanism from the piles to the soil. The cap-soil contact pressure greatly reduces the shear stresses in the soil around the upper part of the piles, and at the same time increases the vertical stress in

the soil under the base of the piles. The shear stresses around the piles are not constant with depth and are very high just above the pile base. Furthermore, the shear stresses are very low in the soil within the group.

The two simplified approaches b) and c) each have some limitations. For both research and design of pile groups, the equivalent axisymmetrical model, approach c), has been used. Hooper (1973) used an axisymmetrical mesh to analyse a piled raft foundation. In the real structure, the piles are arranged approximately in concentric rings; in the finite element mesh these become equivalent annuli. The cross-sectional area of the annuli is greater than that of the piles, and a reduction in the modulus of elasticity of the concrete was made to compensate. The method used was to stimulate each concentric row of piles by a continuous annulus with an overall stiffness (i.e. displacement per unit force) equal to the sum of the stiffnesses of the individual piles. Pressley and Poulos (1986) modelled a square 3x3 pile free-standing group in a similar way, see Fig. 2.25. Sharnouby and Novak (1985) suggested that a square or rectangular group can be replaced by an equivalent axisymmetrical group, in which displacements and forces of all piles in one ring are equal, or by an equivalent cyclically symmetrical circular group. The equivalent pile group gives almost the same group stiffness. The effect of varying the position of the outer boundary was investigated. It was concluded that there was little effect (less than 2%) in increasing the radius of the outer boundary from four to eight times the diameter of the outer annulus representing the pile group, Pressley and Poulos (1986).

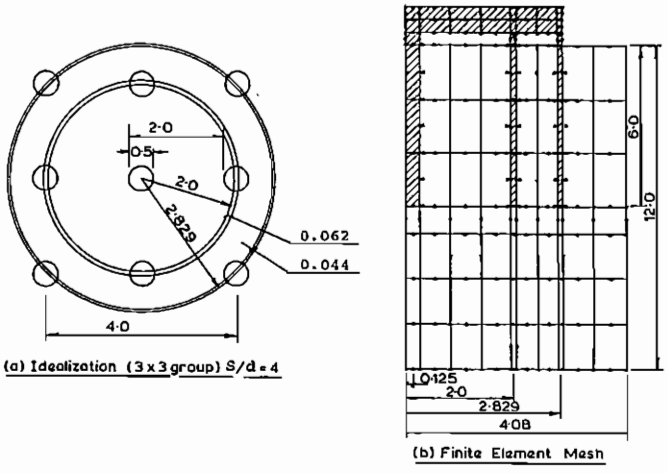

Fig. 2.25 Modelling of square pile group by equivalent axisymmetrical group. (After Pressley and Poulos, 1986)

2.3.3 Computer programs

The complexity of the problem of pile groups/piled footings has necessitated the use of computer-based methods of analysis. A lot of computer programs have been developed for the analysis of pile groups and piled footings. In Table 2.2 a number of available programs are reviewed. The computer programs based on finite element analysis are excluded from this table.

Table 2.2 Selection of computer programs for analysing free-standing pile groups and piled footings.

Program name	Author	Year	Pile group	Piled footing	Remarks	Type
PGROUP	Banerjee et al.	1978	+	+	boundary element method (BEM) complete linear elastic analysis	1
DEFPIG4	Poulos	1986	+	+	nonlinear continuum analysis using interaction factors	1
-	Hain & Lee	1978		+	continuum-based analysis using 4 interaction factors between pile and surface	1
PRAFT	Tomono et al.	1987	+	+	modified Hain & Lee's method	1
SSI J&W	Svensson	1991		+	continuum analysis, considering soil-structure interaction	1
GAFIX	Hewitt	1988	+		nonlinear continuum analysis complete solution	1
PGRAFT	Kuwabara	1991	+	+	boundary element method (BEM) complete linear elastic analysis	1
PILG3	Lazaridis & O'Neill	1989	+		hybrid, non-linear soil reponse, linear pile-soil-pile interaction	2
SPLICE	Clausen et al.	1984	+		hybrid approach, analysing structure-pile-soil interaction	2
P12-2	Chow	1986a	+		continuum-based non-linear hybrid analysis	2
PIGLET	Randolph	1980	+		simplified continuum analysis using interaction factors	3
PGVARIAB	Clemente	1990b	+		simplified analytical method	3
GROUP	Lieng & Svanö	1985	+		no pile-soil-pile interaction	5
PAUL	Jendeby et al.	1987	+	+	calculating settlement with known pile and cap loads	5
TPR	Fatemi-Ardakani	1988		+	thick plate on an elastic medium piles replaced by springs	5
UNIPILE	Fellenius et al.	1990	+		equivalent raft at neutral plane	5

Note: Type of program: 1= integral equation method; 2= hybrid approach; 3= approximate analytical method; 5= other method.

Programs PGROUP, DEFPIG4, P12-2, PIGLET, PGVARIAB were written on the basis of the algorithms presented in Section 2.3.2, with some extensions or improvements. Program P12-1 was contributed by Chow (1986a), and presented in Smith et al. (1988). The main features of the other programs are described bellow.

Program PRAFT, written by Tomono et al. (1987), is a method of estimating load distribution between piles and raft, raft settlement and secondary stress in the raft due to differential settlement which are necessary for the design of a piled raft foundation. The method takes into account the interaction between the raft, piles and soil by combining the finite element analysis and the pile settlement analysis based on Mindlin's first solution of elasticity.

Program SSI J&W was developed at Jacobson & Widmark AB, Sweden for analysing piled rafts on overconsolidated soft clay. In the program, the vertical stress increase in the soil due to the raft-soil contact pressure is calculated according to Boussinesq's solution. The stress increase induced by the piles is determined using Mindlin's equation for a pile with linear variation of skin friction. The superstructure (raft and basement walls) is modelled by the Finite Element Method. The settlement is then calculated on the basis of the stress increase using the initial compression modulus.

PGRAFT, written by Kuwabara (1991), is a program for analysing the behaviour of pile group and piled footings, using a boundary element technique developed by Poulos. The method enables the determination of stresses acting on all elements of the piles and the cap. The program is, however, limited to pile groups consisting of a number of identical piles arranged in a square configuration.

PILG3 is a version, adapted to personal computer by Lazaridis and O'Neill (1989), of the original program PILG based on the method suggested by O'Neill et al. (1977) with a number of simplifying assumptions.

Program SPLICE was written by Clausen et al. (1984) to analyse the interaction between an offshore jacket type linear structure and its non-linear foundation system consisting of single piles or pile groups. The program is based on the hybrid method, i.e. using t-z and p-y curves for individual piles and Mindlin's solution for pile-soil-pile interaction. The program was developed to obtain a consistent solution for both the superstructure and the pile foundation system, i.e. a solution that is compatible with respect to both forces and displacements at the structure-pile interface.

Program GROUP, written by Lieng and Svanö (1985), is a program for calculating the load distribution among piles in a pile group. GROUP is based mainly on Aschenbrenner's three-dimensional method with a few additions and changes. As a basis for a total stress analysis, GROUP utilises t-z (axial) and p-y (lateral) curves in order to attain the soil stiffness used in computation. The displacement of a pile in the group is not influenced by those of the other piles, i.e. no pile-soil-pile interaction is taken into account.

Program PAUL was devised at Chalmers University of Technology for calculating the settlement of a pile group or a piled footing in the case that pile loads and surface loads are already known. The surface loads, which are rectangular and have constant intensity over each individual rectangle, can be placed at any depth. The additional stress due to the surface loads is then calculated according to Frölich's theory. A pile load, which is given as the load at the pile top, will be transformed into a number of point loads along the pile according to a chosen load distribution along the pile. The additional stress due to the pile loads is then calculated by means of Mindlin's solution. The settlement of the point in question is calculated assuming the deformations to be one-dimensional.

Program TPR, written by Fatemi-Ardakani A. (1988), was developed to deal with the analysis and design of a raft foundation on an elastic medium or a pile reinforced elastic medium, using the "thick plate-bending" finite elements to model the raft and the surface element method to model the soil. The piles are then replaced by elastic springs, whose flexibility is estimated by means of the equations obtained from the parameter study for the vertical flexibility of a single pile, undertaken by Fatemi-Ardakani B. (1987) by using the computer program PGROUP3.1 (1981). Pile-soil-pile interaction is taken into account according to Randolph's approach.

Program UNIPILE is based on the method called "the unified design of piles and pile groups considering capacity, settlement, and negative skin friction" suggested by Fellenius et al. (1990). In the program, the settlement of a pile group is determined as the settlement of an equivalent footing located at the elevation of the neutral plane, with the load spreading below the equivalent footing calculated by the 2:1-method. Neither pile-soil-pile interaction nor cap-soil-pile interaction is taken into account.

Discussions

Most of the existing programs for analysing pile groups and piled footings have

been based on the theory of elasticity. They are therefore not suitable for non-cohesive soil. In consequence, some of conclusions obtained from theoretical studies are contrary to the results obtained from the experimental ones. For example, from the tests on pile groups in sand, a corner pile always takes a higher load than the center pile of the group. Calculations based on the theory of elasticity give a contrary result. From the calculations based on the theory of elasticity it has been concluded that the increase in stiffness of a piled footing due to the cap in direct contact with soil is small, although a significant load may be carried by the cap, see e.g. Butterfield and Banerjee (1971), Poulos and Davies (1980), Randolph (1983), Kuwabara (1989). This is, however, very different from the behaviour of piled footings in sand. For analysing pile groups and piled footings in non-cohesive soil, more sophisticated soil models, e.g. Mohr-Coulomb model, should be used.

3 LARGE-SCALE FIELD MODEL TESTS

Large-scale model tests were carried out in an abandoned sand pit at Gråbo, 35 km northeast of Göteborg. Fig. 3.1 shows a bird's eye view of the test field at Gråbo.

Fig. 3.1 A bird's eye view of the test field at Gråbo

3.1 General Features

The main purpose of the field test was to study the problem of pile-cap-soil interaction of piled footings in sand. The problem includes interaction between the piles in the group, named as pile-soil-pile interaction, as well as between the pile group and the pile cap when it is in contact with the soil surface, named as pile-cap interaction. As discussed in Chapter 2, such a study ought to include piled footings, free-standing pile groups, single piles, as well as shallow footings under equal soil condition. (The *shallow footing* will sometimes be called *unpiled footing* or *cap alone).* Comparisons of test results on single piles and on free-standing pile groups will show the pile-soil-pile interaction, while comparisons of the test results on piled footings, free-standing pile groups, and on caps alone will clarify the interaction between the cap and the pile group (the cap-pile group interaction). To make possible a study of the settlement-reducing effect of piles, the load-settlement behaviour of shallow footings and of piled footings should be directly comparable. For the above purposes three different test series were performed, each of which consisted of

four separate tests comprising shallow footing, single pile, free-standing pile group, and piled footing under equal soil conditions and with equal geometry.

The three test series, denoted as T1, T2, T3, were performed with different pile spacings. In each series, the test on cap alone (shallow footing) was denoted as C; the test on single pile, S; the test on free-standing pile group, G; and the test on piled footing, F. With these notations, test T2S, for example, should be understood as the test on a single pile in the second test series. The names of all the separate tests are summarised in Table 3.1

Piles and pile groups

The model piles used in the field tests were hollow steel piles with a square cross-section, 60 mm by 60 mm, and a wall thickness of 5 mm. The pile tip had a pyramidal shape with an apex angle of 60 degrees. The pile length was about 2.3m and the depth of embedment of the piles in each separate test varied slightly, depending on the testing procedure. In the tests on single piles, the depth of embedment of the piles was 2 m; in the tests on free-standing pile groups 2.1 m; and in the tests on piled footings, 2.3 m. The surface of the piles was covered with sand (grain size < 0.125 mm) glued to the surface.

All the test pile groups were square and consisted of five piles: one central pile, pile No.1, and four corner piles, piles Numbers 2 to 5, according to the driving order. As the main purpose of the research was to study the settlement-reducing effect of the piles, the pile spacing was chosen to be relatively large. The centre-to-centre pile spacing was four times pile widths ($4b_p$) in the first test series, and $6b_p$, $8b_p$ in the second and the third series.

Footings (caps)

The footings were made of pre-fabricated reinforced concrete and were absolutely rigid. They were used both as footings in the tests on shallow footings and as pile caps in the tests on pile groups and piled footings. For this purpose, each footing was provided with five holes to admit placement of the piles later on. The size of the footings depended on the pile spacing chosen. In the first test series, the footing was 46cm by 46cm in plan and 30cm in thickness. In the second and the third test series , the footing size was 63cm by 63cm by 35cm, and 80cm by 80cm by 40 cm, respectively. The distance from the edge of the footing to the centre of the corner piles was always 60 mm, Fig. 3.2.

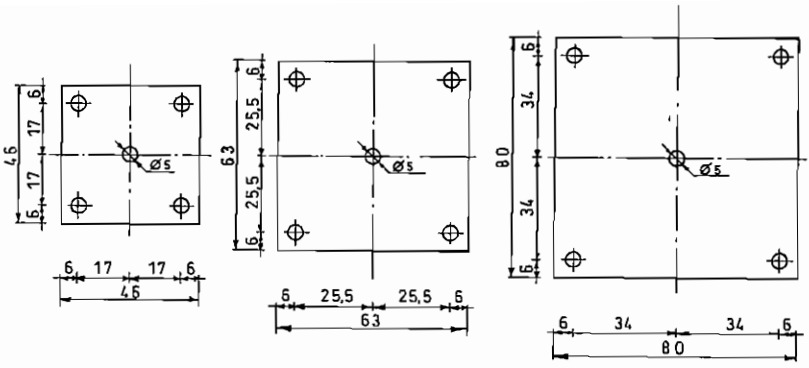

Fig. 3.2 Model footings in plan. Dimensions given in cm. (a) footing used for Test series T1; (b) for Test series T2; (c) for Test series T3.

Soils

The test pit was about 3 m by 3 m at the base and 3m deep. The pit wall had an inclination of about 2:1 (2 vertical to 1 horizontal). The excavation was filled with sand which was compacted in 20 cm thick layers. The soil properties were determined by means of a volumeter and different field methods: cone penetration test (CPT), dilatometer test (DMT) and pressuremeter test (PMT). The results can be seen in details in Chapter 4. In the first test series, the relative density of sand was about 38%; in the second series, about 67%; and the third series, slightly lower, 62%. Descriptions of these test series are given in Table 3.1.

Table 3.1 Summary of the field model tests

Test Series	Pile Group and Cap	Sand	Pile Length (m)	Separate Tests
T1	five piles spacing $S=4b_p$ 46cmx46cmx25cm	I_D = 38%	- 2.0 2.1 2.3	T1C, shallow footing T1S, single pile T1G, pile group T1F, piled footing
T2	five piles spacing $S=6b_p$ 63cmx63cmx35cm	I_D = 67%	- 2.0 2.1 2.3	T2C, shallow footing T2S, single pile T2G, pile group T2F, piled footing
T3	five piles spacing $S=8b_p$ 80cmx80cmx40cm	I_D = 62%	- 2.0 2.1 2.3	T3C, shallow footing T3S, single pile T3G, pile group T3F, piled footing

3.2 Test Instrumentation

In the field tests, the following measurements were made: axial pile loads, total applied load, lateral pressure against the pile shaft and displacement of the footings and of the ground surface.

Measurement of axial pile loads

Axial pile loads were measured by means of load cells at the base and head of every pile. The load was also measured in the middle of one pile, pile No. 5. The load cells consisted of a 170 mm long hollow steel cylinder with an inner diameter of 25 mm and an outer diameter of 35 mm. The pile loads were measured by means of a full Wheatstone bridge that consisted of two active and two passive strain gauges glued to the steel cylinder. The load cells were protected by a cover of pile material, which was fixed by screws to the upper part of the load cell, and leaving an opening of 2 mm at the bottom part of the load cell, thereby allowing for compression of the load cell. In this way only the axial load (and not the skin friction along the load cell) was transferred via the bottom of the load cell, Fig. 3.3. All load cells were calibrated before and after each test series. The load cells behaved perfectly linearly up to 80 kN, which was the maximum load applied during the calibrations. The scatter during calibration was extremely small. The measurements of the axial pile loads were governed by means of a microcomputer-based data acquisition system, which also provided build-in amplifiers for the pile load transducers.

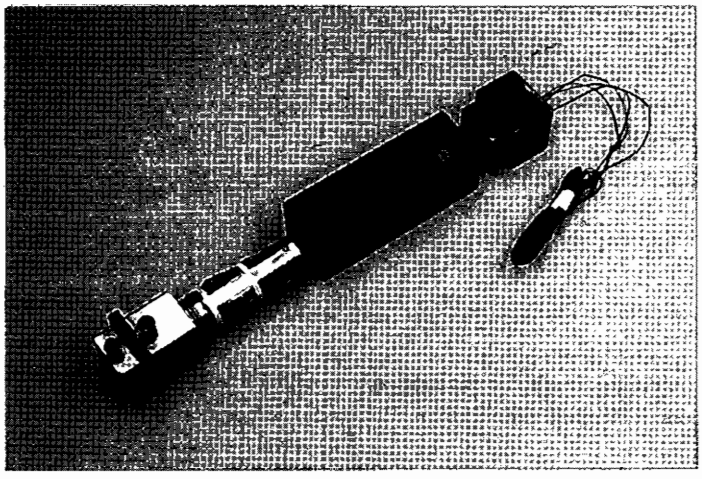

Fig. 3.3 Load transducer used in the field model test

Measurement of horizontal pressure against the pile shaft

The lateral earth pressure against the pile shaft was measured along the pile in the centre of the pile groups by means of Glötzl total stress cells. Twelve cells, each 45 mm in diameter, were installed flush with the pile surface, and were placed symmetrically on all the four sides of the pile, Fig. 3.4. The Glötzl cell is a hydraulic measuring system, which is based on the compensation method: the earth pressure is measured by a continuous stream of dry compressed air, which releases a membrane when equilibrium is reached between the air pressure and the pressure on the steel surface of the Glötzl cell.

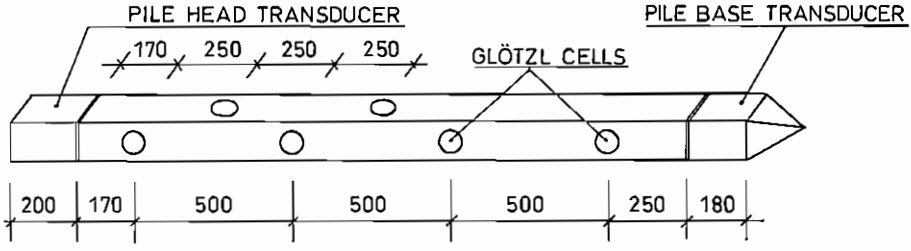

Fig. 3.4 Location of Glötzl cells on the central pile.

Measurement of displacements

Displacements of the pile head in the single pile tests, and of the upper surface of the footing and also of the ground surface in other tests, were measured by means of electric resistance transducers, Novotechnik, with a stroke of 25, 50, or 100 mm. The displacements were measured against two reference beams, each 6 m long, which were protected against wind and sunshine by tarpaulins. The reference beams were founded on footings that rested 30 cm under the soil surface. Levelling showed that movements of the reference beams were negligible. The displacement measurements were also monitored by the data logger. The displacement transducer used in the tests and the reference beam system are shown in Fig. 3.5.

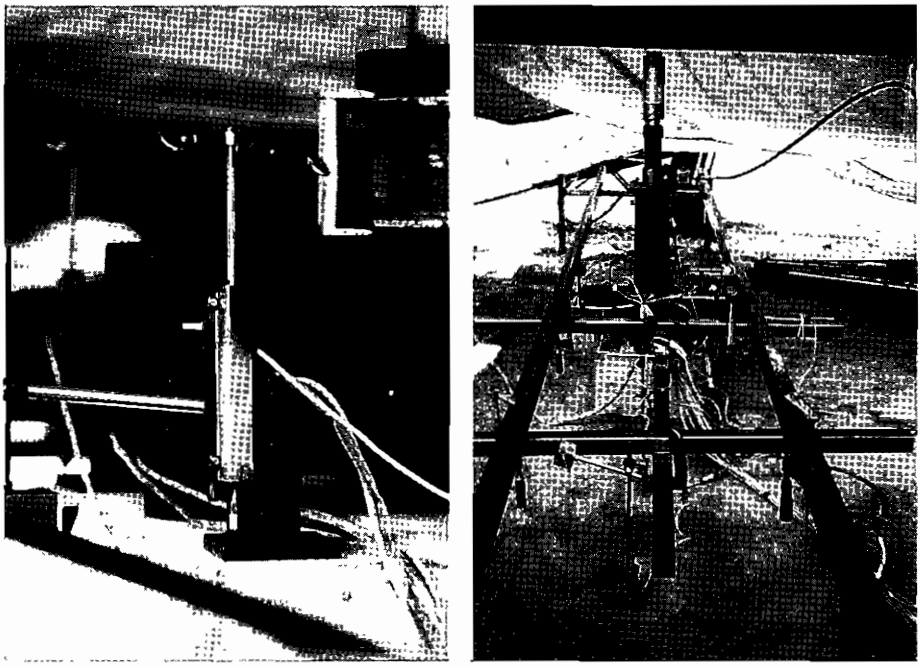

Fig. 3.5 Measurement of displacement: (a) displacement transducers; (b) reference beam system.

Data acquisition system

The system consisted of a data-logger ORION 3530, a personal computer IBM PC 286 and a printer. The logger had up to 200 channels, of which at most 40 channels were used in the tests. The logger was set up and controlled by the PC computer. The set-up routine is a program written in the logger's control language which defines the type and timing of logging and control routines, as well as parameters for all channels. In the tests, all channels were measured at 15 second intervals. The data for each load step was saved in a separate file on the hard disk or floppy disk of the computer. Simultaneously, the data was printed out on the printer.

Jacking system

Different kinds of hydraulic jacks were used in the field tests depending on the ultimate load levels. A small jack with a maximum capacity of 100 kN was used for all the single pile tests. Larger jacks with a maximum capacity of 600 kN and 1000 kN were used for tests on caps, free-standing pile groups and piled

footings. Total loads applied in all the tests were monitored by an independent electric load cell, which was either a small cylindrical cell used together with the small jack, or a larger ring cell used with the larger jacks.

3.3 Installation and Test Procedures

To make possible a comparison between the results of separate tests in one series, all the tests have to be carried out under equal soil conditions. Initially, in one series, tests on a cap, on a free-standing group and on a piled footing were intended to be performed in different sand pits, i.e. after each test the sand would be excavated and refilled under controlled conditions to obtain the same soil condition as before. In the field, however, no matter how carefully it is done, it is almost impossible to reproduce a soil condition identical to the previous one. The four tests in one and the same series were therefore performed in the same sand pit. Under the reaction beam, the test pit was divided into two areas: one for the test on the shallow footing, which was always the first test in a series; and the other for the remaining tests. In the latter area, the central pile was driven and tested first. Afterwards, the other piles were driven, then connected to the cap, and the free-standing group was tested. The test on the piled footing was finally performed after the free--standing pile group was pushed down until the cap came into contact with the ground surface (according to the first procedure of testing), or until the cap was about 20 mm above the ground surface (according to the second procedure). One of the problems met with was to avoid any influence from the test on the shallow footing. Therefore, the tests were placed as far as possible from each other and any possible influence from the test on the shallow footing was checked by measuring the settlement of the soil surface at different distances from the footing. The measurements in all the three test series showed that the displacement of the soil surface at a distance of 1.2 m from the edge of the shallow footing was negligible, only 0.01mm. Figure 3.6 shows the layout of the test site.

Reaction system

Four 400mm-diameter expander bodies, E400, were used as reaction piles. The expander bodies were placed at a depth of 10 m from the ground surface . To avoid the effects of the reaction piles on the test results, casings down to a depth of 8 m were used to isolate the pile steel rods from the soil. An H-beam, HEB600, with a height of 600mm and a length of 6.5m was used as the main

reaction beam. Two double U-320 beams with a length of 2m were used as secondary beams. The whole beam system was placed on two other steel beams so that it could be easily moved away from the test position and back again by handle jacks. A small hand wire-rope hoist that could move along the main beam was used to lift the cap when joining it to the pile group. Figure 3.6 shows the reaction beam system used in the field test.

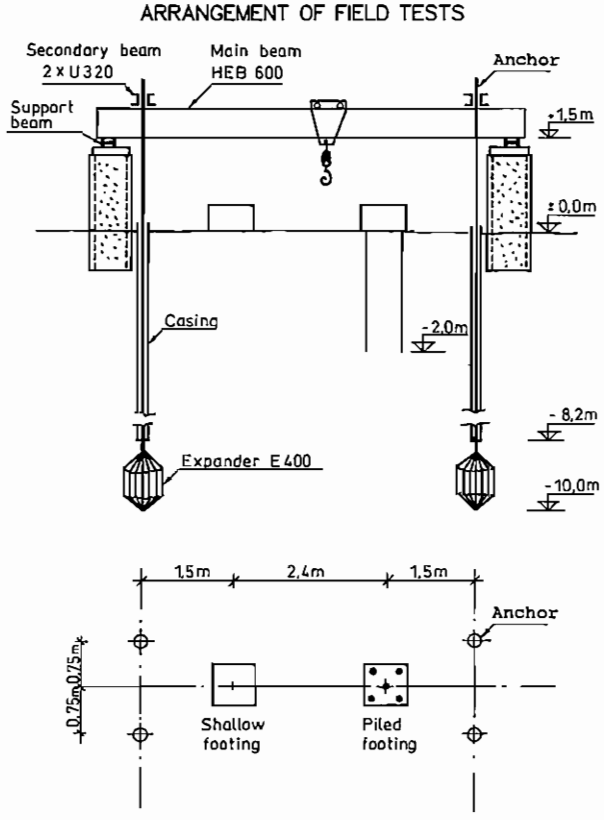

Fig. 3.6 Arrangement of the test site.

Pile driving and pile-cap joint

The piles were driven mechanically by means of a hollow ram (80 kg, height = 0.6m) with an average drop height of 20-30 cm. The central pile was always driven first and then tested as a single pile. Afterwards the corner piles were driven to form a pile group. All the top pile load transducers were not attached to the pile until the completion of driving to avoid possible damage.

The concrete caps were pre-fabricated with five 50mm-diameter holes for bolts by which the piles were attached to the cap. The bolts were hollow in order that the load transducer cables and the pressure cell tubes could be led through. The outer and inner diameters of the bolts were 33 mm and 22 mm, respectively, for the central pile, and 20 mm and 10 mm for the corner piles. After driving all the piles, the bolts were first fixed to the piles by nuts. The cap was then lifted onto the pile group and attached with the pile bolts by nuts. Additional nuts were used to adjust the levels in order to obtain a good contact between the cap and all the piles while the cap was in a hanging position. A detachable cover was used to make the pile cross-section constant, Fig. 3.7.

To be sure that the pile bolts would fit into the cap holes, the position and inclination of the piles had to be checked very carefully during driving. A special positioning steel plate was used to keep the piles in the right position in plan. In this way, the piles fitted naturally into the cap holes in all three test series. This was important as a guarantee that no lateral force on the pile heads influenced the test results.

Test procedure

All the tests were carried out using the same standard procedure as the quick maintained load test. In this method of testing, the applied load is increased every fifteen minutes by a constant amount, approximately 5% of the estimated ultimate load. Settlement gauges are read 0.5, 1, 2, 4, 8 and 15 minutes after application of a new load increment has been started. A new load increment is applied immediately after the 15 minutes reading. Using the computer-based data acquisition system, however, all data from the settlement transducers and from the pile load transducers were automatically collected every fifteen seconds. And each load step was only maintained for eight minutes.

In order to consider residual loads in the piles, the pile load transducers were always read before and after driving, as well as before and after testing. The direct method of measuring residual loads, discussed by Briaud et al. (1985), was used, in which the readings of the pile load transducers, while the pile is hanging under its own weight, is considered as zero values.

In each test series the installation and testing order can be summarised as follows: (a) placing the cap in test position and driving the central pile; (b) two-day break; (c) testing the cap alone as shallow footing; (d) testing the

single pile; (e) driving the corner piles and joining them with the cap; (f) two-day break; (g) testing the free-standing group; (h) one-day break; (i) testing the piled footing.

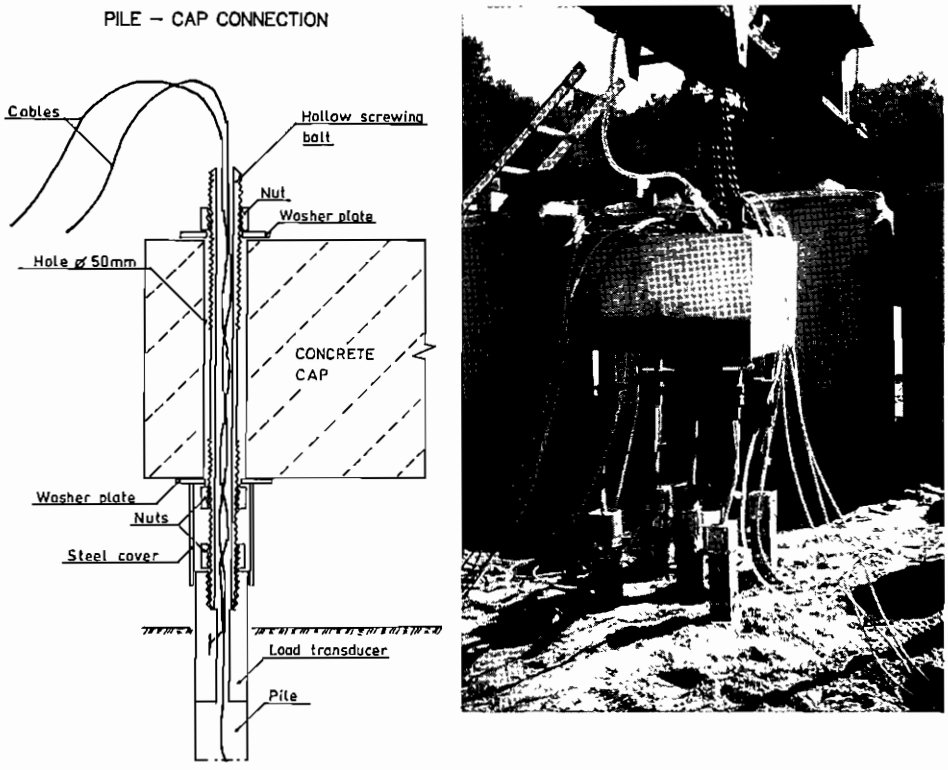

Fig. 3.7. Pile - cap joint. a) detail, b) during installation

The tests on piled footings were performed using two different procedures. On completion of the test on free-standing pile group, the whole footing was pushed down, in Test series T1 until the cap was in contact with the soil surface, and in Test series T2 and T3 until the cap was 20 mm above the soil surface, before the test on the piled footing was started. Each way of testing has its own advantages. Using the first procedure, it is easier to compare directly the behaviour of the piled footing with those of the shallow footing and of the free-standing pile group; while using the second procedure the effect on the behaviour of the piles of the cap being in contact with the soil can be seen clearly, as shown later in Chapters 5 and 6. Figure 3.8 shows a general view of a load test arrangement.

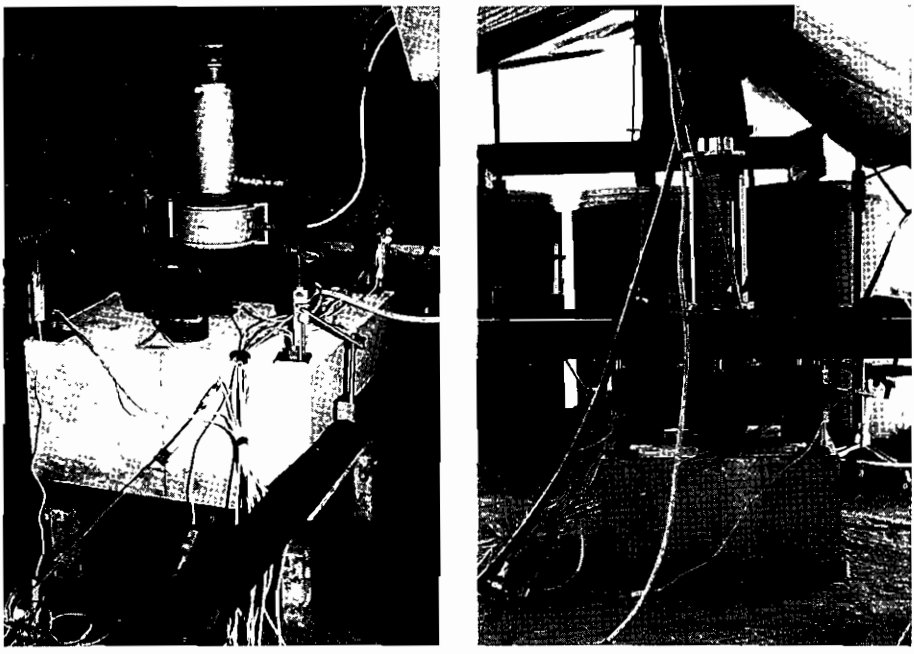

(a) (b)

Fig. 3.8 General view of arrangement of load tests: (a) Test on a free-standing pile group; (b) Test on a piled footing.

3.4 Comparison of Separate Tests in Each Test Series

Traditionally, group efficiency and settlement ratio are obtained by comparing the results from tests on a free-standing group with those on a single pile under equal soil conditions. The results show the pile-soil-pile interaction. Many authors used the same concepts even to study the behaviour of piled footings. This is illogical because the contribution of the footing is quite independent of the number of piles, pile spacing, pile length, and mainly depends on its size. In this study, to compare the bearing capacities of a single pile, a free-standing pile group, a piled footing and a shallow footing under equal conditions, different definitions, called *load efficiencies*, instead of group efficiency, will be suggested in Section 6.3. In the same way, the settlement behaviour of a single pile, a free-standing pile group, a piled footing and a shallow footing under equal conditions will be compared by means of new definitions of *settlement ratios*, see Section 6.4.

4. SOIL INVESTIGATION

The large-scale model tests were carried out in an abandoned sand pit in Gråbo, 35 km northeast of Göteborg. The geological formation of the site is glaciofluvian delta created during two phases of the latest deglaciation. The delta is built up mainly of sand, but lenses of clay and coarser gravel are also found in the deposit. As about 10 metres of the original deposit had been excavated during the years when the sand pit was in use, the *in situ* deposits at the test site were over-consolidated, Liedberg (1991).

The test pit was about 3 m by 3 m at the base and 3 m deep. For each test series, the excavation was refilled with sand, that was compacted in layers of about 20 cm thickness up to the original level. Soil investigations, both field and laboratory tests, were carried out before and after each test series. In this chapter, the results from the soil investigations are presented and discussed.

4.1 Laboratory Tests

The laboratory soil investigation comprised grain size distribution, density, water content and void ratio, and compaction characteristics. Other properties, such as angle of internal friction and deformation characteristics, were obtained from the results presented by Ekström (1989) and Liedberg (1991), who both made a large number of laboratory tests on the same soil material and whose results are in good agreement.

4.1.1 Basic soil properties

Grain size distribution

The grain size distribution of the soil was investigated by sieve analyses, and the results were in good agreement with those published by Ekström and Liedberg. The results showed the average coefficient of uniformity, C_u= 3.4, and a mean grain diameter, d_{50}= 0.34 mm.

Density, water content and void ratio

The specific gravity, ρ_s, determined by the pycnometer method, had a mean value of 2.68 t/m^3.

Density tests were carried out both before and after each test series using a volumeter consisting of a thin steel cylinder, with a diameter of 260 mm and a wall thickness of 1.5 mm. The cylinder was pushed down to a shallow depth into the sand , and the soil within the cylinder was excavated. The volume of the sample was determined by measuring the distance from a reference level to the soil before and after excavation.

During compaction, soil samples were taken at different places for each layer. During excavation, samples were taken inside the pile group at every 20 cm depth to the bottom of the excavation. The values of bulk density, water content, dry density, and void ratio before and after the three test series are given in Figures 4.1, and their mean values are summarised in Tables 4.1 and 4.2.

Table 4.1 Density and water content. Before tests.

	Mean value	Standard deviation	Coefficient of variation	Number of samples
Test series T1				
ρ (t/m^3)	1.67	0.09	5.4%	8
ρ_d (t/m^3)	1.56	0.08	5.1%	8
w (%)	5.94	0.19	3.1%	8
e	0.73	0.09	12.3%	8
Test series T2				
ρ (t/m^3)	1.79	0.05	2.8%	12
ρ_d (t/m^3)	1.68	0.05	3.0%	12
w (%)	6.11	0.36	5.9%	12
e	0.60	0.04	6.6%	12
Test series T3				
ρ (t/m^3)	1.77	0.05	2.8%	13
ρ_d (t/m^3)	1.66	0.05	3.0%	13
w (%)	6.31	0.39	6.1%	13
e	0.62	0.05	6.4%	13

where ρ= bulk density, ρ_d= dry density, w= water content, e= void ratio

Compaction characteristics

The maximum dry density was ρ_d=1.84 t/m^3 (corresponding to a minimum void ratio e_{min}= 0.45). The maximum void ratio e_{max}= 0.90 was obtained by pouring sand into a large oedometer ring. The mean values of the relative density of sands I_D before and after each test series are summarised in Table 4.3, in which $I_D = (e_{max}-e)/(e_{max}-e_{min})$.

Table 4.2 Density and water content. After tests (inside the pile group).

	Mean value	Standard deviation	Coefficient of variation	Number of samples
Test series T1				
ρ (t/m^3)	1.73	0.06	3.4%	7
ρ_d (t/m^3)	1.63	0.06	3.7%	7
w (%)	5.73	0.76	13.2%	7
e	0.65	0.06	9.2%	7
Test series T2				
ρ (t/m^3)	1.85	0.08	4.4%	8
ρ_d (t/m^3)	1.74	0.08	4.6%	8
w (%)	5.75	0.57	9.9%	8
e	0.55	0.07	12.7%	8

Table 4.3 Relative density of sand before and after testing

Test series	Before testing	After testing
T1	38%	56%
T2	67%	78%
T3	62%	-

4.1.2 Deformation characteristics

Constrained modulus

The constrained modulus of compressibility can be determined from oedometer tests. According to Janbu (1963), the tangent constrained modulus M can be expressed as:

$$M = m\,\sigma_r \left[\frac{\sigma}{\sigma_r}\right]^{1-\beta} \qquad (4.1)$$

where, m = modulus number
β = stress exponent
σ' = effective vertical stress
σ_r = reference stress = 100 kPa

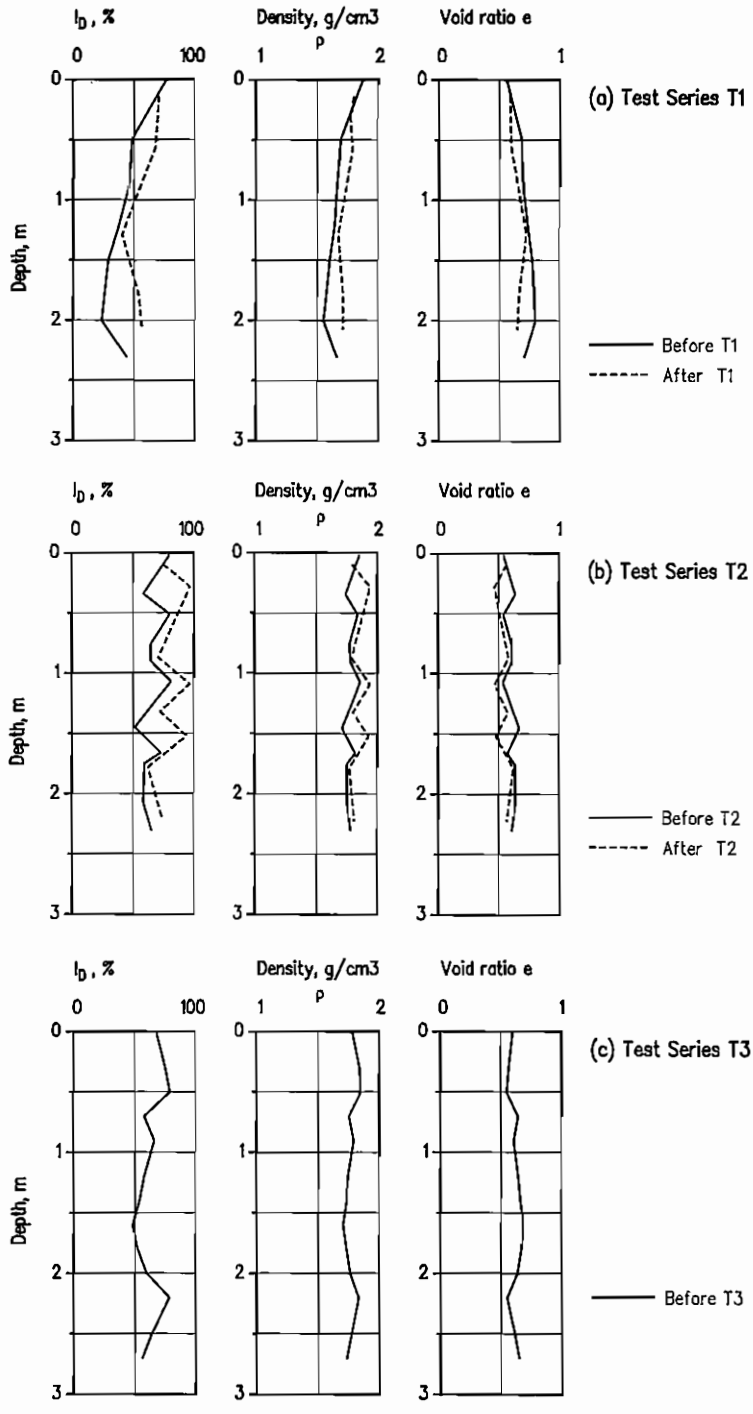

Fig. 4.1 Results from the volumeter tests before and after the model tests: (a) Test series T1; (b) Tests series T2; (c) Tests series T3

Andreasson (1973) suggested that for sand with a mean grain size d_{50} < 5mm, the m and β values could be determined as

$$m = 295\ C_u^{-0.78} e^{-2.65} \tag{4.2}$$

$$\beta = 0.29 \log\left(\frac{d_{50}}{0.01}\right) - 0.065 \log(C_u) \tag{4.3}$$

where, C_u = coefficient of uniformity
d_{50} = mean grain size, in mm
e = initial void ratio

In the case of Gråbo medium sand, Liedberg (1991) showed that Eq. (4.3) seems to give reasonable β values, while the m value determined by Eq. (4.2) is too high. Based on a large number of laboratory tests, Liedberg suggested

$$m = 64.2\ e^{-2.82} \tag{4.4}$$

where, e = initial void ratio

Young's modulus

From triaxial tests, the initial modulus of elasticity can be given by Eq.(4.5), Janbu (1963):

$$E_i = k_E\ \sigma_r \left[\frac{\sigma_3'}{\sigma_r}\right]^{n_E} \tag{4.5}$$

where, k_E = modulus number
n_E = stress exponent
σ_3' = minor principle stress
σ_r = reference stress = 100 kPa

From the triaxial tests on Gråbo sand, the mean value of the stress exponent n_E was found to be 0.58, and the k_E value can be estimated from initial void ratio (Liedberg, 1991):

$$k_E = 16.9\ e^{-5.66} \tag{4.6}$$

where, e = initial void ratio

The tangent modulus of elasticity E_t can then be calculated, e.g. according to Duncan and Chang (1970).

Bulk modulus

As in the case of the modulus M and E_i, the bulk modulus K_B can be expressed in term of a modulus number k_B and a stress exponent n_B as follows:

$$K_B = k_B \, \sigma_r \left[\frac{p'}{\sigma_r} \right]^{n_B} \tag{4.7}$$

where, k_B = modulus number
n_B = stress exponent
$p' = \sigma'_1 = \sigma'_2 = \sigma'_3$ = effective isotropic pressure
σ_r = reference stress = 100 kPa

For Gråbo sand, Liedberg found that the mean value of n_B was 0.56, and the modulus number k_B for any void ratio e can be determined from the equation:

$$k_B = 42.9 \, e^{-3.505} \tag{4.8}$$

The bulk modulus K_B can, also be calculated from E_i using the following equation:

$$K_B = \frac{E_i}{3(1-2\nu)} \tag{4.9}$$

Poisson's ratio

Knowing M and E_i, Poisson's ratio ν can be calculated from the equation:

$$M = \frac{E_i(1-\nu)}{(1+\nu)(1-2\nu)} \tag{4.10}$$

Assuming that Poisson's ratio ν varies linearly with the void ratio e, for Gråbo sand, Liedberg found that:

$$\nu = (e - 0.163)/1.518 \tag{4.11}$$

This equation is valid for a maximum void ratio of 0.92.

4.1.3 Shear strength

For Gråbo sand, Ekström (1989) performed a number of direct shear tests and triaxial tests to evaluate the angle of internal friction ϕ'. From the results of direct shear tests, the ϕ' value varied from 37° to 46°, when the dry density of soil changed from 1.55 to 1.81 t/m^3. From the results of triaxial tests on sand with density 1.60 to 1.83 t/m^3, the ϕ' value changed from 40 to 47°, which is rather similar to the results obtained by Liedberg (1991). The following correlation was obtained using regression analysis with a correlation coefficient of 0.931, Ekström (1989)

$$\tan \phi' = \frac{1}{1.47e + 0.237} \tag{4.12}$$

where, e = initial void ratio

Bolton (1986) performed an extensive study on the strength and dilatancy of sands and presented a relative dilatancy index I_R, which is defined as:

$$I_R = I_D \, (Q - \ln p') - R \tag{4.13}$$

where, I_D = relative density of sand
$p' = (\sigma'_1+\sigma'_2+\sigma'_3)/3$ = mean effective isotropic stress at failure
Q = function of the mean critical isotropic stress p'_{crit}, which is the stress just sufficient to eliminate dilation by grain crushing
R = 1.0

Bolton also stated that the conventional effective strength parameters (c',ϕ') can only describe the full range of soil strength if both are allowed to vary with density and stress

$$\phi' = \phi'_{cv} + F_t \, I_D \, [(10 - \ln p') - 1] \tag{4.14}$$

where, ϕ'_{cv} = effective angle of internal friction at no dilation (no volume change) during shear
F_t = factor equal to 3 for triaxial strain condition, and equal to 5 for plane strain

For Gråbo sand, Liedberg found that:

$$\phi' = 34.8 + 3\mu' \, I_D \, [(\, 10.95 - \ln p') - 1] \tag{4.15}$$

where, μ' = 0.79 (factor allowing for grain shape and roughness, suggested by Larsson, 1989)

4.2 Field Tests

Different field test methods were used, before and after each test series: pressuremeter test (PMT), penetration test (CPT), and dilatometer test (DMT). The arrangements of the field tests for the three test series are showed in Figure 4.2.

4.2.1 Pressuremeter tests (PMT)

Pressuremeter tests were performed before each test series using a Menard mini-pressuremeter. The pressuremeter was installed by direct insertion of the probe inside a driven slotted tube, which is a rather common way of installation in Sweden. The slotted tube has an outer diameter d_t= 44 mm, and an inner diameter (diameter of the probe) d_p= 32 mm, and the length of the measuring cell l_c= 150 mm. The tests were carried out at every half metre down to a depth of about 2.5 to 3.0 m. The results are summarised in Table 4.4.

Table 4.4 Summary of results from pressuremeter tests. Before testing

Test series	Depth (m)	E_{pr} (MPa)	p_1 (MPa)	p_{cr} (MPa)
T1	0.5	3.19	0.18	0.17
	1.0	1.74	0.22	0.18
	1.5	1.15	0.13	0.11
	2.0	2.32	0.22	0.18
	2.5	1.10	0.11	0.10
	2.9	3.87	0.41	0.29
T2	0.5	3.62	0.30	0.25
	1.0	8.17	0.66	0.38
	1.5	10.21	0.86	0.62
	2.0	8.30	0.52	0.38
	2.5	5.38	0.35	0.27
T3	0.5	4.74	0.33	0.33
	1.0	2.55	0.22	0.15
	1.5	5.89	0.47	0.32
	2.0	8.23	0.53	0.38
	2.5	6.33	0.52	0.37

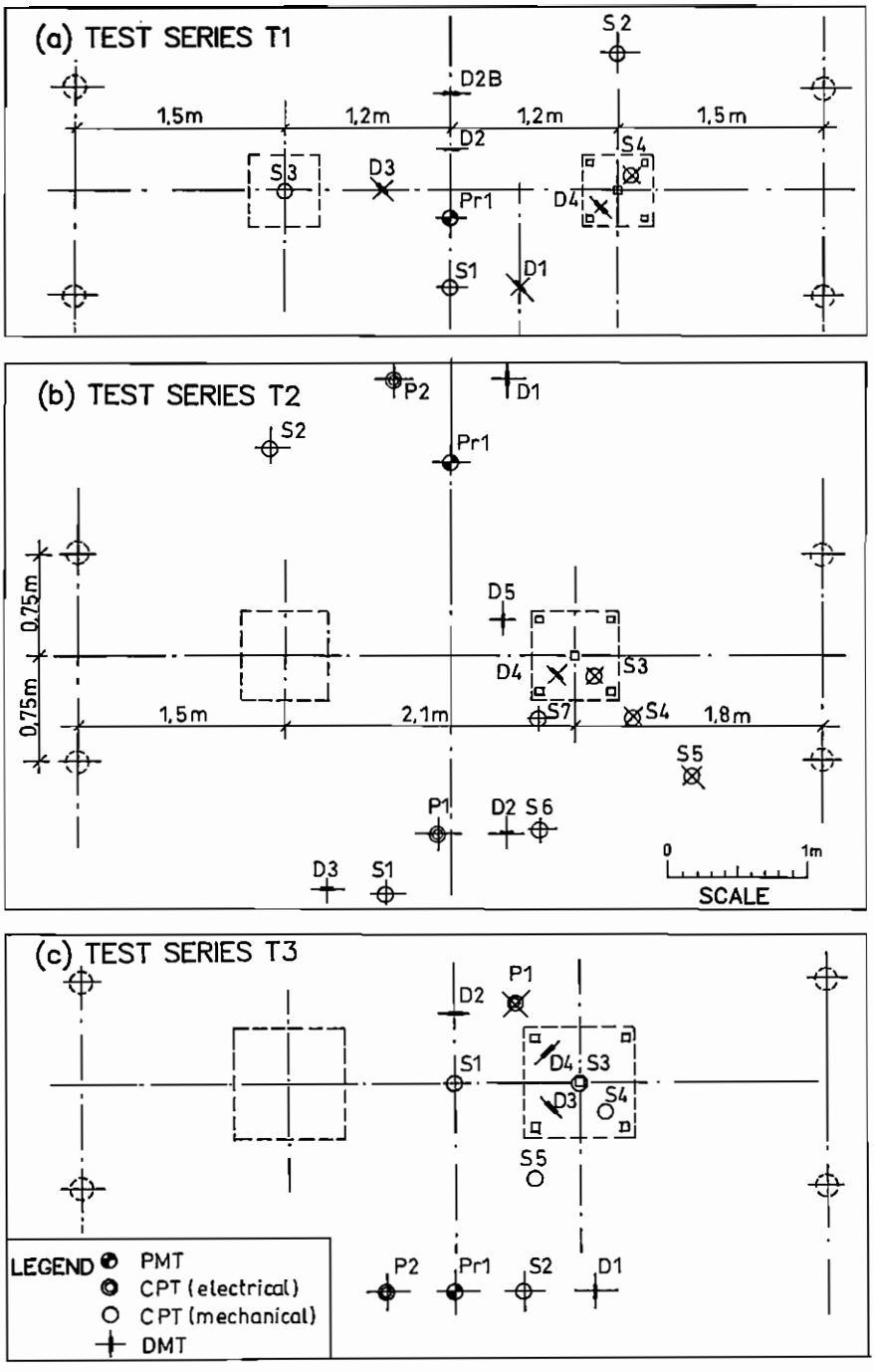

Fig. 4.2 Layout of the soil investigations in the field for: (a) Test series T1; (b) Test series T2; (c) Test series T3

4.2.2 Cone Penetration Tests (CPT)

Two types of CPT equipment were used in the test field: mechanical and electrical penetrometers. The electrical one was only used before Test series T2 and T3 in which the point resistance q_c and the skin friction f_s were measured separately. The mechanical penetrometer, a Swedish Geotech in which only the total penetration force is measured, was used before and after every test series. Since the skin friction of the rod of the mechanical penetrometer was extremely small for the shallow depths in question, the total penetration force could be assumed to correspond with the point resistance. Comparison with the results obtained from the electrical penetrometer indicated that this assumption is reasonable. The average point resistance $\bar{q}_c$ measured by the mechanical penetrometer, and the average $\bar{q}_c$ and $\bar{f}_s$ measured by the electrical one are shown in Tables 4.5 and 4.6. For easier data treatment, all the CPT results were digitalised for every 0.1 m in depth. The original test results are shown in Appendix B.

Table 4.5 Average cone resistance value $\bar{q}_c$ (MPa), mechanical penetrometer Before and after testing.

Test series	Before testing	After testing
T1	0.85	1.88
T2	2.94	3.77
T3	2.90	2.93

Table 4.6 Average resistance $\bar{q}_c$ and $\bar{f}_s$ (MPa), electrical penetrometer. Before Test series T2 and T3.

Test series	$\bar{q}_c$	$\bar{f}_s$	ratio $\bar{f}_s/\bar{q}_c$
T2	3.86	0.023	0.0060
T3	2.87	0.010	0.0035

The q_c values before and after each test series were compared in Figures 4.3. The comparison is also presented in the form of the ratio between the q_c value before and after the tests. It was found that after all three test series, the q_c values increased in soil near the soil surface, which was the soil-footing interface, and also under the level of pile base, both inside the pile group and at a distance of 0.3 m from the edge of the footings. The increase can be

explained by the compaction due to pile driving, as well as the compaction under the footing and under the pile base where the load was transferred to the soil. In Test series T1, the initial soil was much looser than in the other two series, and therefore the effect due to pile driving was much clearer.

4.2.3 Dilatometer tests (DMT)

Dilatometer tests were carried out after each soil preparation, i.e. before each test series, as a control of the homogeneity of the sand. The tests were also performed inside and outside the pile groups after each test series so that the soil properties before and after the tests could be compared. A total of about 160 measurements were performed in all the three test series. The major results are given below in Section 4.3, where the interpreted soil properties obtained from the different soil investigation methods are discussed.

4.3 Discussions on Soil Properties

Soil properties interpreted from the different soil investigation methods performed in the field are discussed and compared with the laboratory test results using the void ratios or dry densities interpolated from the volumeter tests for corresponding soil layers. For convenience, the average values are also studied.

Soil material

Compared with other field test methods, the dilatometer test gives a clearer classification of the soil. In the dilatometer test, the material index I_d is used to classify the soil material. In all three test series, the mean I_d value varies from 2.6 to 4.1 and the soil was designated as silty sand to sand. These results also showed that the dilatometer test gives a rather good indication of the soil type with the actual grain size.

Soil density

The bulk density of the soil was also estimated empirically by means of the dilatometer tests, using the dilatometer material index I_d. The mean bulk density values, determined by the volumeter and the dilatometer tests, are compared in Table 4.7. The comparison shows that the densities obtained from the

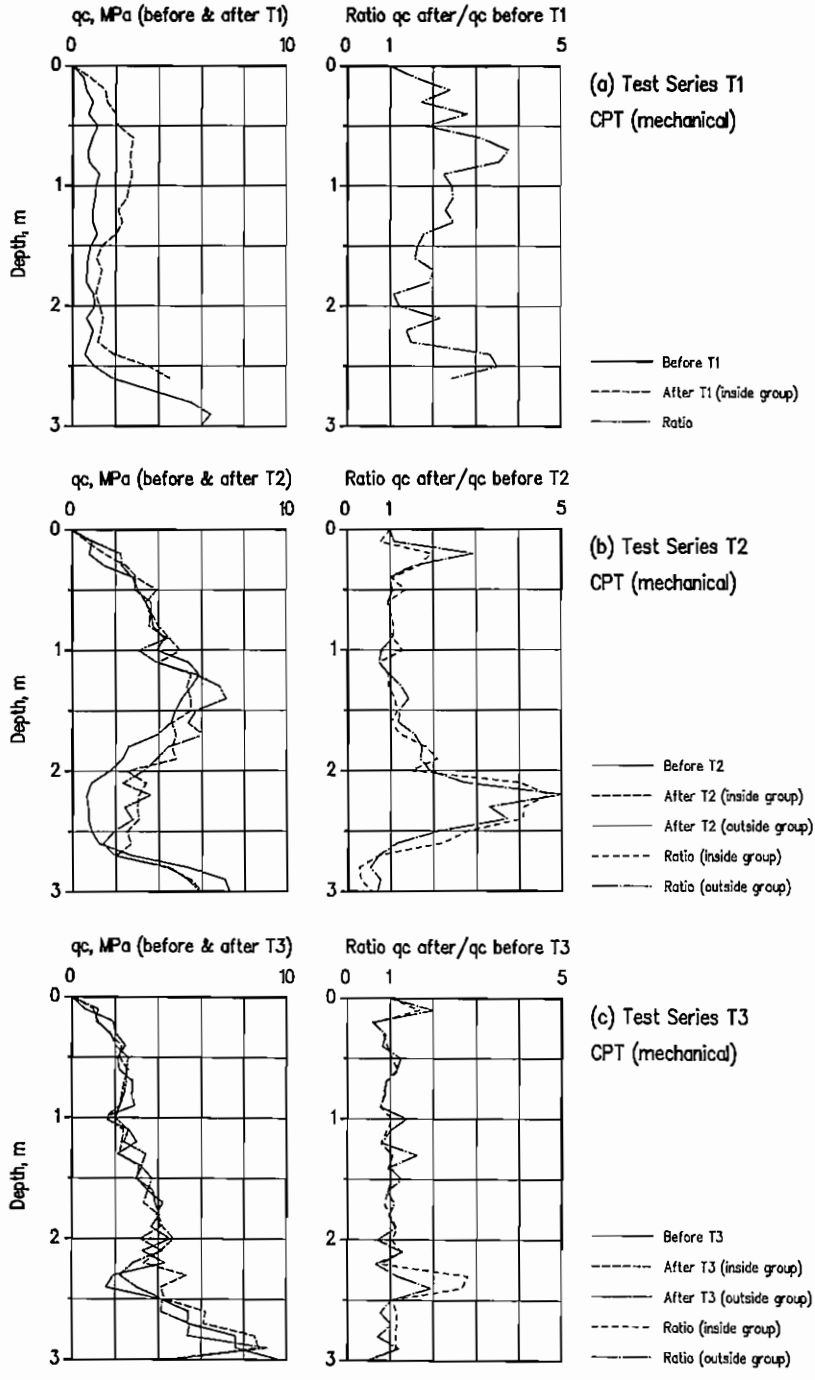

Fig. 4.3 Digitalised results from the mechanical penetrometer tests - Comparison before and after the model tests: (a) Test series T1; (b) Test series T2; (c) Test series T3.

dilatometer tests are in quite good agreement with those obtained from the volumeter test. From the dilatometer tests it can be seen that the initial bulk density, before each test series, was rather constant with depth. After each test series, the density increased significantly. The increase can be explained as a result of the compaction due to pile driving and due to the cap being in contact with the soil surface. The increase is much clearer in loose sand (Test series T1) than in dense sand. The increase is also high in the vicinity of the cap-soil interface.

Table 4.7 Measured bulk density and density evaluated from dilatometer test (DMT), t/m³

	Mean value	Standard deviation	Coefficient of variation	Number of samples
Test series T1				
before: ρ	1.67	0.10	5.4%	8
ρ_{DMT}	1.70	0.03	1.7%	41
after: ρ	1.73	0.06	3.4%	7
ρ_{DMT}	1.73	0.05	2.8%	8
Test series T2				
before: ρ	1.79	0.05	2.8%	12
ρ_{DMT}	1.79	0.07	3.9%	31
after: ρ	1.85	0.09	4.9%	9
ρ_{DMT}	1.87	0.05	2.6%	11
Test series T3				
before: ρ	1.77	0.05	2.8%	13
ρ_{DMT}	1.79	0.07	3.9%	24

where, ρ= measured bulk density, ρ_{DMT}= bulk density evaluated from DMT tests

Angle of internal friction

The effective angle of internal friction ϕ' will be interpreted from different field test results in this section. The values thus obtained will be compared with the laboratory tests performed by Ekström (1989) and Liedberg (1991), using the void ratio or dry density values interpolated from the volumeter tests for the depths corresponding to the field tests. Such laboratory-based values will later be referred to as laboratory test results. Of course, this way of comparison will result in a large scatter, but it is a good way of evaluating the soil properties calculated from the field test results.

In the CPT tests, the ϕ' value can be calculated from the correlation proposed by Robertson and Campanella (1983), which can be converted to Equation (4.16):

$$\tan \phi' = 0.38 \log_{10} \frac{q_c}{\sigma_v'} + 0.10 \qquad (4.16)$$

where, σ_v' = effective vertical stress

The ϕ'-values estimated according to Equation (4.16) are compared with those obtained from the triaxial tests, made by Ekström (1989) and Liedberg (1991) in Figure 4.4. In this figure, the dry densities corresponding to the CPT-based ϕ' values are interpolated from the volumeter tests for the corresponding depths. The calculation was made at every 0.1 m depth. The figure indicates that the ϕ' values estimated from CPT are in rather good agreement with the results of triaxial tests.

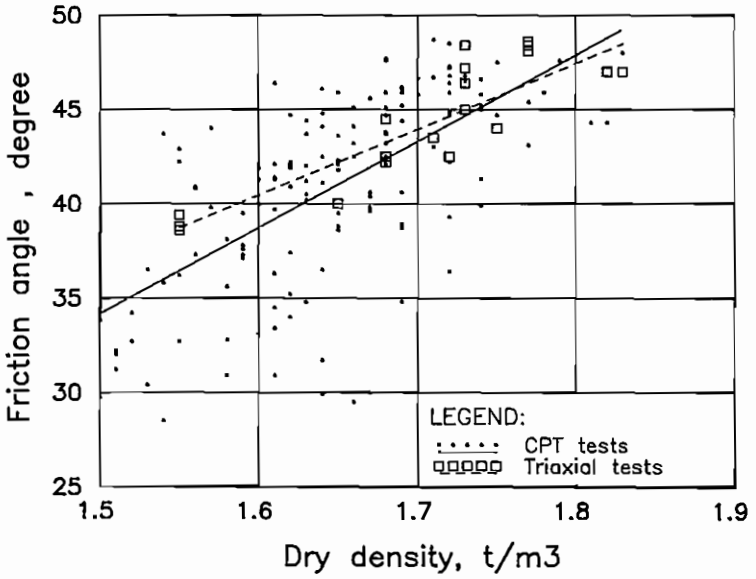

Fig.4.4 Internal friction angle, ϕ', estimated from CPT - Comparison with laboratory tests.

In the dilatometer test, there are four different procedures for estimation of the effective friction angle. In the first procedure, for soils with I_d>1.2, the ϕ' values can be estimated from the material index I_d, the dilatometer modulus E_d, and the effective overburden stress σ_v', using Equation (4.17), Marchetti and Crapps (1981):

$$\phi' = 25 + 0.19\ (I_d R_c - 100)^{0.5} \qquad (4.17)$$

where, $R_c = 500 + \dfrac{(E_d/\sigma_v') - 500}{1+(E_d/\sigma_v' - 500)/1500}$ if $\sigma_v'>50$ or $E_d/\sigma_v'<500$

$R_c = E_d/\sigma_v'$ if $\sigma_v'<50$ or $E_d/\sigma_v'>500$

Schmertmann (1982) suggested a method of calculating a plane strain, effective friction angle ϕ'_{ps}, from DMT combined with measurement of the penetration thrust. Marchetti (1985) proposed the third method, a procedure for evaluating axisymmetrical effective friction angle ϕ'_{ax}, so-called CPT-linked method which is similar to Schmertmann's method , but based on the q_c value from the CPT test instead of the DMT penetration thrust. In the last-mentioned procedure, the calculated friction angle may be normalised to a reference stress value (see Schmertmann, 1988a).

In this section, the first method, Marchetti and Crapps (1981), and the third method, Marchetti (1985), were used to determine the angle of internal friction ϕ'. The calculations were made at every 0.2 m depth and the results are also compared with the triaxial tests, Figures 4.5 (a) and (b). In these figures, the dry densities are also interpolated from the volumeter tests for the corresponding soil layers. The ϕ' value estimated according to Marchetti and Crapps (1981) is found to be too small in comparison with the triaxial tests. The CPT-linked method of Marchetti (1985), gives a better agreement with the results of the laboratory tests. However, in a number of cases unreasonable values, both of K_o and ϕ', were obtained . This can be explained by the fact that "...since sand deposits normally have a high variability, the use of even closely spaced soundings involves an inherent error in obtaining "matching" q_c and K_D values in this method" (Schmertmann ,1988). In Figure 4.5b, the values out of practical limits, e.g., corresponding to negative K_o values, were disregarded.

The large scatters in Figures 4.4 to 4.5 , similarly, may be explained by the unmatchability of the calculated ϕ' values and the dry densities interpolated from the volumeter tests. Besides, in the figures, the stress dependence of ϕ' values is not taken into account. Calculation according to Schmertmann (1982) seems to give better results, see Jan Ekström (1989).

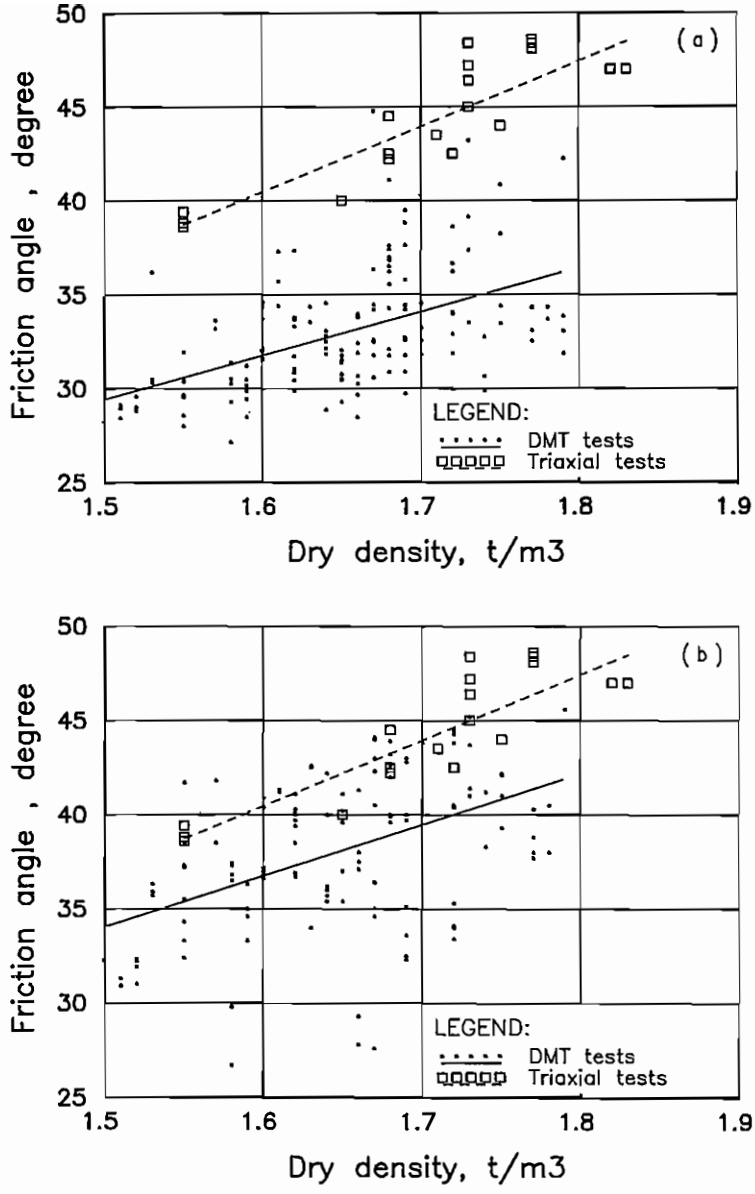

Fig. 4.5 Internal friction angle, ϕ', estimated from DMT - Comparison with laboratory tests : a) estimation according to Marchetti and Crapps (1981), b) according to Marchetti (1985)

In the pressuremeter test the angle of internal friction ϕ' can be obtained , e.g., according to Equation (4.18), proposed by Centre d'Etudes Menard, see Baguelin et al. (1978):

$$p_l^* = 2.5 \cdot 2^{\frac{\phi'-24}{4}} \qquad (4.18)$$

where, $p_l^* = p_l - p_o$, net limit pressure, in bar (1 bar = 100 kPa)

The ϕ' values estimated from Eq. (4.18) are, however, too small to be true. In Table 4.8, the average ϕ' values estimated from different method are compared. The comparison shows that ϕ' values obtained from CPT are in the best agreement with the laboratory test results.

Table 4.8 Comparison of average angle of internal friction ϕ' estimated from different methods

	Laboratory tests	DMT Marchetti & Crapps(1981)	DMT Marchetti (1985)	CPT	PMT
Before T1	37.7	30.7	35.1	36.3	23.0
After T1	40.0	34.7	40.0	41.9	-
Before T2	41.8	33.8	39.6	42.0	28.4
After T2	44.1	35.1	39.9	45.1	-
Before T3	41.0	32.8	40.5	41.6	26.8
After T3	-	34.9	37.6	43.3	-

Deformation characteristics

The deformation moduli are estimated from the different field test methods and compared with the laboratory test results in the same way as regarding the angle of internal friction.

In the dilatometer test, the constrained tangent modulus M_{DMT} can be determined as:

$$M_{DMT} = R_M E_D \qquad (4.19)$$

where, E_D = dilatometer modulus
R_M = correlation factor dependent on K_D and material index I_D (see Schmertmann, 1988)

The modulus M_{DMT} estimated from DMT according to Eq.(4.19) is compared with the laboratory test results in Fig 4.6. The figure indicates that the M_{DMT} is often larger than the M value derived from oedometer tests. Similar results can be seen in Ekström's study.

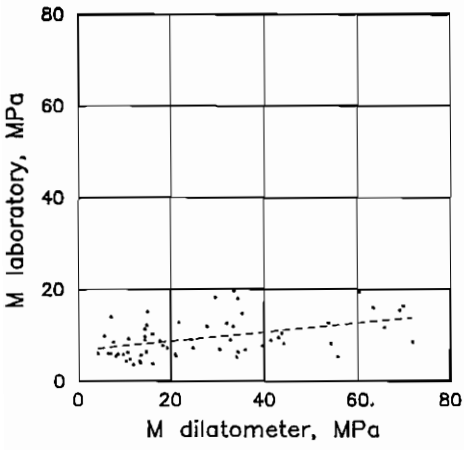

Fig. 4.6 Deformation modulus estimated from DMT - Comparison with laboratory tests.

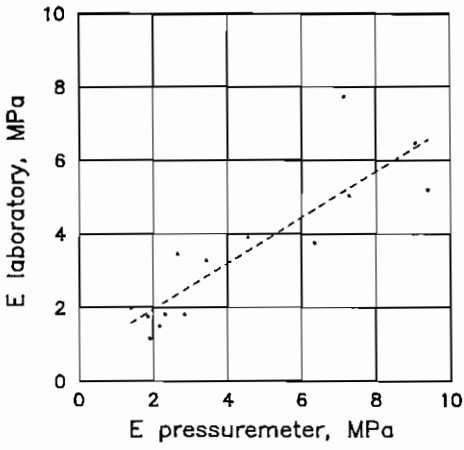

Fig. 4.7 Deformation modulus estimated from PMT - Comparison with laboratory tests.

In the pressuremeter test, the pressuremeter modulus can be estimated as (Hansbo & Pramborg, 1990):

$$E_{pr} = 2(1+\nu)\sqrt{(V_c + V_m)(V_t + V_m)}\,\Delta p/\Delta V \qquad (4.19)$$

where, V_c = initial volume of measuring cell
V_t = corresponding effective volume of tube
V_m = $V_o+\Delta V/2$ = mean value of V over the straight line portion of the pressuremeter curve, corrected for the stiffness of the plotted tube
$\Delta p/\Delta V$ = inclination of the straight line portion of the corrected pressuremeter curve
ν = Poisson's ratio of the soil

The pressuremeter modulus E_{pr} is also compared with the modulus from laboratory tests, Fig. 4.7. To avoid the complexity of estimation of σ_3' in Eq. (4.5), the laboratory modulus E_{lab} was calculated from M_{lab} using Eq.(4.10). The comparison showed that the two values E_{pr} and E_{lab} are in rather good agreement.

As regards the CPT test, it is suggested that the modulus M is estimated as:

$$M = \alpha\, q_c \qquad (4.20)$$

where, α = correclation factor

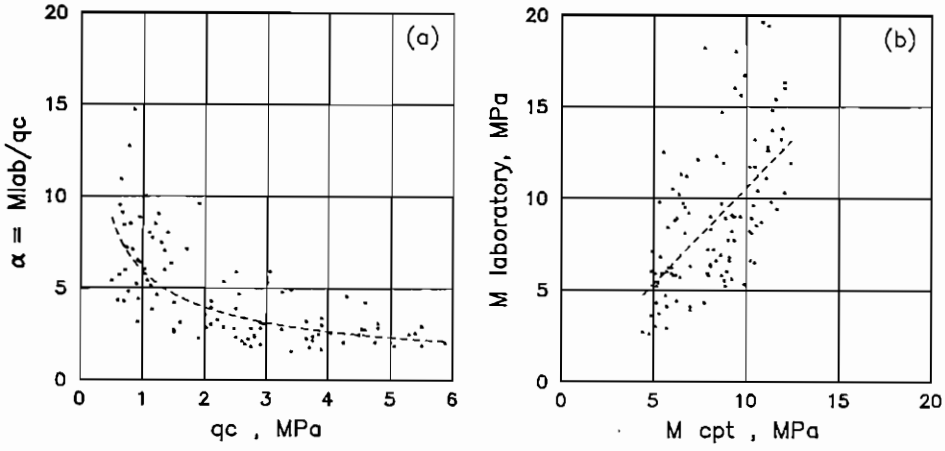

Fig. 4.8 Deformation modulus estimated from CPT : (a) relationship between factor α and q_c; (b) comparison with laboratory tests.

There are different suggestions regarding the α value. Vesic (1970), for example, proposed $\alpha=2(1+I_D^2)$, where I_D is the relative density of soil. However, comparison between the M values from the laboratory tests and the q_c values in Fig. 4.8a indicates that the correlation factor α strongly depends on the q_c value, according to Eq. (4.21):

$$\alpha = 5.909\ q_c^{-0.581} \tag{4.21}$$

This may be because of a rather low level of q_c, 0.5 to 6.0 MPa. With q_c values large enough (q_c > 2 MPa), the mean value of α is less than 4. Using Eq. (4.21), the modulus M is estimated and compared with the laboratory tests in Fig. 4.8b.

For comparison, the secant modulus of elasticity E_i is also back-calculated from the tests on the shallow footings. The settlement of a rigid square footing on a semi-infinite homogeneous elastic solid can be estimated as:

$$s = \frac{0.815\ qb\ (1-\nu^2)}{E_i} \quad \text{or} \quad = \frac{0.815\ P\ (1-\nu^2)}{E_i b} \tag{4.22}$$

where, s = settlement of footing
b = width of footing
q = uniform applied load
P = concentrated applied load = qb^2

Using Eq. (4.22), the secant modulus of elasticity is estimated at 25% and 50% of the failure load from the tests on the shallow footings T1C, T2C and T3C.

In Table 4.9, the average values of M and E_i, estimated by different methods, are compared. The table shows that, in comparison with the laboratory test results, the dilatometer modulus is much higher, while the pressuremeter modulus is rather reasonable. The modulus estimated from CPT is in good agreement with the laboratory test results provided that a reasonable α-value is chosen, e.g. according to Eq. (4.21). However, in comparison with the modulus back-calculated from the tests on the model shallow footings, the modulus obtained from the laboratory, the pressuremeter and the penetrometer tests are all much smaller. The M modulus, back-calculated from the tests on the shallow footings, can be estimated on the basis of the moduli E_{25} and E_{50}, according to Eq. (4.10), multiplied by 1.77 for Test T1C (ν = 0.37) and by 1.35 for Tests T2C and T3C (ν = 0.3). The M value evaluated from the dilatometer tests seems to be of comparable size, but it is still smaller than the back-calculated modulus. According to Briaud (1992), the elastic modulus in compression E is 2 to 3 times larger than the pressuremeter "first-load" modulus. Besides, the settlement predicted according to the pressuremeter method also includes ten years of creep. This can also explain why in Table 4.9 the pressuremeter modulus is smaller than others.

Table 4.9 Comparison of average deformation modulus estimated from different methods, MPa

	M_{lab}	M_{DMT}	M_{CPT}	E_{lab}	E_{pr}	E_{25}	E_{50}
Before T1	6.0	8.5	5.5	3.4	2.05	18.0	6.5
After T1	7.5	19.8	7.7	4.9	-	-	-
Before T2	10.4	29.8	9.3	7.9	7.14	30.4	18.7
After T2	13.2	50.6	10.3	10.4	-	-	-
Before T3	10.2	27.9	9.1	7.6	5.55	23.5	14.2
After T3	-	32.4	9.4	-	-	-	-

Note: M_{lab} = modulus M estimated from laboratory tests
M_{DMT} = modulus M estimated from DMT tests
M_{CPT} = modulus M estimated from CPT tests, using Eqs (4.20) and (4.21)
E_{lab} = modulus E calculated from M_{lab} using Eq. (4.10)
E_{pr} = modulus E estimated from PMT tests
$E_{25,50}$ = secant modulus E back-calculated from tests on shallow footings, at 25% and 50% of failure load

5. BASIC RESULTS OF FIELD MODEL TESTS

In this chapter, the basic results of the the field model tests in the three test series, denoted as T1, T2, T3, will be presented. In all the three series, the pile groups were square and consisted of five piles. The three test series were performed with different pile spacings, cap dimensions and soil conditions. In each test series four separate tests were carried out: tests on a shallow footing (cap alone), on a single pile, on a free-standing pile group, and on a piled footing. All the load tests were carried out using the same standard procedure, the quick maintained load test (ML test). In the interpretation of the test results, the weight of the jack system is always taken into account as an initial load step, which, for simplicity, is not included in the description of the tests below. The maximum load given in the figures should, therefore, be understood as the maximum applied load plus the weight of the jack system.

5.1 The First Test Series (T1)

In the first test series T1, the pile group had a centre-to-centre pile spacing of four pile widths, and the cap dimensions were 46 cm x 46 cm x 30 cm. The sand was loose, with an average relative density I_D= 38%. The excavation was filled in layers of about 20 cm in thickness by pouring sand from a height of about 2 m without compaction by machine.

Shallow footing T1C

The test was carried out by first loading to 22.5 kN using load steps of 1.5 kN, then unloading to 0 kN with load steps of about 3 kN, and reloading again up to 39 kN with load steps of 3 kN. The load-settlement curve for the first loading is shown in Fig.5.1, in which the point of failure, interpreted according to Vesic (1969) and Mazurkiewicz (1972), is presented.

Single pile T1S

The test consisted of only one loading sequence to failure and was performed with very small load steps of about 0.5 kN. Failure occurred by plunging just after six load steps because the sand was so loose. The results, however, are good enough for further analyses, and are shown in Fig. 5.2. The plunging load could be considered as the failure load.

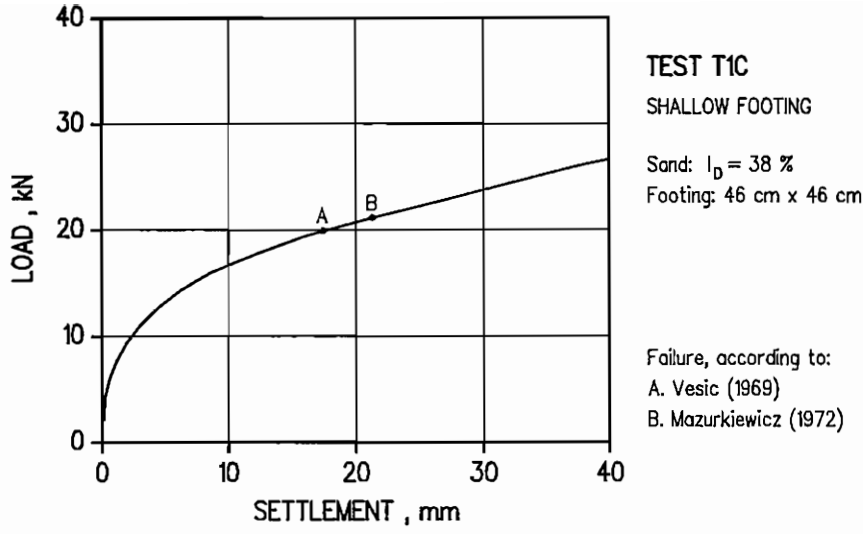

Fig. 5.1 Test on the shallow footing T1C - load-settlement curve

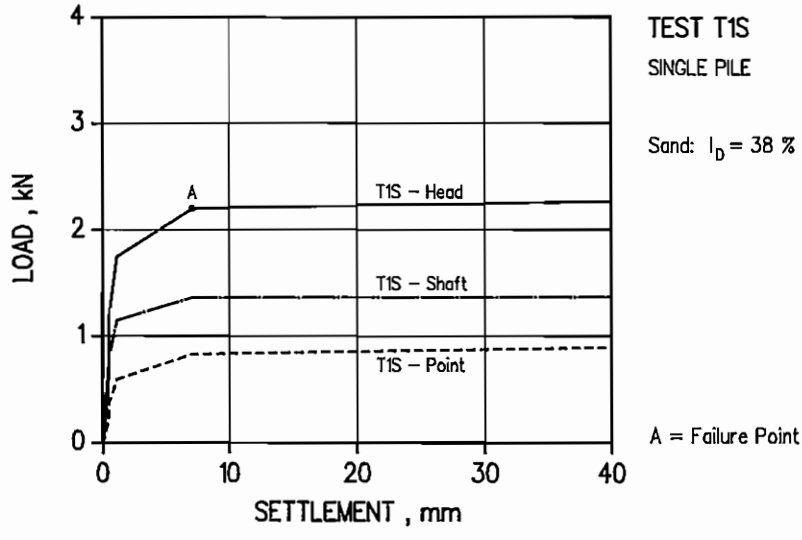

Fig. 5.2 Test on the single pile T1S - Load-settlement curve

Free-standing pile group T1G

The test was performed by one loading sequence to failure, with a maximum load of about 26 kN and a load step of 2 kN. As in the test on the single pile T1S, the failure also occurred by plunging. Consequently, the plunging load could be taken as the failure load. From the test results it can be seen that the centre pile always takes the largest portion of the load. In the first few load steps, the load distribution among the piles in the group is random, and afterwards it seems to depend on the driving order: the later the pile was driven the lower the load, with one exception, Pile 5, Fig.5.3.

The point loads of the piles are independent of the driving order and are of the same magnitude for all the piles. The shaft loads, like the head loads, seem to depend on the driving order, except for Pile 5. In comparison with the single pile test, the increase in shaft loads is considerably larger than in point loads. This means that compaction of the soil due to pile driving has its maximum influence on the pile shaft friction. In other words, the shaft group efficiency was larger than the point group efficiency. The average (head, shaft and point) loads per pile in Test T1G are shown in Fig.5.4. Comparing Fig.5.4 with Fig.5.2 it can be seen that the total, shaft, and base group efficiencies are 2.4, 2.6 and 2.0, respectively.

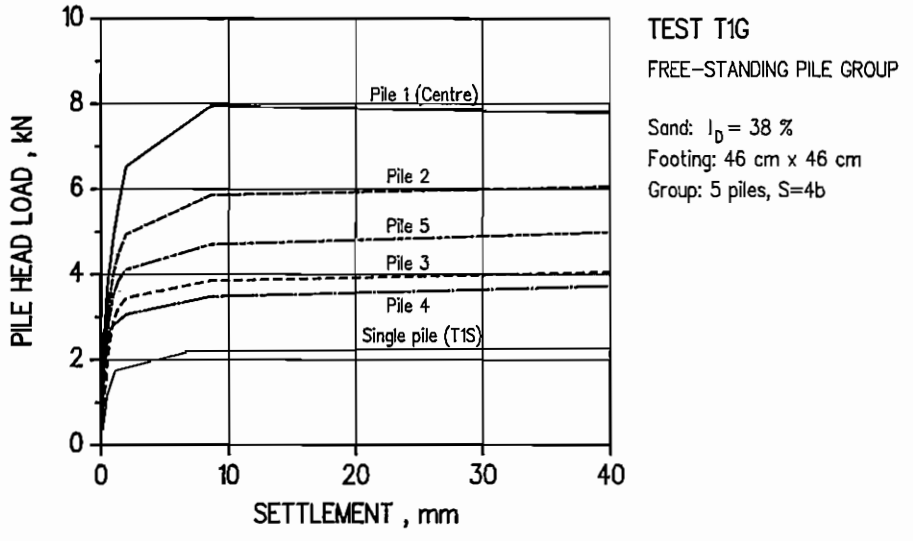

Fig 5.3 Test on the free-standing pile group T1G - Load-settlement curve

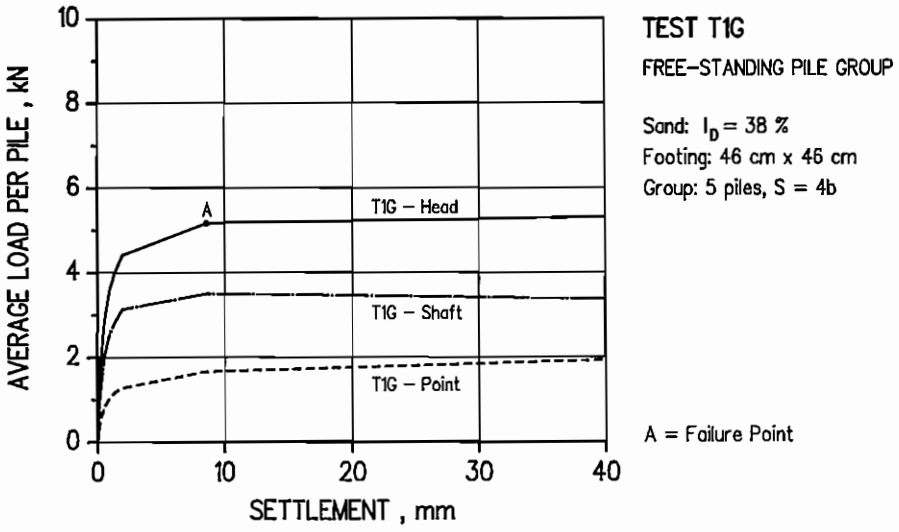

Fig. 5.4 Test on the free-standing pile group T1G - Average load per pile

Piled footing T1F

On completion of the test on the free-standing pile group T1G, the footing was pushed down until the cap came into contact with the soil surface. Test T1F was then started according to the first testing procedure, see Section 3.3. The test was performed as follows: (a) loading up to about 80 kN with a load step of about 2.5 kN (totally 30 steps); (b) unloading to 0 kN with steps of 7.5 kN; (c) reloading to 97.5 kN with steps of 7.5 kN; and (d) unloading again to 0 kN with load steps of 15 kN.

Fig.5.5 shows the load-settlement curve for the first loading in Test T1F. Failure did not occur by plunging, as in Test T1S on the single pile and in Test T1G on the free-standing pile group, but was characterised by settlement-hardening. This is obviously due to the effect of the cap in contact with soil.

The portions of load taken by the cap and the piles in Test T1F can also be seen in Fig.5.5. The share of the applied load between the cap and the piles varies with the load level. In the first sixteen load steps, up to about 40 kN, the load is mainly transferred to the piles, and the load carried by the cap is small and increasing from 10 to 20% of the total load, which was somewhat higher than the average load taken by one pile. Thereafter, with increasing load on the footing, the load taken by the cap increases rather rapidly up to 32 kN, about 38% of the

total load. Meanwhile, the load taken by the piles increases at a rather low rate, and the average load per pile decreases to about 12% of the total load, Fig.5.6. This also means that when the load is applied on the piled footing the piles at first take a major portion of the load. Not until pile failure is a considerable portion of load transferred to the cap.

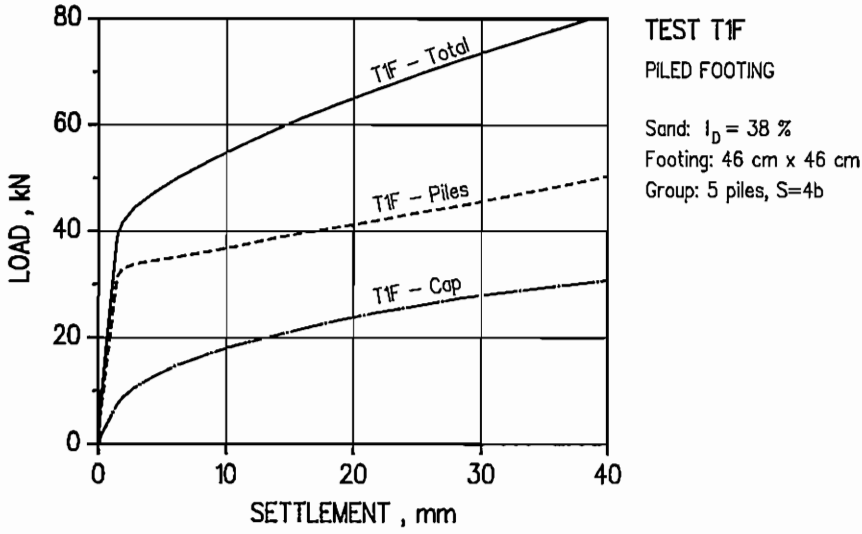

Fig 5.5 Test on the piled footing T1F - Load-settlement curve

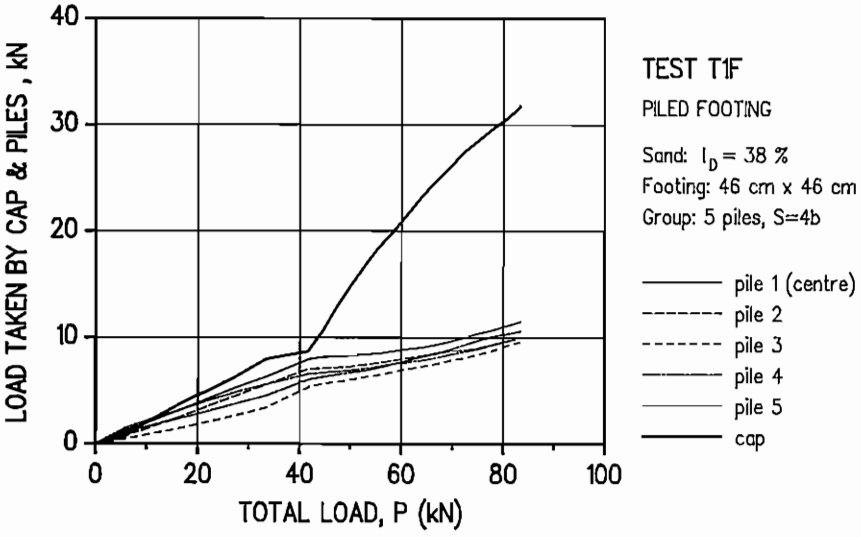

Fig. 5.6 Test T1F - Load distribution between cap and individual piles versus total load

The load distribution among the piles seems to be random during the first few load steps. Afterwards, the centre pile takes the largest portion of load, while the load carried by the corner piles becomes more uniformly distributed, not so dependent on the driving order.

The cap in contact with soil has a large influence on pile bearing capacity. The increases in pile loads in the piled footing, compared with those in the corresponding free-standing pile group, may be caused by several factors, among which are: stress increase due to the cap being in contact with soil, recompression effect (due to the test on the piled footing being made after the test on the free-standing pile groups), and a deeper penetration of pile. The recompression effect, similar to a reloading test, has mainly an influence on the initial stiffness of a footing under working loads, and can be ignored when studying the behaviour of footings at failure (or at rather large settlement). A deeper pile penetration may cause both a certain increase in pile shaft load due to a larger shaft area and a change in pile point load due to a change in soil properties under the pile point. Such a change can be checked by reading all the pile transducers while the footing is pushed down after the test on free-standing pile groups. In Test T1F, however, this effect can be ignored because the pushing loads were nearly equal to the maximum loads in Test T1G, see Fig. 5.7.

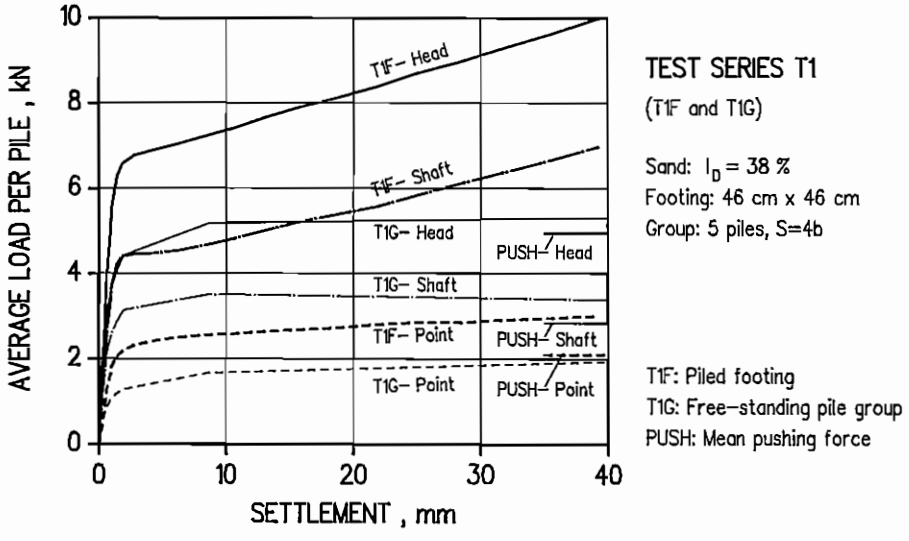

Fig. 5.7. Test series T1 - Average load per pile in Tests T1G and T1F

The increase in average pile (head, shaft and point) loads in Test T1F, in comparison with Test T1G, are thus mainly due to the cap being in contact with soil. Figure 5.7 indicates clearly that due to the cap, the failure of the piles in Test T1F occurs progressively, i.e the load on the piles is gradually increasing during failure. The increase is considerable for the pile shaft load, and very small for the point load. In other words, the contact pressure developed against the cap mainly affects the pile shaft friction. The increase in pile shaft load due to the cap becomes higher with increasing settlement of the footing. Loads taken by all the piles at failure, according to Vesic's criterion in Tests T1G and T1F, as well as those at settlements s = 20 mm and s = 30 mm in Test T1F, are summarised in Table 5.1.

Table 5.1 Load distribution on piles in the group - Test T1G and T1F

a) Head loads, kN

Pile No (1)	T1G at failure (2)	T1F at failure (3)	T1F s = 20 mm (4)	T1F s = 30 mm (5)
1	7.9	8.2	9.2	10.1
2	5.9	7.0	8.4	8.9
3	3.8	5.6	7.4	8.2
4	3.5	6.2	8.2	9.4
5	4.7	6.6	8.0	8.8
All piles	25.8	33.6	41.2	45.4

b) Shaft loads, kN

(1)	(2)	(3)	(4)	(5)
1	6.4	6.0	6.6	7.4
2	4.1	4.7	5.5	6.1
3	2.2	3.2	4.4	5.1
4	2.1	3.6	5.2	6.2
5	2.6	4.7	5.6	6.4
All piles	17.4	22.2	27.3	31.2

c) Point loads, kN

(1)	(2)	(3)	(4)	(5)
1	1.5	2.2	2.6	2.7
2	1.8	2.3	2.8	2.8
3	1.6	2.4	3.0	3.1
4	1.4	2.6	3.2	3.3
5	2.1	1.9	2.3	2.4
All piles	8.4	12.4	13.9	14.3

Note: (1) = pile number, according to driving order

(2), (3) = pile loads at failure in Tests T1G and T1F

(4), (5) = pile loads at settlements s= 20 mm and s= 30 mm in Test T1F

The results from Tests T1F, T1C and T1G show that the load taken by the piles in Test T1F is considerably larger than that in Test T1G. The increase is much higher as the settlement of the footing increases, and it takes place only in the pile shaft load. The load carried by the cap in Test T1F is also higher than that in Test T1C. However, the increase is not as large as the increase in the pile load, Fig. 5.8.

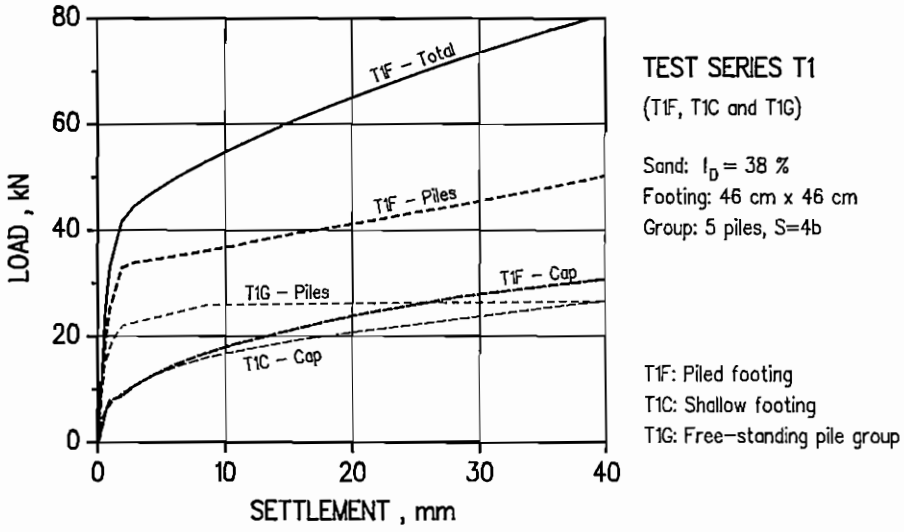

Fig. 5.8 Test series T1 - Comparison of separate tests

5.2 The Second Test Series (T2)

In Test series T2, the pile group had a pile spacing of six pile widths, and the cap dimensions were 63 cm x 63 cm x 35 cm. The sand was dense, with an average relative density I_D= 67%. The excavation was filled in layers of about 20 cm in thickness by pouring sand from a height of about 2 m with two compaction passes by a 70-kg vibratory plate compactor.

Shallow footing T2C

The test was carried out by first loading to 172.5 kN, using load steps of 7.5 kN, then unloading to 0 kN with load steps of about 15 kN, and reloading again up to 210 kN with load steps of 30 kN. The load-settlement curve for the first loading is shown in Fig.5.9, in which the point of failure, interpreted according to Vesic (1973) and Mazurkiewicz (1972), is presented.

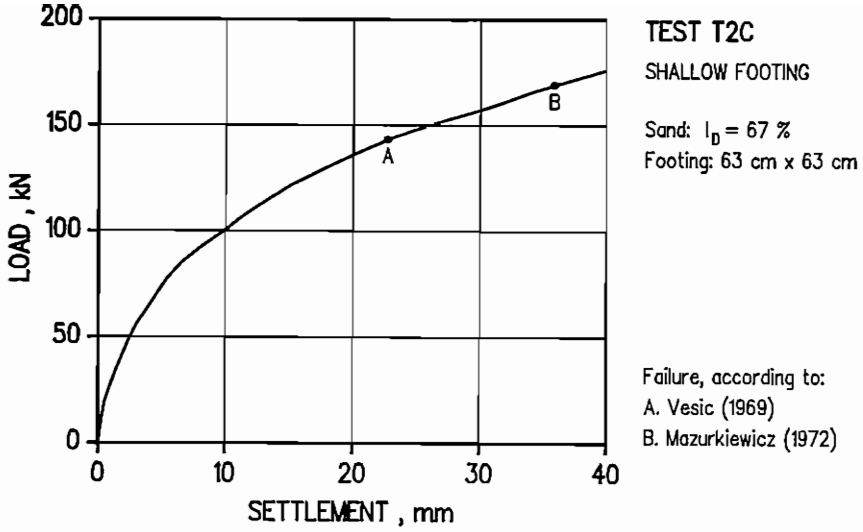

Fig. 5.9 Test on the shallow footing T2C - load-settlement curve

Single pile T2S

The test consisted of only one loading sequence to failure and was performed with load steps of about 1 kN up to a maximum load of 17 kN. The failure did not occur by plunging. The test result is shown in Fig.5.10, in which the point of failure, interpreted according to Vesic (1969) and Mazurkiewickz (1972), is presented.

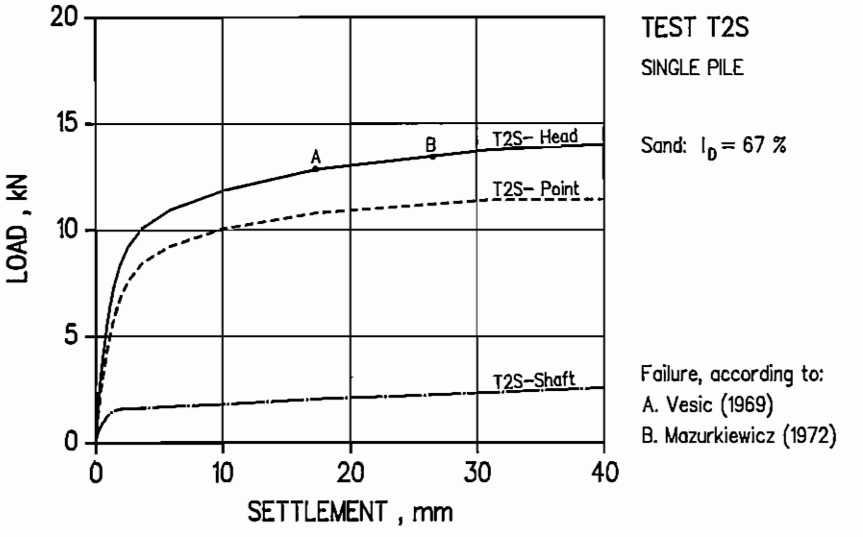

Fig. 5.10 Test on the single pile T2S - Load-settlement curve

Free-standing pile group T2G

The test was performed using one loading sequence to failure, with a maximum load of about 85 kN and load steps of 5 kN. Like in the test on single pile T2S, the failure did not occur by plunging. The point of failure of the group is determined according to Vesic's and Mazurkiewicz's methods using the load-settlement curve for the average pile, Fig.5.12. As in Test T1G in the first test series, the centre pile always takes the largest load portion. The dependence of the load distribution on the driving order is rather clear: the later the pile was driven, the lower the load, except for the first few load steps, in which case the load distribution is fairly random, Fig.5.11.

As in Test T1G, the point loads of the piles are independent of the driving order and are of the same order of magnitude for all the piles. The point loads are even smaller than that of the single pile. The shaft loads, like the head loads, clearly depend on the driving order and are much higher than that of the single pile. This means that compaction of soil due to pile driving has mainly influenced pile shaft friction. The average (head, shaft and point) loads per pile in Test T2G are shown in Fig.5.12. Comparison of Figures 5.12 and 5.10 shows that the total, shaft and base group efficiencies are 1.1, 3.2 and 0.85, respectively.

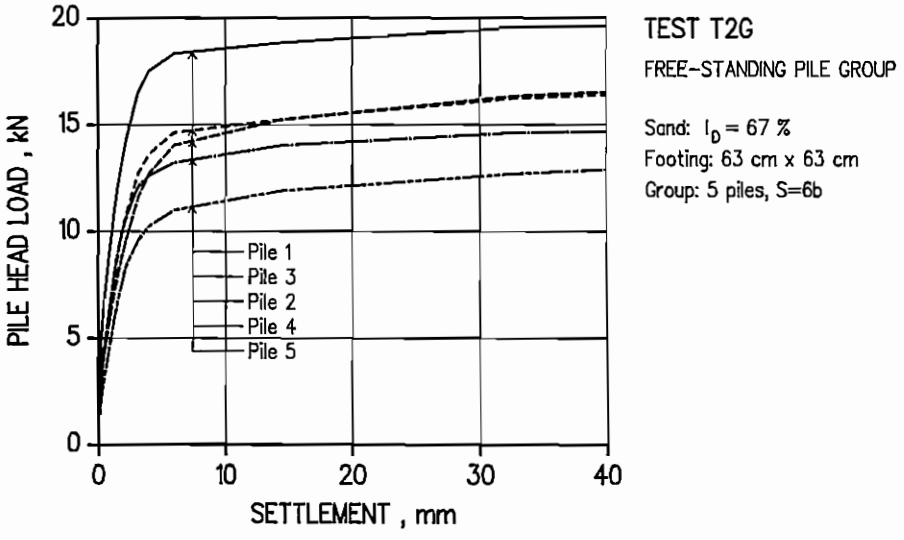

Fig 5.11 Test on the free-standing pile group T2G - Load-settlement curve

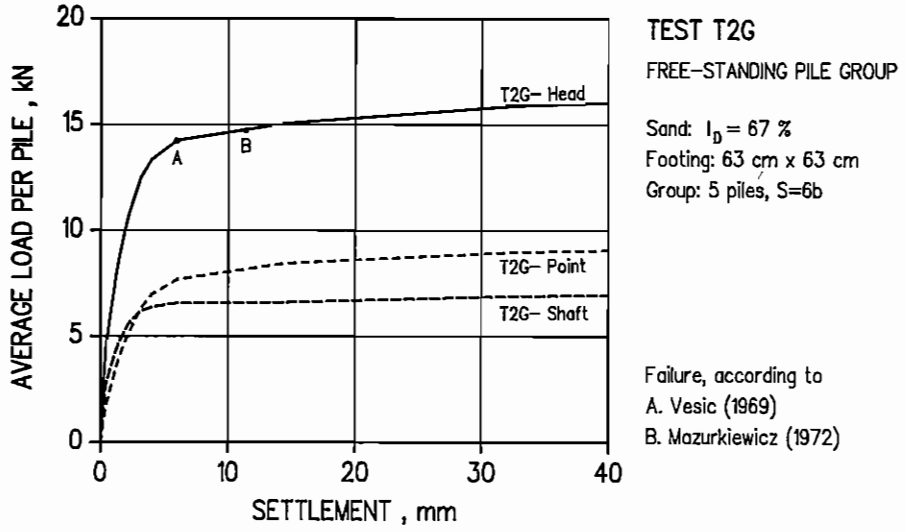

Fig. 5.12 Test T2G - Average load per pile.

Piled footing T2F

On completion of the test on the free-standing pile group T2G, the whole footing was pushed down until the bottom of the cap was about 20 mm above the soil surface. Test T2F was then started according to the second procedure of testing, see Section 3.3. This way of testing shows very clearly the effect of the cap on the behaviour of the piles. The test was performed as follows: (a) first loading up to about 340 kN, with a load step of about 20 kN (totally 17 steps); and (b) unloading to 0 kN with steps of 40 kN.

Fig.5.13 shows the load-settlement curve for the first loading in Test T2F. The cap comes into contact with the soil surface at a settlement of 24 mm. The initial part of the curve, when the settlement is less than 24 mm, shows the behaviour of the free-standing group before the cap comes into contact with soil, and the final part shows the behaviour of the piled footing.

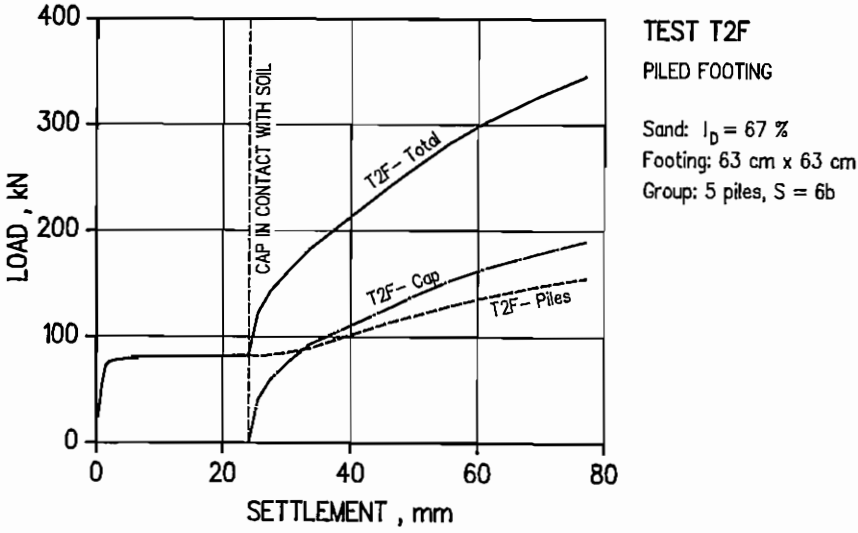

Fig 5.13 Test on the piled footing T2F - Load-settlement curve (original)

Failure of the free-standing pile group occurs by plunging before contact between the cap and the soil, and the failure load is nearly the same as in Test T2G. After contact, the applied load begins to be transferred to the cap, followed at first by a slight decrease in the pile load, and then a significant increase. Of course, the increase is due to the cap being in contact with the soil, and the decrease may be explained by the fact that immediately after contact, the downward movement of the soil under the cap causes a certain reduction in skin friction, Fig.5.14. Failure of the piles in the piled footing did not occur by plunging, and the settlement-hardening type of failure in Test T2F, in which the load on the piles progressively increases, is clearly due to the effect of the cap being in contact with soil. Fig.5.14 also shows that the cap mainly affects the pile shaft load and has no, or very small, influence on the point load. The decrease in the average pile point load in comparison with Test T2G can be explained by the fact that the pile point in Test T2F penetrated into in a deeper soil layer which was softer than that in Test T2G, see the CPT test results in Fig.4.2.

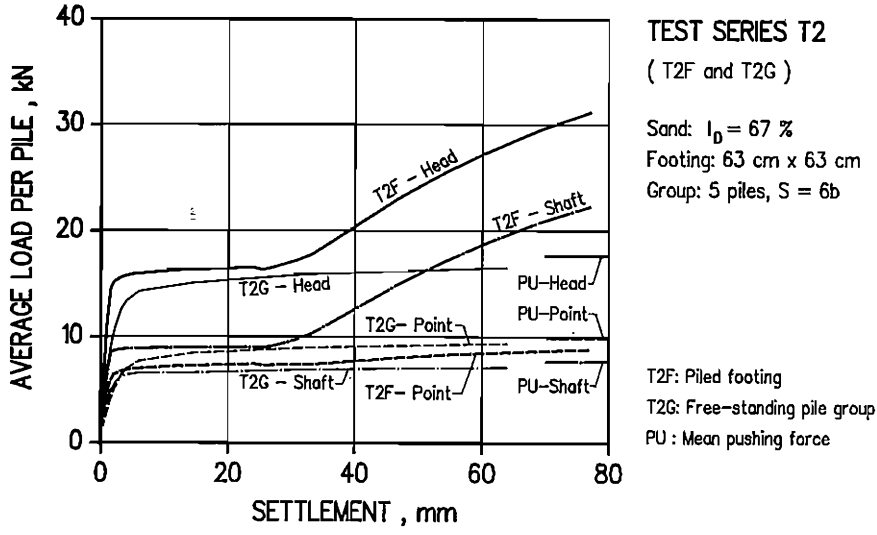

Fig. 5.14 Test series T2 - Average load per pile in Tests T2G and T2F

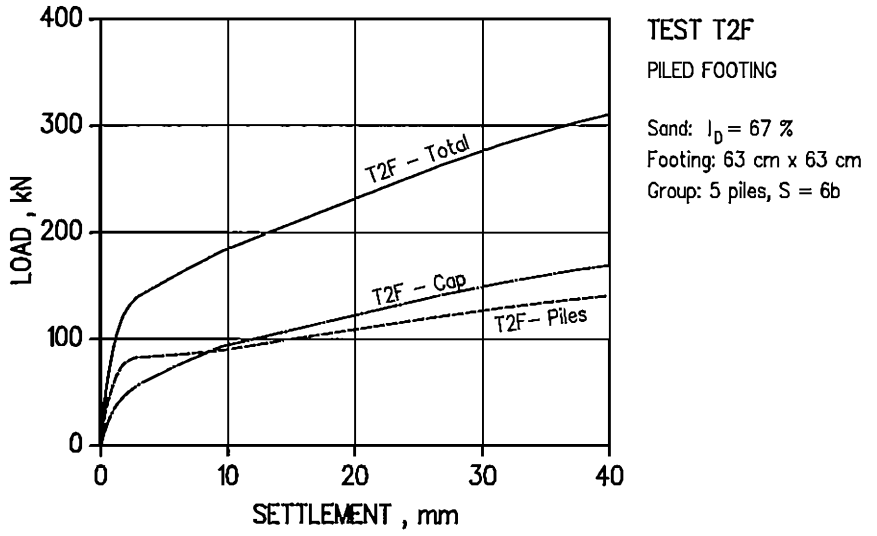

Fig 5.15 Test T2F - Load-settlement curve (modified from Fig.5.13)

This testing procedure shows very clearly the effect of the cap on the behaviour of the piles. However, the results cannot be directly compared with the results of the other tests in the series. For the sake of comparison, the original load-settlement curves in Fig 5.13 are modified in the following way: a) the load taken by the cap is exactly the same as in Fig.5.13, i.e. equal to the measured total load minus the load taken by the piles, but the corresponding settlement starts from zero; b) the pile load is taken as the initial part of the original pile load-settlement curve (before cap-soil contact) for small settlements, and as the final part of the original curve (after cap-soil contact) for larger settlements with the corresponding settlement starting from zero, and a transient curve is used to adapt the two parts of the modified curve, see Appendix A; and c) the total load on the footing is then equal to the sum of the loads taken by the cap and by the piles obtained in the previous steps a) and b). Fig.5.15 shows the curves obtained by modifying the original curves in Fig.5.13. The approximation concerns the load taken by the piles. It is based on a remark from Test series T1 that the initial stiffness of the piles in the piled footing (T1F) is almost the same as that of the free-standing pile group (T1G). The modified pile load-settlement curve is therefore approximated for small settlements, but accurate for large enough settlements.

Loads taken by the piles at failure in the free-standing pile group and in the piled footing are compared in Table 5.2. In the table, the pile loads at failure in the free-standing pile group are taken both from Test T2G, Column (2), and from the initial part of Test T2F before the contact, Column (3). Pile failure in the piled footing, according to Vesic's criterion, occurs at a settlement of 2.6 mm in the modified curve, that is equivalent to s = 26.6 mm in the original curve, Column (4). Load taken by the piles at settlements s = 20 mm and 30 mm in the modified curves, that are equivalent to s = 44 mm and 54 mm in the original curve, are also summarized in Table 5.2, Columns (5) and (6). By comparing the values in Column (3) with those in the three last columns in the table the influence of the cap can be directly seen and the other effects, such as deeper pile penetration, reconsolidation and recompression, are easily eliminated.

In Test T2F, the load distribution among the piles does not depend on the driving order. However, as in Test T2G, the centre pile always takes the largest load portion, even at pile failure. With increasing settlement, the load distribution becomes more uniform.

Table 5.2 Load distribution on piles in the group - Test T2G and T2F

a) Head loads, kN

Pile No. (1)	T2G at failure (2)	T2F initial (3)	T2F at failure (4)	T2F s = 20 mm (5)	T2F s = 30 mm (6)
1	18.4	18.0	19.2	24.5	28.2
2	14.0	14.4	14.9	21.0	24.4
3	14.6	16.7	18.5	23.6	27.1
4	13.2	14.7	16.0	21.4	24.9
5	11.0	13.7	14.1	19.4	22.7
All piles	71.2	77.5	82.7	109.9	127.3

b) Shaft loads, kN

(1)	(2)	(3)	(4)	(5)	(6)
1	11.6	11.4	11.9	16.8	20.3
2	5.6	8.4	8.1	13.7	16.7
3	6.0	9.0	9.6	14.0	17.0
4	5.6	7.1	7.5	12.0	15.1
5	4.1	8.3	8.3	13.4	16.3
All piles	32.9	44.2	45.4	69.9	85.4

c) Point loads, kN

(1)	(2)	(3)	(4)	(5)	(6)
1	7.9	6.6	7.3	7.7	7.9
2	9.6	6.0	6.8	7.3	7.7
3	9.5	7.7	8.9	9.6	10.1
4	8.3	7.6	8.5	9.4	9.8
5	7.7	5.4	5.8	6.0	6.4
All piles	43.0	33.3	37.3	40.0	41.9

Note: (1) = pile number, according to driving order
(2) = pile loads at failure according to Vesic's criteria in Test T2G
(3) = pile loads at failure in initial stage of Test T2F, before contact (free-standing pile group)
(4) = pile loads at failure in modified curve, equivalent to s=26.6 mm in original curve, Test T2F
(5), (6) = pile loads at s=20 mm and 30 mm in modified curve, equivalent to s=44 and 54 mm in original curve, Test T2F

The load portions taken by the cap and the piles in Test T2F can be also seen in Fig.5.16, which is established from the modified load-settlement curve in Fig.5.15. The distribution of the applied load among the cap and the piles varies with the load level. In the beginning of the test, the cap carries about 30 % of the total load and the average pile, about 14 %. At pile failure, the load carried by the cap increases rather quickly up to about 50 - 55 % of the total load. Meanwhile, the load taken by the piles increases at a rather low rate, and the average load per pile decreases to about 9 % of the total load, Fig.5.16.

Thus, when the load is applied on the piled footing, the piles start taking an important portion of the load, and, not until pile failure, a considerable load portion is transferred to the cap.

The results of Tests T2F, T2C and T2G are compared in Figs 5.17a and 5.17b using the original and modified load-settlement curves from Test T2F. The figures show that in comparison with Test T2G, the load taken by the piles in Test T2F is considerably larger. The increase occurs only in the pile shaft load due to the cap, and is much higher as the settlement of the footing increases. The load carried by the cap in Test T2F is somewhat lower than that in Test T2C at corresponding settlements. However, the two curves approach each other with increasing settlement. Presumably, the downward movement of the soil-cap interface, caused by downward pile displacement, slightly affects the load-settlement relationship of the cap. In the case of loose sand this effect is counteracted by soil compaction due to pile driving with consequential increase in cap load capacity.

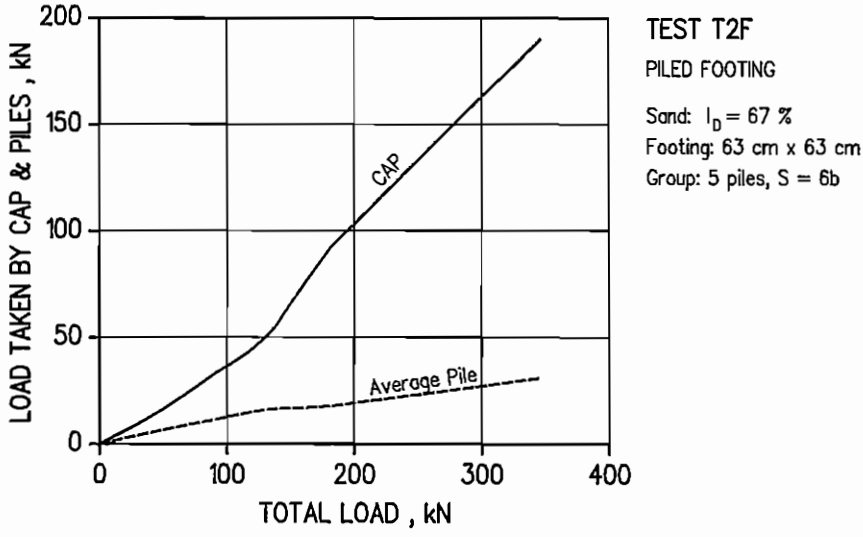

Fig. 5.16 Test T2F - Load distribution between cap and piles versus total load

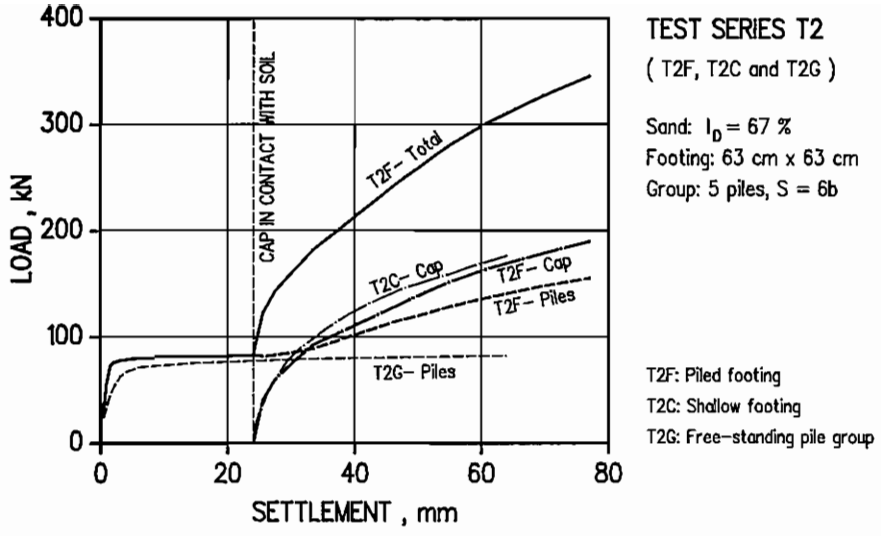

Fig. 5.17a Test series T2 - Comparison of separate tests, original T2F curves

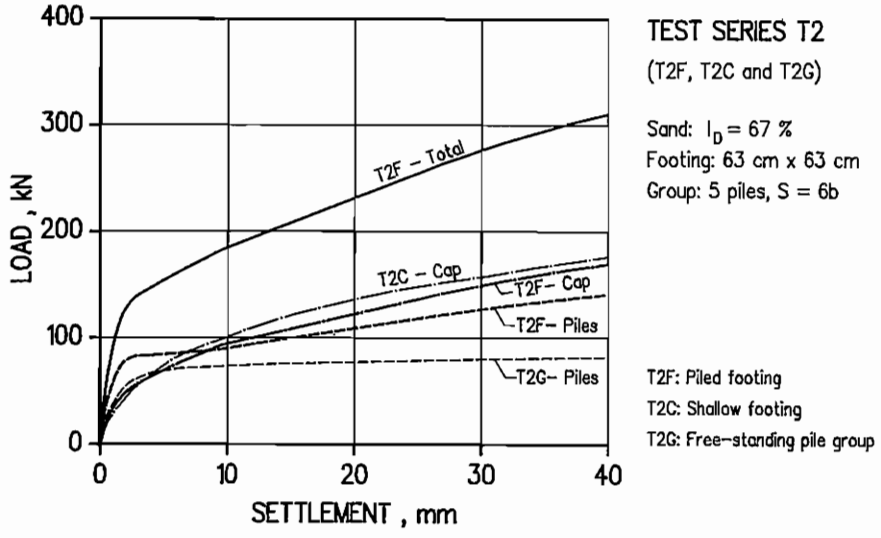

Fig. 5.17b Test series T2 - Comparison of separate tests, modified T2F curves

5.3 The Third Test Series (T3)

In Test series T3, the pile spacing was eight times the pile width, and the cap dimensions were 80 cm x 80 cm x 40 cm. The sand was slightly looser than that in Test series T2, with an average relative density I_D= 62%. The excavation was filled in layers of about 20 cm in thickness by pouring sand from a height of about 2 m, with one compaction pass by the same compactor used in Test series T2 (70 kg).

Shallow footing T3C

The test was carried out by first loading to 225 kN using load steps of 15 kN, then unloading to 0 kN with load steps of about 30 kN, and reloading again up to 270 kN with load steps of 30 kN. The load-settlement curve for the first loading is shown in Fig.5.18, in which the point of failure, interpreted according to Vesic (1973) and Mazurkiewicz (1972), is presented.

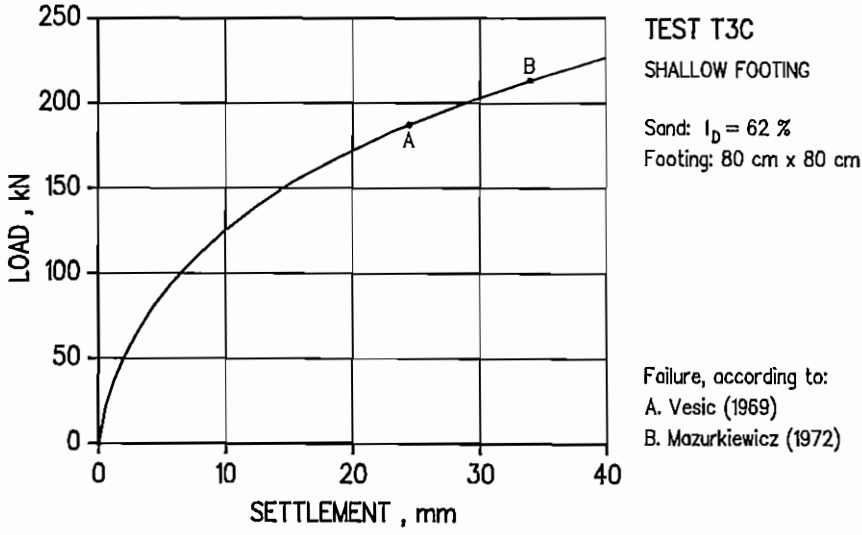

Fig. 5.18 Test on the shallow footing T3C - load-settlement curve

Single pile T3S

The test consisted of only one loading sequence to failure and was performed with load steps of about 1 kN up to a maximum load of 10 kN. The failure did not occur by plunging. The test result is shown in Fig. 5.19 and the point of failure, interpreted according to Vesic's and Mazurkiewicz's methods, is presented.

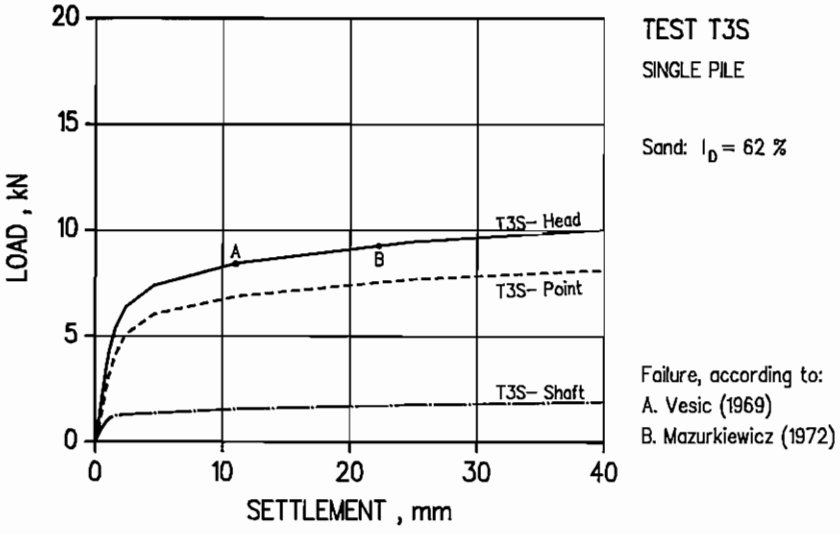

Fig. 5.19 Test on the single pile T3S - Load-settlement curve

Free-standing pile group T3G

The test was performed by one loading sequence to failure, with a maximum load of about 62.5 kN and load steps of 2.5 kN. Like in the test on single pile T2S, the failure did not occur by plunging. The failure point of the pile group is determined according to Vesic's and Marzukiewicz's methods using the load-settlement curve for the average pile, Fig.5.21. Before failure the centre pile carries the largest load portion. The load distribution seems to depend on the driving order: the later the pile was driven, the lower the load, except for Pile No.5. After failure, however, the influence of the driving-order seems to disappear, and even the centre pile takes a lower load than Pile No.2, Fig.5.20. From the measurement results it can be seen that the distribution of the pile shaft loads clearly depends on the driving order and the shaft load of the centre pile is almost double that of the other piles. After failure, the shaft load of the centre pile is reduced (strain-softening), and those of the other piles become more uniform. The point loads are independent of the driving order and are almost of the same magnitude for all the piles. As the point loads are predominant over the shaft loads, the driving-order dependence of the pile head loads is not clear.

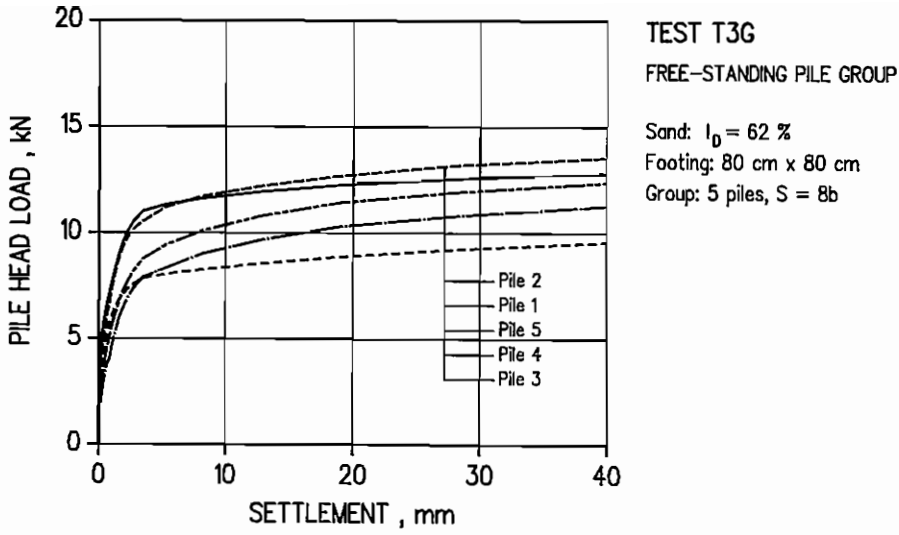

Fig 5.20 Test on the free-standing pile group T3G - Load-settlement curve

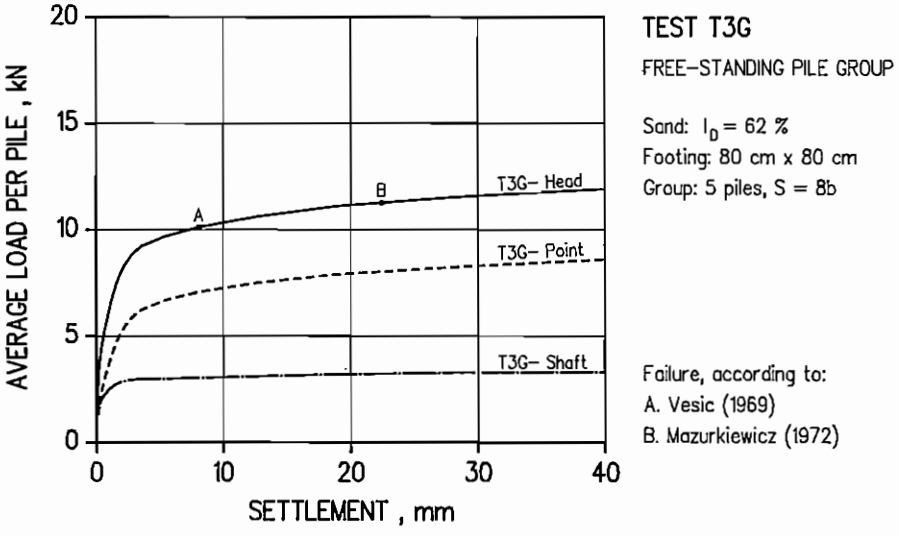

Fig. 5.21 Test T3G - Average load per pile

The point loads are quite comparable with that of the single pile. This means that compaction of soil due to pile driving has no, or very small, influence on the pile point loads. However, the pile shaft loads are higher than that of the

single pile. In particular, the shaft load of the centre pile is almost three times higher than that of the single pile. This means that compaction of soil due to pile driving mainly affects the pile shaft friction and the effect is considerable, although the pile spacing is as large as eight times the pile width, the largest spacing in all three test series. The average (head, shaft and point) loads per pile in Test T3G are shown in Fig.5.21. Comparison of Figures 5.21 and 5.19 shows that the total, shaft and base group efficiencies are 1.2, 2.0 and 1.03, respectively. Though the shaft efficiency is rather high, the total efficiency is near unity because the point loads are predominant over the shaft loads and the point efficiency is almost unity.

Piled footing T3F

As in the test series T2, on completion of the test on the free-standing pile group T3G, the whole footing was pushed down until the bottom of the cap was about 20 mm above the soil surface. Test T3F was then started according to the second testing procedure, see Section 3.3. Test T3F was performed as follows: (a) first loading up to about 360 kN with a total number of 20 load steps, using load steps of 10 kN for the first six steps (before contact) and load steps of 20 kN for the last thirteen steps (after contact); (b) unloading to 0 kN with load steps of 40 kN.

Fig.5.22 shows the load-settlement curve for the first loading in Test T3F. The cap comes into contact with the soil surface at a settlement of 20 mm. The initial part of the curve, when the settlement is less than 20 mm, shows the behaviour of the free-standing group, and the final part of the curve shows the behaviour of the piled footing, with the pile cap being in contact with soil.

The failure of the free-standing pile group (before cap-soil contact) occurs by plunging. After cap-soil contact, the applied load begins to be transferred to the cap, while the pile load slightly increases at first, then significantly increases later on. Pile failure in the piled footing did not occur by plunging, and the settlement-hardening feature of failure is clearly due to the effect of the cap being in contact with soil, Fig.5.22. The average (head, shaft and point) loads per pile in Tests T3F and T3G are compared in Fig.5.23. The pile point load after cap-soil contact is the same as before contact. On the other hand, the shaft load begins to increase after contact. This means that the cap affects only the pile shaft load and has no influence on the point load.

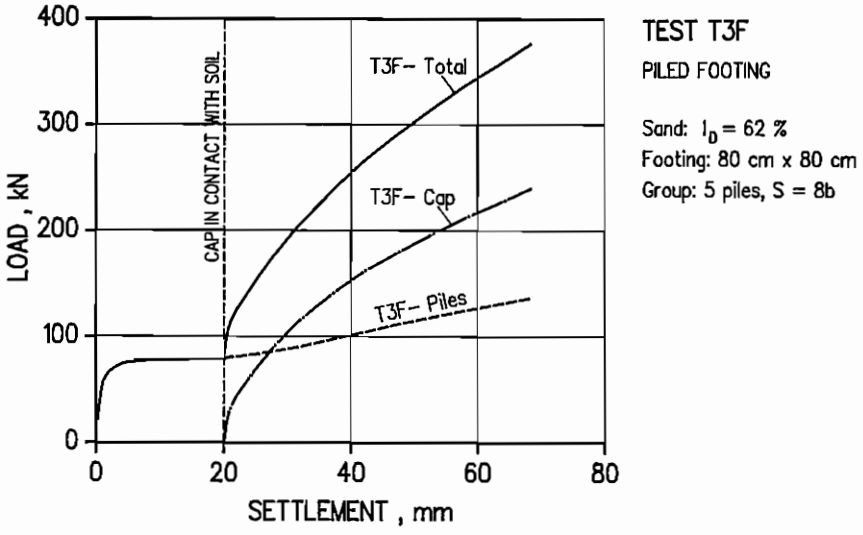

Fig 5.22 Test on the piled footing T3F - Load-settlement curve (original)

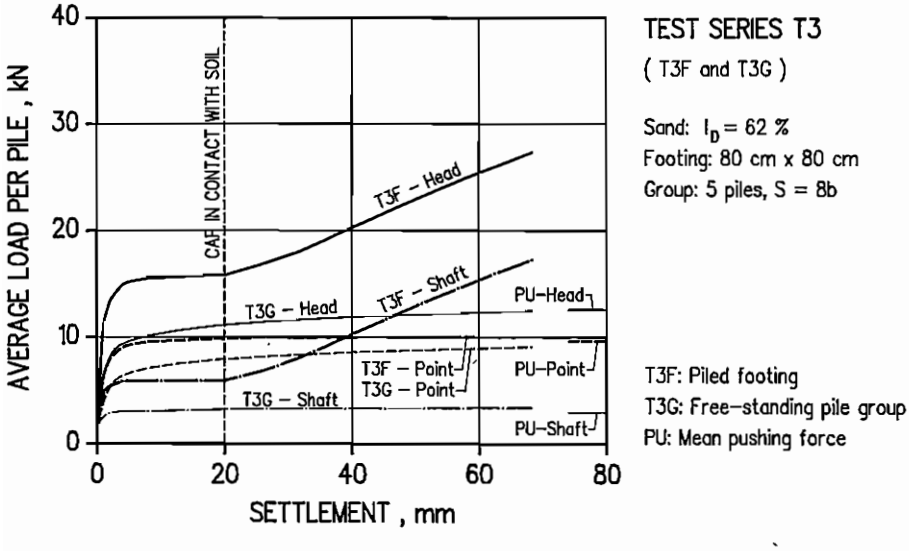

Fig. 5.23 Test series T3 - Average load per pile in Tests T3G and T3F

In order to facilitate a comparison of the different separate tests in the test series, the modified curves in Fig.5.24 are created from the original curves in Fig.5.22 in the same way as in Test T2F. Loads taken by the piles at failure in the free-standing pile group and in the piled footing are compared in Table 5.3. The pile loads at failure in the free-standing pile group are taken both from Test T3G, Column (2), and from the initial part of Test T3F before cap-soil contact, Column (3). Pile failure in the piled footing, according to Vesic's criterion, occurs at a settlement of 4 mm in the modified curve, corresponding to s = 24 mm in the original curve, Column (4). Loads carried by the piles at settlements s = 20 mm and 30 mm in the modified curves, which correspond to s = 40 mm and 50 mm in the original curve, are also summarised in Table 5.3, Columns (5) and (6). By comparing the values in Column (3) with those in the three last columns in the table, the influence of the cap can be directly seen and the other effects, such as deeper pile penetration, reconsolidation and recompression effects, are easily eliminated. It can bee seen that the increase in pile shaft load in the piled footing at failure, Column (4), in comparison with that in the free-standing pile group, Column (3), is not so large. However, the increase becomes much larger with an increasing settlement of the footing, Columns (5) and (6).

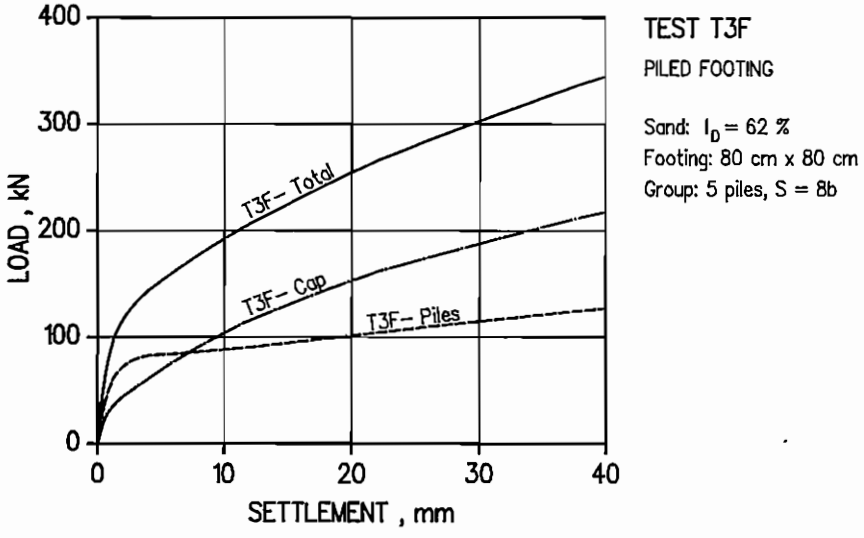

Fig 5.24 Test T3F - Load-settlement curve (modified from Fig.5.22)

Table 5.3 Load distribution on piles in the group - Test T3G and T3F

a) Head loads, kN

Pile No. (1)	T3G at failure (2)	T3F initial (3)	T3F at failure (4)	T3F s = 20 mm (5)	T3F s = 30 mm (6)
1	11.6	15.7	17.3	18.4	22.8
2	11.7	14.3	15.8	17.0	22.3
3	8.2	13.8	15.8	17.5	23.7
4	9.0	15.1	16.4	17.5	22.6
5	10.1	15.9	17.3	18.2	23.3
All piles	50.6	74.8	82.6	88.6	114.7

b) Shaft loads, kN

(1)	(2)	(3)	(4)	(5)	(6)
1	5.1	6.3	7.4	8.9	13.3
2	2.8	4.1	4.7	5.8	11.1
3	2.7	6.0	7.3	8.3	14.2
4	2.5	6.5	7.0	8.1	13.1
5	2.1	6.3	6.5	7.6	12.8
All piles	15.2	29.2	32.9	38.7	64.5

c) Point loads, kN

(1)	(2)	(3)	(4)	(5)	(6)
1	6.5	9.4	9.9	9.5	9.5
2	8.9	10.2	11.1	11.2	11.2
3	5.5	7.8	8.5	9.2	9.5
4	6.5	8.6	9.4	9.4	9.5
5	7.9	9.6	10.8	10.6	10.5
All piles	35.4	45.6	49.7	49.9	50.2

Note: (1) = pile number, according to driving order
(2) = pile loads at failure according to Vesic's criterion , Test T3G
(3) = pile loads at failure in free-standing pile group, Test T3F - initial stage, before contact
(4) = pile loads at failure in modified curve, corresponding to s=24 mm in original curve, T3F
(5),(6) = pile loads at s=20 mm and 30 mm in modified curve, corresponding to s=40 and 50 mm in original curve, Test T3F.

In Test T3F, the load carried by the various piles is quite equal, not dependent on the driving order, neither on the pile position (centre or corner). After failure, with increasing settlement, the load distribution becomes even more uniform.

The load portions taken by the cap and the piles in Test T3F can be also seen in Fig.5.25, which is established from the modified load-settlement curve in Fig.5.24. The share of the applied load between the cap and the piles varies with the load level. In the beginning of the test, the cap carries about 32 % of the total load and the average pile about 13 %. After pile failure, the load taken by

the cap increases rather rapidly up to about 63 % of the total load. Meanwhile, the load taken by the piles increases at a rather low rate, and the average pile load decreases to about 7 % of the total load, Fig.5.25. In consequence, an important part of the load applied was first carried by the piles, and not until pile failure, a considerable portion of the load was transferred to the cap.

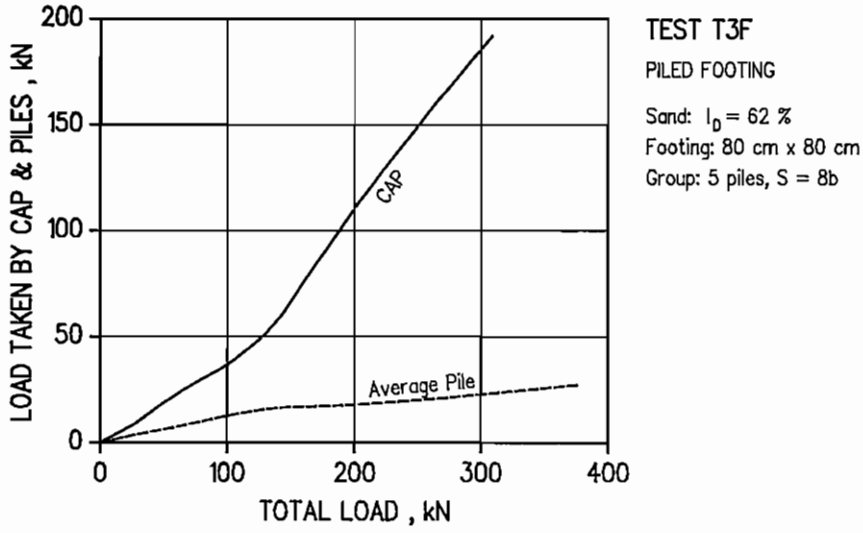

Fig. 5.25 Test T3F - Load distribution between cap and piles versus total load

The results of Tests T3F, T3C and T3G are compared in Figs 5.26a and 5.26b using the original and modified load-settlement curves from Test T3F. The figures show that in comparison with Test T3G, the load taken by the piles in Test T3F is considerably larger. The increase occurs only in the pile shaft load due to the cap, and is much higher as the settlement of the footing increases. As in Test series T2, the load taken by the cap in Test T3F is somewhat lower than that in Test T3C at corresponding settlements. However, the two curves approach each other with increasing settlement.

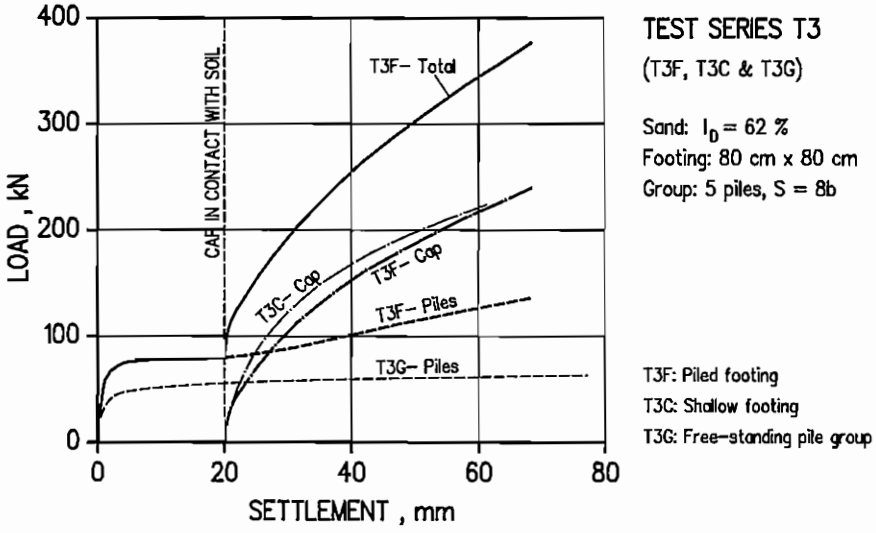

Fig. 5.26a Test series T3 - Comparison of separate tests, original T3F curves

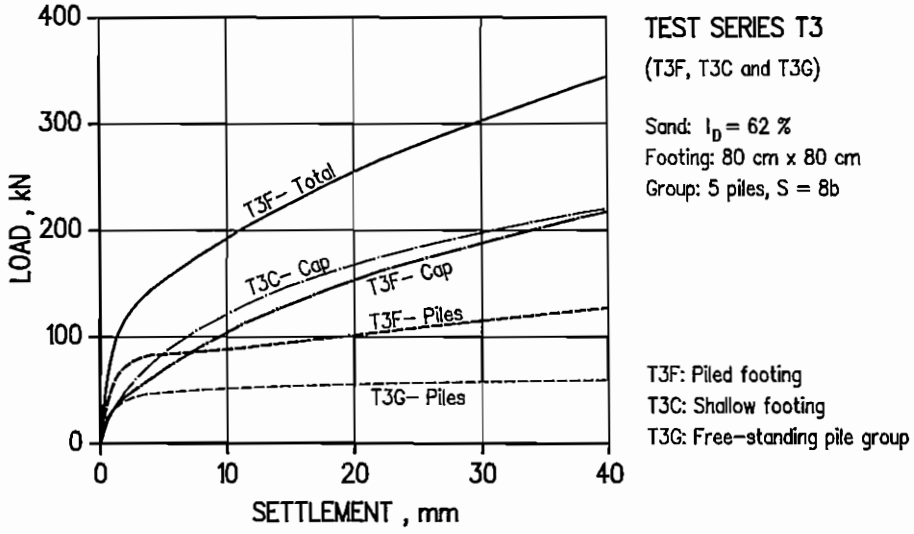

Fig. 5.26b Test series T3 - Comparison of separate tests, modified T3F curves

6. ANALYSIS OF THE FIELD MODEL TEST RESULTS

6.1 Lateral Earth Pressure against the Pile Shaft

The lateral earth pressure against the pile shaft was measured for Pile No.1, (i.e. the pile in the centre of the groups) by means of Glötzl total stress cells. The main purpose of the measurement was to study the effect of the cap being in contact with the soil on the pile behaviour. In the test on the piled footings, the cells were read every second load step. Moreover, the cells were read before and after each test series, before and after driving each pile, as well as before and after the tests on single piles and free-standing pile groups. The results will be shown in the form of the increase in lateral pressure against the pile shaft as compared with the readings before the test. The intention is to separate the effect of the cap on the lateral pressure from other sources such as compaction effects due to pile driving, time effects, testing effects (change of lateral pressure before and after the tests on the single pile and the free-standing pile group).

In Test series T1, the measurement data were unreliable due to malfunction. In Test series T2 and T3, eight new cells were installed on the two opposite sides of the pile, A and C. In the tests on the piled footings, Cells A1 and C1 were located at a depth of 0.5 m from the cap; Cells A2, C2 at 0.75 m; Cells A3, C3 at 1.25 m; and Cells A4, C4 at 1.75 m. The pile point was located at 2.3 m. As Tests T2F and T3F were performed according to the second testing procedure, see Section 3.3, the increase in lateral pressure on the pile shaft can be observed for both the free-standing pile groups (before cap-soil contact) and for the piled footings (after cap-soil contact).

Test T2F - measurement results

In Fig.6.1, the (total) increase in lateral pressure against the pile shaft is plotted versus settlement for sides A and C of the pile. For a certain reason, Cell A3 did not work. The initial part of the curves, when the settlement is less than 24 mm, corresponds to the free-standing group before the cap comes into contact with the soil, and the final part corresponds to the piled footing after cap-soil contact.

Before cap-soil contact, the lateral pressure increases only at the lower cells C3, A4, and C4, while the readings from the upper cells A1, C1, A2, C2 are

almost zero. This can be explained by the fact that a compacted zone develops around the pile tip at pile failure. The compacted zone causes the pressure to increase only at the lower cells, not at the upper cells near the ground surface. Another possible reason is that the volume of sand increases due to dilatancy. This effect is larger the higher the stress level is.

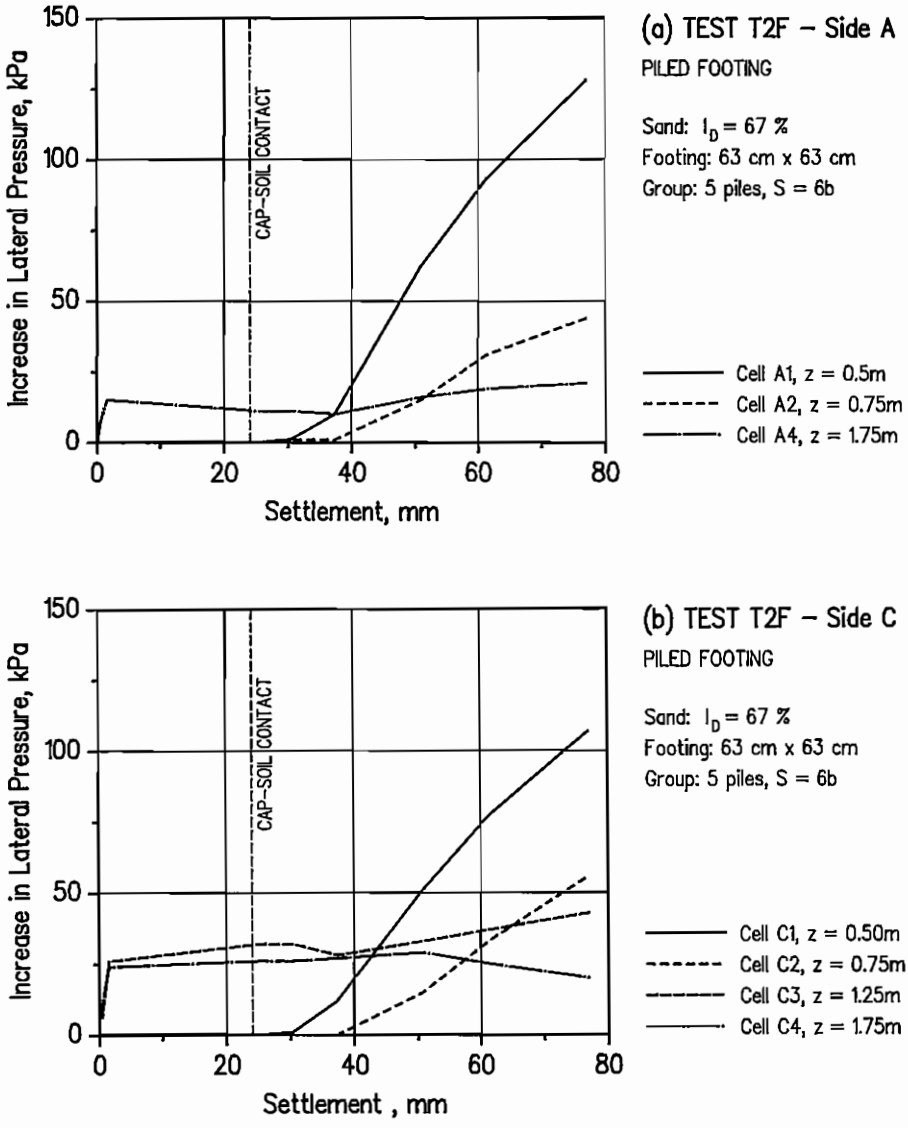

Fig. 6.1. Test T2F - Increase in lateral earth pressure against the pile shaft, total effect. (a) Side A; (b) Side C.

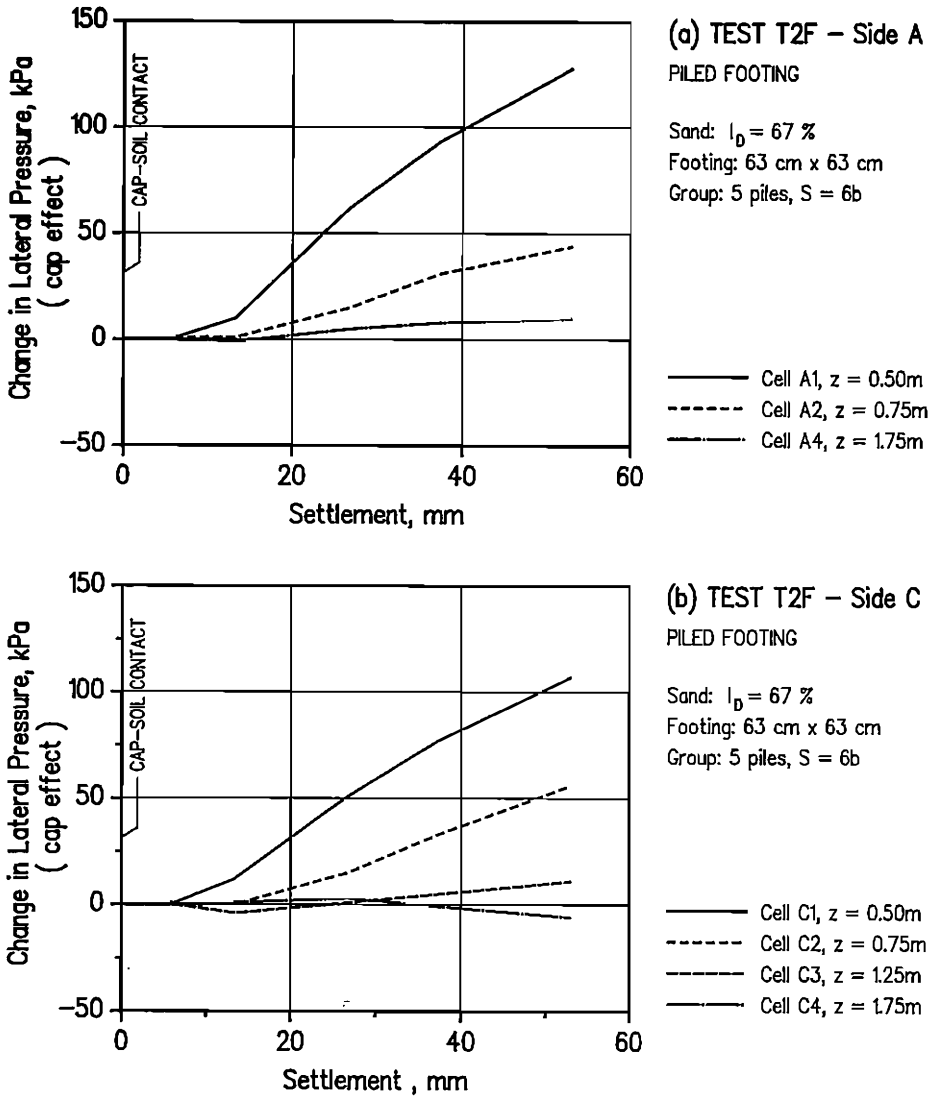

Fig. 6.2. Test T2F - Change in lateral pressure against pile shaft due to cap effect versus settlement (after contact). (a) Side A; (b) Side C

The pressure increase due to the cap coming into contact with soil will add to the effect of the pile failure zone. The effect of the cap-soil contact is predominant for the upper cells, while the effect of the pile failure zone is predominant for the lower cells. The pressure change due to the cap can be obtained by subtracting the pressure increase at cap-soil contact from the total increase. The term "pressure change due to the cap" may not be completely

correct here because the pile failure zone may still have some influence on the lower cell after contact. This term should be understood as the change in earth pressure in comparison with the value at cap-soil contact, and therefore it can have even a negative value. The changes in lateral pressure against the pile shaft due only to the effect of the cap are plotted versus the settlement of the piled footing (after cap-soil contact) in Fig.6.2, as well as versus the load carried by the cap in Fig.6.3.

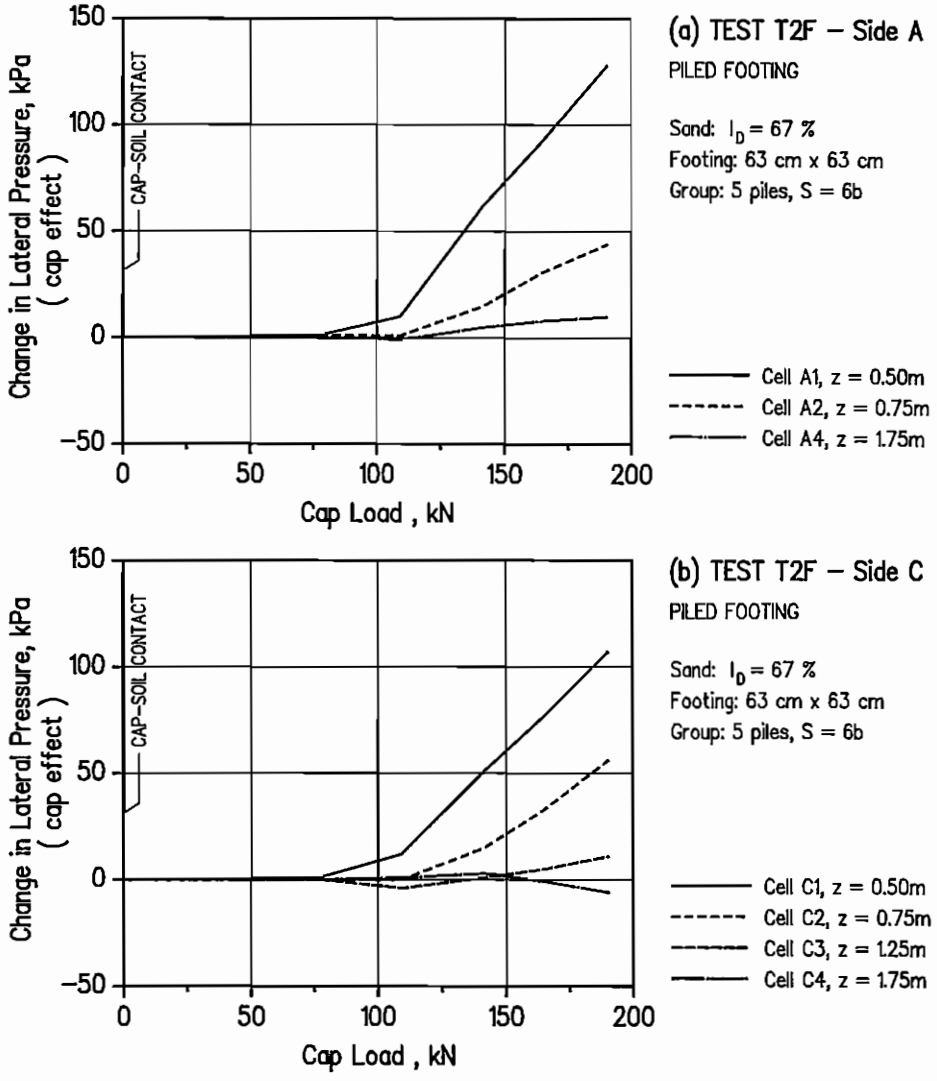

Fig. 6.3. Test T2F - Change in lateral pressure against pile shaft due to cap effect versus cap load (after contact). (a) Side A; (b) Side C

These figures show that the cap-soil contact pressure has a large influence on the lateral earth pressure against the pile shaft, especially for the cells close to the cap. The influence clearly decreases with increasing depth. On the lowest cells A4 and C4, the cap has no or very little influence. From Fig.6.3 it can also be seen that at cap loads smaller than about 100 kN the pressure increase is quite small. Thereafter, it increases very fast with increasing cap load. The changing point seems to correspond fairly well with the failure point of the piled footing, see Fig.5.17b.

The increase in lateral pressure against the pile shaft is plotted versus depth in Fig.6.4. Fig.6.4a shows the increase in pressure before contact due to pile failure (pile effect). Fig.6.4b shows the total increase in pressure due to both pile and cap effects (total effect). In Fig.6.4c, the pressure change due only to the cap-soil contact (cap effect), relative to the readings at contact, is presented. In Fig.6.4, P_{ft} means the total applied load, and P_{fc} the load carried by the cap. The total load steps in Fig.6.4b correspond to the cap load steps in Fig.6.4.c. From Fig.6.4, it can be seen that pile failure has an influence on the lower part of the pile, close to the pile point , while the cap-soil contact pressure has an influence on the upper part of the pile, close to the cap. The middle part of the pile can be influenced by both the above effects.

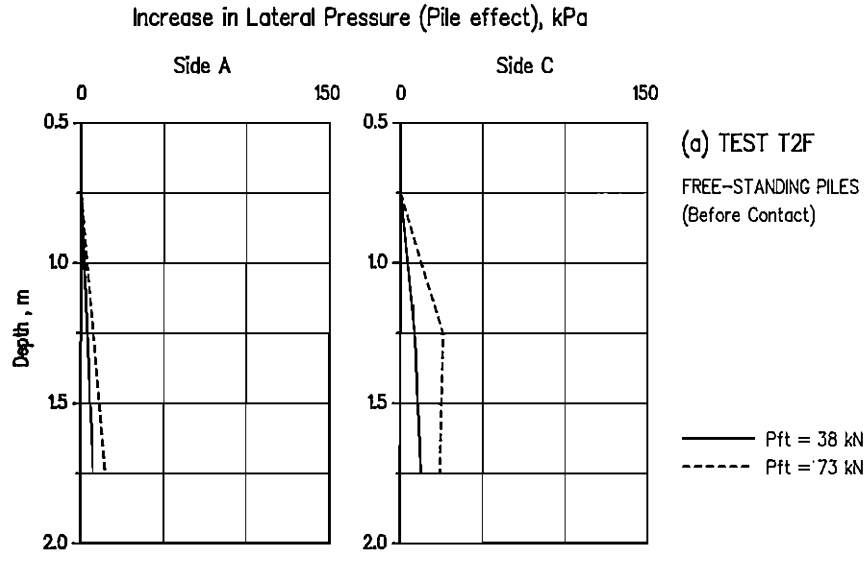

Fig. 6.4. Test T2F - Increase in lateral earth pressure against pile shaft versus depth. (a) Pile effect (before contact)

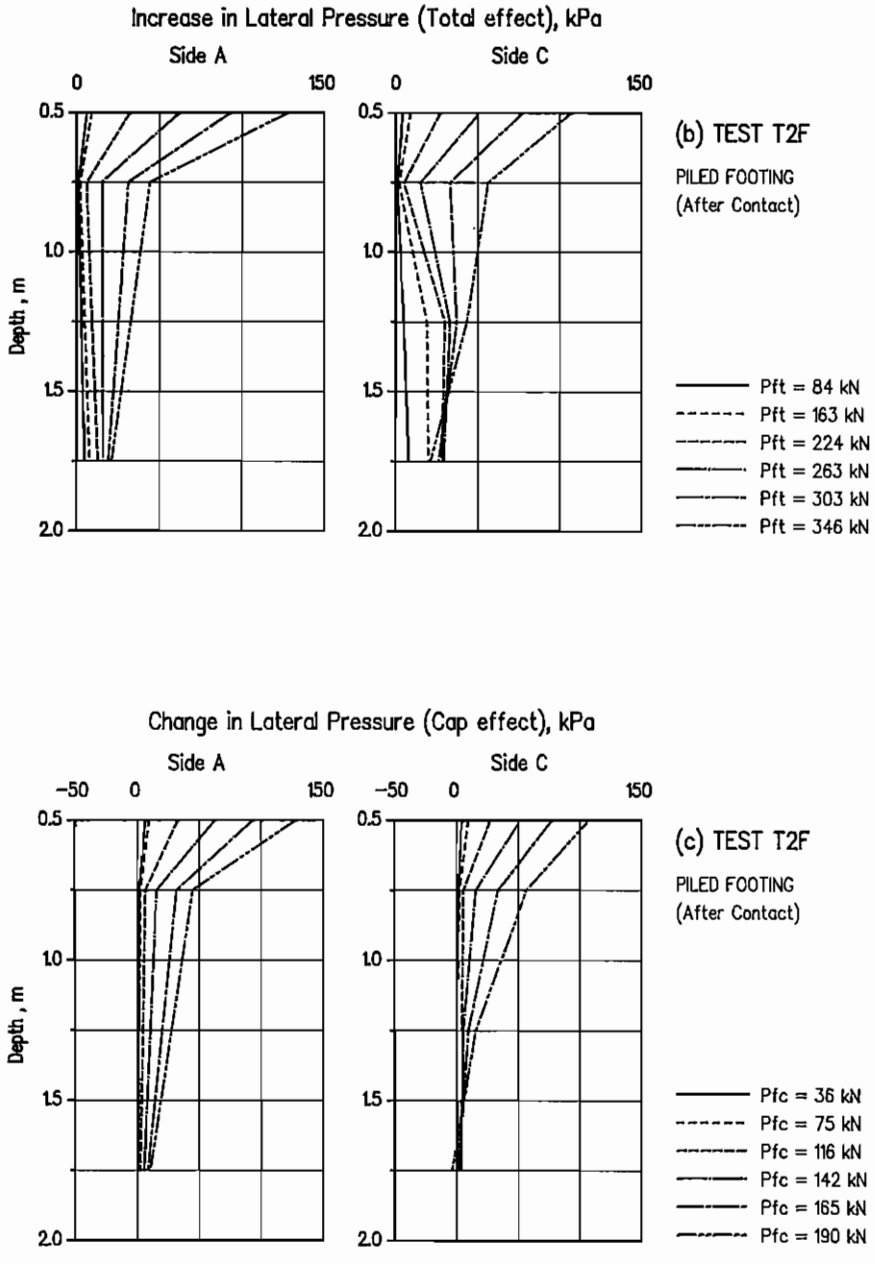

Fig. 6.4. Test T2F - Increase in lateral earth pressure against pile shaft versus depth. (b) Total effect (after contact); (c) Cap effect (after contact).

Test T3F - measurement results

The increase in lateral pressure against the pile shaft for Test T3F is plotted versus settlement in Fig.6.5 . As in Test T2F, Cell A3 did not work. The initial part of the curves, when the settlement is less than 20 mm, corresponds to the free-standing piles before the cap comes into contact with the soil, and the final part corresponds to the piled footing after cap-soil contact.

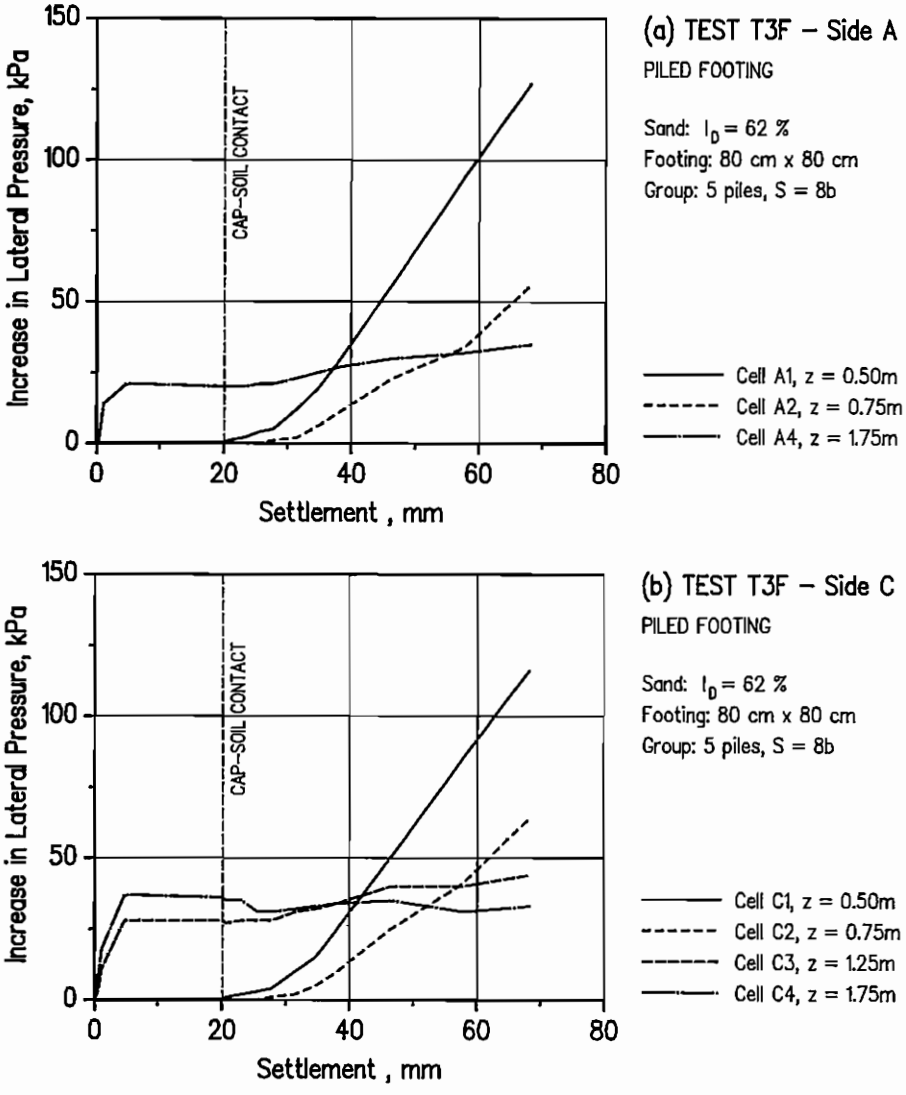

Fig. 6.5. Test T3F - Increase in lateral earth pressure against the pile shaft, total effect. (a) Side A; (b) Side C.

As in Test T2F, the lateral pressure before contact increases only at the lower cells, while the readings from the upper cells are almost zero. As stated above this can be explained as an effect caused by pile failure.

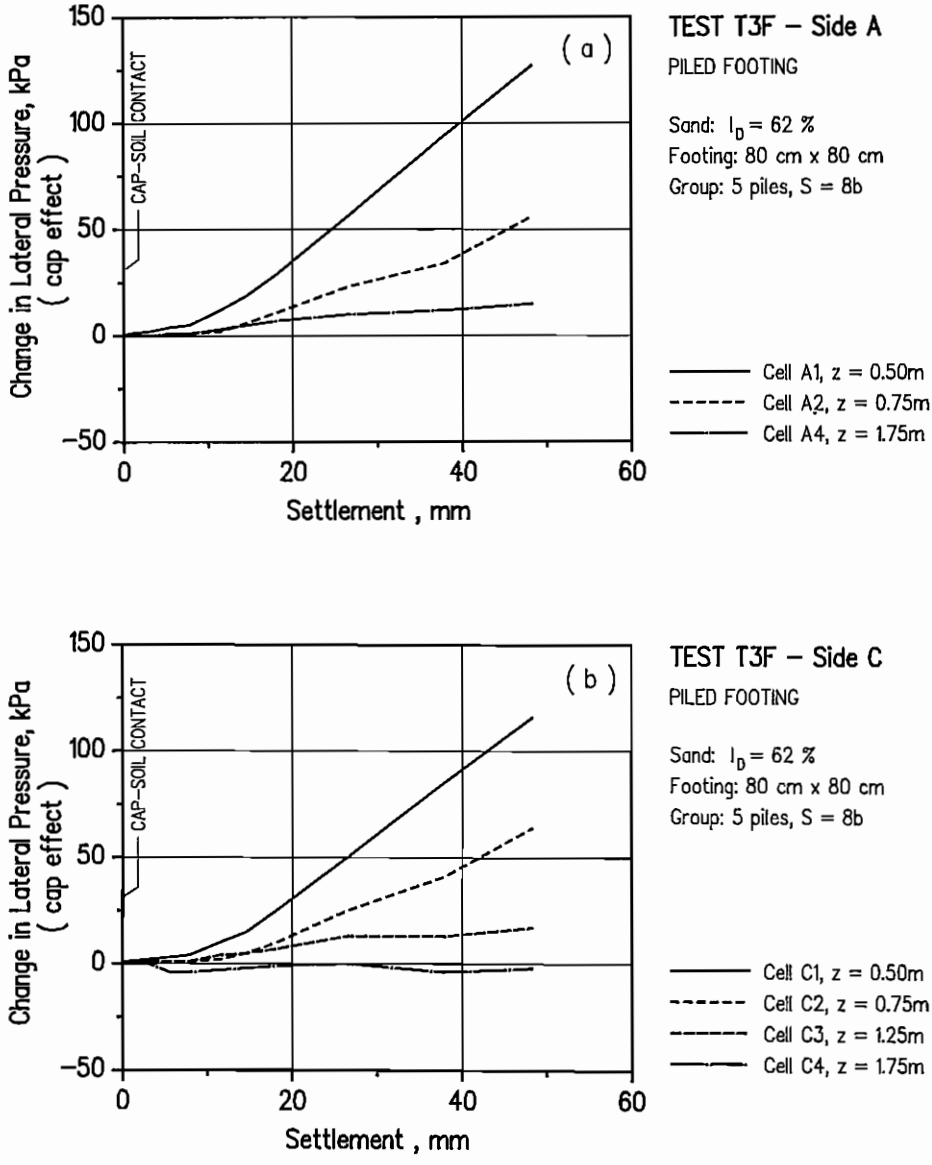

Fig. 6.6. Test T3F - Change in lateral pressure against pile shaft due to cap effect versus settlement (after contact). (a) Side A; (b) Side C

After cap-soil contact, the cap has a large influence on the lateral pressure against the pile shaft, especially against the upper part of the pile (Cells A1, A2, C1, C2). The change in lateral pressure against the pile shaft due to the

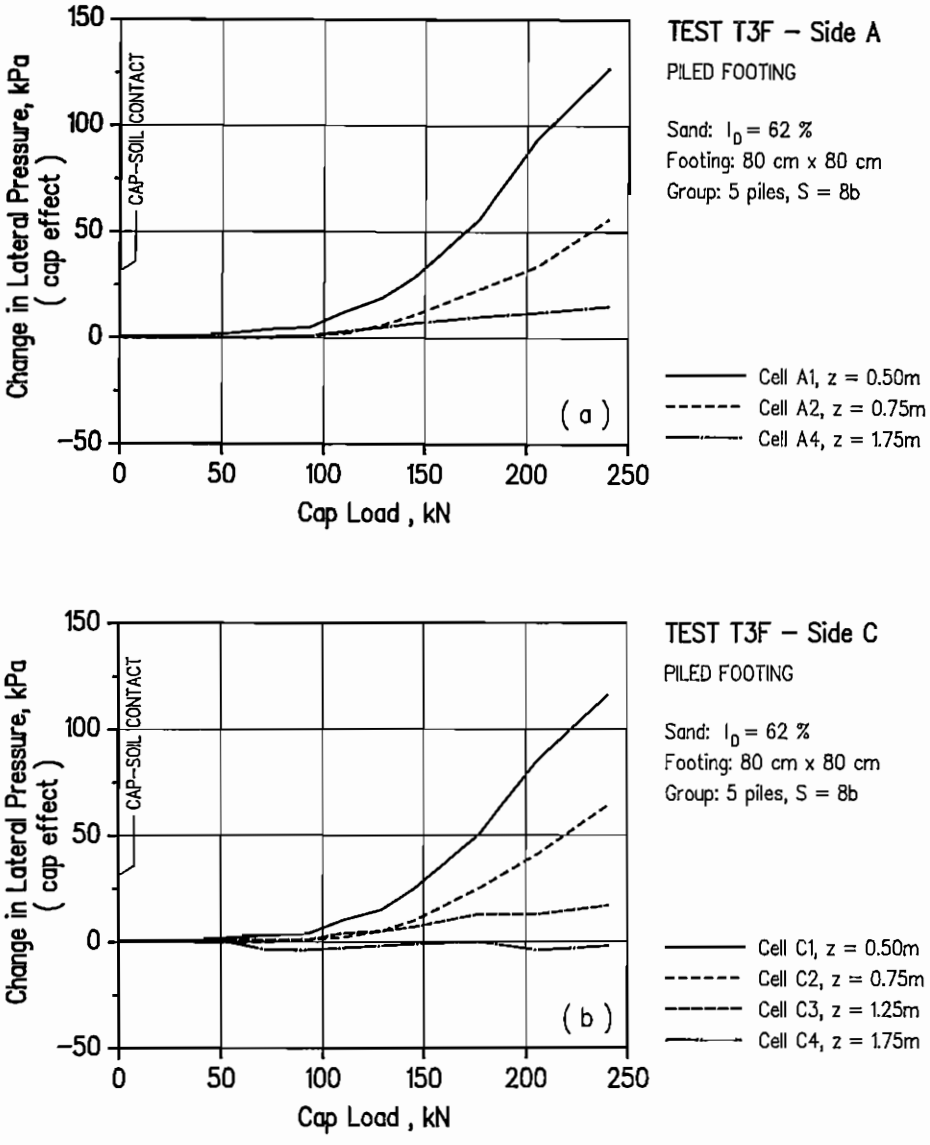

Fig. 6.7. Test T3F - Change in lateral pressure against pile shaft due to cap effect versus cap load (after contact). (a) Side A; (b) Side C

cap alone in relation to the readings at contact, is plotted versus the settlement of the piled footing in Fig. 6.6, as well as versus the load carried by the cap in Fig. 6.7. These figures show that the cap has a large influence on lateral earth pressure against the pile shaft, especially for the cells close to the cap. The influence clearly decreases with increasing depth. At the lowest cells A4 and C4, the cap has no or very little influence. As in Test T2F, it can also be seen in Fig.6.7 that for cap loads smaller than about 100 kN the pressure increase is quite small. Thereafter, it increases very quickly with increasing cap load. The changing point seems to correspond to the failure point of the piled footing.

The increase in lateral pressure against the pile shaft is plotted versus depth in Fig.6.8. The total load steps in Fig.6.8b correspond to the cap load steps in Fig.6.8c. Similar conclusions as in Test T2F can be obtained from Fig.6.8, namely that pile failure has an influence on the lower part of the pile , while the contact pressure against the cap has an influence on the upper part, close to the cap. The middle part of the pile can be influenced by both the above effects.

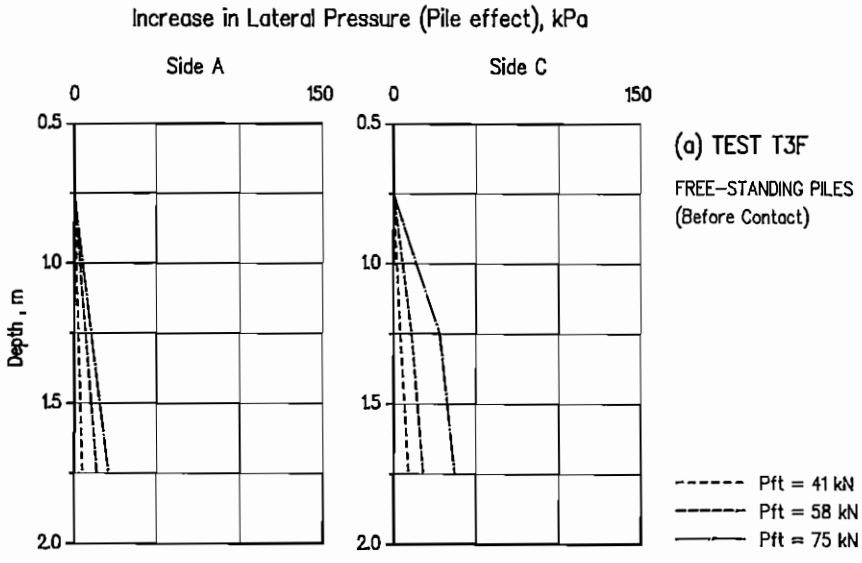

Fig. 6.8. Test T3F - Increase in lateral earth pressure against pile shaft versus depth. (a) Pile effect (before contact)

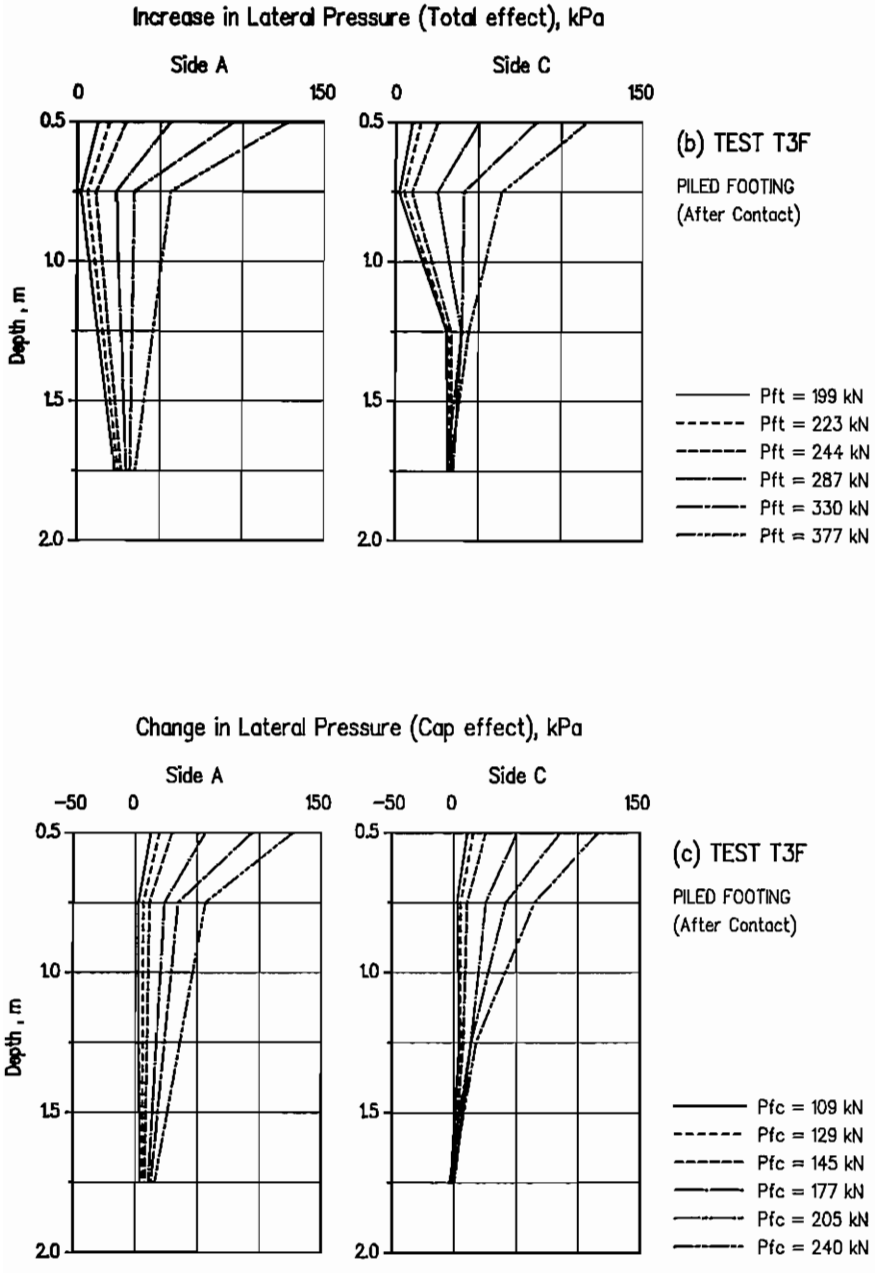

Fig. 6.8. Test T3F - Increase in lateral earth pressure against pile shaft versus depth. (b) Total effect (after contact); (c) Cap effect (after contact).

6.2 Distribution of Axial Pile Load

The distribution of the axial load of the pile with depth was measured for Pile No.5, the last driven corner pile of the group. In addition to the pile top and the pile tip transducers, an extra load transducer was placed in the middle of the pile.

Free-standing Pile Group

The distribution of the axial pile load is shown in Fig.6.9 for all three tests on the free-standing pile groups, T1G, T2G and T3G, for selected total loads applied on the groups P_g. In these tests, the ratio between pile length and pile width is the same, L/b = 35. According to the results of the tests, the shape of the curves is almost identical in the three tests: the skin friction in the upper part of the pile is very small and the point resistance contributes considerably to the total pile load, especially in denser sands, T2G and T3G.

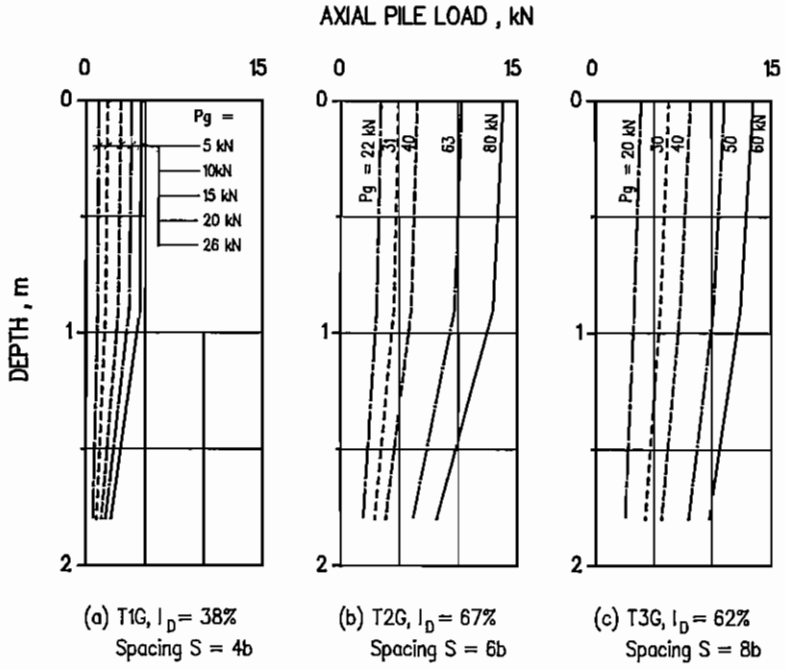

Fig 6.9 Free-standing pile group - Distribution of axial pile load versus depth (a) Test T1G; (b) Test T2G; (c) Test T3G

These results are quite typical for short, stiff piles in sand, see Joshi et al. (1989) and Ekström (1989). One of the reasons why the skin friction is so small in the upper part of the pile is the loss of contact between pile and soil due to pile driving. This can happen even for full scale piles. Joshi et al. (1989) performed a number of laboratory model tests on single piles, in which the pile dimensions and the sand were rather similar to the present tests, but with more detailed pile load measurement. They found that as a result of low pile deformation and corresponding high relative displacement between pile point and adjacent soil, the skin friction distribution is basically triangular and the ultimate skin resistance remained constant beyond a L/d ratio of 21, in which d is the pile diameter.

Piled Footing

The tests on the piled footings were performed in two different ways: Test T1F according to the first procedure, and Tests T2F and T3F according to the second procedure, see Section 3.3. Fig 6.10 shows the load-settlement curves for pile head, middle and point loads in all three test series. The distribution of the axial pile load is shown in Fig.6.11 for selected cap loads P_{fc}. One of the main purposes of the measurement was to study the change in pile behaviour under the effect of cap-soil contact pressure. The changes in axial pile loads in relation to the values obtained just before cap-soil contact show the cap effect alone. This way of treating the test results can only be done for Tests T2F and T3F, which were performed according to the second test procedure. The increase in axial pile loads due to the cap effect is shown in Fig.6.12 for selected cap loads P_{fc} in Tests T2F and T3F. The figure indicates that the cap-soil contact pressure has a large influence on the upper part of the pile, and almost no influence on the lower part. This is very similar to the conclusions obtained from the measurement of lateral earth pressure against the pile shaft, see Section 6.1.

As with lateral pressure against the pile shaft, the increase in pile axial load can be plotted against the settlement of the footing, Fig. 6.13a and c, and against the load carried by the cap, Fig. 6.13b and d. From these figures, conclusions similar to those in Section 6.1, can be drawn, namely that the increase in the axial pile load is quite small at small cap load levels, but grows very quickly at large enough cap load levels. The changing point corresponds to the ultimate load of the piled footings at a settlement of about 5 to 7 mm after cap-soil contact.

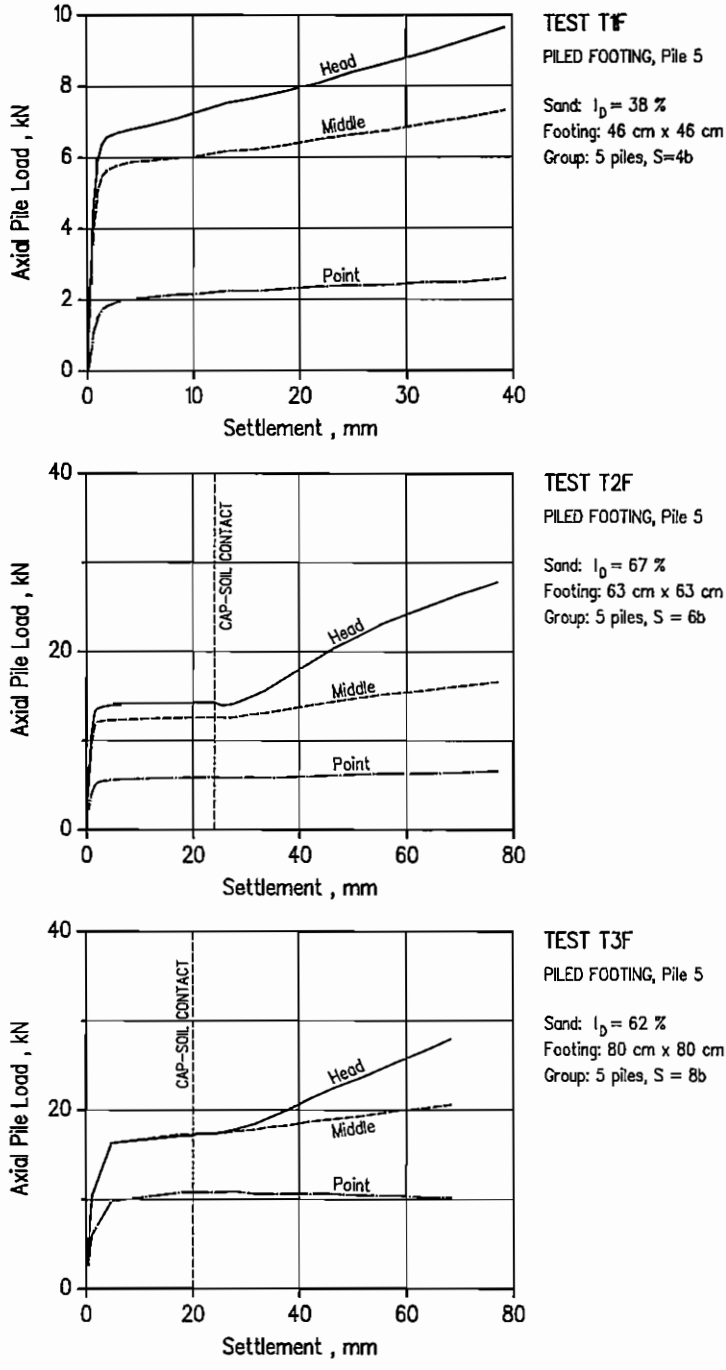

Fig.6.10 Piled footing - Pile head, middle, point load versus settlement curves (a) Test T1F; (b) Test T2F; (c) Test T3F.

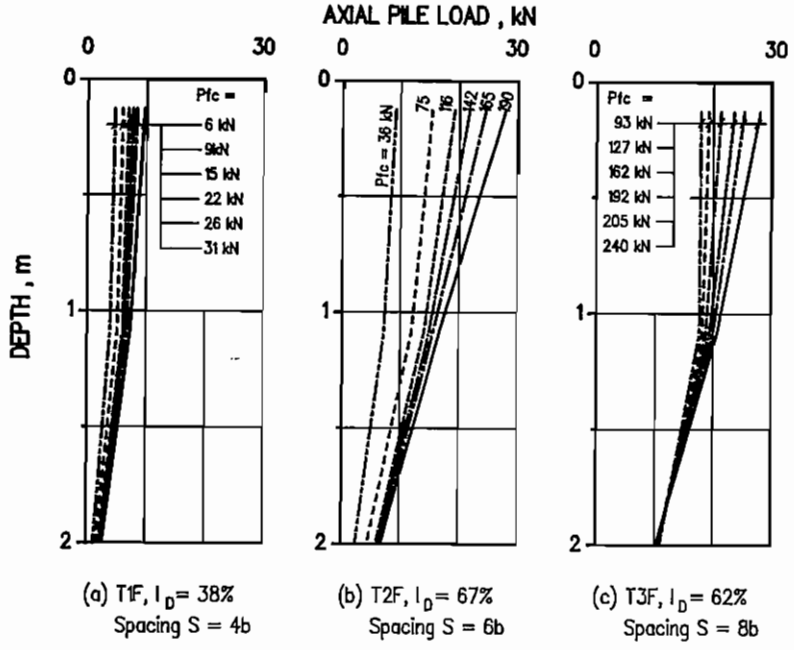

Fig.6.11 Piled footings - Distribution of pile axial load versus depth, total effect. (a) Test T1F; (b) Test T2F; (c) Test T3F.

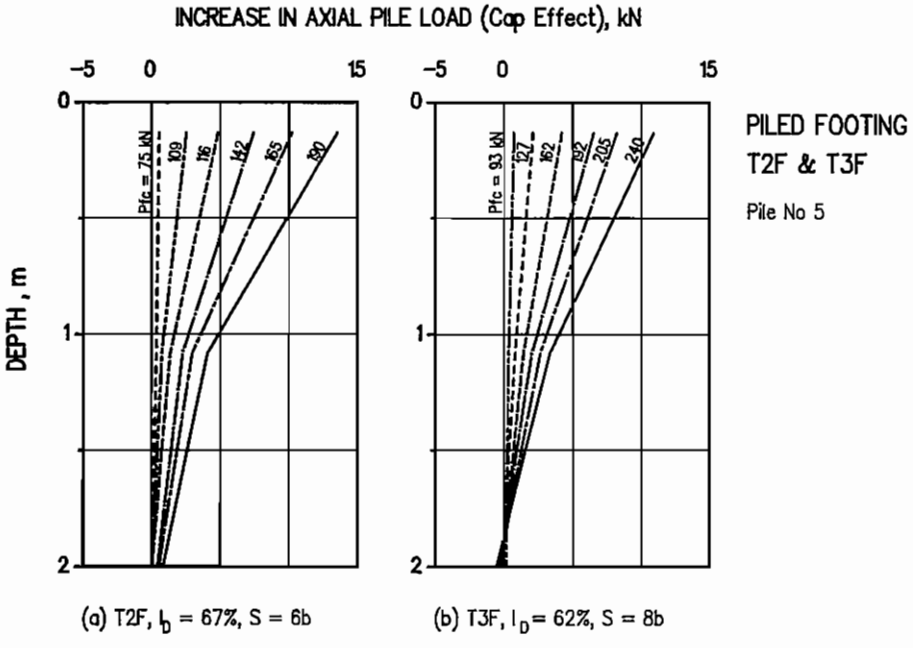

Fig.6.12 Piled footings - Increase in pile axial load due to cap effect versus depth. (a) Test T2F; (b) Test T3F.

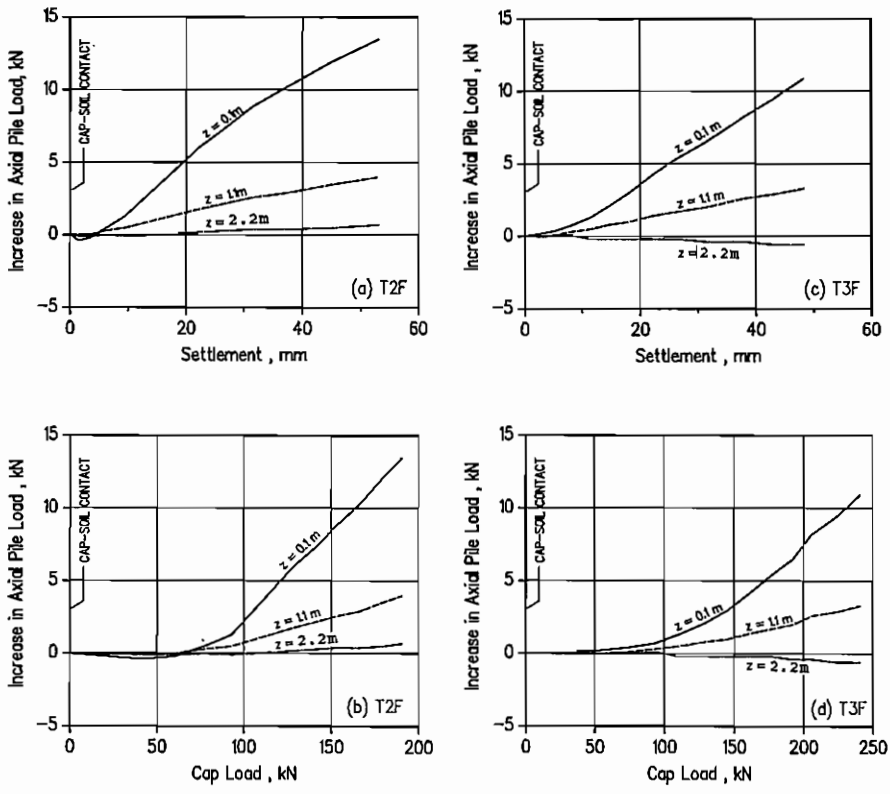

Fig.6.13 Piled footing - Increase in pile axial load due to cap effect versus settlement and versus cap load. (a),(b) Test T2F; (c),(d) Test T3F

The increase in the axial pile load due to the cap effect can be calculated by integrating the skin friction distribution using the increase in lateral pressure against pile shaft $\Delta\sigma_h'$ measured from the Glötzl cells, shown in Section 6.1. Calculation in this way gives the pile head load in good agreement with the measured values. However, the calculated axial load at half pile length is considerably below the measured value.

6.3 Load Efficiency and Bearing Capacity

The concept of group efficiency was originally used to compare the ultimate bearing capacity of a free-standing pile group with that of a single pile under equal soil conditions. The efficiency shows the pile-soil-pile interaction and it is suitable for free-standing groups. Many researchers, however, used the same concept for piled footings. This is not logical as the contribution of the cap is quite independent of the number of piles, pile spacing, pile length, and mainly depends on its size. In order to compare bearing capacities of single piles, free-standing pile groups, piled footings and shallow footings under equal conditions different definitions which are called *load efficiencies*, instead of group efficiency, are suggested below, see Table 6.1.

Table 6.1. Definitions of load efficiencies

Symbol	Definition	comparison between
η_1	P_{gr}/nP_s	free-standing pile group and single pile
η_2	P_{fp}/nP_s	piled footing and single pile
η_3	P_{ft}/nP_s	piled footing and single pile
η_4	P_{fp}/P_{gr}	piled footing and free-standing pile group
η_5	P_{ft}/P_{gr}	piled footing and free-standing pile group
η_6	P_{fc}/P_c	piled footing and shallow footing
η_7	P_{ft}/P_c	piled footing and shallow footing

where, n = number of piles
P_s = load applied on a single pile
P_{gr} = load applied on a free-standing pile group
P_{ft} = total load applied on a piled footing
P_{fp} = load carried by piles in a piled footing
P_{fc} = load carried by cap in a piled footing
P_c = load applied on a shallow footing (cap alone)

From the definitions in Table 6.1, it can be seen that the efficiency η_1 shows pile-soil-pile interaction, in which compaction due to pile driving plays the most important role. Efficiencies η_4, η_5 show the influence of the cap-soil contact pressure, or cap-soil-pile interaction, on the pile behaviour. Efficiencies η_2, η_3 show the total effect, which consists both of pile-soil-pile interaction and cap-soil-pile interaction on the pile behaviour, i.e. $\eta_2 = \eta_1 \cdot \eta_4$ and $\eta_3 = \eta_1 \cdot \eta_5$. Efficiency η_6 shows the influence of the cap-soil-pile interaction on the cap behaviour.

The efficiencies η_1 and η_3 have been used in the literature with one and the

same notation η, while the others have never been used before. In the old concept of group efficiency, the ultimate bearing capacity of a pile group is compared with that of a single pile. However, there are a number of different failure criteria which lead to different values of failure load for a specific test. As a result, the efficiencies obtained are also different. To avoid this problem, the load efficiencies will be evaluated by comparing loads *at the same settlement* in the two tests studied. Notice that, in the old definition, loads are compared at different settlements because failure of a free-standing pile group and of the corresponding single pile often occur at different settlements. All the figures in this section will be plotted using loads at the same settlement. For comparison, the load efficiency is also estimated according to the old definition, in which the failure loads are determined using Vesic's method.

Comparison of free-standing pile groups and single piles

The load efficiency η_1, based on the failure load of the free-standing pile groups and that of the single piles, using Vesic's criterion, is shown in Table 6.2a for pile head, shaft and point (base) loads. The indices "$_s$" and "$_b$" indicate pile shaft and base. From this table, it can be seen that the base efficiency η_{1b} is close to unity in medium to dense sand, Test series T2 and T3. In Test T2, however, η_{1b} is slightly less than unity. This can be explained by the fact that the pile point penetrated into a softer soil layer, see Chapter 4. In Test T1 (loose sand), the base efficiency is much higher than unity, possibly because the soil below the pile point was compacted by pile driving. The shaft efficiency η_{1s} is always larger than unity, showing a compaction effect due to pile driving on the pile shaft load at all sand densities investigated. In the literature, there is a general agreement that in loose to medium dense sand the (total) group efficiency is larger than unity, with a peak value at a pile spacing between 2 and 3 pile diameters, and approaches unity at a spacing between 6 and 10 pile diameters. This may only be correct for the total efficiency in the case where the point load contributes considerably to the total load, as in Tests T2 and T3, see Table 6.2a. However, it may not be correct for the shaft efficiency. In Test series T3, the pile spacing is as large as eight times the pile diameter, but η_{1s} is still much higher than unity.

Fig. 6.14 shows the load efficiency η_1, calculated as the ratio of the load per pile in the free-standing pile groups to that of the single piles at the same settlement for the pile head, shaft and point loads.

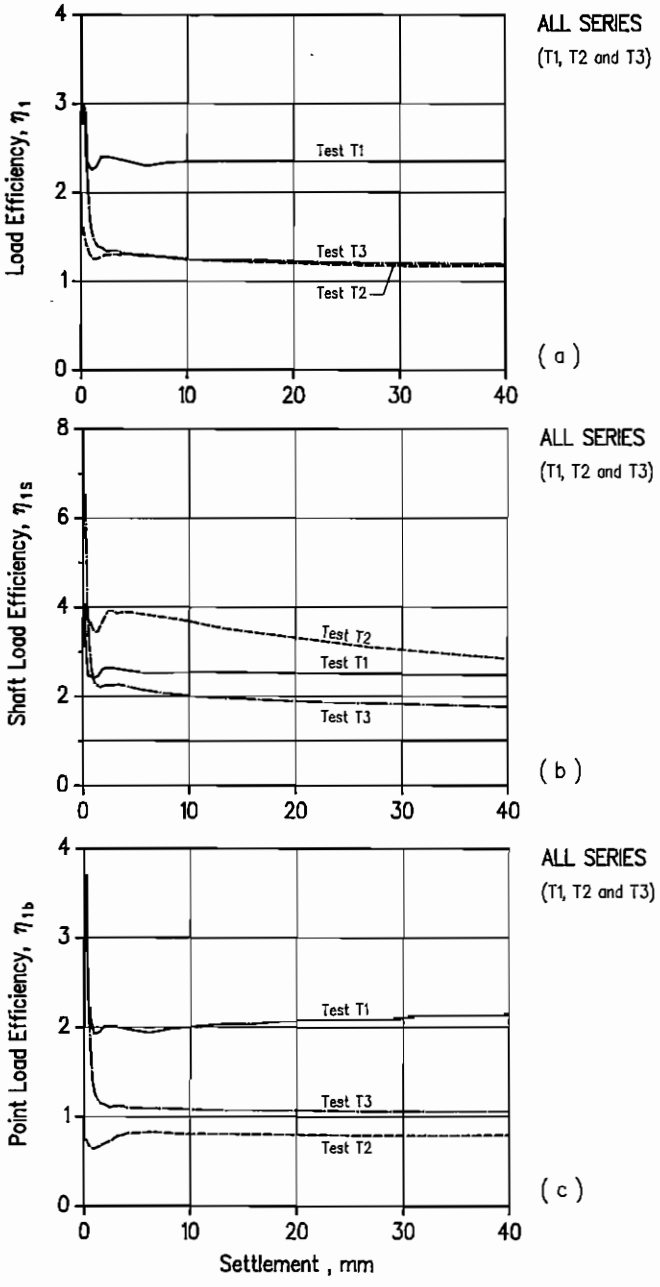

Fig. 6.14 Load efficiency η_1 - Comparison of free-standing pile groups with single piles for: (a) pile head load, (b) pile shaft load, (c) pile point load. Test series T1: relative density of sand I_D=38%, pile spacing $S=4b_p$; Test T2: I_D=67%, $S=6b_p$; Test T3: I_D=62%, $S=8b_p$.

As can be seen, the load efficiency η_l calculated in this way is very high at small settlements, then drops very quickly at settlement between 2-3 mm, and approaches a stable value at settlements larger than about 5 mm, except for the shaft efficiency in Test series T2. The stable values of the load efficiency are shown in Table 6.2b. The efficiency estimated in this way is extremely close to that calculated using the ultimate loads. In practice such differences can be ignored, and the new definition is therefore suggested to be used, in which the load efficiency is calculated using the pile load in the two tests studied *at the same settlement.* Moreover, calculation according to the new definition has the advantage that it shows very clearly the change of efficiency η_l in the whole loading process. Fig. 6.14c seems to show that the base load efficiency η_{lb} mainly depends on the initial relative density of sand.

Table 6.2a Load efficiency η_l calculated using ultimate loads, (old definition)

Test series	Soil I_D %	Spacing S/b	Single pile load, kN Head	Shaft	Point	Load efficiency η_l Head,η_l	Shaft,η_{ls}	Base,η_{lb}
T1	38	4	2.2	1.4	0.8	2.36	2.56	2.00
T2	67	6	12.9	2.1	10.8	1.10	3.19	0.85
T3	62	8	8.4	1.5	6.9	1.20	2.00	1.03

Table 6.2b Load efficiency η_l calculated using loads at the same settlement

Test series	I_D %	Spacing	Head, η_l	Shaft, η_{ls}	Base, η_{lb}
T1	38	4	2.34	2.50	2.00 - 2.16
T2	67	6	1.21	2.71 - 3.60	0.81
T3	62	8	1.16	1.76 - 2.00	1.06

Comparison of piled footings and single piles

There are two ways of comparing the pile loads in a piled footing with that of a single pile: using the load carried by the piles or using the total load applied on the piled footing. The former case corresponds to the load efficiency η_2 and the latter case to the efficiency η_3, according to Table 6.1. The efficiency η_2 is more logical because it does not include the contribution of the cap, which is more dependent on the cap size than on the group geometry. The efficiency η_3, however, is used more commonly in the literature. Similarly to η_l, the efficiency η_2 can be estimated for the pile head, shaft and point loads, while η_3 can only be estimated for the pile head load. The efficiency η_2 shows both the group effect (pile-soil-pile interaction), and the effect of cap-soil contact pressure (cap-pile-soil interaction), on the pile loads.

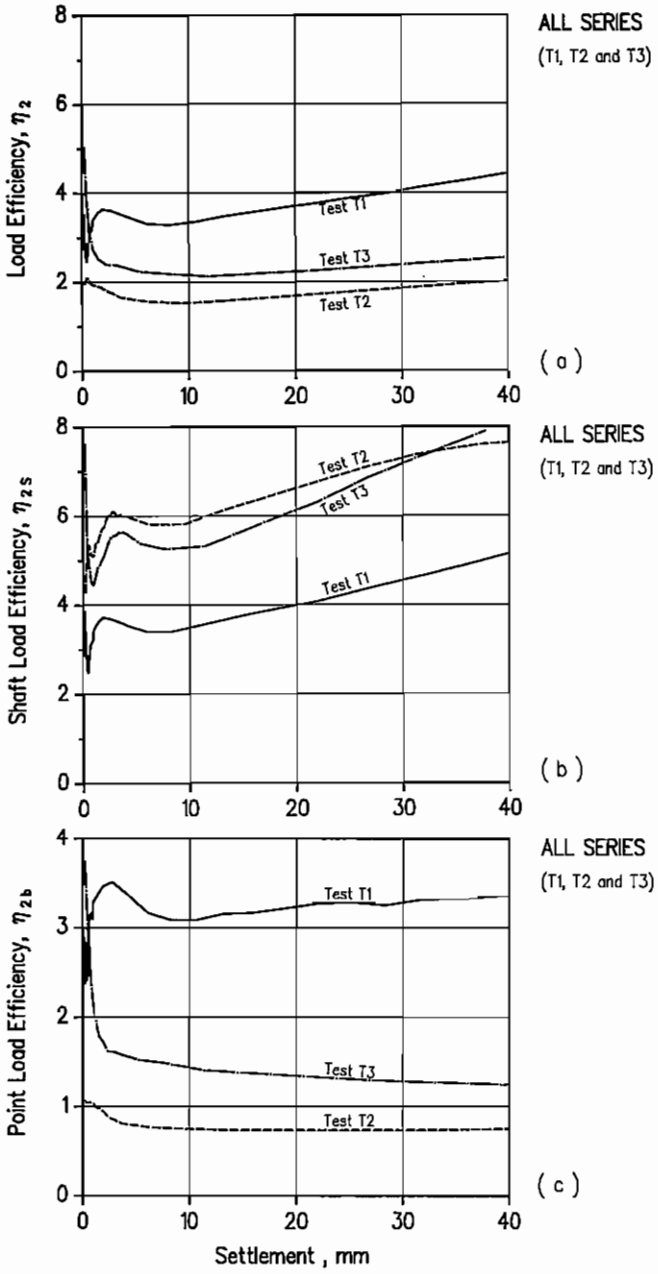

Fig. 6.15 Load efficiency η_2 - Comparison of pile load per pile in piled footings with single piles for: (a) pile head load, (b) pile shaft load, (c) pile point load. Test series T1: relative density of sand I_D=38%, pile spacing $S=4b_p$; Test series T2: I_D=67%, $S=6b_p$; Test series T3: I_D=62%, $S=8b_p$.

Because pile failure in a piled footing occurs progressively, i.e. the pile load increases with an increasing settlement, the efficiencies η_2 and η_3 will be estimated by comparing the loads at failure, and at a settlement of 20 mm and 30 mm in the piled footing tests with the failure load of the single piles, see Tables 6.3 and 6.4. In Figures 6.15 and 6.16, however, the efficiencies η_2 and η_3 are calculated using loads at the same settlement.

Table 6.3. Load efficiency η_2 using pile load per pile in a piled footing

Test series	Loads at failure			Loads at s=20mm			Loads at s=30mm		
	Head	Shaft	Base	Head	Shaft	Base	Head	Shaft	Base
T1	3.05	3.24	2.98	3.74	3.98	3.35	4.13	4.45	3.44
T2	1.28	4.42	0.70	1.71	6.80	0.74	1.98	8.30	0.78
T3	1.96	4.40	1.39	2.11	5.16	1.45	2.73	8.60	1.45

From Fig. 6.15, it is found that the shaft efficiency η_{2s} increases considerably in all the three test series. The larger the cap and the denser the sand, the higher the increase. This is evidently due to the effect of cap-soil contact pressure. The base load efficiency η_{2b}, however, is rather constant and approaches unity in Tests T2 and T3. This means that the cap being in contact with soil surface has no or very little influence on η_{2b}. In Test T1, η_{2b} is much larger than unity mainly because of pile installation, as stated above. The total (head) load efficiency η_2, in general, has a tendency to increase with increasing settlement, but the increase is not so large in denser sands, where the pile point load is predominant (Tests T2F and T3F).

Piled footings and single piles can be compared in the way some researchers did before by estimating the load efficiency η_3 on the basis of total load per pile in the piled footing. This efficiency, however, can only be estimated for the pile head load. The results are shown in Table 6.4 and Fig. 6.16. The efficiency η_3 is very high because it also includes the capacity of the cap. This efficiency is, therefore, very much dependent on the capacity of the cap relative to that of the piles. As commented above, η_3 is not a logical efficiency.

Table 6.4. Load efficiency η_3 using total load per pile in piled footing

Test series	I_D %	Spacing	at failure	at s=20mm	at s=30mm
T1	38	4	3.32	5.41	6.68
T2	67	6	2.12	3.64	4.25
T3	62	8	3.53	6.12	7.21

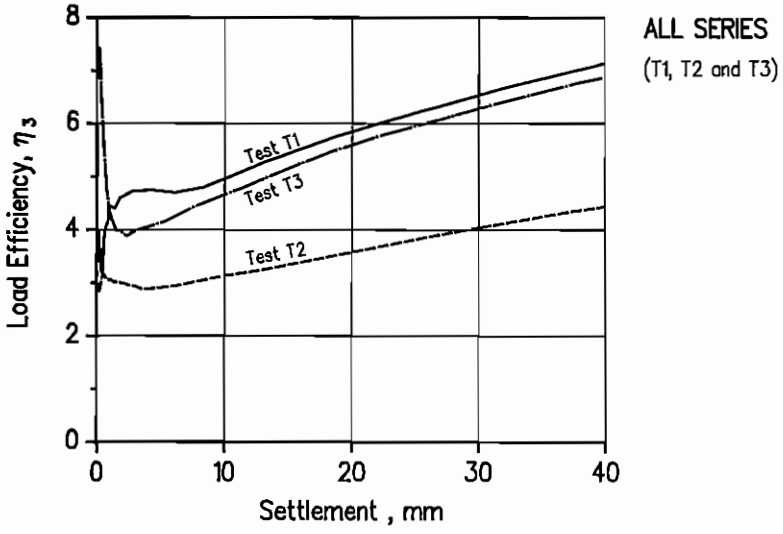

Fig. 6.16. Load efficiency η_3 - Comparison of total load per pile in piled footing with single pile. Test series T1: relative density of sand I_D=38%, pile spacing $S=4b_p$; Test series T2: I_D=67%, $S=6b_p$; Test series T3: I_D=62%, $S=8b_p$.

Comparison of piled footings and free-standing pile groups

Comparison of a piled footing with a free-standing pile group, using the load efficiencies η_4 or η_5, defined in Table 6.1, shows the effect of cap-soil contact pressure on the pile capacity. As previously mentioned, there are two ways of comparing the pile loads in a piled footing with those in a free-standing pile group: using the load carried per pile, excluding the load carried by the cap, or using the total load carried per pile, including the load carried by the cap. The former case corresponds to the load efficiency η_4, defined in Table 6.1, and the latter case, which corresponds to the load efficiency η_5. The efficiency η_4 is more practical since it does not include the capacity of the cap. As with η_2, the efficiency η_4 can be estimated for the pile head, shaft, and point loads, while η_5 can only be estimated for pile head load. In Table 6.5, the load efficiency η_4 is calculated for pile head, shaft and point loads using the failure load in the test on the free-standing groups, and the loads at failure and at a settlement of 20 mm and 30 mm in the piled footing tests. In Figures 6.17 through 6.19, the efficiencies η_4 and η_5 are estimated using loads at the same settlement.

Table 6.5a Load efficiency η_4 using pile load per pile in piled footings TF and failure load in free-standing pile groups TG

Test series	Loads at failure			Loads at s=20mm			Loads at s=30mm		
	Head	Shaft	Base	Head	Shaft	Base	Head	Shaft	Base
T1	1.29	1.27	1.47	1.58	1.56	1.64	1.75	1.78	1.69
T2	1.16	1.38	0.87	1.54	2.12	0.93	1.79	2.60	0.98
T3	1.63	2.17	1.35	1.75	2.54	1.41	2.26	4.24	1.41

Table 6.5b Load efficiency η_4 using pile load per pile in piled footings TF and failure load of free-standing groups in Test TF, before contact.

Test series	Loads at failure			Loads at s=20mm			Loads at s=30mm		
	Head	Shaft	Base	Head	Shaft	Base	Head	Shaft	Base
T2	1.07	1.03	1.10	1.42	1.58	1.20	1.64	1.93	1.26
T3	1.10	1.13	1.09	1.18	1.32	1.09	1.53	2.20	1.10

Note In Tables 6.5a and 6.5b, η_4 is estimated by comparing loads at failure and at s= 20mm and s= 30mm in the tests on the piled footings to the failure load of the free-standing pile groups.

The results shown in Table 6.5a and Fig. 6.17 are obtained by comparing the pile loads in the tests on free-standing pile groups TG with those in the tests on the piled footings TF. No matter how carefully the tests are performed , it is almost impossible to avoid errors caused by recompression effects, for example, a deeper pile penetration, or time effects, see Chapter 5. Table 6.5a and Fig. 6.17 show the load efficiency η_4, estimated from the results of the free-standing pile groups on the one hand and from subsequent tests on the piled footings on the other, with some time interval. The best way to discern the effect of cap-soil contact pressure on the pile behaviour, however, is by taking the test results before cap-soil contact in the continuous tests on piled footing as significant for the free-standing groups, thereby eliminating time and penetration effects. The efficiency η_4, evaluated in this way, using loads at the same settlement, is shown in Table 6.5b and plotted in Fig. 6.18. The results for Test series T1 are not included because the test on the piled footing T1F was performed according to the first testing procedure.

From Fig. 6.18, it can be clearly seen that the base load efficiency η_{4b} is equal to unity. The shaft load efficiency η_{4s} is rather similar for both the test series T2 and T3: it is quite constant and slightly higher than unity at settlements smaller than 10 mm; thereafter it increases very quickly up to 2.0 ÷ 2.5 at a settlement of 40 mm. The total (head) load efficiency η_4 has the same tendency as the shaft efficiency but with a smaller magnitude.

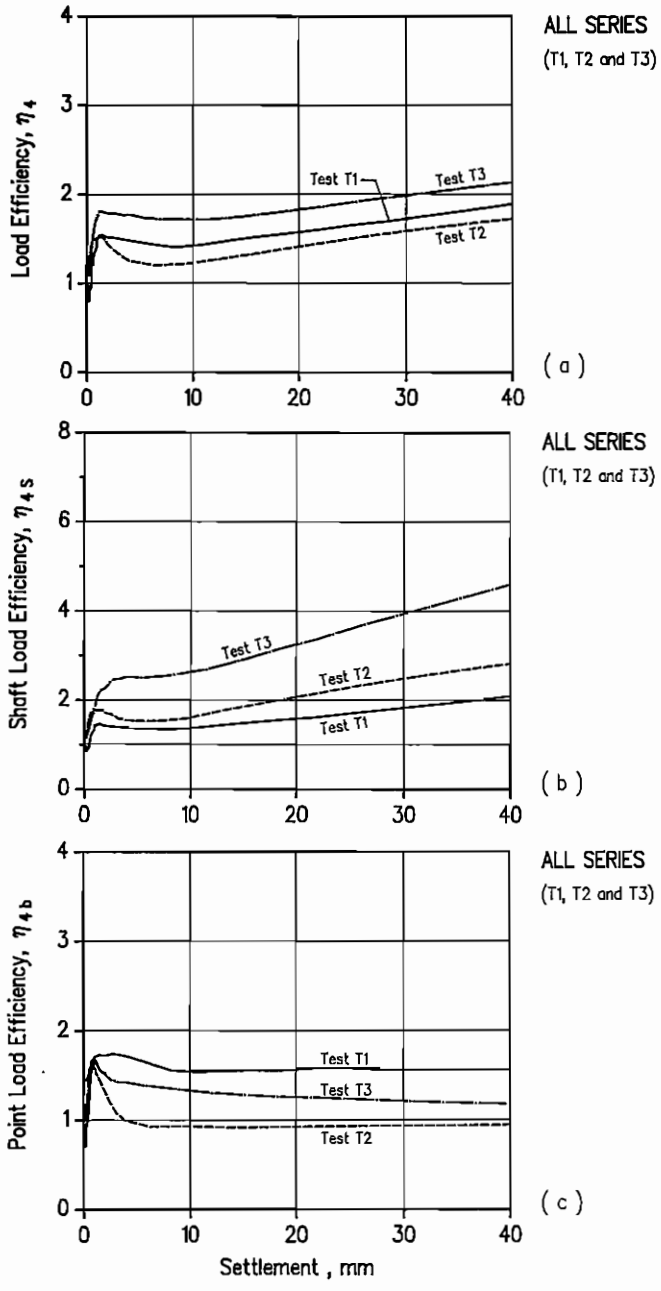

Fig. 6.17 Load efficiency η_4 - Comparison of pile load per pile in piled footings with free-standing pile groups for: (a) pile head load, (b) pile shaft load, (c) pile point load. Test series T1: relative density of sand I_D= 38 %, pile spacing $S= 4b_p$; Test series T2: I_D= 67 % $S= 6b_p$; Test series T3: I_D= 62 %, $S= 8b_p$.

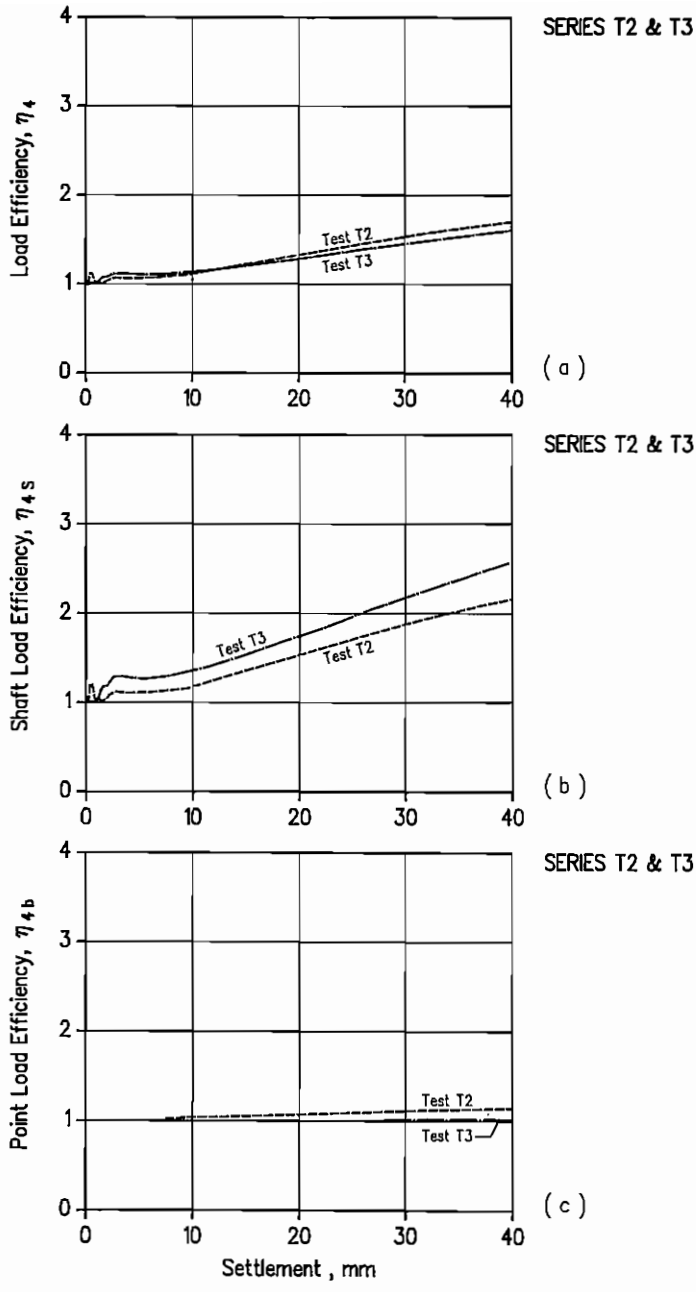

Fig. 6.18 Load efficiency η_4 - Comparison of pile load per pile in piled footings with free-standing pile groups using initial part of test on piled footings TF (before contact) as test on free-standing groups, for: (a) pile head load, (b) pile shaft load, (c) pile point load. Test series T1: relative density of sand I_D= 38%, pile spacing $S= 4b_p$; Test T2: I_D= 67%, $S= 6b_p$; Test T3: I_D= 62%, $S= 8b_p$.

Fig. 6.19 shows the load efficiency η_5, which compares the total load per pile in the piled footings with that in the free-standing groups, using the initial part of the tests on piled footings T2F and T3F (before contact) as tests on free-standing pile groups. As expected, the efficiency η_5 depends mainly on the size of the cap because in the cases studied with short piles, the capacity of the cap is always much larger than that of the piles.

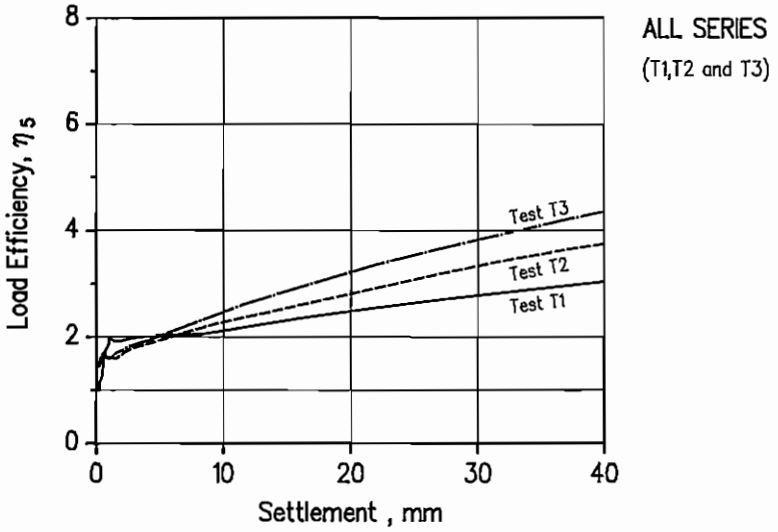

Fig. 6.19. Load efficiency η_5 - Comparison of total load per pile in piled footings with free-standing pile groups using initial part of test on piled footings TF (before contact) as test on free-standing groups. Test series T1: relative density of sand I_D= 38%, pile spacing $S= 4b_p$; Test T2: I_D= 67%, $S= 6b_p$; Test T3: I_D= 62%, $S= 8b_p$.

Comparison of piled footings and shallow footings

The bearing capacity of a piled footing and a shallow footing (cap) of equal size in plan can be compared through the efficiency η_7 defined in Table 6.1. The load carried by the cap in the piled footing is compared with that carried by the shallow footing by using the efficiency η_6. The efficiencies are estimated using the loads at equal settlement, see Figures 6.20 and 6.21.

The efficiency η_6, plotted versus settlement in Fig. 6.20, is very close to unity. It seems, however, that η_6 tends to be higher than unity in loose sand

(Test series T1), and smaller than unity in denser sand but approaching unity at large settlements (Tests series T2 and T3).

From Fig. 6.21, it is found that the η_7-settlement curve has the same shape for all three test series: at small settlements, less than 2-3 mm, the efficiency η_7 has quite high values. Afterwards, it drops rather quickly, and approaches a stable value at a settlement larger than 10 mm. The stable value of η_7 depends mainly on the contribution of the cap to the capacity of the piled footing: the higher the capacity of the cap (larger cap size, denser sand), the lower the η_7 value. The stable values of η_6 and η_7 at s = 40 mm are shown in Table 6.6.

Table 6.6 Load efficiency η_6 and η_7

Test series	Soil I_D %	Spacing S/b	Load efficiency η_6	Load efficiency η_7
T1	38	4	1.15	3.05
T2	67	6	0.99	1.77
T3	62	8	0.97	1.62

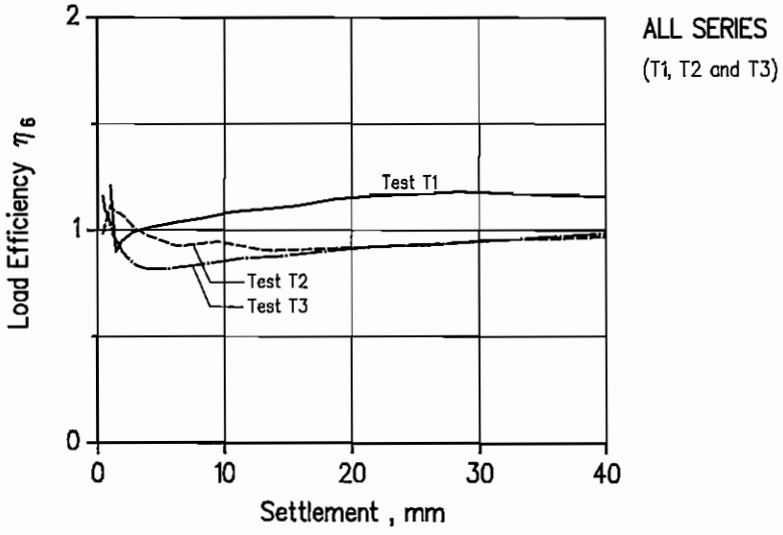

Fig. 6.20 Load efficiency η_6 - Comparison of load carried by cap in piled footings with shallow footings (caps alone). Test series T1: relative density of sand I_D =38%, pile spacing S= $4b_p$; Test T2: I_D= 67%, S= $6b_p$; Test T3: I_D= 62%, S= $8b_p$.

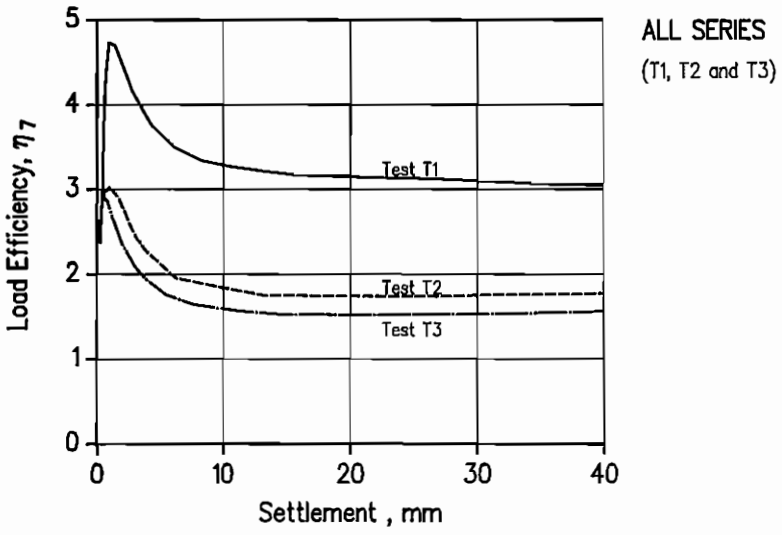

Fig. 6.21. Load efficiency η_7 - Comparison of total load in piled footing with shallow footing (cap alone). Test series T1: relative density of sand I_D =38%, pile spacing S= 4b_p; Test T2: I_D= 67%, S= 6b_p; Test T3: I_D= 62%, S= 8b_p.

Bearing Capacity of a piled footing

As suggested in Chapter 2, in a general case, the bearing capacity of a piled footing P_{ft} can be estimated as follows:

$$P_{ft} = n\,(\beta_s\,\delta_s\,P_{ss} + \beta_b\,\delta_b\,P_{sb}) + \beta_c\,P_c \qquad (6.1)$$

where, n = number of piles in the group,
δ_s, δ_b = influence factor of pile-soil-pile interaction on the pile shaft and pile base capacities,
β_s, β_b, β_c = influence factor of cap-pile interaction on the pile shaft and pile base capacities, and on the capacity of the cap,
P_{ss}, P_{sb} = shaft and base capacities of the reference single pile under equal soil conditions as the pile group,
P_c = capacity of the shallow footing (cap alone).

Comparing Eq. (6.1) with the definitions of load efficiencies in Table 6.1, the following remarks can be made:

(a) influence factors of pile-soil-pile interaction on the pile shaft and base capacities $\delta_s = \eta_{1s}$, and $\delta_b = \eta_{1b}$, see Fig. 6.14 or Table 6.2;
(b) influence factors of cap-pile interaction on the pile shaft and base capacities $\beta_s = \eta_{4s}$, $\beta_b = \eta_{4b}$, see Figures 6.17, 6.18 or Table 6.5;
(c) influence factor of cap-pile interaction on the capacity of the cap $\beta_c = \eta_6$, see Fig. 6.20 or Table 6.6;

The efficiencies η_{1s} and η_{1b} should be estimated by comparing the load per pile in a free-standing pile group with the load of a reference single pile at the same settlement. A specific settlement can be chosen, for example s = 10 mm. To determine the efficiencies η_{4s}, and η_{4b}, tests on a piled footing should be performed according to the second testing procedure, i.e. the test should be started with a free-standing pile group, with the cap being about 20 mm above the soil surface. The number of load steps before cap-soil contact should be large enough to be able to determine correctly the failure load of the free-standing group and the occurrence of cap-soil contact. After contact, the piled footing should be tested to failure. Comparison of pile loads in the piled footing (after contact) with pile loads in the free-standing group, which is taken from the initial stage of the test (before contact), will result in accurate values of η_{4s}, and η_{4b}. The influence factor β_c (= η_6) can be taken as 1.0 for footings on loose sand and 0.9 for footings on medium to dense sand.

6.4. Settlement Ratio

Different definitions of the settlement ratio have been utilised to compare the settlement of a free-standing pile group or a piled footing with that of a reference single pile. As discussed in Chapter 2, the use of different definitions of the settlement ratio leads to different values of the ratio even for one and the same test. This is exemplified for the three test series performed by the Author using the first definition in Section 2.1, with the failure criteria recommended by Vesic (1969) and Mazurkiewicz (1972), and using three different values of factor of safety: 3.0, 2.0 and 1.5. Accordingly, the settlement ratio is estimated as the ratio of the settlement of a free-standing pile group to that of a reference single pile at the same fraction of their failure loads. Thus, according to this definition, the settlement ratio is estimated by comparing the settlement of pile groups and of single piles at different loads per pile, because failure occurs at different pile loads. The results are shown in Table 6.7.

Table 6.7. Settlement ratio calculated according to Eq. 2.2a

Test series	Soil I_D %	Spacing S/b	Vesic (1969) F=3.0	Vesic (1969) F=2.0	Vesic (1969) F=1.5	Mazurkiewicz (1972) F=3.0	Mazurkiewicz (1972) F=2.0	Mazurkiewicz (1972) F=1.5
T1	38	4	0.44	0.88	1.06	0.44	0.88	1.06
T2	67	6	0.65	0.95	0.83	0.80	0.91	0.78
T3	62	8	0.31	0.69	0.85	0.30	0.63	0.71

Obviously, the settlement ratio estimated according to this definition depends very much on the choice of failure criterion and of safety factor. This explains the difficulties in scrutinising previous studies on settlement ratio. Only in Test series T1 are the results independent of the failure criterion, as the single pile and the pile group both failed by plunging, which represents failure no matter which criterion is used.

The definition of the settlement ratio ξ as the ratio of the pile group settlement to the single pile settlement, at comparable working pile loads and at a certain fraction of the failure load of the single pile, may be preferable. The definition based on the ratio of the initial slope of the load-settlement curve, or the initial stiffness, of the pile group to that of the single pile is very similar to the definition mentioned above. These definitions, however, are not suitable for studying behaviour of footings close to failure. Besides, as in the case of load efficiencies, choosing the failure criteria is also difficult. In this section, the settlement ratio of the free-standing pile group or the piled footing as compared with the single pile will be based on settlement comparisons *at the same load per pile*, and that of the free-standing pile group or the shallow footing as compared with the piled footing will be based on a settlement comparison *at the same applied load.*

As mentioned above, the old concept of settlement ratio is used only to compare settlement of a free-standing pile group with that of a single pile. For comparison of the settlements of single piles, free-standing pile groups, piled footings and shallow footings (caps) under equal conditions, the definitions given in Table 6.8 will be used.

Table 6.8. Definition of settlement ratios

Symbol	Definition	comparison between
ξ_1	$\bar{s}_{gr} / s_s$	free-standing pile group and single pile
ξ_2	$\bar{s}_{fp} / s_s$	piled footing and single pile
ξ_3	$\bar{s}_{ft} / s_s$	piled footing and single pile
ξ_5	$\bar{s}_{ft} / \bar{s}_{gr}$	piled footing and free-standing pile group
ξ_7	$\bar{s}_{ft} / \bar{s}_c$	piled footing and shallow footing

where s_s = settlement of single pile

$\bar{s}_{gr}$ = average settlement of free-standing pile group

$\bar{s}_{fp}$ = average settlement of piled footing, corresponds to load taken by piles

$\bar{s}_{ft}$ = average settlement of piled footing, corresponds to total applied load

$\bar{s}_c$ = average settlement of shallow footing (cap)

Note: The ratios ξ_1, ξ_2, ξ_3 are based on settlement comparisons at the same load per pile; while ξ_5, ξ_7, at the same load applied on footings or pile groups.

The indices of the settlement ratios ξ_i presented in Table 6.8 correspond to those of the load efficiencies η_i, presented in Table 6.1. The ratios ξ_1 and ξ_3 have been used in the literature with one and the same notation ξ, while the others are introduced. From the definitions, it can be seen that $\xi_5 = \xi_3/\xi_1$.

Comparison of free-standing pile groups and single piles

The ratio ξ_1 is estimated by comparing the settlement of a free-standing pile group with that of a single pile at the same load per pile, given as a percentage of the failure load of the single pile P_{sf}. In loose sand, Test series T1 (I_D= 38%), the ratio is very small, less than 0.30, with a minimum value less than 0.05 at 100% of the single pile failure load. In denser sand, the maximum value of ξ_1 is higher: less than 0.5 for Test T3 (I_D= 62%), and less than 0.7 for Test series T2 (I_D= 67%), see Fig. 6.22. It is noted that the ratio ξ_1 in all three series is less than unity. This is in agreement with the results obtained by Ekström (1989). A ratio lower than unity seems reasonable for small pile groups, and it can be explained by soil compaction within the group due to pile driving.

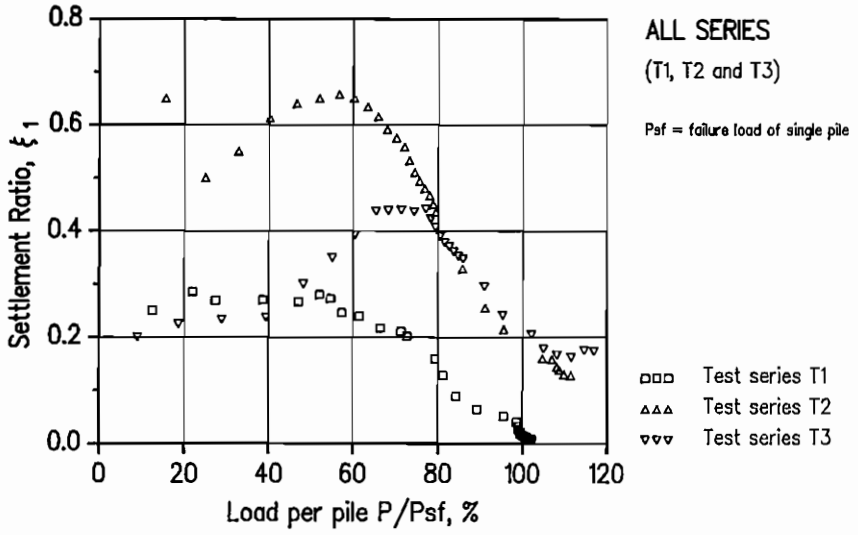

Fig. 6.22. Settlement ratio ξ_1 versus pile load as a percentage of failure load of single pile - Comparison of free-standing pile groups with single piles. Test series T1: relative density of sand I_D= 38 %, pile spacing $S= 4b_p$; Test series T2: I_D= 67 %, $S= 6b_p$; Test series T3: I_D= 62 %, $S= 8b_p$.

Comparison of piled footings and single piles

Comparison of the settlement of a piled footing with that of a single pile can be made by estimating the ratios ξ_2 and ξ_3. The ratios ξ_2 and ξ_3, Table 6.8, are both estimated at the same load per pile, given as a percentage of the failure load of the single pile P_{sf}. The results are shown in Figures 6.23 and 6.24. It is obvious that ξ_3 is always smaller than ξ_2. This is due to the contribution of the cap to the total load. There is a clear tendency in all three test series that both ξ_2 and ξ_3 are quite stable up to 60% of P_{sf} and from then onwards drop rather quickly to very small values at 100% of P_{sf}.

Typical values of the ratios ξ_1, ξ_2 and ξ_3 are summarised in Table 6.9. From the table, it can be seen that in Test series T1 these ratios are quite close to each other even at 100% of P_{sf}. This means that the contribution of the cap to the overall stiffness of the piled footing is insignificant. However, in Tests T2 and T3 the contribution of the cap is considerable and the ratios ξ_2 and ξ_3 are therefore much smaller than ξ_1, especially at loads close to P_{sf}.

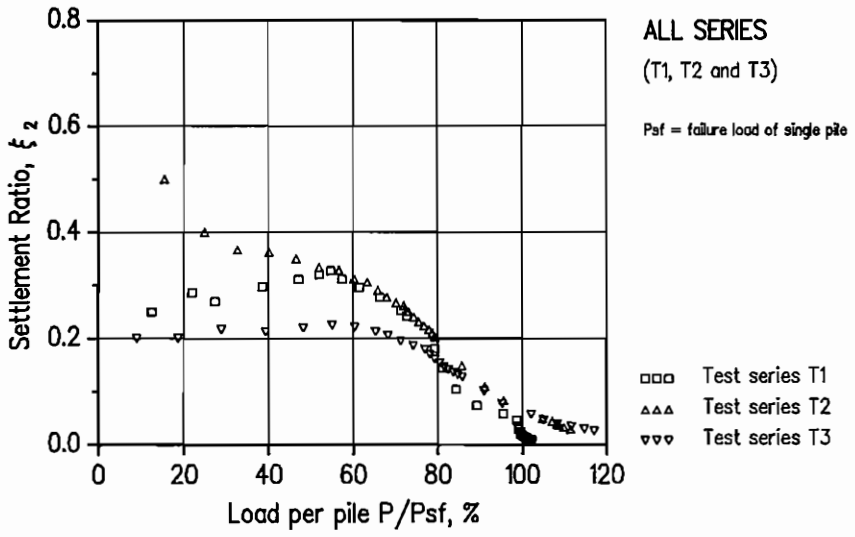

Fig. 6.23. Settlement ratio ξ_2 - Comparison of piled footings with single piles. Test series T1: relative density of sand I_D=38%, pile spacing $S=4b_p$; Test series T2: I_D=67%, $S=6b_p$; Test series T3: I_D=62 %, $S=8b_p$.

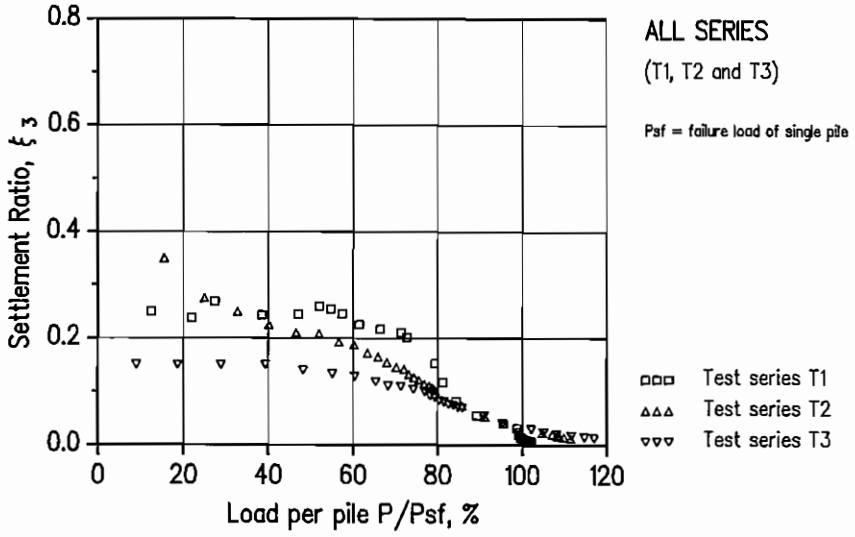

Fig. 6.24. Settlement ratio ξ_3 - Comparison of piled footings with single piles. Test series T1: relative density of sand I_D=38%, pile spacing $S=4b_p$; Test series T2: I_D=67%, $S=6b_p$; Test series T3: I_D=62 %, $S=8b_p$.

Table 6.9 Settlement ratios ξ_1, ξ_2, and ξ_3

Test series	P/P_{sf}=20%			40%			60%			80%			100%		
	ξ_1	ξ_2	ξ_3	ξ_1	ξ_2	ξ_3	ξ_1	ξ_2	ξ_3	ξ_1	ξ_2	ξ_3	ξ_1	ξ_2	ξ_3
T1	.29	.29	.24	.27	.30	.24	.25	.31	.24	.16	.18	.15	.04	.05	.03
T2	.58	.45	.32	.61	.36	.23	.65	.31	.19	.44	.20	.10	.18	.06	.03
T3	.23	.20	.15	.25	.21	.15	.40	.22	.13	.38	.15	.08	.21	.06	.03

Comparison of piled footings and free-standing pile groups

Comparison of the settlement of a piled footing with that of a free-standing pile group can be made by estimating the ratio ξ_5, Table 6.8. The ratio is estimated at the same applied load, which is given as a percentage of the failure load of the free-standing pile group P_{gf}. The results are shown in Fig. 6.25. The ratio is always less than unity, showing the contribution of the cap to the overall stiffness of the piled footing. For all the three test series the ratio tends to a maximum value equal to 1.0 for Test series T1 and about 0.6 for the other two test series, at a load level of 20-30% of P_{gf}. The ratio then decreases at an almost constant rate to a minimum value at a load level between 100-120% of P_{gf}. Contrary to the conclusions drawn in most of the theoretical studies, namely that the influence of the contact pressure induced by the cap on the stiffness of a piled footing is insignificant, Fig. 6.25 indicates that the increase

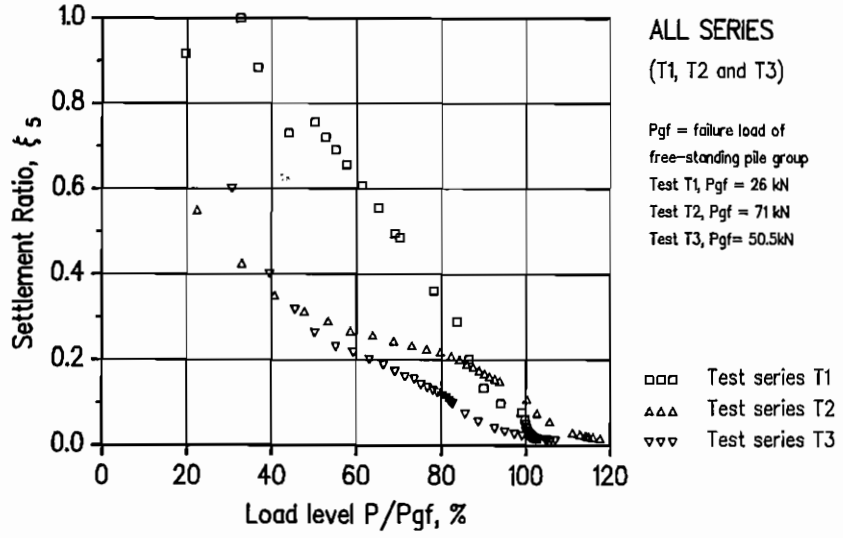

Fig. 6.25. Settlement ratio ξ_5 - Comparison of piled footings with free-standing pile groups. Test series T1: relative density of sand I_D=38%, pile spacing $S=4b_p$; Test series T2: I_D=67%, $S=6b_p$; Test series T3: I_D=62%, $S=8b_p$.

in stiffness of the piled footings is considerable, and the closer to failure load of the free-standing pile groups, the greater the increase. The increase seems to depend on the cap size: the larger the cap, the greater the increase.

Comparison of piled footings and shallow footings

The ratio ξ_7, defined in Table 6.8, is estimated at equal applied load, given as a percentage of the failure load of the shallow footing P_{cf}. The results are shown in Fig. 6.26. This figure indicates that the settlement ratio ξ_7 is always less than unity. The variation of the ratio ξ_7 depends very much on the relative cap capacity α, which is defined as the ratio of the load applied on the shallow footing (cap) to that applied on the piled footing at a certain settlement close to failure. For example, if a settlement of 5 mm is chosen, the relative cap capacity α for Test series T1 can be calculated as the ratio of the load applied on the shallow footing at s = 5 mm (in Test T1C) to the load on the piled footing at the same settlement (in Test T1F). The α value is then equal to 0.27, 0.48 and 0.55 for Test series T1, T2 and T3, respectively. The relative cap capacity shows the relative contribution of a cap to the bearing capacity of a piled footing, and is the inverse of the load efficiency η_7 at the same settlement, i.e. $\alpha = 1/\eta_7$.

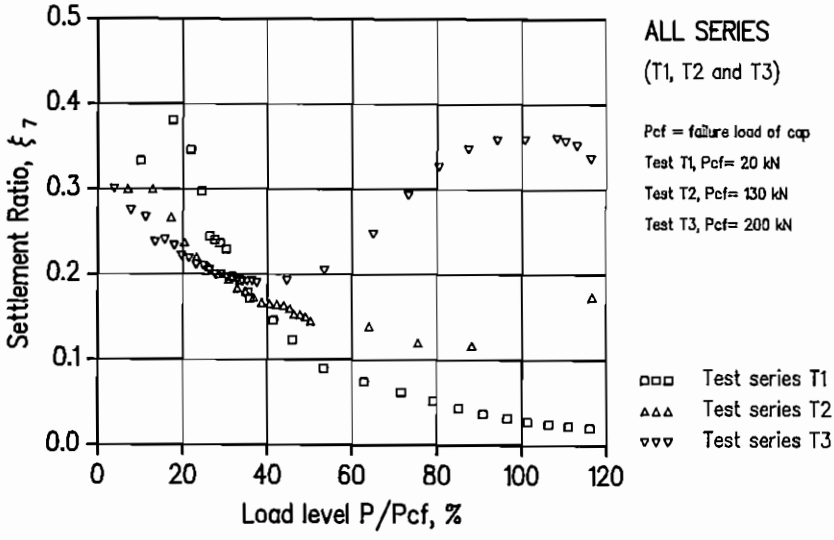

Fig. 6.26. Settlement ratio ξ_7 - Comparison of piled footings with shallow footings. Test series T1:relative density of sand I_D=38%, pile spacing $S=4b_p$; Test series T2: I_D=67%, $S=6b_p$; Test series T3: I_D=62 %, $S=8b_p$.

If the relative cap capacity is low, the ratio ξ_7 will decrease all the time to a very small value, as in Test series T1. If the relative cap capacity is high, the ratio ξ_7 will first decrease at low load levels, and will then increase with loads close to 100% of P_{cf}, as in Test series T2 and T3, Fig. 6.26. The turning point depends also on the relative cap capacity α: the higher the α value, the sooner the turning point occurs.

The settlement ratio ξ_7 can be plotted versus the relative cap capacity α. It is noted that both α and ξ_7 are equal to unity for a shallow footing. For a footing on a large number of high-capacity piles, such as long piles with small pile spacing (the contribution of the cap to the capacity of the piled footing is small compared with that of the piles), the α value is very small as well as the settlement of the footing. In such a case, α and ξ_7 can both be considered equal to zero. Using the α value calculated above (at s = 5 mm), the correlation between α and ξ_7 is presented in Fig. 6.27 for different load levels, from 60% to 120% of P_{cf}. This figure shows a clear tendency with very small scatter. Thus, when α is less than about 0.5, i.e. the contribution of piles to the total

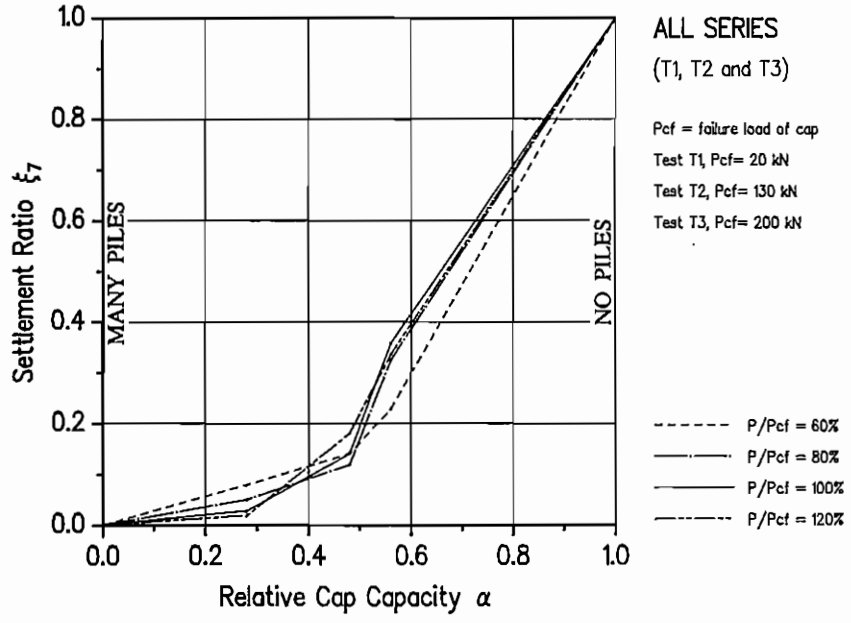

Fig. 6.27. Comparison of piled footings with shallow footings - Settlement ratio ξ_7 versus relative cap capacity α, which is defined as ratio of load carried by the shallow footing to that carried by corresponding piled footing at a settlement of 5 mm.

capacity is large enough, the settlement ratio ξ_7 decreases slowly with a decreasing α value. In other words, with α less than about 0.5, a considerable increase in pile capacity induced by increasing number of piles or pile length will not lead to a significant reduction in the settlement of the footing. However, with an α value higher than 0.5, i.e. when the capacity of the cap is predominant, the contribution of the piles has a clear effect in reducing the settlement of the footing.

6.5 Load Sharing between Piles and Cap

The load share between piles and cap in the piled footings is shown in Chapter 5, Figures 5.6, 5.16, 5.25. These figures show a clear tendency that the load share between cap and piles varies with load level and that the piles carry an important part of the load until pile failure, thereafter the load carried by the cap increases very quickly. Fig. 6.28 is a modification of the above-mentioned figures, in which the load carried by the cap or by an average pile as a percent of the total load applied is plotted versus load level. The load level is defined as a percentage of the load applied in relation to the total load at a settlement of 40 mm. According to Fig. 6.28, the percentage of load carried by the cap depends first of all on its size: the larger the cap, the higher the load it takes. Moreover, in the beginning the piles always carry a larger portion of the load, ranging from 90% (Test T1F) to about 70% (Tests T2F and T3F). After pile failure, a large percentage of the load applied is transferred to the cap. The load share is also plotted against settlement, Fig. 6.29.

The load sharing between piles and cap in a piled footing, in general, depends on the construction procedure. However, the influence on the load sharing of the construction sequence may be important only in the beginning of the loading process. As soon as the cap comes into good contact with the piles and the ground surface, a considerable part of the load will be transferred to the piles until they reach failure. In other words, as soon as the cap, the piles and the subsoil are in good contact, the load share will be governed by the settlement. At very small settlement, the piles take an important part of the load. At a settlement large enough to mobilise the full capacity of piles, a considerable portion of the load applied will be transferred to the cap. Thereafter, the load sharing between the cap and the piles becomes almost constant, Fig. 6.29. However, the load carried by the cap on the one hand and by the piles on the other both increase.

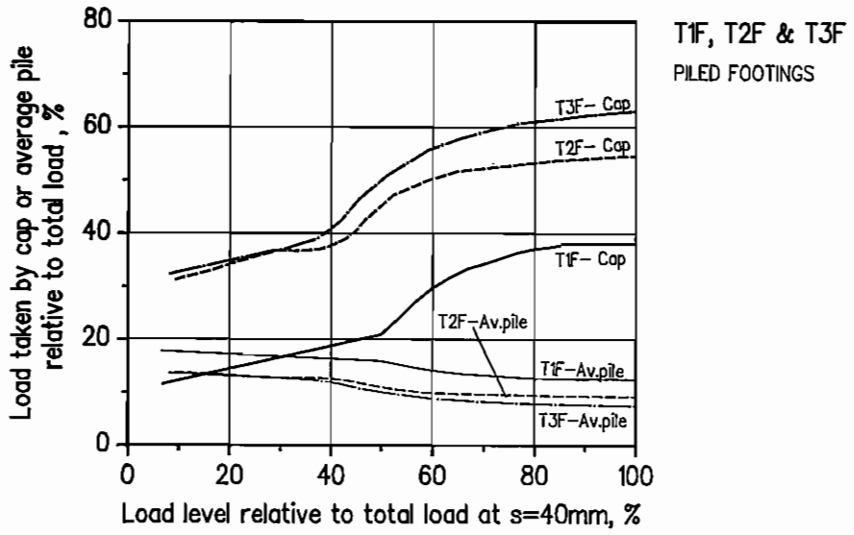

Fig. 6.28 Percentage of load taken by cap and by average pile versus load level Test T1F: relative density of soil I_D=38%, cap size: 46cmx46cm; Test T2F:I_D=67%, cap:63cmx63cm; Test T3F:I_D=62%, cap:80cmx80cm;

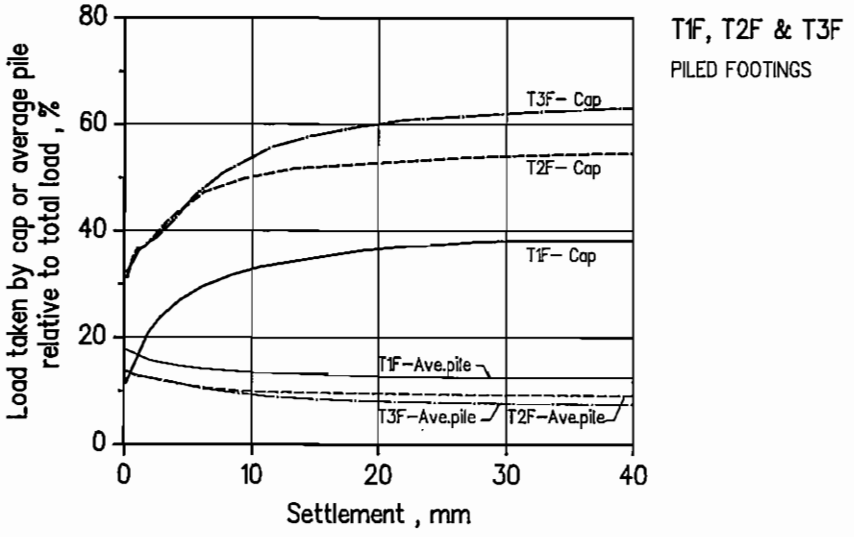

Fig. 6.29 Percentage of load taken by the cap and by average pile versus settlement Test T1F: relative density of soil I_D=38%, cap size: 46cmx46cm; Test T2F:I_D=67%, cap:63cmx63cm; Test T3F:I_D=62%, cap:80cmx80cm

6.6 Creep Behaviour

An advantage of using electrical displacement transducers and a data logger for the purpose of measuring settlement of footings is that the creep behaviour can be interpreted with great accuracy. Thus, settlements could be read exactly every fifteen seconds. In this section, the creep from 1 minute to 8 minutes of observation will be presented. The creep behaviour of the shallow footings will be compared with that of the piled footings. In Tests T2F and T3F, the creep is interpreted only after cap-soil contact because these tests were performed according to the second testing procedure. Figures 6.30 through 6.32 compare the creep-load curves of the shallow (unpiled) footings to those of the piled footings. There are two creep-load curves representing the tests on a piled footing: one representing the creep behaviour of the cap in the piled footing, corresponding to the load taken by the cap, and the other representing the overall creep behaviour of the footing, corresponding to the total load applied on the footing. From these figures, it can be noted that under an equal load applied, the creep of the piled footing is always smaller than that of the shallow footing.

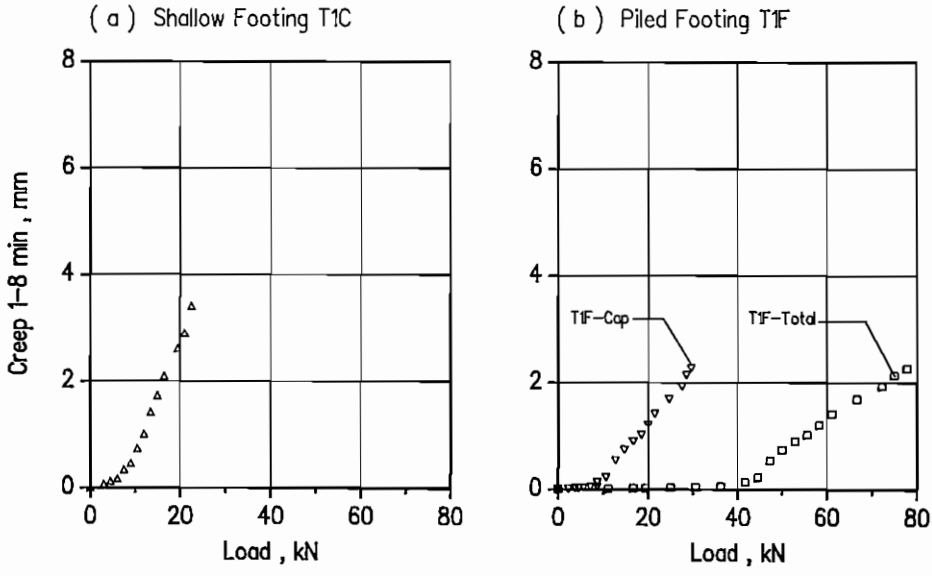

Fig. 6.30 Creep 1-8 min. versus load - Test series T1: relative density of sand I_D= 38 %, pile spacing S= $4b_p$: (a) shallow footing T1C, (b) piled footing T1C.

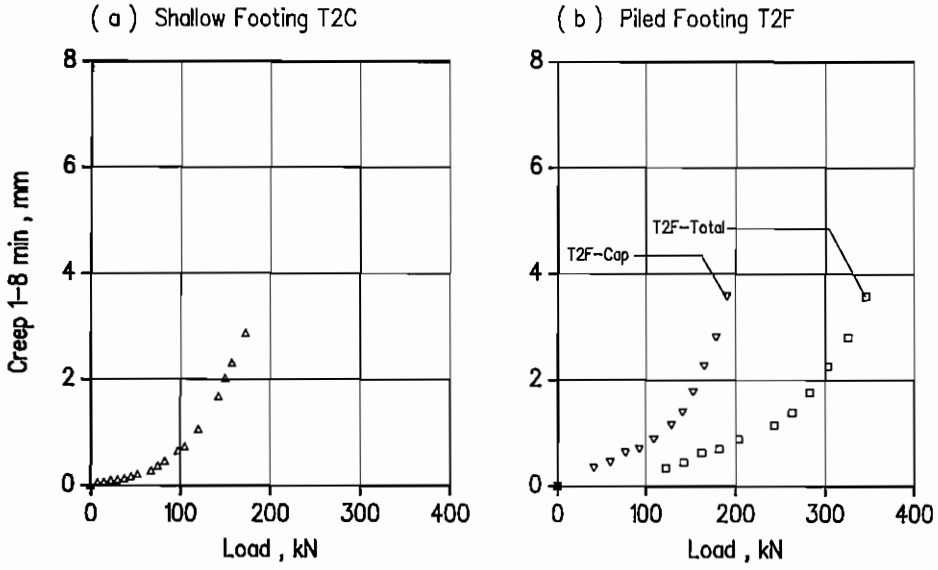

Fig. 6.31 Creep 1-8 min. versus load - Test series T2: relative density of sand I_D= 67 %, pile spacing S= $6b_p$: (a) shallow footing T2C, (b) piled footing T2C.

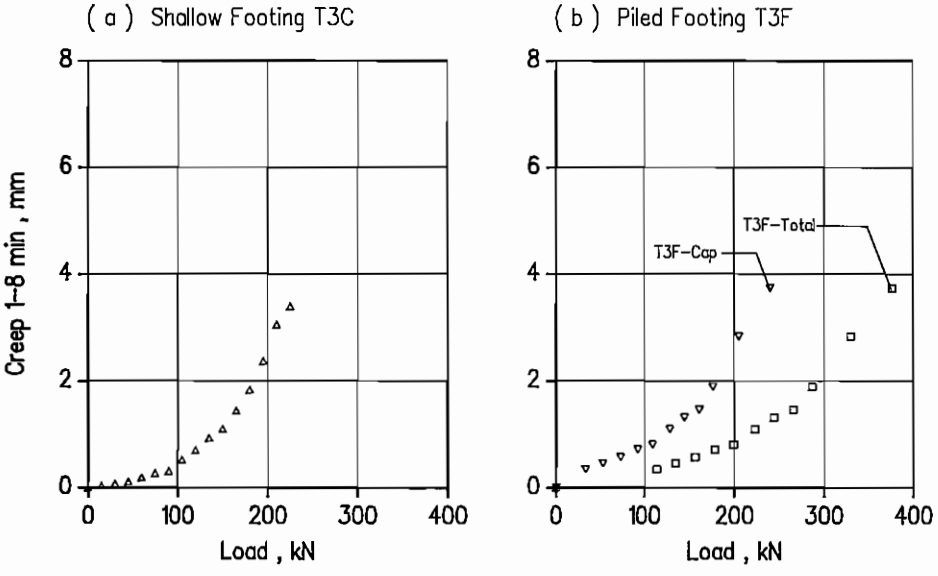

Fig. 6.32 Creep 1-8 min. versus load - Test series T3: relative density of sand I_D= 62 %, pile spacing S= $8b_p$: (a) shallow footing T3C, (b) piled footing T3C.

In loose sand (Test series T1) the creep of the cap in the piled footing is smaller than that of the shallow footing, see Fig. 6.30. In medium and dense sand (Test series T2 and T3), at small load levels, the creep of the cap in the piled footings is larger than that of the shallow footing, while at large loads, the creep seems to be equally large, see Figs 6.31 and 6.32. This can be seen more clearly in Figures 6.33 through 6.35, in which the creep is plotted versus time for both the shallow and the piled footings at a similar level of load taken by the cap. In these figures, P_c denotes the load applied on the shallow footing, while P_{fc} denotes the load carried by the cap and P_{ft} the total load applied on the piled footing. In Test T1, loose sand, the creep of the shallow footing seems always to be larger than that of the cap in the piled footing. In Tests T2 and T3, medium to dense sand, at a low level of load taken by the cap, the creep of the cap in the piled footing is larger than that of the shallow footing. However, from a certain level of load taken by the cap, 93 kN in Test T2 and 107-109 kN in Test T3, the creep is quite similar. As expected, the creep-log time relationship is quite linear for both the shallow and the piled footings. It can therefore be used for prediction of the long-term creep settlement of the footings.

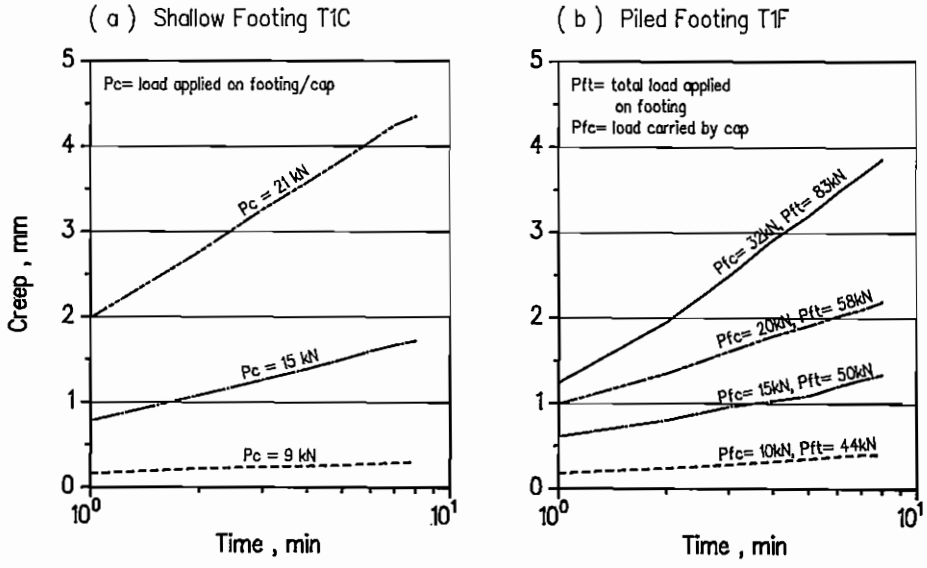

Fig. 6.33 Creep 1-8 min. versus time - Test series T1: relative density of sand I_D= 38 %, pile spacing S= $4b_p$: (a) shallow footing T1C, (b) piled footing T1C.

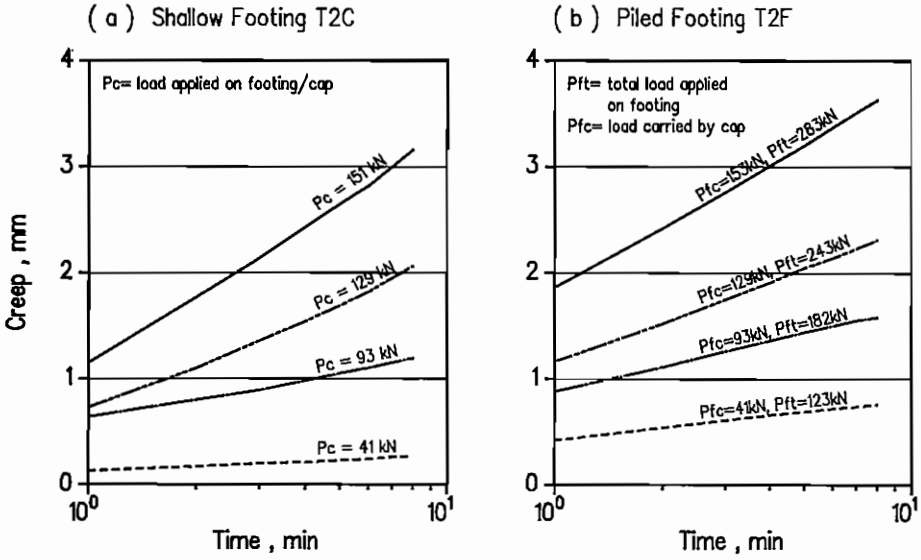

Fig. 6.34 Creep 1-8 min. versus time - Test series T2: relative density of sand I_D= 67 %, pile spacing S= $6b_p$: (a) shallow footing T2C, (b) piled footing T2C.

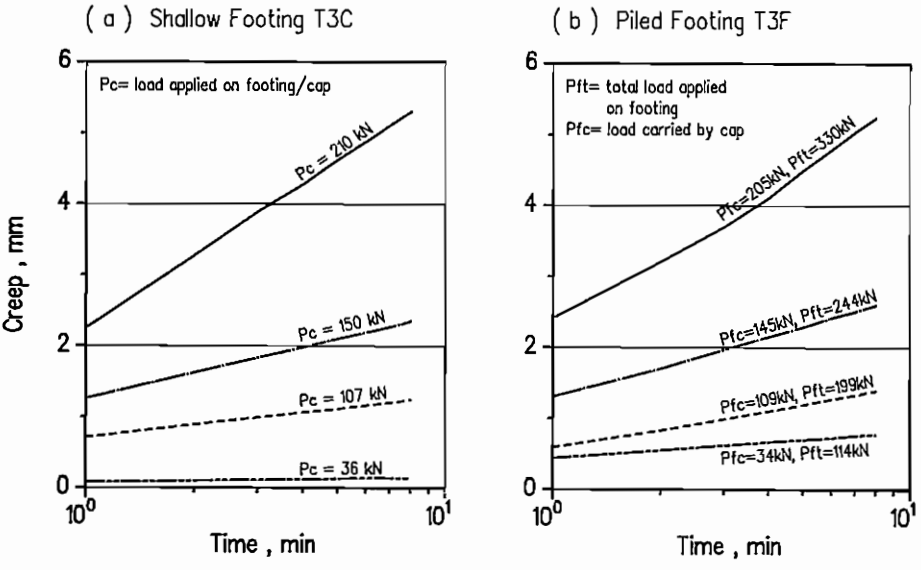

Fig. 6.35 Creep 1-8 min. versus time - Test series T3: relative density of sand I_D= 62 %, pile spacing S= $8b_p$: (a) shallow footing T3C, (b) piled footing T3C.

6.7. Increase in Skin Friction along a Pile

In a piled footing, the skin friction of a pile consists of friction due to pile-soil-pile interaction (as for single piles and free-standing pile groups), and friction due to an increase in lateral earth pressure caused by the cap-soil contact pressure and by the influence of the failure zone at the pile tip, as shown in Section 6.1.

The skin friction due to an increase in horizontal stress will be discussed here. The ultimate skin friction is generally expressed as:

$$f_{su}(z) = \sigma_h'(z) \tan\delta \tag{6.2}$$

where, σ_h' = horizontal effective stress
δ = pile-soil friction angle

The relative displacement between pile and soil $s_{ps}(z)$ should be large enough to mobilise full friction. In the general case, with a given value of the relative displacement $s_{ps}(z)$, the skin friction f(z) can be calculated as:

$$f_s(z) = \sigma_h'(z)\, F(z) \tan\delta \tag{6.3}$$

where, F(z) = level of mobilization of skin friction, which can be estimated as:

$$F(z) = \begin{cases} s_{ps}(z) / s_{psu} & \text{for } s_{ps} < s_{psu} \\ 1 & \text{for } s_{ps} \geq s_{psu} \end{cases} \tag{6.4}$$

where, s_{psu} = relative displacement between pile and soil required to mobilise full skin friction

The movement of the pile shaft relative to the surrounding soil, required to mobilise ultimate pile shaft resistance, is almost independent of the pile diameter and is in the order of 2 to 5 mm.

When the pile cap comes into contact with the ground, it causes an increase in the horizontal pressure against the pile shaft, called $\Delta\sigma_h'$. At the same time it causes the underlying soil to settle, called $s_c(z)$, and as a result the relative displacement between the pile shaft and the surrounding soil will be reduced in the region close to the cap. If the settlement of the pile head s_p and the pile

compression $\delta_p(z)$ are known, and ignoring the settlement of soil due to the pile load, the relative pile-soil displacement becomes, see Fig. 6.36b:

$$s_{ps}(z) = s_p - s_c(z) - \delta_p(z) \tag{6.5}$$

where, $s_{ps}(z)$ = relative displacement between pile and soil at depth z
s_p = settlement of the pile head
$s_c(z)$ = settlement of soil due to the cap
$\delta_p(z)$ = compression of pile

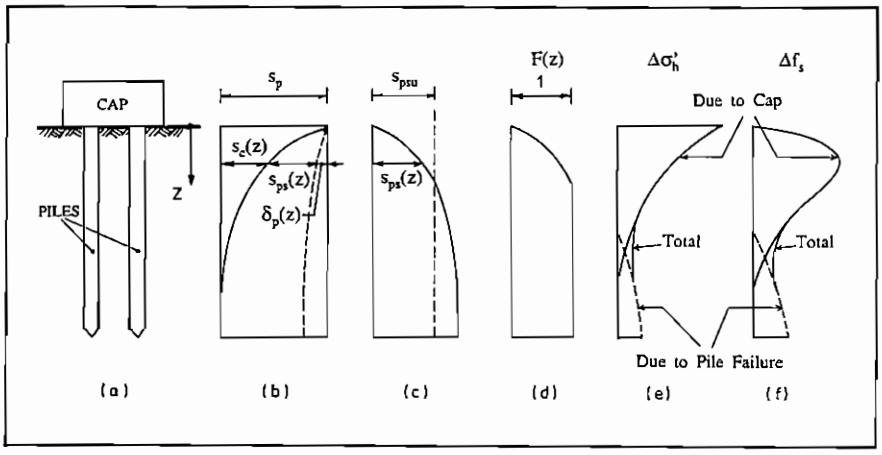

Fig. 6.36 Increase in skin friction along a pile due to effect of cap being in contact with soil and effect of pile failure.

At the pile head, depth z = 0, $s_{ps}(0) = 0$ because $s_p = s_c(0)$, and $\delta_p(0) = 0$. At a depth large enough $s_c(z) = 0$, and Eq. (6.5) returns to the usual form: $s_{ps}(z) = s_p - \delta_p(z)$. The increase in skin friction Δf_s due to the cap in contact with soil will be zero at the cap-soil interface. It will then increase to a maximum value at a certain depth, where the relative soil-pile displacement is large enough, and thereafter decrease because $\Delta\sigma_h'$ reduces with depth, see Fig. 6.36f. In Tests T2F and T3F, the depth, where the increase in skin friction Δf_s due to the cap reach the maximum value, is equal to or less than 0.5 m, because from this depth downwards $\Delta\sigma_h'$ always decreases. It should be noted that the reduction in relative displacement between the pile shaft and soil due to the cap being in contact with soil also makes the skin friction due to pile-soil-pile interaction reduced in vicinity of the bottom of cap. The effect of diminishing the relative displacement between piles and soil nearest below the cap can be seen, though not so clearly, in Test T2F, just after cap-soil contact. Close to the pile base, both $\Delta\sigma_h'$ and Δf_s increase due to the effect of pile failure.

7. COMPARISONS BETWEEN THEORETICAL AND OBSERVED RESULTS

In this chapter, some of the calculation methods, presented in Chapter 2, are applied to analyse the model tests and the results will be compared with the test results.

7.1 Analysis of piled footings using program DEFPIG

The program DEFPIG, presented by Poulos (1980a), is one of the most commonly used computer programs. As discussed in Section 2.3, most of the available computer programs for analysing pile groups and piled footings are based on the theory of elasticity and DEFPIG is one of them. The program was chosen to be used here for the following reasons: (1) DEFPIG has been found to be in close correspondence with other familiar computer programs, such as PIGLET and PGROUP (see Poulos and Randolph, 1983), or PILG (see O'Neill and Ha, 1982); (2) DEFPIG is based on the theory of elasticity, but it allows for the possibility of slippage between the piles and the soil under axial loading, and can therefore be used to predict the load-settlement behaviour of piles; and (3) the program is sufficiently compact to be run on a personal computer. DEFPIG4 (Poulos,1986), a later version of DEFPIG, will be used here to predict the load-settlement behaviour of the piled footings T1F, T2F and T3F, and the calculated results will be compared with the measured results.

Soil Properties

DEFPIG can give quite acceptable predictions of pile group performance, if the required soil parameters are well selected (Poulos, 1980b). The most significant parameters required for the analysis of pile behaviour under static axial loading by means of DEFPIG are: (a) Young's modulus and Poisson's ratio of the soil, E_s and ν_s, (b) the limiting vertical pile-soil stress (adhesion) for pile shaft elements f_{su}, (c) the limiting vertical pile-soil stress for pile base elements q_{bu}, and (d) the limiting vertical pile-soil pressure for pile cap elements q_{cu}. The Poisson's ratio of soil ν_s, estimated according to Eq. (4.11), is 0.37 for the first test series, and 0.30 for the second and the third test series. The Young's modulus of the soil E_s is taken as 22.8 MPa, 37.6 MPa and 30 MPa for Test series T1, T2 and T3, respectively, according to the parameter study presented in Section 7.2. The limiting values f_{su}, and q_{bu} are estimated from the results of the tests on the free-standing pile groups, shown in Chapter

5, by dividing the maximum pile shaft and pile base loads by the corresponding pile shaft and pile base areas. The limiting value q_{cu} is estimated from the results of the tests on the shallow footings by dividing the failure loads by the footing areas. The selected soil parameters are summarised in Table 7.1.

Table 7.1. Soil parameters used in analyses by DEFPIG4

Test	E_s (MPa)	ν_s	f_{su} (kPa)	q_{bu} (kPa)	q_{cu} (kPa)
T1F (I_D=38%)	22.8	0.37	5.7	250	100
T2F (I_D=67%)	37.6	0.30	20.8	2960	380
T3F (I_D=62%)	30.0	0.30	14.2	2100	300

Calculation results

The settlement calculated by means of DEFPIG4 is compared with the measured results of the tests on the piled footings in Fig. 7.1. It can be seen that with well-selected soil properties, DEFPIG4 predicts quite well the load-settlement behaviour of the piled footing under the working load (or the elastic stage). The soil properties here are chosen directly from the field model tests. However, the program fails to simulate the "settlement-hardening" response of the piled footing. The calculated results show a plunging failure. This may be because the method is based on the theory of elasticity, in combination with the "load cut-off" procedure for simulating soil-pile slippage. For each test, two different values of the shaft efficiency 1.0 and 2.5 were used. The base efficiency was accepted to be unity for all the cases. As mentioned above, the limiting shaft friction f_{su} is chosen from the test on the free-standing pile group. This also means that the shaft efficiency for the free-standing pile groups in relation to the single piles η_{1s} is already taken into account in the selected f_{su} values. The efficiency mentioned here refers to the shaft efficiency for the piles in the piled footings in relation to the free-standing pile groups η_{4s}. A η_{4s} value of 2.5 is chosen from Fig. 6.18b, while a unity value means no increase in the pile shaft resistance due to the cap-soil contact effect. Using η_{4s}= 1.0, the maximum applied load is much lower than the measured value, while using η_{4s}= 2.5 the results seem to be better.

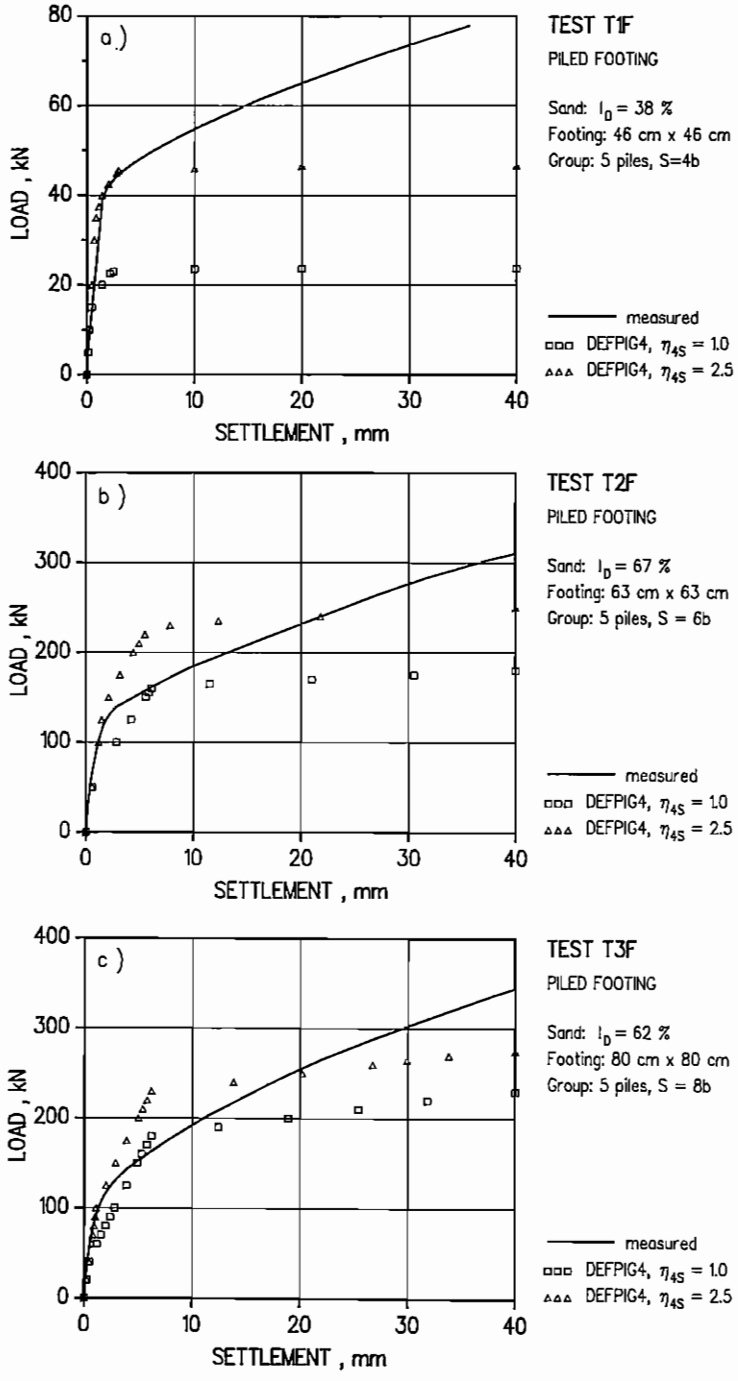

Fig. 7.1 Comparison between measured settlements of piled footings and calculated settlements using Program DEFPIG4. (a) Test T1F; (b) Test T2F; (c) Test T3F.

In principle, DEFPIG4 can be used for analysing single piles or free-standing pile groups and piled footings. However, there is an error in the resulting pile base pressure, since this is different from that obtained by dividing the resulting pile base load by the pile base area. This also results in a premature indication of pile failure. This conclusion was also confirmed by the author of the program, Poulos (1993). Therefore, the program can not be used for single piles and free-standing pile groups, in which the pile base resistance is the factor indicating the pile failure. For piled footings, however, the decisive indication of failure is the cap-soil contact pressure, and the results of the analysis are then acceptable. If the error is corrected, the program can surely be used for single piles and pile groups, and can predict better settlement of piled footings. Another remark is that the approximate procedure for computing the response of individual piles in the group works reasonably well when the pile-soil conditions are elastic, but gives poor answers when a significant amount of pile-soil slip occurs.

7.2 Analysis of shallow footings by means of FLAC

FLAC (Fast Lagrangian Analysis of Continua) is a two-dimensional explicit finite difference code, based on a Lagrangian calculation scheme (ITASCA, 1991). FLAC has several built-in constitutive models. The initial intention was to use FLAC for analysing piled footings, using the equivalent axisymmetrical model, presented in Section 2.3.2, and to compare the calculated results with the test results. Unfortunately, the program does not work well with interfaces which are not placed on a straight line. The soil properties are chosen from a parameter study based on the load-settlement behaviour of the shallow footings, presented below. Using these soil properties, the capacity of the single piles, the free-standing pile group and the piled footings will be overestimated if the interface elements are not used in the analysis. Based on one of the most important remarks drawn from Chapters 5 and 6, namely that the behaviour of the cap in the piled footings is very similar to that of the individual cap, the effect of the cap in contact with soil on the behaviour of the piles can be studied by analysing the cap alone. From the test results, it is obvious that the increase in the pile shaft resistance is much greater than the change in pile base resistance or the change in the cap capacity. This increase in the shaft resistance is induced by the increase in lateral earth pressure against the pile shaft due to the contact pressure at the cap-soil interface. This effect will be studied below by analysing the behaviour of the cap alone using the FLAC code.

For the analysis of the shallow footings, axisymmetrical geometry is used. The square footing is replaced by an equivalent circular one with the same area. The soil media is divided by a mesh composed of quadrilateral elements as shown in Fig. 7.2. The left vertical boundary represents the axis of symmetry. To minimise the boundary effect, the radius to the right vertical boundary and the depth of the soil mass in question are both chosen as large as ten times the radius of the equivalent footing. A linearly elastic- perfectly plastic material according to the Mohr-Coulomb failure criteria is used for modelling the soil. The in-situ stress condition is assumed to be caused by the self-weight of the soil. To simulate a rigid footing, a constant velocity boundary condition is applied in the negative y-direction across the footing width, i.e. the grid points representing the footing are moved rigidly. In order to minimise shocks to the system thus modelled, the velocity V is kept as small as $-1 \cdot 10^{-6}$ m/step. The number of steps N, required to reach a given displacement D of the footing, is then equal to N= D/V.

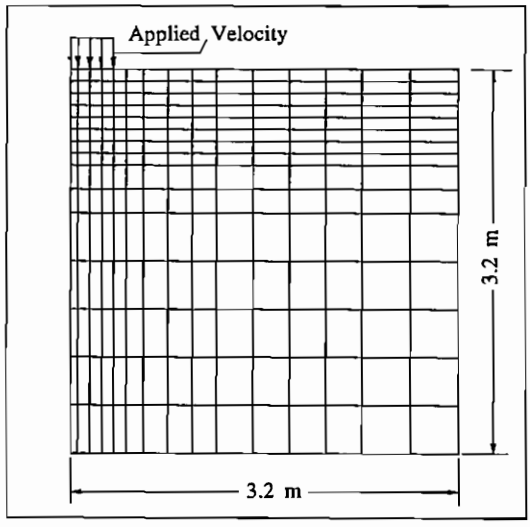

Fig. 7.2 Difference element grid used in FLAC analysis of shallow footing T2C

Soil properties - parametric study

For Test T1C, FLAC was run with 18 different combinations of the values of the elastic modulus E_s, the internal friction ϕ', and the dilation angle ψ, with E_s values ranging between 13 and 26 MPa, ϕ' between 32° and 38°, and ψ between -18° and 0°. The E_s value is chosen on the basis of E_{25}, modulus back-calculated from

the test on the shallow footing at 25% of the failure load, using Eq. (4.22). The Poisson's ratio of soil is 0.37. The elastic shear modulus G, and elastic bulk modulus K, used in the program, are calculated from the Young's modulus and the Poisson's ratio according to the common elasticity formulae: G=E/2(1+ν), and K=E/3(1-2ν). The parameter study for Test T1C, shown in Fig 8.3a, indicates that the footing behaviour calculated by FLAC using the soil properties: E_s= 22.8 MPa, ϕ= 34°,and ψ= -18° (the data file 1v7c) is in best agreement with the observed behaviour.

For Test T2C, FLAC was run with 21 different combinations of the values of E_s, ϕ', and ψ, with E_s ranging between 30 and 42 MPa, ϕ' between 35° and 43°, and ψ between 0° and 20°. The parameter study for Test T2C, presented in Fig 8.3b, shows that the footing behaviour calculated using E_s= 37.6 MPa, ϕ'= 38° to 39°, and ψ= 0° to 3° is in best agreement with the observed behaviour (the data files 2v7 and 2v7a).

For Test T3C, FLAC was run with 23 different combinations of the values of E_s, ϕ', and ψ, with E_s ranging between 20 and 35 MPa, ϕ' between 35° and 41°, and ψ between 0° and 10°. From the parameter study for Test T3C, shown in Fig 8.3c, we find that the behaviour of the footing can be best predicted by FLAC using E_s= 30 MPa, ϕ= 37° and ψ= 0° (the data file 3v9e).

Table 7.2 Soil parameters back-calculated by FLAC

Test	E_s (MPa)	ν_s	ϕ' (degree)	ψ (degree)
T1C (I_D=38%)	22.8	0.37	34	-18
T2C (I_D=67%)	37.6	0.30	38 ÷ 39	0 ÷ 3
T3C (I_D=62%)	30.0	0.30	37	0

From the parameter study, some remarks can be drawn: FLAC can predict the load-settlement behaviour of shallow footings excellently well if reasonable soil parameters are chosen and if the soil is modelled as a Mohr-Coulomb material. The modulus of elasticity of the soil is of the same order of magnitude as that back-calculated from the tests on the shallow footing at loads betweens 18% and 25% of the failure load. Among the soil investigation methods, the dilatometer tests seems to give a modulus of comparable size, although it is still smaller than E_{25}. The angle of internal friction ϕ' evaluated from the dilatometer tests according to the CPT-linked method, Marchetti (1985), is closest to the value

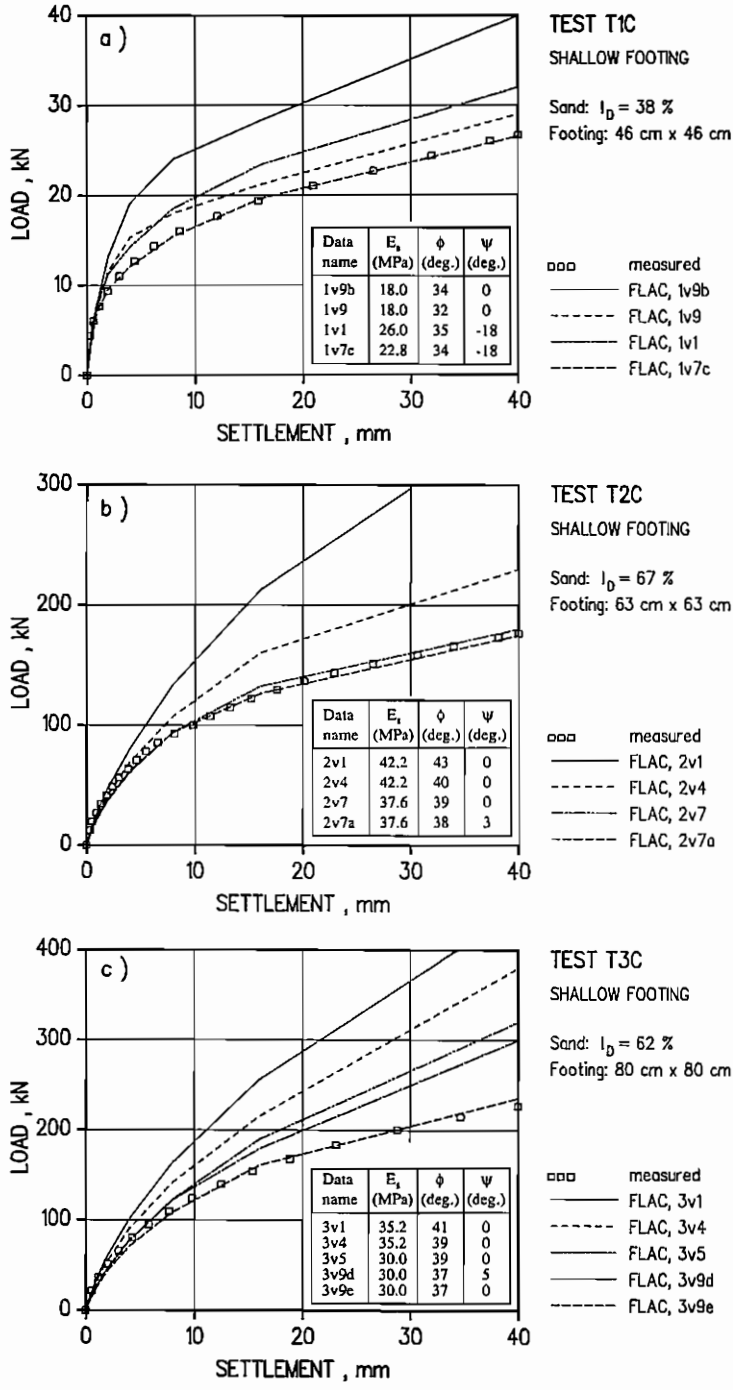

Fig. 7.3 Analyses of shallow footing by FLAC - Parameter study on soil properties. (a) Test T1C; (b) Test T2C; (c) Test T3C.

back-calculated by FLAC, although it is slightly larger. For loose sand, a negative dilation angle ψ should be used, while for medium dense or quite dense sand a value equal to, or slightly higher than, zero can be used.

Horizontal soil stress induced by shallow footings

The horizontal soil stress induced by the shallow footings, analysed above using the Mohr-Coulomb model will now be compared with that obtained using the elastic soil model. The elastic analysis was also made using the FLAC code. In both cases, axisymmetrical geometry was used as shown above. The soil properties back-calculated by FLAC, see Table 7.2, were used in the analysis. The elastic soil model had the same values of E_s and ν_s as those of the elastic-plastic model. The distribution of the horizontal soil stress versus depth under the centre of Footings T2C and T3C thus obtained is shown in Figures 7.4 and 7.5. The horizontal soil stress, shown in these figures, is only due to the applied load which is 175 kN in the case of Footing T2C and 225 kN for Footing T3C. The corresponding average cap-soil contact pressures are 441 kPa and 351 kPa, respectively. The calculated horizontal stress induced by the shallow footings is also compared with the increase in the measured lateral earth pressure along the pile shaft due to the cap effect in the corresponding piled footings at the equal cap load level.

According to Figures 7.4 and 7.5, the theory of elasticity underestimates the induced horizontal soil stress. Using the Mohr-Coulomb soil model, the horizontal pressure in the soil is much higher, and the depth of influence is much greater. It is interesting to see that the measured lateral pressure against the pile shaft due to the cap effect in the piled footings, has a surprising correspondence with the horizontal soil stress under the corresponding shallow footings analysed by the elastic-plastic theory. This fact once again supports the assumption that the behaviour of the cap in a piled footing is similar to that of a corresponding unpiled footing. This can also be used as a basis for a theoretical estimation of the cap effect on the pile shaft resistance in a piled footing.

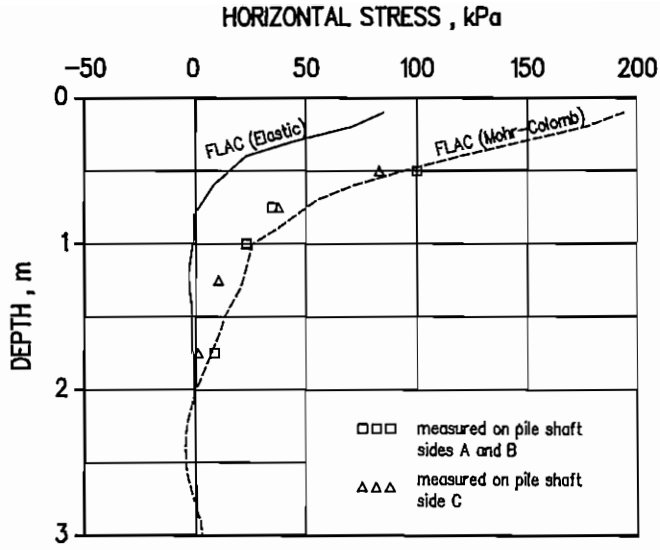

Fig. 7.4 Comparison of the horizontal soil stress under the shallow footing T2C analysed by FLAC with the measured earth pressure against the pile shaft due to the cap effect in the piled footing T2F at the load level $P_c = P_{fc}$ *= 175 kN.*

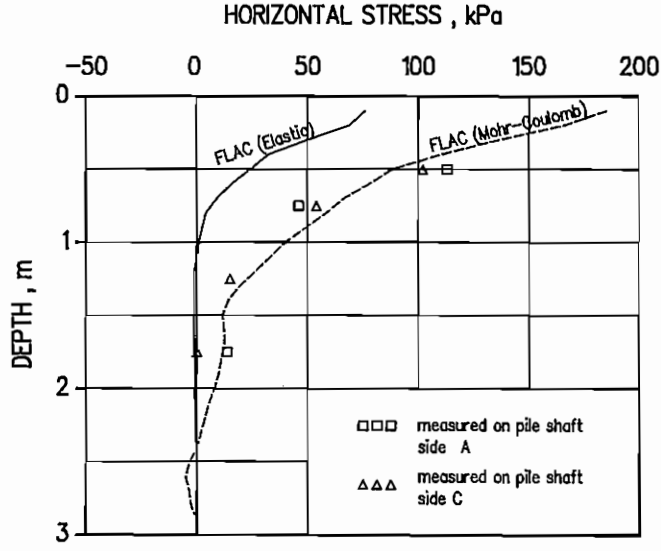

Fig. 7.5 Comparison of the horizontal soil stress under the shallow footing T3C analysed by FLAC with the measured earth pressure against the pile shaft due to the cap effect in the piled footing T3F at the load level $P_c = P_{fc}$ *= 225 kN.*

8. PROPOSED SIMPLIFIED METHOD OF CALCULATING SETTLEMENT OF PILED FOOTINGS IN SAND

Based on the conclusions drawn in Chapters 5 and 6, some simplified methods for estimating settlement of piled footings in non-cohesive soil are suggested in this chapter. The settlement of piled footings in sand can be calculated using the results of the corresponding tests on shallow footings and single piles.

8.1 Calculating settlement of piled footings

The results in Chapter 5 indicate that the behaviour of the cap in a piled footing is very similar to that of the corresponding shallow footing (cap alone). In comparison with the cap alone, the stiffness of the cap in loose sand in the piled footing is slightly higher (Test T1), while in medium dense to dense sand it is slightly lower (Tests T2 and T3). However, in both cases, it can be considered that the behaviour of the cap in a piled footing is approximately equal to that of the corresponding shallow footing. This means that if the load carried by the cap P_{fc} in a piled footing is known, the settlement of the piled footing can be approximately estimated as the settlement of the shallow footing at the same load level. In the piled footing, the load carried by the cap P_{fc} is equal to the total applied load P_{ft} minus the load taken by the piles P_{fp}:

$$P_{fc} = P_{ft} - P_{fp} \tag{8.1}$$

The key factor is now to estimate the load carried by the piles P_{fp} in the piled footing. Based on the result of load tests on single piles, provided that the load efficiency for a free-standing pile group in relation to a single pile η_1 (at the same settlement) is known, the load taken by the piles can be estimated as:

$$P_{fp} = n \cdot \eta_1 \cdot P_s \tag{8.2}$$

where, n = number of piles in the group
P_s = load applied on the single pile at the same settlement

If the load efficiency for piles in a piled footing in relation to a free-standing pile group η_4 (due to the cap effect) is also known, the P_{fp} value can be estimated as:

$$P_{fp} = n \cdot \eta_1 \cdot \eta_4 \cdot P_s \tag{8.3}$$

From Fig. 6.17, Chapter 6, we find that η_4 is always higher than unity whatever the relative density of the sand. Generally, the efficiency η_4 increases when the settlement increases. Of course, the η_4 value is rarely known in practice. However, it can be estimated by means of the theory of plasticity as shown in Chapter 7. The proposed method of settlement analysis will now be exemplified for the piled footings in all three test series using the results of the corresponding tests on single piles and on shallow footings, shown in Chapter 5, as well as the load efficiencies $\eta_1$and η_4 obtained in Chapter 6.

Test series T1

From the test on the piled footing T1F shown in Fig. 5.5, the total applied load P_{ft} at a given settlement is known. Using, for this load, the result of the test on the single pile T1S shown in Fig. 5.2, the load taken by the piles P_{fp} can be estimated according to the first method, Eq. (8.2), or the second method, Eq. (8.3). The load efficiency η_1 is determined from Fig. 6.14, and the efficiency η_4 from Fig. 6.17. The load carried by the cap P_{fc} is then calculated according to Eq. (8.1). Using the result of the test on the shallow footing T1C, shown in Fig. 5.1, the settlement of the piled footing can be estimated approximately as the settlement of the shallow footing at the same load level P_{fc}. The estimated results are summarised in Table 8.1 and are shown in Fig. 8.1a.

Table 8.1 Estimation of settlement of the piled footing T1F

s_0 (mm)	P_{ft} (kN)	P_s (kN)	η_1	P_{fp1} (kN)	P_{c1} (kN)	s_1 (mm)	η_4	P_{fp2} (kN)	P_{c2} (kN)	s_2 (mm)
2.5	43.5	1.85	2.4	22.0	21.0	18	1.5	33.0	10.5	2.7
5.0	48.0	1.90	2.4	23.0	25.0	30	1.5	34.5	13.5	5.3
7.5	51.5	2.20	2.35	25.8	25.7	35	1.4	36.1	15.4	7.7
10.0	55.0	2.20	2.35	25.8	29.2	-	1.45	37.4	17.6	11.5
15.0	61.0	2.20	2.35	25.8	35.2	-	1.5	38.8	22.2	24.0
20.0	65.0	2.20	2.35	25.8	39.2	-	1.6	41.4	23.6	28.0
30.0	73.0	2.25	2.35	26.4	47.2	-	1.75	46.2	26.8	39.0

Note: s_0= settlement in question; P_{ft}= corresponding total load in the piled footing test; η_1, η_4 = load efficiencies, P_{fp1}, P_{fp2} = loads taken by the piles in piled footing calculated according to the first method, Eq. (8.2), and the second method, Eq.(8.3); P_{c1}, P_{c2} = loads carried by the cap in piled footing corresponding to P_{fp1}, P_{fp2}; and s_1, s_2 = settlements calculated according to the first method and the second method, respectively.

Test series T2

The settlement of the piled footing T2F is estimated in the same way as above, using Fig. 5.9 for the shallow footing T2C, Fig. 5.10 for the single pile T2S, and Fig. 5.15 for the piled footing T2F. The load efficiencies η_1 and η_4 are also determined from Figures 6.14 and 6.17. The estimated results are summarised in Table 8.2 and are shown in Fig. 8.1b.

Table 8.2 Estimation of settlement of the piled footing T2F

s_0 (mm)	P_{ft} (kN)	P_s (kN)	η_1	P_{fp1} (kN)	P_{c1} (kN)	s_1 (mm)	η_4	P_{fp2} (kN)	P_{c2} (kN)	s_2 (mm)
2.5	133	9.2	1.3	60	73	5.0	1.35	81	52	2.5
5.0	154	10.6	1.3	69	85	6.5	1.2	83	71	4.8
7.5	170	11.3	1.25	71	99	9.5	1.2	85	85	7.0
10.0	184	11.8	1.25	74	110	12.0	1.2	89	95	9.5
15.0	208	12.4	1.2	75	133	20.0	1.3	97	111	13.5
20.0	231	13.0	1.2	78	153	26.0	1.3	101	130	19.0
30.0	276	13.5	1.2	81	195	-	1.65	133	143	24.0
40.0	310	14.0	1.2	84	226	-	1.7	143	167	35.0

Test series T3

For analysing settlement of the piled footing T3F, Fig. 5.18 is used for the shallow footing T3C, Fig. 5.19 for the single pile T3S, and Fig. 5.24 for the piled footing T3F. The load efficiencies η_1 and η_4 are also determined from Figures 6.14 and 6.17. The estimated results are summarised in Table 8.3 and are shown in Fig. 8.1c.

Table 8.3 Estimation of settlement of the piled footing T3F

s_0 (mm)	P_{ft} (kN)	P_s (kN)	η_1	P_{fp1} (kN)	P_{c1} (kN)	s_1 (mm)	η_4	P_{fp2} (kN)	P_{c2} (kN)	s_2 (mm)
2.5	125	6.4	1.35	43	82	4.5	1.75	76	49	2.0
5.0	153	7.4	1.30	48	105	7.2	1.70	82	71	4.0
7.5	173	7.8	1.25	49	124	10.4	1.70	83	90	5.7
10.0	192	8.2	1.25	51	141	13.5	1.70	87	105	7.7
15.0	225	8.7	1.25	54	171	20.0	1.75	95	130	11.5
20.0	255	9.1	1.20	55	200	30.0	1.80	99	156	17.0
30.0	303	9.6	1.20	58	245	-	2.00	116	187	26.5
40.0	345	10.0	1.20	60	285	-	2.10	126	219	39.0

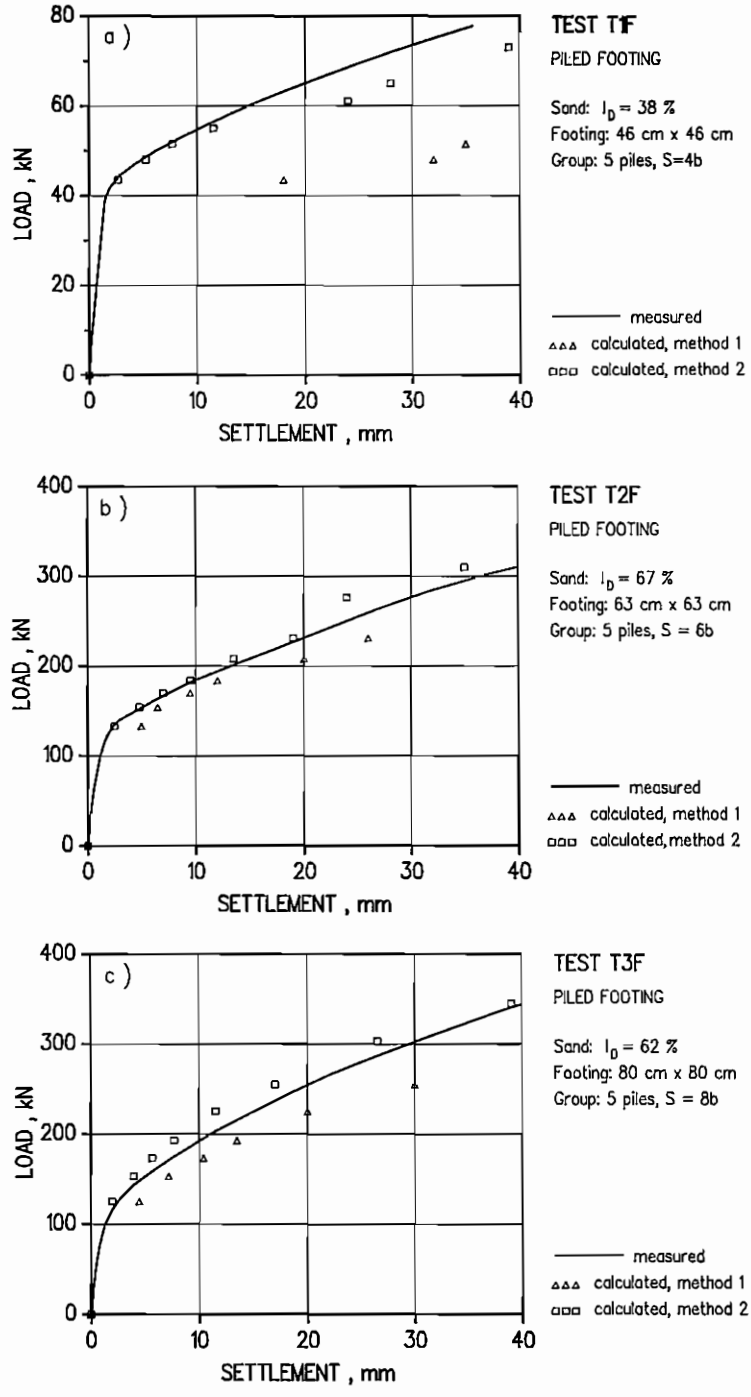

Fig. 8.1 Comparison between the settlements calculated according to the proposed simplified methods and the measured values. (a) Test series T1; (b) Test series T2; (c) Test series T3.

Discussions

From Fig. 8.1 it can be seen that the settlement calculated according to the first simplified method is always higher than the measured value. This can be explained by the fact that using Eq. (8.2) the load taken by the piles is always underestimated. In reality, the influence of the cap in contact with soil on the pile capacity is significant. However, it is ignored in Eq. (8.2). This method can be applied in practice because it is simple and always conservative.

The settlement estimated according to the second simplified method is in good agreement with the measurement results due to the consideration of the cap effect in Eq. (8.3). However, in comparison with the measured values, the calculated settlement is still larger in loose sand, and slightly smaller in dense sand. Considering Fig.6.20, we notice that, for a settlement larger than 10 mm, the load taken by the cap in the piled footing is larger than the load applied on the corresponding shallow footing in loose sand (about 10 to 15 %), and lower in medium to dense sand (about 10%). Based on this remark, if the load taken by the cap is decreased 10-15% for loose sand, and increased about 10% for medium to dense sand, the calculated settlement will be in excellent agreement with the measured value.

8.2 Estimating settlement-reducing effect

In Section 6.4, the concept of relative cap capacity α was introduced. The relationship between the settlement ratio ξ_7 and the relative cap capacity α, shown in Fig. 6.27, will be used in this section as the basis of a quick method for estimating the settlement-reducing effect. The settlement ratio ξ_7, defined as the ratio of the settlement of a piled footing to that of the corresponding shallow footing, means the level of settlement reduction due to the use of piles for a shallow footing. The relative cap capacity α of a piled footing is defined as the ratio of the load applied on the corresponding shallow footing to the load applied on the piled footing at a certain settlement close to failure. The α value refers to the relative contribution of the cap to the capacity of the piled footing. With a given relationship between α and ξ_7, similar to that shown in Fig.6.27, the settlement reduction will be known if the relative cap capacity is known.

We now assume that the load-settlement curve for a shallow footing is already known. Then, if the ultimate capacity of the single pile P_s and the load

efficiency η_1 are known, the reduction in settlement of the corresponding piled footing (ξ_7) can be predicted according to the following procedure: (a) At a certain settlement s_c, called the reference settlement, the load applied on the shallow footing P_c is taken from the load-settlement curve for the shallow footing; (b) the load applied on the piled footing P_{ft} is then equal to the sum of P_{fc}, which is considered to be equal to the load applied on the shallow footing P_c, and the load taken by the piles P_{fp}, which can be estimated, e.g. according to Eq.(8.2); (c) the relative cap capacity at this reference settlement is estimated as: $\alpha = P_c/P_{ft}$; (d) the reduction in settlement of the corresponding piled footing ξ_7 can be obtained, e.g. from Fig. 8.2, in which the α-ξ_7 curve is the upper limit of the curves in Fig. 6.27; (e) the settlement of the piled footing can be estimated as: $s_f = \xi_7 \cdot s_c$. This method can also be used to predict the settlement of piled footing as the third simplified method.

The method proposed above is exemplified for the prediction of the settlement of the piled footings T1F, T2F, and T3F. The calculation results are shown in Tables 8.4 to 8.6.

Table 8.4 Estimation of the settlement reduction - piled footing T1F

Ref. set. s_c (mm)	P_c (P_{fc}) (kN)	P_s (kN)	η_1	P_{fp} (kN)	P_{ft} (kN)	α	ξ_7	calculated s_f (mm)	measured s_f (mm)
10	16.7	2.20	2.35	25.8	42.5	0.39	0.12	1.2	2.1
20	20.7	2.20	2.35	25.8	46.5	0.44	0.15	3.0	3.9
30	23.7	2.25	2.35	26.4	50.1	0.47	0.18	5.4	6.2
40	26.7	2.27	2.35	26.7	53.4	0.50	0.23	9.2	8.3

Table 8.5 Estimation of the settlement reduction - piled footing T2F

Ref. set. s_c (mm)	P_c (P_{fc}) (kN)	P_s (kN)	η_1	P_{fp} (kN)	P_{ft} (kN)	α	ξ_7	calculated s_f (mm)	measured s_f (mm)
10	101	11.8	1.25	73.8	174.8	0.58	0.38	3.8	7.6
20	133	12.9	1.20	77.4	210.4	0.63	0.46	9.2	12.6
30	158	13.7	1.20	82.2	240.2	0.66	0.51	15.3	17.4
40	175	14.0	1.20	84.0	259.0	0.68	0.54	21.6	20.8

Table 8.6 Estimation of the settlement reduction - piled footing T3F

Ref. set. s_c (mm)	P_c (P_{fc}) (kN)	P_s (kN)	η_1	P_{fp} (kN)	P_{ft} (kN)	α	ξ_7	calculated s_f (mm)	measured s_f (mm)
10	121	8.2	1.25	51.2	172.2	0.70	0.56	5.6	7.3
20	168	9.1	1.22	55.5	223.5	0.75	0.64	12.8	14.7
30	198	9.6	1.20	57.6	255.6	0.77	0.67	20.1	20.1
40	221	10.0	1.20	60.0	281.0	0.79	0.69	27.6	25.1

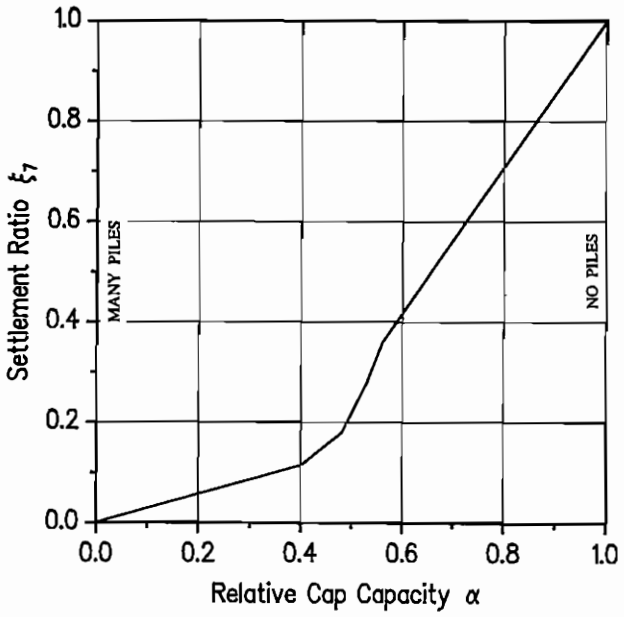

Fig. 8.2 Settlement reduction factor ξ_7 of piled footings, in relation to shallow footings, versus relative cap capacity α

Although the calculated values are smaller than those measured at small settlements of the piled footings, the results in Tables 8.4 to 8.6 show a very good agreement between the calculated and the measured settlements. This method is promising, especially in the period of preliminary design of a piled footing. The number of piles required to reduce the settlement of the footing to a permissible level can be quickly estimated with reasonable accuracy. However, it has to be realised that the method is empirical and approximate. Thus, the α value is defined at the same settlement, but it is estimated, according to the proposed procedure, from the loads applied on the shallow footing and the piled footing at different settlements. However, by assuming that the behaviour of the cap in the piled footing is similar to that of the cap alone ($P_c = P_{cf}$), the ratio $\alpha = P_c/P_{ft} = P_{fc}/P_{ft}$ still has the meaning of "the relative contribution of the cap to the capacity of the piled footing". It is noticed that, for a piled footing, α is not a fixed value, it varies with varying settlement. Fig. 6.27, the basis for Fig 8.2, was based on the α values calculated for Test series T1, T2 and T3 at a settlement of 5 mm. It could be based on α values calculated at another settlement, e.g. 10 or 20 mm. However, the settlements calculated using the α-ξ_7 curve based on a settlement of 5 mm are closest to the measured values.

9. CONCLUSIONS

The behaviour of piled footings in non-cohesive soil with the cap in contact with the soil surface is quite a complicated problem. The main purpose of this investigation is to obtain a better knowledge of the load-transfer mechanism, the pile-cap-soil interaction, as well as of the load-settlement behaviour of piled footings in non-cohesive soil. Simplified methods of estimating the settlement of piled footings in sand have been proposed, where the piles are used for the mere purpose of reducing the settlement of the footings to a permissible level.

The main conclusions gained from the field tests and the analyses are summarised in this chapter.

Bearing capacity

The bearing capacity of the piled footings were studied in this thesis by using the different load efficiencies defined in Table 6.1. All these efficiencies do not have a fixed value. They vary depending on the settlement level. The most practical efficiencies are η_1, η_4, η_6 and η_7.

The bearing capacity of a piled footing P_{ft} can be calculated according to Eq. (6.1), which can be modified to the following form:

$$P_{ft} = n\,(\eta_{1s}\,\eta_{4s}\,P_{ss} + \eta_{1b}\,\eta_{4b}\,P_{sb}) + \eta_6\,P_c \qquad (9.1)$$

where, n = number of piles in the group,

η_{1s}, η_{1b} = influence factors of pile-soil-pile interaction on the pile shaft and pile base capacities,

η_{4s}, η_{4b}, η_6 = influence factors of cap-pile interaction on the pile shaft and and pile base capacities, and on the capacity of the cap,

P_{ss}, P_{sb} = shaft and base capacities of the reference single pile under equal soil conditions as the pile group,

P_c = capacity of the shallow footing (cap alone).

The load efficiencies η_{1s} and η_{1b} represent pile-soil-pile interaction, which is mainly caused by the pile installation effect. The pile base efficiency η_{1b} can be taken as unity for piles in medium to dense sand, but it seems to be larger than unity for piles in loose sand. The pile shaft efficiency η_{1s} is always higher than unity even for pile groups with large pile spacing. In Test series T3, with a pile spacing of eight times the pile width ($S = 8b_p$), η_{1s} is still quite large, $\eta_{1s} \simeq 2$.

The load efficiencies η_{4s}, η_{4b}, and η_6 represent the effect of the cap-soil contact pressure. The pile base efficiency η_{4b} is probably higher than unity for very short piles, but can be taken as unity when the piles are long enough, e.g. $l_p >$ (1.5 to 2) B_c, where B_c is the width of the cap. The pile shaft efficiency η_{4s} is the most important factor in the cap-pile interaction problem. It seems to increase linearly with increasing settlement. The efficiency η_{4s} also depends on the size of the cap: the larger the cap, the greater the efficiency. The efficiency η_{4s} can be estimated theoretically by analysing the corresponding shallow footing using the Mohr-Coulomb soil model, as shown in Section 7.2. The cap efficiency η_6 is very close to unity: it is between 1.1 and 1.2 for Test series T1 in loose sand, and 0.8 to 1.0 for Test series T2 and T3 in medium dense to dense sand. For practical design purposes, it can be taken as 1.0 for loose sand, and 0.9 for medium to dense sand.

Lateral earth pressure against the pile shaft

The increase in the capacity of a piled footing due to the cap-soil-pile interaction is mainly caused by the increase in the pile shaft resistance which in turn, is induced by the increase in horizontal pressure against the pile shaft under the cap-soil contact pressure.

The increase in lateral earth pressure against the pile shaft in a piled footing consists of two components: the increase due to the cap in contact with soil on the one hand, and to the effect of the pile failure zone on the other. The effect of cap-soil contact is predominant for the upper part of the pile, while the effect of the pile failure zone is predominant for the lower part. However, in comparison with the increase in lateral pressure due to the cap effect, the increase due to the pile failure effect is small and can be ignored in practice.

At a small cap load P_{fc}, the increase in lateral pressure due to the cap effect is small. When the cap load is large enough, it increases in proportion to the increase in the cap load. This can be explained by the fact that, at small cap loads, the soil under the cap remains in an elastic state and that, therefore, the horizontal stress induced in the soil is small. At a large enough cap load, the soil becomes plastic, and in consequence the horizontal stress increases both in magnitude and in depth of influence, as shown in Section 7.2.

The lateral pressure against the pile shaft clearly decreases with increasing depth. It has a largest magnitude at the cap-soil interface and reduces to zero

at a certain depth depending on the size of the cap.

Load sharing between piles and cap

With a good cap-soil contact, the distribution of the load between the cap and the piles will be governed by the settlement. At very small settlement, the piles take an important part of the load. When the settlement is large enough to mobilise the full capacity of the piles, a considerable portion of the applied load will be transferred to the cap. Thereafter, the load sharing between the cap and the piles becomes almost constant. The percentage of load carried by the cap is identical with the concept of relative cap capacity α at a specific settlement. As in the case of a free-standing pile group, the central pile in a piled footing in sand takes a higher load than the corner piles.

Load-settlement behaviour

The failure of a piled footing in non-cohesive soil is progressive, i.e. the applied load increases with increasing settlement. The increase in the applied load is significant and is due to the cap-soil contact pressure which makes the pile shaft resistance increase considerably.

The load-settlement behaviour of the cap in a piled footing is very similar to that of a corresponding shallow footing (cap alone). This remark, which is one of the most important conclusions drawn from the field model tests, is used as the basis for the simplified method of estimating the settlement of a piled footing in sand, as proposed in Chapter 8.

The conventional settlement ratio, defined by comparing the settlement of a single pile with that of a pile group, has little practical meaning in estimating the settlement of piled footings. The settlement ratio ξ_7, defined as the settlement of a piled footing to that of a corresponding shallow footing at the same applied load, seems to be more useful. The ratio ξ_7 depends clearly on the relative cap capacity α, and can be used for a quick estimate of the reduction in settlement of the footing.

Creep behaviour

In loose sand, the creep of the cap in a piled footing is smaller than that of a corresponding shallow footing. In medium dense to dense sand, the creep

behaviour of the cap in a piled footing is quite similar to that of a corresponding shallow footing. As expected, the creep - log time relationship is quite linear for both the shallow and the piled footings. It can, therefore, be used for prediction of the long-term creep settlement of the footings.

Proposed calculation methods

Based on the second conclusion on the load-settlement behaviour of a piled footing, simplified methods of predicting the settlement of piled footings in non-cohesive soil have been proposed in Chapter 8. Thus, the settlement of a piled footing can be approximately estimated as the settlement of a corresponding shallow footing at the same cap load level. The load-settlement behaviour of a shallow footing, in turn, can be calculated according to any method preferred by the reader. However, the Author suggests that the Mohr-Coulomb soil model should be used in the analysis.

The reduction in settlement of a piled footing in relation to the corresponding shallow footing can also be quickly estimated according to another simplified method, with the help of the relative cap capacity, which represents the contribution of the cap to the capacity of the piled footing. The results of the simplified methods are in good agreement with those obtained from the field tests.

Test Procedure

Tests on a piled footing can be performed using two different procedures. The first procedure, in which the test is started when the pile cap is already in good contact with the soil, has the advantage of making possible a direct comparison between the behaviour of a piled footing and those of a shallow footing and a free-standing pile group. However, using the second procedure, in which the test is started when the pile cap was 20 mm above the soil surface, the effect on the pile behaviour of the cap being in contact with soil is more obvious. Comparisons with other tests can be made by using the load-settlement curve, modified from the original one according to the method shown in Appendix A. The second test procedure is strongly recommended for testing piled footings both in sand and clay.

Further research

This study has presented a basis for the analysis of the behaviour of a piled footing with the cap in contact with the soil surface by performing an extensive program of large-scale field model tests. However, the scale effect may have a certain influence on the test results. Full-scale tests should be carried out, according to the test procedures used in this study, to verify the results obtained.

The existing calculation methods, based on the theory of elasticity, show disadvantages when predicting the behaviour of a piled footing in non-cohesive soil, especially for footings with settlement-reducing piles, in which the piles are close to or at failure. Methods of analysis based on the elastic-plastic soil model are, therefore, strongly needed.

Studies of the load distribution among the piles in a pile group or in a piled footing in sand often show a higher capacity for the central pile/piles in relation to the corner and edge piles. This can be simulated by using a greater soil stiffness inside the pile group than outside.

The field tests were carried out during a short time. It is known that the capacity of a single pile, for example, could change with time. The long term behaviour of a piled footing could, therefore, be different from the results obtained in this research. The long-term behaviour of piled footings in sand needs further investigation.

REFERENCES

Andreasson L. (1973). Compressibility of cohesionless soils. A laboratory investigation. Rapport R 36:1973, Byggforskningen, Stockholm. (In Swedish)

Akinmusuru, J.O. (1980). Interaction of piles and cap in piled footing. Proc. ASCE, JGED, Vol. 106, No. GT11, pp. 1263- 1268.

Atkinson, J.H., Sällfors, G. (1991). Experimental determination of stress-strain time characteristics in laboratory and insitu tests, Proc. 10th ECSMFE, Florence, Vol. 3, pp. 915-956.

Banerjee, P.K., Driscoll, R.M. (1978). Program for the analysis of pile groups of any geometry subjected to horizontal and vertical loads and moments, PGROUP (2.1). HECB/B/7 Department of Transport, HECB, London.

Baguelin, F., Jezequel, J.F., Shields, D.H. (1978). The pressuremeter and foundation engineering. Trans Tech Publications, Clausthal.

Beredugo, Y.O. (1966). An experimental study of the load distribution in pile groups in sand. Canadian Geotech. J., Vol. 3, No. 3, pp. 145-166.

Berezantsev, V.G., Khristoforov, V.S., Golubkov, V.S. (1961). Load bearing capacity and deformation of piled foundations. Proc. 5th ICSMFE, Paris, Vol.2, pp. 11-15.

Bjerrum, L., Jönsson, W., Ostenfeld C. (1957). The settlement of a bridge abutment on friction piles. Proc. 4th ICSMFE, London, Vol. 2, pp. 14-18.

Bolton, M.D. (1986). The strength and dilatancy of sands. Geotechnique, Vol. 36, No. 1, pp. 65-78.

Briaud, J.L., Tucker, L., Lytton, R.L., Coyle, H.M. (1985). Behaviour of piles and pile groups in cohesionless soils. US Department of Transportation, FHWA, Report No. FHWA/RD-83/038, Washington, D.C.

Briaud, J.L. (1992). Pressuremeter. Balkema Publishers, Rotterdam.

Burland, J.B., Broms, B.B., De Mello, V.F.B. (1977). Behaviour of foundations and structures. Proc. 9th ICSMFE, Tokyo, Vol. 2, pp. 495-546.

Burland, J.B., (1986). The value of field measurements in the design and construction of deep foundations. Proc. Int. Conf. on Deep Foundations, Beijing, Vol. 2, pp. 177-187.

Butterfield, R. and Banerjee, P.K. (1971). The problem of pile group - pile cap interaction. Geotechnique, Vol. 21, No. 2, pp. 135-142.

Butterfield, R. and Douglas, R.A. (1981). Flexibility coefficients for the design of piles and pile groups. CIRIA, Technical Note No. 108, London.

Brown, P.T., Poulos, H.G., Wiesner, T.J. (1976). Pile raft foundation design. Research Report No. R299, University of Sydney, N.S.W.

Cambefort, H. (1953). La force portante des groupes de pieux. Proc. 3rd ICSMFE, Zurich, Vol. 2, pp. 22-28.

Chow, Y.K. (1986a). Analysis of vertically loaded pile groups. Int. J. for Numerical and Analytical Methods in Geomech., Vol. 10, pp. 59-72.

Chow, Y.K. (1986b). Discrete element analysis of settlement of pile groups. Computers & Structures, Vol. 24, No. 1, pp. 157-166.

Clancy, P., Griffiths, D.V. (1990). Finite element analysis of pile group interactions. Proc. European Specialty Conference on Numerical Methods in Geotechnical Engineering, Santander.

Clausen, C.J.F., Aas, P.M., Hasle, E. (1984). SPLICE - A computer program for analysing structure-pile-soil interaction problems. NGI, Publication No.152, Oslo, pp.1-7.

Clemente, J.L.M. and Polo, J.M. (1988). Micro-computer analysis of pile group settlement using independent point and shaft loads. Computers & Structures, Vol. 29, No. 2, pp. 241-255.

Clemente, J.L.M. (1990a). Nonlinear analysis of settlement and load distribution in pile groups. Computers & Structures, Vol. 36, No. 2, pp. 203-210.

Clemente, J.L.M. (1990b). PGVARIAB - computer program. (Personal communication)

Cook, R.W. (1986). Piled raft foundation on stiff clays - A contribution to design philosophy. Geotechnique, Vol. 36, No. 2, pp. 169-203.

Combarieu, O. and Evrard, H. (1979). Les fondations mixtes, semelle-pieux. Bulletin de Liaison des Laboratoires des Ponts et Chaussées, No. 102, pp. 49-58.

Combarieu, O., Morbois, A. (1982). Fondations mixtes semelle-pieux. Annales de l'institut technique du batiment et des travaux publics, Sols et Fondations, No. 410, pp. 3-34.

Coyle, H.M., Reese, L.C. (1966). Load transfer for axially loaded piles in clay. Proc. ASCE, JSMFD, Vol. 92, No. SM2, pp. 1-26.

Davis, E.H. and Poulos, H.G. (1972). The analysis of pile raft systems. Australian Geomech. J., Vol. G2, No. 1, pp. 21-27.

Desai, C.S. (1974). Numerical design analysis for piles in sands. Proc. ASCE, JGED, Vol. 100, No. GT6, pp. 613-635.

Desai, C.S., Johnson L.D., Charles M.H. (1974). Analysis of pile-supported gravity lock. Proc. ASCE, JGED, Vol. 100, No. GT9, pp. 1009-1029.

Di Millio, A.F., NG, E.S., Briaud, J.L., O'Neill, M.W. et al. (1987). Pile group prediction symposium: summary. Vol. 1: Sandy soil. US Department of Transportation, FHWA, Publication No. FHWA-TS-87-221, Georgetown Pike, McLean, Virginia.

Duncan, J.M., Chang, C-Y. (1970). Nonlinear analysis of stress and strain in soils. Proc. ASCE, JSMFD, Vol. 96, No. SM5, pp. 1629-1653.

Ealy, C.D. (1982). Progress report No. 1, Instrumentation installation and initial monitoring pier EA-31. Shannon & Wilson Inc. Geotechnical Consultants, Seattle, Washington.

Ellison, R.D., D'Appolonia, E., Thiers, G.R. (1971). Load-deformation mechanism for bored piles. Proc. ASCE, JSMFD, Vol. 97, No. SM4, pp. 661-678.

Ekström, J. (1989). A field study of model pile group behaviour in non-cohesive soils - Influence of compaction due to pile driving. PhD thesis, Chalmers University of Technology, Göteborg.

Fatemi-Ardakani, A. (1988). Analysis of raft foundations, piled-raft foundations and ground floor slabs. PhD thesis, University of London.

Fatemi-Ardakani, B. (1987). A contribution to the analysis of pile-supported raft foundations. PhD thesis, University of Southampton.

Feagin, L.B. (1948). Performance of pile foundation of navigation locks and dams on the Upper Mississippi River. Proc. 2nd ICSMFE, Rotterdam, Vol. 4, pp. 98-106.

Fellenius, B.H., Goudreault, P. (1990). UNIPILE (Version 1.0), User's manual. Bengt Fellenius Consultants Inc., Ottawa.

Feng, G.D., Liu, Z.D., Huang, S.K. (1989). Determination of the load transfer parameters of pile foundations. Proc. 12th ICSMFE, Rio de Janeiro, Vol. 2, pp. 1053-1056.

Fleming, W.G.K. (1958). The bearing capacity of piles. PhD thesis. Queens Univ. of Belfast.

Fleming, W.G.K., Weltman, A.J., Randolph, M.F., Elson, W.K. (1992). Piling engineering. Blackie & Son, Glasgow, and John Wiley & Sons, New York, etc.

Garg, K.G. (1979). Bored pile groups under vertical load in sand. Proc.ASCE, JGED, Vol. 105, No. GT8, pp. 939-956.

Hain, S.J., Lee, I.K. (1978). The analysis of flexible raft-pile systems. Geotechnique, Vol. 28, No. 1, pp. 65-83

Hanna, T.H. (1963). Model studies of foundation groups in sand. Geotechnique, Vol. 13, No. 4, pp. 334-351.

Hanna, T.H. (1992). Personal communication.

Hansbo, S, (1984). Foundations on friction creep piles in soft clays. Proc. 1st Int. Conf. on Case Histories in Geotechnical Engineering, St. Louis, pp. 914-915.

Hansbo, S. (1989). Common-sense foundation design. Proc. 2nd Int. Conf. on Case Histories in Geotechnical Engineering, St. Louis, pp. 1337-1342.

Hansbo, S., Pramborg, B. (1990). Experience of Menard pressuremeter in foundation design. Proc. 3rd Int. Symp. on Pressuremeters. Thomas Telford Ltd, London, pp. 361-370.

Hartikainen, J. (1972a). On the distribution of pile loads in a friction pile foundation. University of Oulu, Dept. of Civil Engineering, Series C Technica No. 3, Mechanica No. 2.

Hartikainen, J. (1972b). On the influence of compaction piling on contact pressure distribution. Helsinki Univ. of Technology, Research paper No. 39.

Hewitt, C.M. (1988). Cyclic response of offshore pile groups. PhD thesis, University of Sydney, N.S.W.

Hooper, J.A. (1973). Observations on the behaviour of a piled-raft foundation on London clay. Proc. Inst. Civ. Engrs, Vol. 55, Part 2, pp. 855-877.

Hooper, J.A. (1979). Review of behaviour of piled raft foundations. CIRIA Report No. 83, London.

Hooper, J.A., Levy, J.F. (1981). Behaviour of a flexible pile foundation. Proc. 10th ICSMFE, Stockholm, Vol. 2, pp. 735-740.

ITASCA Consulting Group, Inc. (1991). FLAC (Fast Lagrangian Analysis of Continua), Version 3.0 - User's manual. Minneapolis, Minnesota.

Janbu, N. (1963). Soil compressibility as determined by oedometer and triaxial tests. Proc. ECSMFE, Wiesbaden, Vol.1, pp. 19-25.

Janardhanam , R. (1987). Effect of pile driving on group efficiency. Proc. Int. Symp. on Prediction and Performance in Geotechnical Engineering, Calgary, pp. 119-126.

Jendeby, L. (1986). Friction piled foundations in soft clay - A study of load transfer and settlement. PhD thesis, Chalmers University of Technology, Göteborg.

Jendeby, L., Ekström, J. (1987). User's manual to program PAUL - a computer program for calculating settlement. Göteborg Computer Centre. (in Swedish)

Joshi, R.C., Sharma, H.D., Sparrow, D. (1989). Skin friction distribution along driven piles. Proc. 12th ICSMFE, Rio de Janeiro, Vol.2, pp. 929-932.

Kakurai, M., Yamashita, K., Tomono, M. (1987). Settlement behaviour of piled raft foundation on soft ground. Takenaka Technical Research Report No. 38, Tokyo, pp. 191-198.

Kerisel, J. (1961). Fondations profondes en milieux sableux. Proc. 5th ICSMFE, Paris, Vol. 2, pp. 73-83.

Kezdi, A. (1957). Bearing capacity of piles and pile groups. Proc. 4th ICSMFE, London, Vol. 2, pp. 46-51.

Kezdi, A. (1960). Bemerkungen zur Frage der Tragfähigkeit von Pfahlgruppen. Proc. Symp. on the Design of Pile Foundations, Stockholm.

Ko, H.Y., Atkinson, R.H., Goble, G.G., Ealy, C.D. (1984). Centrifugal modeling of pile foundations. Proc. ASCE Symp. on Analysis and Design of Pile Foundations, San Francisco, pp. 21-40.

Kishida, H., Meyerhof, G.G. (1965). Bearing capacity of pile groups under eccentric loads in sand. Proc. 6th ICSMFE, Toronto, Vol. 2, pp. 270-274.

Kishida, H. (1967). Ultimate bearing capacity of piles driven into loose sand. Soils and Foundations, Vol. 7, No. 3, pp. 20-29.

Kuwabara, F. (1989). An elastic analysis for piled raft foundations in a homogeneous soil. Soils and Foundations, Vol. 29, No. 1, pp. 82-92.

Kuwabara, F. (1991). PGRAFT - computer program. (Personal communication).

Larsson, R. (1989). Strength of non-cohesive soils. SGI Information No. 8, Linköping. (In Swedish)

Lazaridis, A. and O'Neill, M.W. (1989). Numerical method for pile group response. University of Houston, Department of Civil and Environmental Engng, Report No. UHCE 89-7.

Lee, I.K. (1977). Interaction analysis of rafts and raft-pile systems. Proc. Int. Symp. on Soil-Structure Interaction, Roorkee, pp. 513-520.

Leonards, G.A. (1972). Settlement of pile foundations in granular soil. ASCE Speciality Conference on Performance of Earth and Earth-Supported Structures, Purdue University, Lafayette, Vol. 1, Part 2, pp. 1169-1184.

Liedberg, S. (1991). Earth pressure distribution against rigid pipes under various bedding conditions - Full-scale field tests in sand. PhD thesis, Chalmers University of Technology, Göteborg.

Lieng, J.T., Svanö, G. (1989). GROUP - Version 02, User's manual. NTH, SINTEF Geotechnical Engng. Report No. STF69-F89030, Trondheim.

Liu, J.L., Yuan, Z.L., Zhang K.P. (1985). Cap-pile-soil interaction of bored pile groups. Proc. 11th ICSMFE, San Francisco, Vol. 4, pp. 1433-1436.

Marchetti, S., Crapps, D.K. (1981). Flat dilatometer manual. GPE, Inc., Gainesville.

Marchetti, S. (1985). On the field determination of K_o in sand. Panel discussion. Proc. 11th ICSMFE, San Francisco, Session 2A.

Mazurkiewicz, B.K. (1972). Load testing of piles according to the Polish regulations. Swedish Pile Commission, Report No. 35, Stockholm.

Meyerhof, G.G. (1959). Compaction of sands and bearing capacity of piles. Proc. ASCE, JSMFD, Vol. 85, No. SM6, pp. 1-29.

Millan, A.A., Townsend, F.C., Bloomquist, D. (1987a). Bearing capacity of pile groups in sand from centrifugal model tests. Proc. 8th Pan. Am. Conf. SMFE, Cartagena, Vol.2.

Millan, A.A., Townsend, F.C., Bloomquist, D. (1987b). Deformation of pile groups in sand from centrifugal model tests. Proc. 8th Pan. Am. Conf. SMFE, Cartagena, Vol.2.

Naylor, D.J., Hooper J.A. (1974). An effective stress finite element analysis to predict the short- and long-term behaviour of a piled-raft foundation on London clay. Proc. Int. Conf. on Settlement of Structures, Cambridge, pp. 394-402.

Nordal, S. (1983). Elasto-plastic behaviour of soils analysed by the finite element method. PhD thesis, NTH, Trondheim.

Ottaviani, M. (1975). Three-dimensional finite element analysis of vertically loaded pile groups. Geotechnique, Vol. 25, No. 2, pp. 159-174.

O'Neill, M.W., Ghazzaly, O.I., Ha, H.B. (1977). Analysis of three-dimensional pile groups with non-linear soil response and pile-soil-pile interaction. Proc. 9th Annual Offshore Technology Conference, Vol. 2, pp. 245-256.

O'Neill, M.W., Hawkins, R.A., Mahar, L.J. (1981). Field study of pile group action. U.S. Federal Highway Administration, Report No. FHWA/RD-81/002, Washington, D.C.

O'Neill, M.W., Hawkins, R.A., Mahar, L.J. (1982). Load transfer mechanism in piles and pile groups. Proc. ASCE, JGED, Vol. 108, No GT12, pp. 1605-1623.

O'Neill, M.W., Ha, H.B. (1982). Comparative modelling of vertical pile groups. Proc. 2nd Int. Conf. on Numerical Methods in Offshore Piling, ICE.

O'Neill, M.W., Heydinger, A.G. (1982). Observations on full-scale pile group performance. Public Roads, Vol. 46, No. 3, pp. 106-111.

O'Neill, M.W. (1983). Group action in offshore piles. ASCE Conf. on Geotechnical Practice in Offshore Engineering, Austin, pp. 25-64.

Padfiel, C.J., Sharrock, M.J. (1983). Settlement of structures on clay soils. CIRIA Special Publication No. 27, PSA Civil Engineering Technical Guide 38, London.

Pepper, A.E.J. (1961). An interim report on a laboratory study on groups of piles in sand. Proc. Symposium on Granular Soils, The Midland SMFE Society, Birmingham, Vol. 4, pp. 187-203.

Phung Duc Long (1992). Tests on piled footings and pile groups in non-cohesive soil - A literature survey. SGI Varia No. 369, Linköping.

Polo, J.M. (1982). Analysis of settlements of pile groups. PhD thesis, Duke University, Durham, N.C.

Polo, J.M., Clemente, L.M. (1988). Pile-group settlement using independent shaft and point loads. Proc. ASCE, JGED, Vol. 114, No. 4, pp. 469-487.

Poulos, H.G. (1968). Analysis of the settlement of pile groups. Geotechnique, Vol. 108, pp. 449-471.

Poulos, H.G. (1980a). User's guide to program DEFPIG - Deformation analysis of pile groups. University of Sydney, School of Civil Engineering, N.S.W.

Poulos, H.G. (1980b). Comparison between theoretical and observed behaviour of pile foundations. Research Report No. R365, University of Sydney, N.S.W.

Poulos, H.G. (1986). DEFPIG4 - computer program. (Personal communication)

Poulos, H.G. (1987). From theory to practice in pile design. Research Report No. R559, University of Sydney, N.S.W.

Poulos, H.G. (1988). Marine geotechnics. Unwin Hyman, London.

Poulos, H.G. (1989). Pile behaviour-theory and application. The Rankine lecture. Geotechnique, Vol. 39, No. 3, pp. 365- 415.

Poulos, H.G. (1992). Pile foundation settlement prediction - Hand and computer methods, Proc. Int. Conf. on New Technology for Foundation Engineering, Hanoi.

Poulos, H.G. (1993). Personal communication.

Poulos, H.G., Davis, E.H. (1980). Pile foundation analysis and design. John Wiley and Sons, New York, etc.

Poulos, H.G., Randolph, M.F. (1983). Pile group analysis : a study of two methods. Proc. ASCE, JGED, Vol. 109, No. 3, pp. 355 -372.

Press, H. (1933). Die Tragfähigkeit von Pfahlgruppen in Beziehung des Einzelpfahles. Bautechnik, Vol. 11, pp. 625-627.

Pressley, J.S., Poulos, H.G. (1986). Finite element analysis of mechanism of pile group behaviour. Research Report No. R518, School of Civil and Mining, Engng, University of Sydney, N.S.W.

Randolph, M.F. (1980). PIGLET: A computer program for the analysis and design of pile groups under general loading conditions. Cambridge University, Engineering Department, Research Report, Soils TR91.

Randolph, M.F. (1983). Design of piled raft foundations. Cambridge University, Engineering Department, Research Report, Soils TR143.

Ranpolph, M.F. (1985). Settlement of pile groups. Cambridge University, Engineering Department, Research Report, CUED/D - Soils TR 163.

Randolph, M.F., Wroth, C.P. (1978). Analysis of deformation of vertically loaded piles. Proc. ASCE, JGED, Vol. 104, No.GT12, pp. 1465-1488.

Randolph, M.F., Wroth, C.P. (1979). An analysis of the vertical deformation of pile groups. Geotechnique, Vol. 29, No. 4, pp. 423-439.

Robertson, P.K., Campanella, R.G. (1983). Interpretation of Cone Penetration Tests - Part I (Sand). Canadian Geotech.J., Vol. 20, No. 4, pp.718-733.

Robertson, P.K., Campanella, R.G. (1988). Guidelines for using CPT, CPTU and Marchetti DMT for geotechnical design, Vol.2: Using CPT and CPTU data. US Department of Transportation, FHWA, Report No. FHWA-PA-87-023+84-24, Washington, D.C.

Sayed, M.S., Bakeer R.M. (1992). Efficiency formula for pile groups. Proc. ASCE, JGED, Vol.118, No.2, pp. 278-299.

Samson, L., Authier J. (1986). Change in pile capacity with time: case histories. Canadian Geotech. J., Vol. 23, pp. 174-180.

Sellgren, E. (1981). Friction piles in non-cohesive soils. Evaluation from pressuremeter tests. PhD thesis, Chalmers University of Technology, Göteborg.

Schmermann, J.H. (1982). A method for determining the friction angle in sands from the Marchetti dilatometer test. Proc. 2nd European Symposium on Penetration Testing, ESOP II, Vol. 2, pp. 853-861.

Schmermann, J.H. (1988a). Guidelines for using CPT, CPTU and Marchetti DMT for geotechnical design, Vol.3: DMT test methods and data reduction. US Department of Transportation, FHWA, Report No. FHWA-PA-87-024+84-24, Washington, D.C.

Schmermann, J.H. (1988b). Guidelines for using CPT, CPTU and Marchetti DMT for geotechnical design, Vol.4: DMT design methods and examples. US Department of Transportation, FHWA, Report No. FHWA-PA-87-025+84-24, Washington, D.C.

Shanouby, B.E., Novak, M. (1985). Static and low-frequency response of pile groups. Canadian Geotech. J., Vol. 22, No. 1, pp. 79-94.

Smith, I.M., Griffiths, D.V. (1988). Programming the finite element method (2nd ed.). John Wiley and Sons, Chichester, etc.

Skempton, A.W. (1953). Piles and pile foundations, settlement of pile foundations. Discussions. Proc. 3th ICSMFE, Zurich, Vol. 3, p. 172.

Stuart, J.G., Hanna, T.H., Naylor, A.H. (1960). Note on the behaviour of model pile groups in sand. Proc. Symp. on the Design of Pile Foundations, Stockholm, pp. 97-103.

Svensson, L. (1991). Soil-structure interaction of foundations on soft clay - Experience during the last ten years. Proc. 10th ECSMFE, Florence, Vol. 2, pp. 583-586.

Swedish Pile Commission (1979). Recommendations for pile driving tests with subsequent load testing. Report No. 59, Stockholm.

Tejchman, A.F. (1973). Model investigations of pile groups in sand. JSMFD, ASCE, Vol. 99, No. SM2, pp. 199-217.

Terzaghi, K. (1943). Theoretical soil mechanics. John Wiley & Sons Inc., New York.

Thaher, M., Jessberger, H.L. (1990a). Influence of the configuration of piles supporting the foundation raft on the settlement behaviour of high-rise buildings. Proc. Int. Seminar on Geotechnical and Water Problems in Lowland, Saga, Japan.

Thaher, M., Jessberger, H.L. (1990b). Settlement reduction of high-rise buildings by a limited number of piles supporting the foundation raft. Proc. Conf. on Deep Foundation Practice, Singapore, pp. 247-256.

Thaher, M., Jessberger, H.L. (1991). Investigation of the behaviour of pile-raft foundations by centrifuge modelling. Proc. 10th ECSMFE, Florence, Vol. 2, pp. 597-603.

Timoshenko, S., Goodier, J.N. (1951). Theory of elasticity. McGraw-Hill Book Company, New York, etc.

Tomono, M., Kakurai, M., Yamashita, K. (1987). Analysis of settlement behaviour of piled raft foundations. Takenaka Technical Research Report No. 37, Tokyo, pp. 115-124.

Trochanis, A.M., Bielak, J., Christiano, P. (1991a). Three-dimensional nonlinear study of piles. Proc. ASCE, JGED, Vol. 117, No. 3, pp. 429-447.

Trochanis, A.M., Bielak, J., Christiano, P. (1991b). Simplified model for analysis of one or two piles. Proc. ASCE, JGED, Vol. 117, No. 3, pp. 448-466.

Trofimenkov, A.M. (1977). Panel discussion. Proc. 9th ICSMFE, Tokyo, Vol. 3, pp. 370-371.

Trofimenkov, J.G., Lioshin, G.M. (1979). Piled-mat foundation for heavy buildings and structures. Proc. 6th Asian Regional Conf. on SMFE, Singapore, Vol. 1, pp. 361-364.

Van Impe, W.F. (1991). Deformations of deep foundations. Proc. 10th ECSMFE, Florence, Vol. 3, pp. 1031-1062.

Vesic, A.S. (1969). Experiments with instrumented pile groups in sand. Performance of Deep Foundations, ASTM STP 444, pp. 177-222.

Vesic, A.S. (1970). Tests on instrumented piles, Ogeechee River site. Proc. ASCE, JSMFD, Vol. 96, No. SM2, pp. 265-290.

Vesic, A.S. (1977). Design of pile foundations. Synthesis of Highway Practice No. 42, Transportation Research Board, Washington.

Whitaker, T. (1957). Experiments with model piles in groups. Geotechnique, Vol.7, No. 4, pp. 147-167.

Wiesner, T.J., Brown, P.T. (1980). Laboratory tests on model piled raft foundations. JGED, ASCE, Vol. 106, No. GT7, pp. 767-783.

Wood, L.A. (1978). A note on the settlement of piled structures. Ground Engineering, Vol. 11, No. 4, pp. 38-42.

Woodward-Clyde Consultants (1969). Results and interpretation of pile driving effects test program, existing locks and dam No.26, Mississippi River, Alton, Illinois. Phase IV Report, Vol. 3, Dept. of the Army, St.Louis District, Corps of Engineers, pp. 8.1-8.7.

Yamaguchi, H. (1984). Effect of depth of embedment on foundation settlement. Soils and Foundations, Vol. 24, No. 1, pp. 151-156.

Yamashita, K., Tomono, M., Kakurai, M. (1987). A method for estimating immediate settlement of piles and pile groups. Soils and Foundations, Vol. 27, No. 1, pp. 61-76.

APPENDIX A Modification of pile load-settlement curves in tests on a piled footing using the second test procedure.

As described in Section 3.3, the tests on piled footings were performed using two different procedures. According to the second procedure, the test on the piled footing was started when the the cap was 20 mm above the soil surface. Tests T2F and T3F were carried out by this procedure. This way of testing has the excellent advantage in that the effect on the behaviour of the piles of the cap in contact with the soil can be seen clearly. The other effects, such as time and penetration effects, can be eliminated by taking the test results before cap-soil contact in the continuous test on the piled footing as those obtaining for the free-standing pile group. However, using this procedure the test results can not be directly compared with those of the other tests in the same series. In order to make possible a comparison, the original pile load-settlement curve was modified in the way described in this appendix.

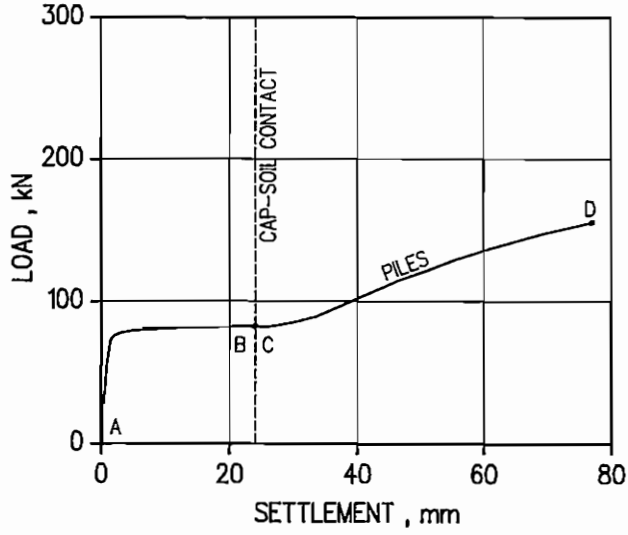

Fig. A.1 The original pile load-settlement curve in a piled footing test carried out according to the second test procedure

The original pile load-settlement curve in a piled footing test, carried out according to the second testing procedure, is shown in Fig.A.1. In this figure,

AB corresponds to the free-standing pile group (before cap-soil contact), and CD corresponds to the behaviour of the piles in the piled footing (after contact). Based on a remark from Test series T1, stating that the initial stiffness of the piles in the piled footing is very similar to that of the corresponding free-standing pile group, curve AB can be used as the initial part of the modified curve. Curve CD, of course, can be used for the final part of the modified curve with the corresponding settlement starting from zero, Fig A.2. EF is a transient part to adapt the two curves. The modified pile load-settlement curve is AEFD. The modified curve is approximate for small settlements, but accurate for large enough settlements.

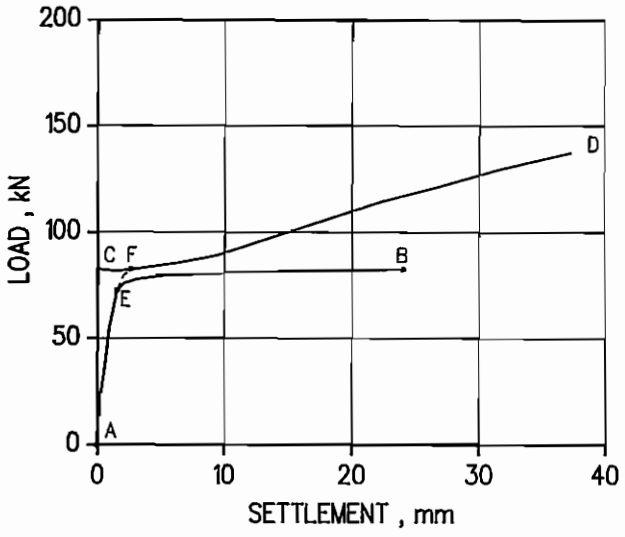

Fig. A.2 Establishment of modified pile load-settlement curve

APPENDIX B Electrical CPT Tests - Typical Results (Before Tests)

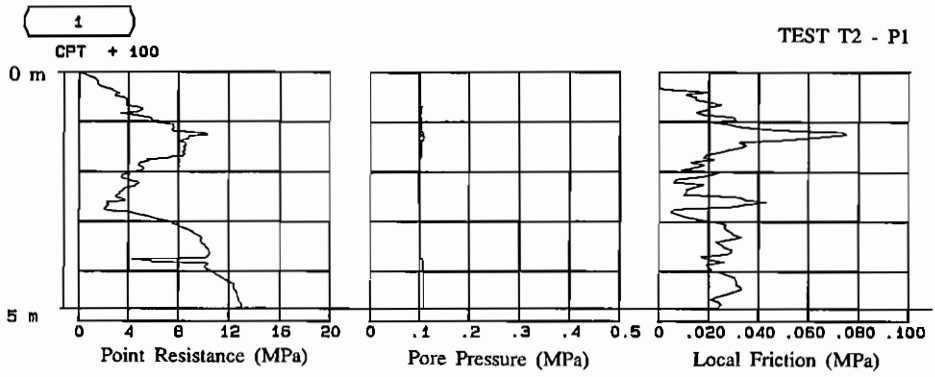

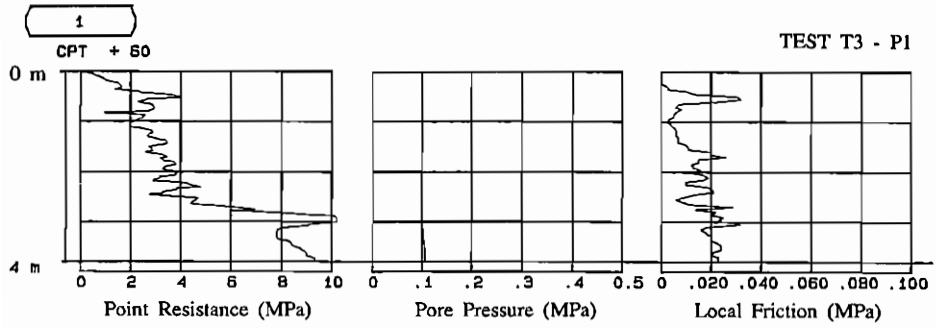

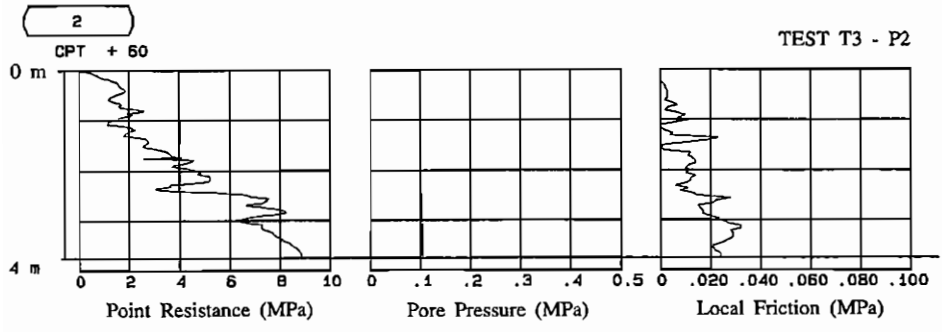

Distribution: Department of Geotechnical Engineering
Chalmers University of Technology
S-412 96 Göteborg, Sweden

Price: 200 Sw.Crs.

ISBN 91-7032-833-1